# Solid-State Chemistry of Drugs

Stephen R. Byrn

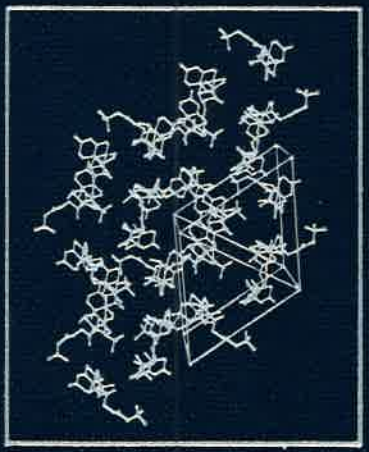

# Solid-State Chemistry of Drugs

STEPHEN R. BYRN

*Department of Medicinal Chemistry and Pharmacognosy*
*School of Pharmacy and Pharmacal Sciences*
*Purdue University*
*West Lafayette, Indiana*

ACADEMIC PRESS 1982

*A Subsidiary of Harcourt Brace Jovanovich, Publishers*

New York London
Paris San Diego San Francisco São Paulo Sydney Tokyo Toronto

# Contents

# 1 Introduction

# 1 Introduction

The branch of science termed solid-state chemistry of drugs is unusually broad. It includes the areas of physical pharmacy and industrial pharmacy (including powder technology and formulation). It also includes the areas of stability of solids, kinetics of solid-state reactions, and molecular details of solid-state reactions.

Studies of the molecular details of solid-state reactions aim at providing an explanation of the products and rate of the reaction in terms of the molecular change (chemical reaction) that occurs. These studies usually use the crystal structure and other molecular information to provide such an explanation.

The aim of this book is to review the molecular details of solid-state reactions of drugs and to bring these details to bear on pharmaceutical problems. It is thus an attempt to provide a molecular basis for understanding the solid-state chemistry of drugs. Related aims in the areas of biology and chemistry (i.e., attempts to put these areas on a molecular basis) have led to the rapid development of these branches of science. A similar rapid development of the area of solid-state chemistry of drugs is also expected.

# I. Crystallization and Properties of Crystals

The process of crystallization is one of ordering. During this process, randomly organized molecules in a solution, a melt, or the gas phase take up regular positions in the solid. The regular organization of the solid is responsible for many of the unique properties of crystals, including the diffraction of x-rays, defined melting point, and sharp, well-defined crystal faces.

The first step in crystallization involves nucleation. The formation of nuclei is not well understood but could be related to impurities, dust in the flask, or small conglomerates of molecules of the compound, a few angstroms in size.

Once formed, the nuclei grow into crystals by deposition of molecules on the crystal faces. This is an equilibrium process, with the molecules in equilibrium between the solution and the solid. (It should be noted that dissolution is the reverse process.) The rate of crystallization also depends on the concentration of the solution, the temperature, and the degree of agitation or stirring of the solution.

## A. FORCES HOLDING CRYSTALS TOGETHER

At this point it is appropriate to consider the forces responsible for crystallization and the forces responsible for holding crystals together. Crystals are held together by noncovalent interactions. These interactions are either hydrogen-bonding or noncovalent attractive forces. Kitaigorodskii described the forces holding crystals together in his classic book entitled "Organic Chemical Crystallography" (1961). Both hydrogen-bonding and noncovalent interactions result in the formation of a regular arrangement of molecules in a crystal. Noncovalent attractive interactions, which are sometimes called nonbonded interactions, depend on the dipole moments, polarizability, and electronic distribution of the molecules. Hydrogen bonding, of course, requires donor and acceptor functional groups.

Another important factor is the symmetry of the molecules. The molecule's symmetry (or lack of symmetry) determines how it is packed in the crystal and, in some cases, the overall symmetry of the crystal. Molecules with symmetries that allow them to fit together in a close-packed arrangement form better crystals and crystallize more easily than nonregular molecules.

Kitaigorodskii (1961) has advanced the close-packing theory to explain the forces holding crystals together. He suggests that the basic factor that affects free energy is the packing density. The denser or more closely packed crystal has the smaller free energy. This means that the heat of

sublimation (and, to a first approximation, melting point) increases as the packing density increases, and that in a series of polymorphs the densest polymorph is the most stable.

Kitaigorodskii (1961) pointed out that symmetry is also important. The free energy of a crystal undoubtedly increases as the number of independent molecules in the crystal increases. This tendency to higher symmetry may conflict with the tendency toward close packing. However, close packing generally affects the internal energy of the crystal, while symmetry affects its entropy.

## B. CRYSTAL HABITS

The faces of a crystal that grow most rapidly are those to which the molecules are bound most tightly. This feature is displayed in the shapes of crystals of organic ring compounds. Molecules containing planar aromatic or nonaromatic rings such as cytosine, caffeine, or theophylline usually form needlelike crystals. The relatively strong interaction between the planes of these rings (i.e., pi–pi interaction) causes more rapid growth in the stacking direction than in other directions. Thus in these crystals the rings are arranged perpendicular to the needle axis.

In this case the external shape of the crystal, its *habit,* reflects the internal structure. Thus a knowledge of the crystal habit sometimes provides important information on its molecular organization. The relationship between the external shape of the crystal and its internal structure can be confirmed by determination of the crystal structure.

It is not uncommon for the same compound to crystallize in several different crystal habits, as shown in Figure 1. Although crystal habits have the same internal structure and thus have identical single crystal- and powder-diffraction patterns, they can still exhibit different pharmaceutical properties, owing to the fact that different crystal faces are developed (Haleblian, 1975).

Before discussing the different pharmaceutical properties of crystal habits, it is important to point out crystallization conditions that can affect the habits that occur:

1. *Supersaturation.* The extent of supersaturation may affect which habit grows.
2. *Rate of cooling and degree of solution agitation.* When naphthalene is crystallized by rapid cooling it gives thin plates, while when it is slowly crystallized by evaporation it gives compact crystals.
3. *Presence of cosolutes, cosolvents, and adsorbable foreign ions.* When NaCl is crystallized from water only cubic [100] faces are developed, while octahederal [111] faces grow when NaCl is crystallized in the presence of urea.

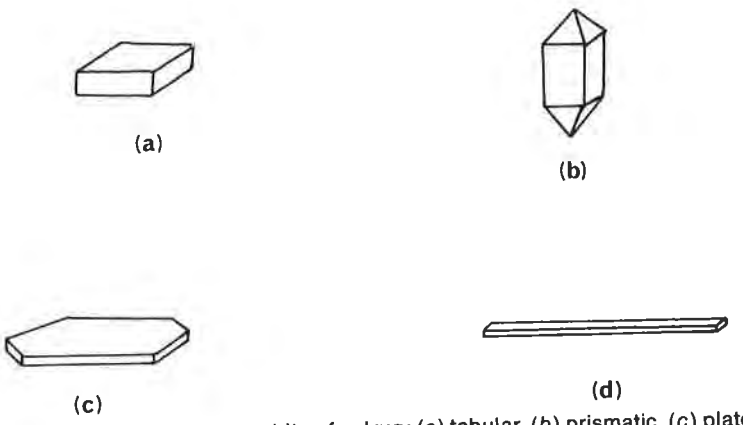


**FIGURE 1.** Different crystal habits of a drug: (*a*) tabular, (*b*) prismatic, (*c*) plate, and (*d*) needle.

Once the crystals obtained have been shown to have habits it is often necessary to characterize these habits. Habits are best characterized using instruments called reflecting or optical goniometers. A reflecting goniometer is shown in Chapter 2 in Figure 9 (p. 38).

Crystal habits influence several pharmaceutical characteristics related to the physical shape and nature of the crystal.

1. *Suspension syringeability*. This parameter is influenced by mostly mechanical factors. For example, a suspension of plate-shaped crystals may be injected through a small needle with greater ease than one of needle-shaped crystals.
2. *Tableting behavior*. Behavior upon compression of crystals is dependent upon the habit present; however, no generalization can be made. It is quite reasonable to expect platelike crystals to exhibit different tableting behavior from needles. However, a priori, it is difficult to predict the differences in behavior.

## C. POLYMORPHS

Crystallization can also result in the formation of several different solvates and/or anhydrates, which have different crystal habits and different x-ray diffraction patterns. These different solvates and/or anhydrates will be referred to as *polymorphs*. Polymorphs are thus different crystal forms of the same compound, and are detected by x-ray diffraction. Polymorphs have different physical and chemical properties. They can be interconverted by phase transformations or a solvent-mediated process. Phase transformations can be induced by heat or mechanical stresses. Different

polymorphs have different dissolution rates and bioavailability. No rules exist that allow prediction of whether a compound will exhibit polymorphism; however, polymorphism is widespread in pharmaceuticals, particularly in steroids, sulfonamides, and barbiturates.

Two special types of polymorphism are termed *conformational* and *configurational* polymorphism. Conformational polymorphism occurs when a molecule adopts a significantly different conformation in different crystal polymorphs. The term "significantly different" is open to interpretation; however, it implies torsion or dihedral angles different by at least three standard deviations. For example, the Schiff's base *p*-(*N*-chlorobenzylidene)-*p*-chloroaniline crystallizes in two polymorphs. The stable form belongs to the triclinic crystal system, while the unstable form belongs to the orthorhombic crystal system. Both polymorphs are disordered but, strikingly, the conformation of the Schiff's base is different in the two polymorphs. Thus, these forms are termed *conformational polymorphs* (Bernstein and Hagler, 1978).

Conformational polymorphism involves the crystallization of different conformers in different crystalline forms, but this term does not adequately describe cases where different types of isomers crystallize in different forms. Thus a new term—*configurational polymorphism*—is defined. Configurational polymorphism exists when different configurations (i.e., cis–trans isomers or tautomers) crystallize in separate crystalline forms. Of course the crystallization of cis and trans isomers of the same compound in different crystalline forms is well known and occurs whenever the pure isomer is crystallized. Similarly, crystallization of a pair of pure tautomers in separate crystals leads to what may be called tautomerizational polymorphs. The crystallization of equilibrating isomers in configurational polymorphs is of significantly more interest. When this occurs, the phenomena of configurational polymorphism can be used to isolate and study the individual isomers.

Polymorphism is very common in the pharmaceutical area. Because they have different crystal structures, polymorphs have different chemical and physical properties. Polymorphs of the same substance show different melting points, different chemical reactivities, different dissolution rates, and different bioavailabilities.

## D. CRYSTAL SOLVATES

Upon crystallization, drugs often entrap solvent in the crystal. This solvent can be in stoichiometric or nonstoichiometric amounts. Crystals that contain solvent of crystallization are termed *solvates*. If water is the solvent of crystallization, the solvates are called *hydrates*. Crystal solvates

and hydrates are extremely important for drugs. In particular, antibiotics are well known for crystallizing with solvent in the crystal. Determination of the crystal structure reveals the nature of interaction of the solvent with the host molecules. A knowledge of this interaction is extremely helpful in understanding and explaining the behavior of solvates.

Crystallization also results in crystals that contain no solvent of crystallization. Such crystals are termed *anhydrates*. Here, the term anhydrate refers to crystals that do not contain solvent of crystallization.

A classification scheme for solvates needs further discussion. Crystal solvates exhibit a wide range of behavior. Some solvates are very stable and require vigorous conditions to bring about desolvation; however, upon desolvation, a different crystal form is produced. Other solvates are much less stable but also give a different crystal form upon desolvation. Still other solvates are relatively unstable but do not give a different crystal form upon desolvation.

The forces holding solvates together explain these types of behavior. For example, in some solvates the solvent plays an important role in holding the crystal together. Formation of a hydrogen-bonding network that includes the solvent is quite common. When these solvates lose solvent, the crystal collapses and recrystallizes in a new crystal form.

In other solvates, the solvent plays little or no role in holding the crystal together. In these cases, a network of hydrogen bonds and nonbonded interactions holds the host molecules together. The solvent molecules are fillers that occupy voids in the crystal. Desolvation of these solvates does not destroy the crystal. For example, Pfeiffer *et al.* (1970) described the behavior of several cephalosporin solvates that can be desolvated and resolvated at will without destruction of the original crystal lattice and without greatly changing the powder diffraction pattern of the crystal. This behavior was termed *crystal pseudopolymorphism*.

Based on these considerations a new classification scheme for crystal solvates is proposed. This classification scheme is based on the crystallographic behavior of solvates rather than the stability. Solvates that transform to another crystal form (different x-ray powder-diffraction pattern) upon desolvation are *polymorphic solvates*. Solvates that remain in the same crystal form (similar x-ray powder diffraction pattern) are *pseudopolymorphic solvates*. Both classes of solvates contain stable and unstable members. An important difference between these two classes is that pseudopolymorphic solvates are readily resolvated, while polymorphic solvates are resolvated only after a phase transformation.

Table I lists the classification of a few solvates that have been investigated at Purdue University or described in publications.

**TABLE I**
*Classification of Solvates*

| Polymorphic solvates | Pseudopolymorphic solvates |
|---|---|
| Cytosine hydrate | Cephalexin hydrate |
| 5-Nitrouracil hydrate | Hydrocortisone *tert*-butylacetate ethanolate |
| Deoxyadenosine hydrate | |

Another possible classification scheme for solvates makes use of diagrams of vapor pressure versus composition. These are constructed by equilibrating the crystal with vapor in a closed container. Diagrams of vapor pressure versus composition are determined easily for water because a range of salt solutions with different water vapor pressures is available. However, for other solvents these diagrams are more difficult to determine because of the difficulties inherent in measuring their vapor pressures.

Diagrams of vapor pressure versus composition have been prepared for a few solvates. For example, Pfeiffer *et al.* (1970) measured vapor pressure versus composition for cephaloglycin–water, cephalexin–water, and cephalexin–acetonitrile (Figure 2). At Purdue, the vapor pressure versus composition of dialuric acid–water has been measured.

Diagrams of vapor pressure versus composition show the conditions under which a given solvate or anhydrate exist. However, examination of the published diagrams shows that there is no obvious trend that could be used as a means of classification of crystal solvates. Thus, classification

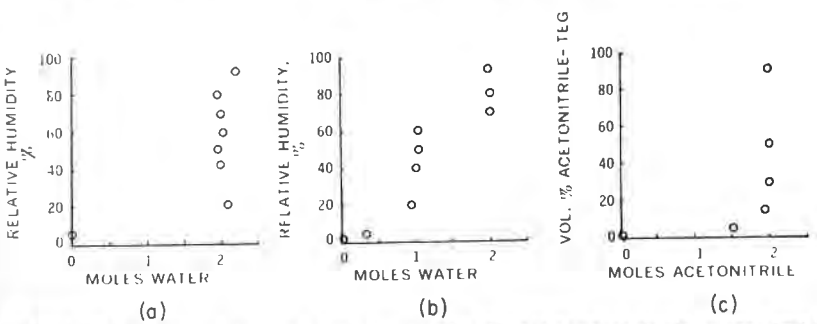


**FIGURE 2.** Vapor pressure versus composition for (*a*) cephaloglycin–water and (*b*) cephalexin–water. The third diagram (*c*) is a plot of the volume percent acetonitrile in triethylene glycol (TEG), which was present in a solution used to provide a range of acetonitrile vapor pressures whose exact magnitude was not determined. (Pfeiffer *et al.*, 1970. Reproduced with permission of the copyright owner.)

based on the x-ray diffraction pattern of solvates and desolvated crystals appears to be the scheme of choice.

## II. Properties of Other Solids

A number of other solids in addition to crystals are encountered in the study of solid pharmaceuticals. The properties of these solids are also of interest.

### A. AMORPHOUS SOLIDS

Amorphous solids have no crystal shape and cannot be identified as either habits or polymorphs. The most common amorphous solid is a glass in which the atoms and molecules exist in a nonuniform array.

An *amorphous form* can also be understood in terms of the size of the crystallites. Starting with a crystalline material, the size of the crystals would be reduced in stages and an x-ray photograph could be taken at each stage. The lines on the photograph would become diffuse when the crystal size falls below about $10^{-5}$ cm. As the crystal size is reduced further, the lines would become increasingly diffuse until the limit is reached at about $10^{-8}$ cm, the region of atomic dimensions. At this point it is impossible for a crystal to exist since, by definition, it is no longer an ordered array of atoms or molecules. Amorphous forms give no diffraction pattern and thus have crystal sizes less than $10^{-5}$ Å.

Amorphous crystals can be prepared by rapid crystallization or by lyophilization. For example, rapid crystallization gave an amorphous form of chloramphenicol palmitate (Kimura and Hashimoto, 1960), and lyophilization gave the amorphous form of fluprednisolone (J. Haleblian *et al.*, 1971).

Amorphous solids are best characterized by x-ray powder diffraction, since these solids give very diffuse lines or no crystal diffraction pattern at all.

While amorphous solids often have desirable pharmaceutical properties such as rapid dissolution rates, they are not usually marketed because of their instability. Since they are noncrystalline, amorphous forms are an energetic form which tend to crystallize to a more stable form. In addition, amorphous forms are often more chemically reactive than their crystalline counterparts (Pikal *et al.*, 1977).

However, in some cases amorphous forms are used and are desirable. An excellent example is novobiocin (Mullins and Macek, 1960). Novobiocin exists in a crystalline and an amorphous form. The crystalline

**TABLE II**
*Plasma Levels (μg/ml) of Novobiocin in Dogs after Administration of Different Forms of Novobiocin*[a]

| Form administered | Hours after dose | | | | | | |
|---|---|---|---|---|---|---|---|
| | 0.5 | 1.0 | 2.0 | 3.0 | 4.0 | 5.0 | 6.0 |
| Sodium novobiocin | 0.5 | 0.5 | 14.6 | 22.2 | 16.9 | 10.4 | 6.4 |
| Amorphous novobiocin acid | 5.0 | 40.6 | 29.3 | 22.3 | 23.7 | 20.2 | 17.5 |
| Crystalline novobiocin acid | Not detectable at any time | | | | | | |

[a] From Haleblian (1975).

form is poorly absorbed and does not provide therapeutically active blood levels; in contrast, the amorphous form is readily absorbed and is therapeutically active. Further studies show that the amorphous form is 70 times more soluble than the crystalline one in 0.1 *N* HCl at 25°C when particles $<10$ μm are used.

Table II shows data for the plasma levels of novobiocin's amorphous and crystalline forms and for sodium novobiocin, which also gives detectable plasma levels but is chemically unstable in solution.

Unless special precautions are taken, the amorphous form is slowly converted to the crystalline form. Several additives have been developed to retard this conversion, with methylcellulose and several alginic acids being most effective.

## B. HYGROSCOPIC SOLIDS

Unfortunately, there is no clear definition of hygroscopic solids. Instead, a solid is *hygroscopic* when it takes up moisture from the atmosphere. Hygroscopicity is determined by both a kinetic term and a thermodynamic term. For example, at equilibrium a solid may only take up a small amount of water but because the uptake is rapid the solid would be termed hygroscopic. Likewise, the solid may absorb a large amount of water at a very slow rate. Because the rate is slow, such a solid is not termed hygroscopic.

In addition, the relative humidity of the atmosphere plays an obviously important role in determining whether or not a solid is hygroscopic. In high relative humidities, many solids are hygroscopic. In atmospheres of low humidity, only a few solids will be hygroscopic.

A third factor influencing hygroscopicity is surface area. The larger the surface area of the solid, the more rapid the uptake of moisture. This is because solids with a larger surface area have more sites for condensation and adsorption of water molecules. In general, amorphous solids are often

hygroscopic, because of their large surface area and possibly because of their disordered structure.

### C. LYOPHILIZED POWDERS

Many antibiotics and some other drugs are marketed as lyophilized powders. Lyophilized powders are produced by freeze drying a solution to a very low moisture content. Freeze drying is accomplished by placing the solution under high vacuum at a low temperature. These powders are reconstituted before use by adding water.

The nature of lyophilized powders ranges from crystalline to amorphous. In some cases the solid crystallizes during freeze drying. In many more cases an amorphous, hygroscopic powder is formed. Lyophilized powders sometimes crystallize upon storage to form a crystalline solid with a much slower dissolution rate.

## III. Solid-State Chemistry of Drugs

The scientific discipline of solid-state chemistry of drugs emphasizes studies of the chemical properties of the various solids just discussed. This includes solid-state phase transformations and polymorphic transformations, reactions in which solvent of crystallization is lost, and a broad range of solid-state chemical reactions.

### A. CRITERIA FOR SOLID-STATE REACTIONS

It is necessary to establish criteria for solid-state reactions. This enables researchers to focus on true solid-state reactions and to avoid identification of a reaction that occurs in a liquid as a solid-state reaction.

Morawetz (1966) suggests four criteria for determining whether a reaction is a true solid-state reaction:

1. A reaction occurs in the solid when the liquid reaction does not occur or is much slower. This criterion is particularly important for determining whether a reaction is a true solid-state reaction.
2. A reaction occurs in the solid when pronounced differences are found in the reactivity of closely related compounds.
3. A reaction occurs in the solid when different reaction products are formed in the liquid state.
4. A reaction occurs in the solid if the same reagent in different crystalline modifications has different reactivity or leads to different reaction products.

A fifth and very important criterion can be added (Paul and Curtin, 1973). A reaction occurs in the solid if it occurs at a temperature below the eutectic point of a mixture of the starting material and products. This criterion can best be understood using the phase diagram shown in Figure 3.

Each solid-state reaction can be represented by a phase diagram, from which important insights can be gained. It is particularly instructive to consider the diagram of temperature versus composition (at constant pressure) for a two-component mixture of A and B where A goes to B upon heating. At least four cases can be visualized (see Figure 3).

Case 1: *Solution reaction.* This case is understood by visualizing that component A is heated to temperature *Z*. At temperature *Y*, melting occurs. The reaction then continues in liquid until 100% of B is formed.

Case 2: *Melting before reaction.* This case is understood by visualizing that component A is heated to temperature *Y*, at which point melting occurs. Component A then reacts to form B until point *Q* is reached. At this point, B crystallizes and the reaction continues in a mixture of liquid and crystalline B until 100% B is formed.

Case 3: *Reaction before melting.* This case is understood by visualizing that component A is heated to temperature *X*. As soon as some B is formed, solid A + liquid will exist until point *U* is reached. The mixture will liquify until point *T* is reached. At this point, B will crystallize and the reaction will continue in a mixture of liquid + crystalline B until reaction is complete.

Case 4: *Solid-state reaction.* This case is understood by visualizing that

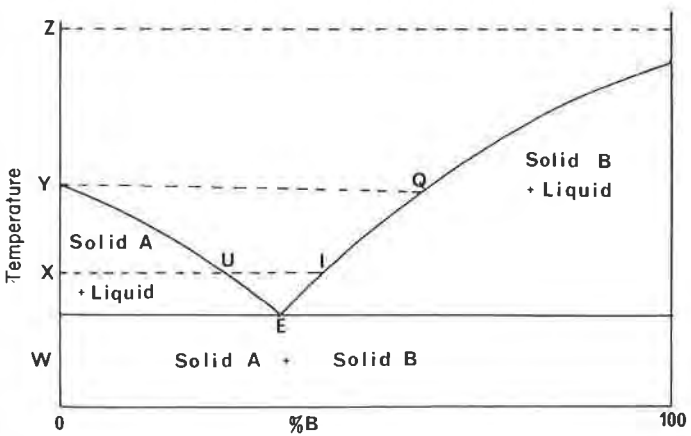


**FIGURE 3.** Hypothetical phase diagram of a solid A and its solid-state reaction product B.

component A is heated to point *W*. The reaction then occurs completely in the solid state until 100% B is formed.

Thus only Case 4 depicts a true solid-state reaction. From this discussion it is clear that care must be taken to ensure that the reaction is being carried out at a temperature below the eutectic temperature of the reactants and products, to be sure that the reaction takes place in the solid state.

## B. STEPS IN A SOLID-STATE REACTION

Once it has been established that the reaction is occuring in the solid state, the reaction is understood in terms of a four-step process (Paul and Curtin, 1973).

1. *Loosening of molecules at the reaction site.* It is reasonable to assume that the extent of loosening required depends on the distortion of the reaction cavity required to accomplish the next step.
2. *Molecular change.* This step is similar to the corresponding solution reaction where the reactants bonds are broken and the product bonds formed.
3. *Solid-solution formation.* During the early stages of the reaction, a solid solution of the product in the starting crystal is formed; however, after the product concentration reaches a certain point the product will separate.
4. *Separation of product.* This step often gives randomly oriented crystals or crystals with an orientation governed by the crystals of the starting material. This latter case is termed a topotactic reaction and will be discussed further.

*Molecular Loosening.* Solid-state reactions begin at one or more nucleation sites and spread through the crystal. In some cases, particularly in desolvations and some thermal reactions, a reaction begins at a nucleation site and spreads through the crystal in a front that advances at a more or less linear rate through the crystal.

Nucleation sites for reaction are developed during crystallization or can sometimes be produced by mechanical deformations such as pricking with a pin or cutting the crystal. Nucleation sites can also sometimes be produced by exposing the starting crystal to product crystals. In other cases, neither mechanical deformation nor exposure to product crystals nucleates the reaction. Obviously, this variability in nucleation and the random number of nucleation sites that are present in crystals can greatly complicate the kinetics of solid state reactions. In fact, the rates of some solid-state reactions can be explained entirely in terms of propagation of nucleation sites through the crystal.

For solid–gas reactions, this molecular loosening step also involves diffusion of the gas to the reactive site. Of course, diffusion of a gas into the crystal requires molecular loosening. Thus for solid–gas reactions the molecular loosening step actually involves simultaneous or sequential molecular loosening and diffusion.

*Molecular Change.* This step is most similar to the solution reaction of compounds: in it, the chemical reaction occurrs. If nucleation and the molecular loosening process can be separated from the molecular change, then the rate of solid-state reactions is explainable by the same factors that explain the rates of solution reactions. Unfortunately, in many cases the molecular loosening process cannot be separated from the molecular change. It is interesting to note that, except in rare instances of favorable orientation, solid-state reactions are usually much slower than their solution counterparts. This is probably due to the compactness of solids and the fact that large movements of functional groups are restricted by the rigid crystal.

*Solid-Solution Formation.* After a small amount of product is formed, it usually exists as a solid solution in the starting crystal lattice. In general, the extent of solid solution formation and the energies required to form solid solutions probably do not greatly influence the rates of solid-state reactions. However, in cases where the energy of the product influences the energy barrier, these factors could play a role. The formation of a solid solution of product in the starting crystal does indicate that methods such as x-ray diffraction that measure the diffraction of the starting crystal may not be suitable for measuring rates of reaction, since during solid solution formation the diffraction pattern of the starting crystal would not change greatly or even predictably.

*Separation of the Product Phase.* After the limit of solubility of the product in the starting crystal lattice is reached, the product will crystallize. This step would not influence the rate of the reaction if the rate is measured by chemically measuring the amount of product formed or the disappearance of the reactant. However, if the rate is measured by measuring the diffraction from the crystal lattice of the product, then this step will contribute to the measured rate of the reaction. Thus rates measured using x-ray diffraction differ from those measured chemically.

It is clear from the above discussion that the rates of solid-state reactions depend on several factors, including nucleation and the molecular change involved.

It is important to realize that the crystal structure and crystal packing profoundly affect the molecular-loosening and molecular-change steps of a solid-state reaction. The crystal packing determines the extent of molecular loosening required for the molecules to get in an orientation to undergo the molecular change required to complete the reaction. The

crystal packing also determines the extent of molecular loosening required for gases to diffuse to the reaction site in solid–gas reactions. Thus, a great deal of insight into solid-state reactions can be attained by determining the crystal structure of the reacting crystals.

In favorable cases, the crystal packing places the molecules in an orientation that results in acceleration of the reaction (Sukenik *et al.*, 1970). In these cases, the solid-state reaction is actually faster than the solution reaction.

## C. THE TOPOCHEMICAL POSTULATE

The topochemical postulate describes the best examples of control of solid-state reactions by crystal packing. Schmidt and his co-workers at the Weizmann Institute were able to explain a variety of solid-state photochemical reactions in terms of the topochemical postulate, which states that reactions in crystals proceed with a minimum of atomic and molecular movement. Thus the products of these reactions are controlled by the crystal packing of the starting crystals (Schmidt, 1964, 1971). This postulate explains a large number of reactions; however, it is obviously limited to reactions that occur in a crystalline matrix.

The topochemical postulate implies the concept of a reaction cavity (Cohen, 1975). The molecules in a solid that are going to react occupy a certain size and shape cavity in the starting crystal. This is defined as the *reaction cavity*. Reactions that proceed according to lattice control and obey the topochemical postulate probably proceed with a minimum distortion of this cavity, since formation of voids or protrusions from it are energetically unfavorable. In addition, in some cases the activated complex and the products fit so well in the reaction cavity that products are produced as a solid solution in the starting crystal. A topochemically controlled reaction is expected to give the product that best fits the reaction cavity.

The concept of a reaction cavity is based on the assumption that topochemically controlled reactions occur in the bulk of the crystal. Studies of the photodimerization of mixed crystals of *trans*-cinnamides and of *trans*-stilbenes give products that are consistent with the dimerization occurring in the bulk phase rather than at defect sites (Cohen and Cohen, 1976).

On the other hand, crystals contain finite populations of impurity molecules and of structural defects of different types, and sometimes crystals react at these sites. When such a crystal is irradiated, most of the light is absorbed by the perfect part of the crystal. However, in general, energy transfer is fast enough that transfer to the impurity molecules or defect

sites occurs (Cohen, 1975). For example, anthracene crystals containing a $10^{-4}$ mole ratio of tetracene absorb light at the anthracene wavelength, but most of the emission is from tetracene. In addition, general experience shows that the rate of a solid-state photochemical reaction is faster for impure crystals and for crystals that contain many mechanical defects. There are also exceptions to the rapid energy transfer to defect sites. In particular, studies of cinnamic acid, cinnamides, and stilbenes lead to the tentative conclusion that in these reactions there is little or no transfer of energy (Hung *et al.*, 1972; Cohen *et al.*, 1973).

Another important example of the influence of the crystal packing of the reactant on a solid-state reaction is the phenomenon of topotaxy. *Topotaxy* occurs when the product crystal has a preferred orientation in a crystallographic direction of the parent. Topotaxy is most common in the solid-state rearrangement reactions of polyvalent iodine compounds and in solid-state polymerizations. From studies of topotaxy in polyvalent iodine compounds, the following observations can be made (Etter, 1976).

1. Topotaxy is a reaction constant unique to the chemistry and crystallography of the transformation.
2. Isomorphism between reactant and product phases is not a necessary criterion for topotaxy.
3. Both bimolecular and unimolecular reactions can give oriented crystalline products.
4. Multiple reaction products can be simultaneously ordered by the reactant lattice.
5. The symmetry directions of the reactant lattice are not necessarily parallel to the product lattice.
6. When the reactant and product lattice symmetry directions are not parallel, twinning of the product phase will occur such that the reactant point-group symmetry is conserved.

These principles provide the basis for understanding yet-to-be-discovered examples of topotactic reactions of drugs.

## D. POLYMORPHIC TRANSFORMATIONS

Polymorphism is the crystallization of the same compound in different crystal forms, in different crystal packing arrangements. Since polymorphs contain molecules with the same molecular structure, polymorphic transformations do not involve a molecular change. Polymorphs can also form solid solutions. Polymorphic transformations thus involve three steps: molecular loosening, solid solution formation, and separation of product.

The molecular-loosening step requires the nucleation of reaction. During this step, the molecules partially unpack from the original crystal lattice. This can in some cases be initiated by a pin-prick or other mechanical deformation. For example, Kitaigorodskii *et al.* (1965) showed that a pin-prick can initiate the transformation of $\alpha$-*p*-dichlorobenzene to $\beta$-*p*-dichlorobenzene. The transformation of $\alpha$- to $\beta$-*p*-dichlorobenzene is delineated by the spread of the reaction front from the nucleation site through the crystal.

A related process is the thermally induced rearrangement of the $\alpha$ to $\beta$ form of *p*-nitrophenol (Coppens and Schmidt, 1965). In this reaction, needle-shaped single crystals rearrange, with the phase boundary moving approximately perpendicular to the needle axis.

Separation of the product phase involves crystallization of the new crystal form. The product appears as microcrystallites with little or no net orientation relative to the starting crystal. This is in contrast to *p*-dichlorobenzene, where the product is a single crystal.

## E. DESOLVATION REACTIONS

Desolvation is related to polymorphic transformation, however the solvent exits the crystal. For polymorphic solvates, the product crystal separates into a new crystal form. For pseudopolymorphic solvates, loss of solvent does not lead to the formation of a new polymorph.

The desolvation of polymorphic solvates involves four steps:

1. Molecular loosening.
2. Breaking of the host–solvent hydrogen bonds (or other associations).
3. Solid solution formation.
4. Separation of the product phase.

The molecular-loosening step involves nucleation and loosening of the crystal packing so that the solvent can escape. Then the forces that hold the solvent to the host molecules in the crystal are broken. Usually this is the breaking of hydrogen bonds. The solvent then exits the crystal and the product separates. Extensive studies in our laboratory show that this reaction is quite similar in mechanism to other solid–state reactions.

Desolvation of pseudopolymorphic solvates involves two steps: (*a*) molecular loosening and (*b*) breaking of host–solvent hydrogen bonds or associations.

## F. CHEMICAL REACTIONS

It is important to realize that many solid-state reactions of drugs involve drug degradation. These reactions are of interest because of a desire

to prevent such degradation. Therefore in many respects the solid-state chemistry of drugs is synonymous with drug degradation.

Drug degradation has been studied mostly on the macroscopic level. In fact, few studies aimed at determining the molecular aspects of the solid-state chemistry of drugs have been published. Even for such common drugs as vitamin $D_2$ and vitamin A, only the structures of a few of the degradation products have been published.

Table III summarizes some of the solid-state chemical reactions of drugs, and is arranged according to the chemical reaction involved. Only solid-state reactions in which the chemical structure of the product(s) is known are included. The classification scheme used in this table is used throughout this book, and each class of reaction is treated in a separate chapter or chapters.

## IV. Stability Testing

One of the practical areas encompassed by the field of solid-state chemistry of drugs is the area of stability testing. Stability tests are conducted on all marketed drugs in order to determine an expiration date after which the drug will not be sold.

Companies are required to ensure that the drugs distributed and marketed are of the best possible quality. However, because the phrase "best possible quality" is vague the government has attempted to define this idea in terms of good manufacturing practices. The most recent good manufacturing practices were published in the "Federal Register" on September 29, 1978. They require, among other things, that

1. Essentially all products must bear an expiration date.
2. All products bearing this date must describe the storage conditions under which this date applies.
3. The stability-testing program must be defined in writing.

An expiration date is required in hopes of assuring that drug products have the identity, purity, structure, and quality described on the label and package insert during their period of use. Obviously the expiration date is only for the storage conditions described. If the product is subjected to extremes, such as higher temperatures than those described, then the actual expiration date will be sooner than the expiration date on the label.

Generally, stability studies and expiration dates should be determined under conditions approximating normal storage conditions rather than under accelerated conditions. However, accelerated stability tests can be very important since they can be used to determine the best storage conditions. Using accelerated tests, a number of storage conditions can be

**TABLE III.**

*Solid-State Chemistry of Drugs*

I. Solid–Gas Reactions

A. Solid-state oxidations (Chapter 6)

1. Vitamin $D_2$

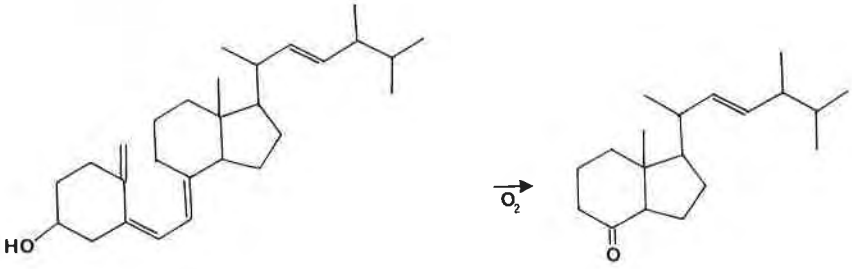


2. Hydrocortisone *tert*-butylacetate

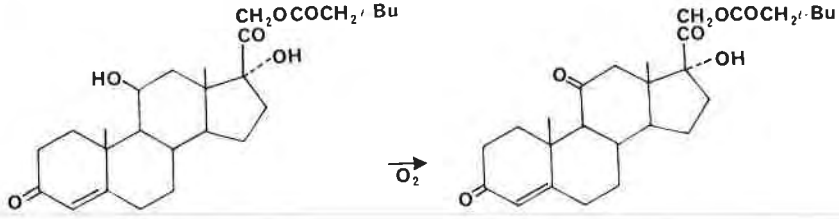


3. Dihydrophenylalanine

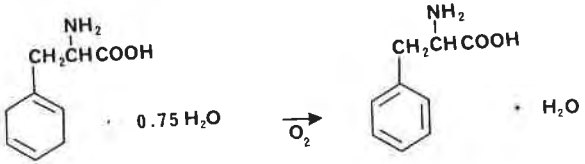


4. Dialuric acid

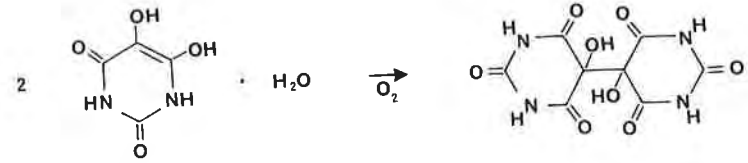


5. Vitamin C

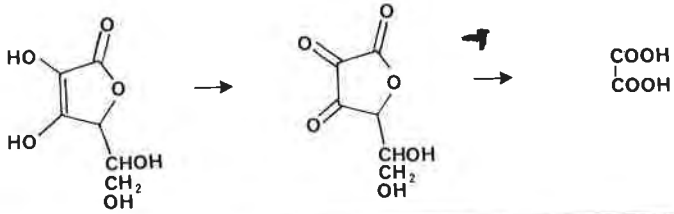

**TABLE III.** (*continued*)

6. Reserpine

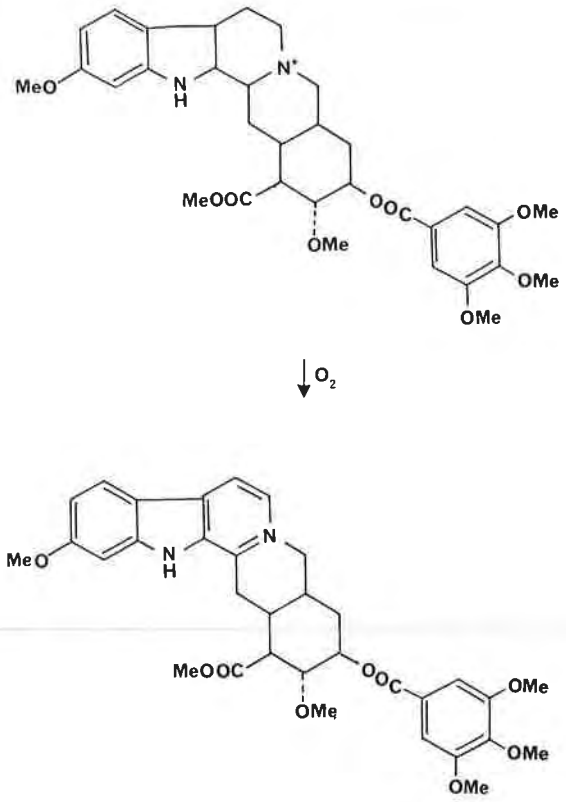


7. Phorbol esters

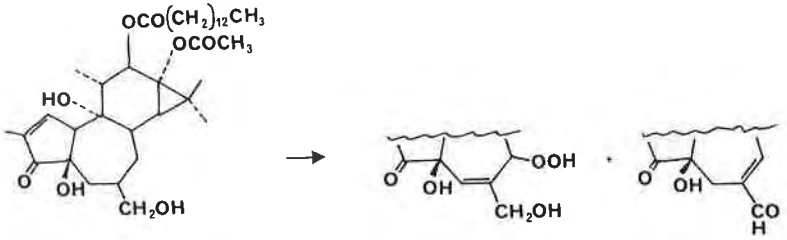


B. Additions of gases to solids—solid-state hydrolyses (Chapter 7)

1. Aspirin

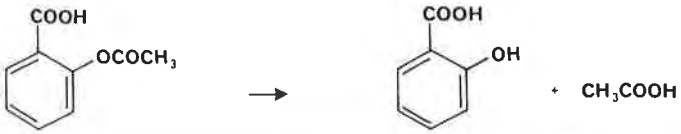

**TABLE III.** (*continued*)

2. Nitrazepam

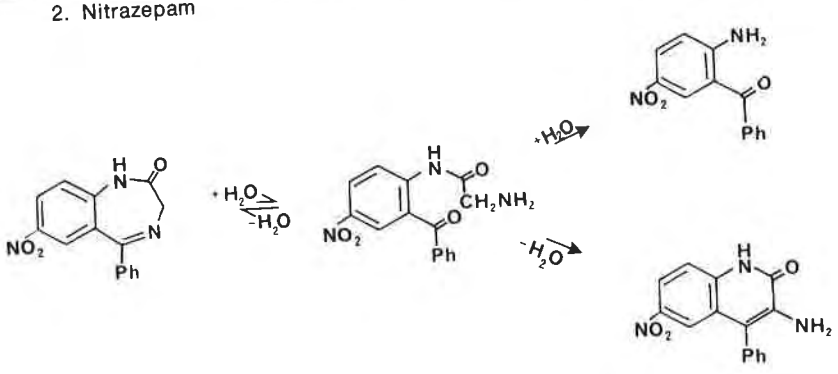

C. Solid-state decomposition reactions of the type A(solid) → B(solid) + C(gas) (Chapter 8)

1. Dehydration of Tetracyclines

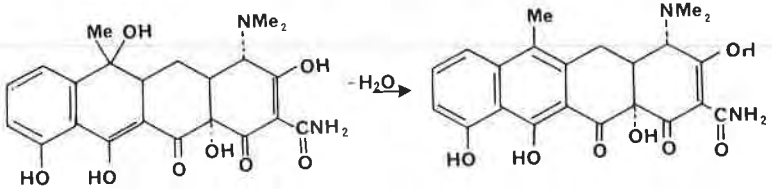

2. Dehydrochlorinations of aminosalicylic acid hydrochlorides

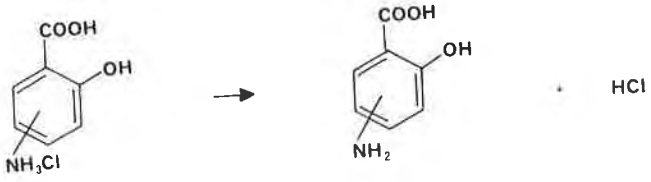

3. Dehydrochlorination of caffeine hydrochloride

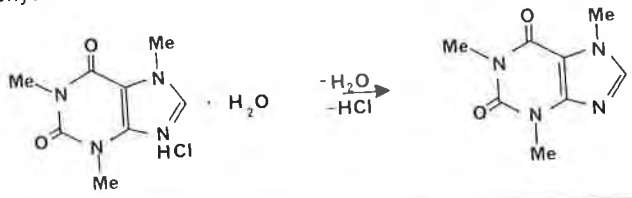

**TABLE III.** (*continued*)

4. Decarboxylation of *p*-aminosalicylic acid

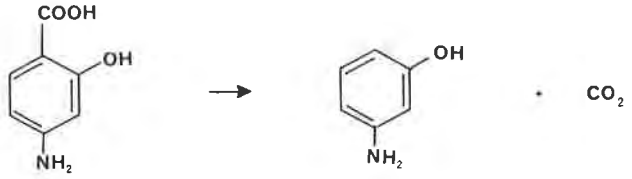


D. Solid-state photochemical reactions (Chapter 9)

1. Gibberellins

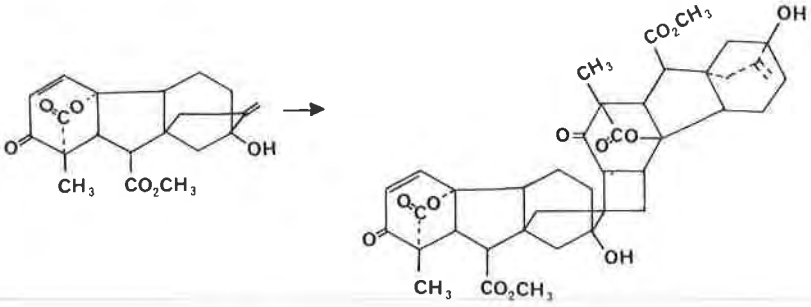


2. Dieldrin

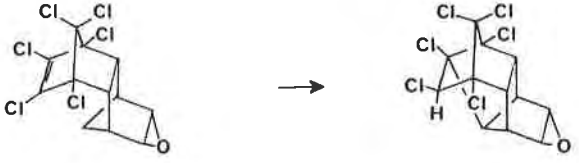


E. Solid-state thermal reactions (Chapter 10)

1. Rearrangement of aspirin anhydride

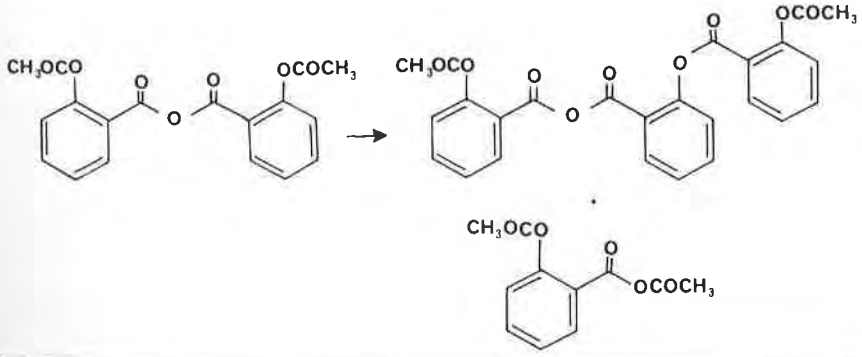

**TABLE III.** (*continued*)

2. Rearrangement of the methyl ester of tetraglycine.

3. Rearrangement of a triazenoimidazole

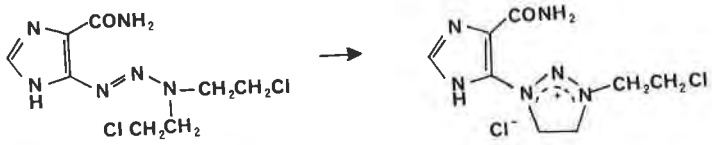

F. Solid–solid reactions (Chapter 11)

1. Reaction of *p*-aminosalicylic acid hydrochloride with sodium carbonate

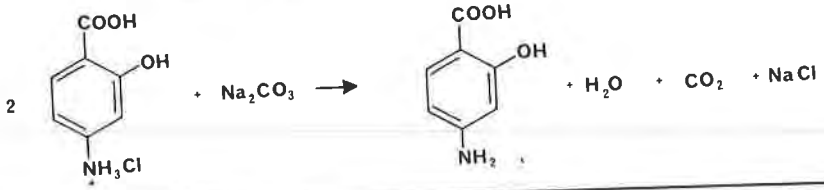

screened rapidly. In addition, knowledge from studies of the mechanisms of degradation of solid drugs can also speed up the determination of the best storage conditions and lead to a more rational approach to discovery of the best method for stabilizing the drug.

For accelerated stability tests, each crystalline form and habit of the pure solid and solid–solid mixtures of the pure solid with excipients and adjuncts should be maintained at approximately 70°C in vials or ampules under the following conditions: inert atmosphere, exposed to air, and exposed to increased humidity. One ampule or vial should be assayed each day using the most sensitive method available. The experiment should be run for at least 2 weeks, and the data should be used to determine the rate of decomposition at 70°C. The rate is conveniently determined using the computer program described in Chapter 3. It should be noted that if 70°C is too close to the melting point of the solid, liquid could form after only a few percent decomposition due to lowering of the melting point by the decomposition products. Under these circumstances, it is probably best to lower the temperature to 50°C and carry out the study for longer times, because solution reactions are often faster than reactions in the solid state.

The activation energy is also of interest. For determination of the activation energy, the kinetics (percentage of decomposition versus time) of the solid-state reactions are determined at several temperatures (at least three). However, the kinetics of solid-state reactions are often much more complicated than in the corresponding solution reactions. Solid-state reactions are usually not clearly zero-order, first-order, etc., but are often of fractional orders. Thus determination of the rate constant at different temperatures is difficult, if not impossible. In addition, because of the slowness of many solid-state reactions, rate studies are usually only carried through one or two half-lives. For this reason, Carstensen (1974) suggests that first-order or zero-order kinetics should be assumed for determination of the activation energy. Thus the rates of decomposition are measured at several temperatures and plotted according to zero-order and first-order kinetics. The equation that gives the best fit by statistical tests is then assumed to give the best rate constants. An attractive alternative approach is the application of the computer program discussed in Chapter 3 to the data.

The rate constants ($k$) are then plotted versus temperature ($T$) according to the Arrhenius equation

$$k = Ae^{-E_a/RT} \qquad (R \text{ is the gas constant})$$

From this plot, $A$ (the preexponential factor) and $E_a$ (the activation energy) are determined and used to determine the rate constant ($k$) at the labeled storage conditions. This rate constant is then used to estimate the expiration date.

The reactivity of the compound in solution at elevated temperatures should also be determined. It should be noted again that solution degradations are usually faster than solid-state degradations.

The stability of the drug in light is also usually determined. Each crystalline form and habit of the pure solid and mixtures with adjuncts and excipients is exposed to light in a light cabinet under the following conditions: inert atmosphere, exposed to air, and exposed to increased humidity. These latter studies can conveniently be done using a glove bag. Samples are assayed each day using the most sensitive method available.

The container in which the drug has the greatest stability is selected. The best container is determined by measuring the rate of degradation of the drug in various containers under various storage conditions. Obviously, the container and storage conditions in which the rate of decomposition is slowest should be chosen.

Once the rate constant is determined and the expiration date and shelf life established, the shelf life is often extended by including a so-called excess. The "United States Pharmacopeia" requires that a tablet or other

dosage form contain between 90 and 110% of the labeled amount. The expiration date is the date when the amount will drop below 90% of the labeled amount. The expiration date can be lengthened by including 110% of the labeled amount in the dosage form. The excess over labeled amount is also sometimes called an *overage*. Overages may not always be cost-effective, since if very stable and very expensive drugs are being marketed the savings in increasing the shelf life may not be offset by the cost of the overage.

It is important to realize that stability testing does not require an understanding of the molecular details of the reaction. Instead, it requires a good analytical method to follow drug degradation and controlled conditions. An understanding of the molecular details of a solid-state reaction requires a much more extensive study of the process.

## V. Summary

This chapter summarizes the scope of the area of solid-state chemistry of drugs. It is clear that this is a broad, relatively unexplored area involving an understanding of crystallization, the properties of crystals, the forces holding crystals together, the properties of other solids (i.e., amorphous solids), the chemical reaction involved, the criteria for solid-state reactions, the kinetics of solid-state reactions, and the broad field of stability testing.

There is a need to develop an understanding of solid-state reactions of drugs in terms of the molecular details of reactions. Of particular interest is a determination of the molecular parameters that can lead to retardation of the solid-state reactions of drugs and thus render drugs more stable.

It is the aim of the rest of this book to further illustrate the importance and value of molecular understanding of solid-state reactions.

## References

Bernstein, J., and Hagler, A. T. (1978). *J. Am. Chem. Soc.* **100,** 673.
Carstensen, J. (1974). *J. Pharm. Sci.* **63,** 1.
Cohen, M. D. (1975). *Angew. Chem. Int. Ed.* **14,** 386.
Cohen, M. D., and Cohen, R. (1976). *J. Chem. Soc., Perkin Trans. 2,* 1731.
Cohen, M. D., Cohen, R., Lahav, M., and Nie, P. L. (1973). *J. Chem. Soc., Perkin Trans. 2,* 1095.
Coppens, P., and Schmidt, G. M. J. (1965). *Acta Cryst.* **18,** 62, 654.
Etter, M. C. (1976). *J. Am. Chem. Soc.* **98,** 5326.
Haleblian, J. K., Koda, R. T., and Biles, J. A. (1971). *J. Pharm. Sci.* **60,** 1485.

Haleblian, J. (1975). *J. Pharm. Sci.*, **64,** 1269.
Hung, J. D., Lahav, M., Luwisch, M., and Schmidt, G. M. J. (1972). *Isr. J. Chem.* **10,** 585.
Kimura, T., and Hashimoto, S. (1960). *Jap. Patent* **60,** 5798.
Kitaigorodskii, A. I. (1961). Organic Chemical Crystallography. Consultants Bureau, New York.
Kitaigorodskii, A. I., Mnyukh, Y. V., and Asadov, Y. G. (1965). *J. Phys. Chem. Solids* **26,** 463.
Morawetz, H. (1966). *Science,* **152,** 705.
Paul, I. C., and Curtin, D. Y. (1973). *Acc. Chem. Res.* **7,** 223.
Pfeiffer, R. R., Yang, K. S., and Tucker, M. J. (1970). *J. Pharm. Sci.* **59,** 1809.
Pikal, M. J., Lukes, A. L., and Lang, J. E. (1977). *J. Pharm. Sci.* **66,** 1312.
Schmidt, G. M. J. (1964). *J. Chem. Soc.*, 2014.
Schmidt, G. M. J. (1971). *Pure Appl. Chem.* **27,** 647.
Sukenik, C. N., Bonapace, J. A. P., Mandel, N. S., Lau, P. Y., Wood, G., and Bergman, R. G. (1977). *J. Am. Chem. Soc.* **99,** 851.
United States Pharmacopeia, XX(1980), U.S. Pharmacopeial Convention, Inc., Rockville, Md. 20852.

# 2 Methods of Analysis

In this chapter, methods of analyzing solids and methods of studying the solid state chemistry of drugs are outlined. The aim of this chapter is to give an idea of the variety of methods available for the study of the solid-state chemistry of drugs. An example of each method from the field of solid-state chemistry is included when possible.

## I. X-Ray Crystallography

X-Ray crystallography is a powerful tool for the investigation of crystalline solids. In the most favorable cases, it can lead to a complete determination of the structure of the solid and the determination of the packing relationship between individual molecules in the solid. This knowledge is often crucial to understanding solid-state chemistry of drugs.

In some respects, x-ray crystallography is analogous to light microscopy. Light microscopy provides an image of objects visible or nearly visible to the naked eye, and x-ray crystallography provides an image of objects of atomic dimensions, which are not visible by light microscopy. While in light microscopy the image is focused with lenses, in x-ray crystallography the atomic image is determined using a Fourier synthesis

(normally calculated on a computer) of the diffracted radiation. This analogy should be helpful to the reader to whom x-ray crystallography is new.

In this section, we provide an overview of crystals and x-ray crystallography. The interested reader should consult one of the books in this area (Glusker and Trueblood, 1972; Stout and Jensen, 1968) for more details.

## A. CRYSTALS

Crystals contain highly ordered arrays of molecules and atoms. This internal ordering is a fundamental characteristic of crystalline solids and is manifested in the external shapes of crystals. Crystals have sharp edges with well-defined angles between these edges. However, because an object contains sharp edges does not mean it is crystalline: i.e., a window pane is not a crystalline solid but rather a glass, since the atoms are not ordered. The fact that crystals are ordered is experimentally demonstrated by showing that a crystal can act as a three-dimensional diffraction grating for x-rays that have a wavelength comparable to the interatomic distances.

Crystals are built up by the repetition of a three-dimensinal structural unit. This unit is best viewed as a parallelepiped that, when repeated in three dimensions, forms the crystal. This parallelepiped is called the *unit cell*. Sometimes it is also convenient to view the unit cell as a point or points and the crystal as a three dimensional array of these points. Such an array is called the *crystal lattice*.

For all crystals there are seven conventional unit cells: triclinic, monoclinic, orthorhombic, tetragonal, hexagonal, rhombohedral, and cubic. However, for drugs only three of these are common: triclinic, monoclinic, and orthorhombic. (Figure 1). The triclinic unit cell has $a \neq b \neq c$ and $\alpha \neq \beta \neq \gamma \neq 90°$. For the monoclinic unit cell $a \neq b \neq c$ and $\alpha = \gamma = 90°$, $\beta \neq 90$; for orthorhombic unit cell $a \neq b \neq c$, $\alpha = \beta = \gamma = 90°$.

Figure 2 shows a crystal, in two dimensions, formed by orthorhombic unit cells. By inspection, the angles between the faces of the crystal are obviously related to the dimensions of the unit cell, $a$ and $b$. The faces labeled (010) and $(0\bar{1}0)$ are parallel to the $a$ axis and intersect the $b$ axis. The faces labeled (110), $(1\bar{1}0)$, $(\bar{1}\bar{1}0)$, and $(\bar{1}10)$ interesect both the $a$ and $b$axis at 1 unit vector from the origin. The angle between the faces labeled (010) and (110) is dependent on the length of $a$ and $b$. If $a = b$, then this angle is 45°.

The numbers used to label the faces are termed Miller indices. The plane with Miller indices $h, k, l$ makes intercepts $a/h$, $b/k$, and $c/l$ with the unit cell axes $a$, $b$, $c$. Thus the (010) face has Miller indices 0,1,0 and interesects the $a$, $b$, and $c$ axes at $\infty$, 1, $\infty$. Similarly, the (110) plane interesects the $a$, $b$, and $c$ axes at 1, 1, $\infty$.

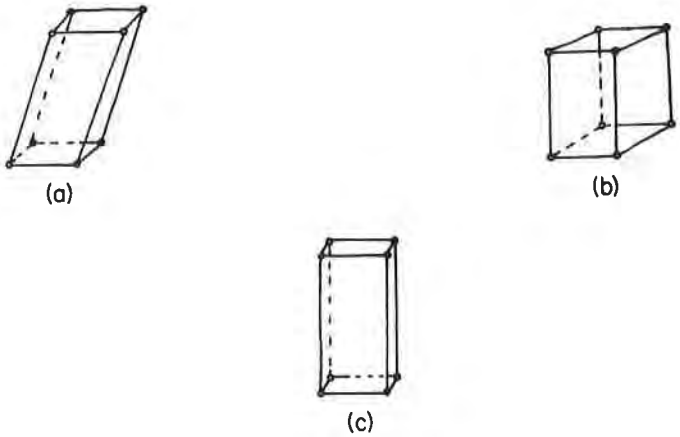


**FIGURE 1.** The most common unit cells for crystals of drugs: (*a*) triclinic—all sides of different lengths, no angles equal to 90°; (*b*) monoclinic—all sides of different lengths, two angles equal to 90°; (*c*) orthorhombic—all sides of different lengths, all angles equal to 90°.

The "law of rational indices" states that the crystal faces have Miller indices that are small whole numbers.

The law of rational indices along with the definition of the Miller indices clearly allows one to orient the unit cell relative to the external shape of the crystal. By definition, the crystal structure locates the atoms relative to the unit cell. A knowledge of the crystal structure and the Miller indices of the crystal faces thus allows one to visualize the atoms in the crystal.

At this point it should be noted that a given unit cell can be arranged in different ways in order to produce crystals with different external shapes but the same internal structure. This is shown in Figure 3.

Crystals that have the same internal structure but different external shapes are called crystal habits.

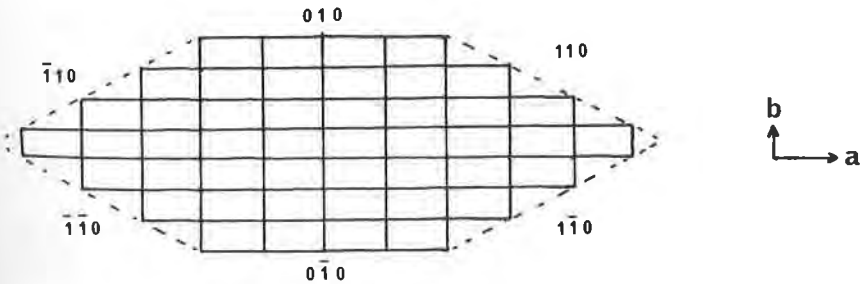


**FIGURE 2.** A schematic view of a crystal built up from two-dimensional unit cells with axial lengths *a* and *b*.

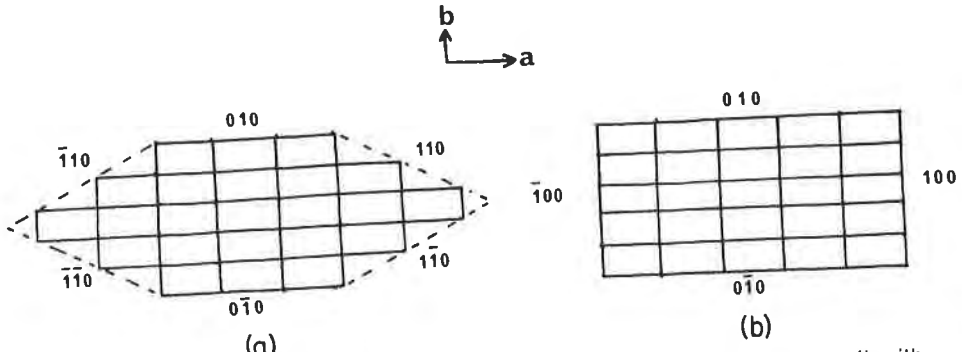


**FIGURE 3.** Two crystals composed of the same two-dimensional unit cell with lengths *a* and *b* but with different external shapes. (*a*) Habit yields pointed crystals. (*b*) Habit yields rectangular crystals.

## B. DETERMINATION OF THE CRYSTAL STRUCTURE

### *1. Diffraction of X-Rays*

X-Rays are scattered by objects in the same way that visible light is scattered. However, there are no known lenses that focus x-rays, so that the determination of the image of the object is not directly possible.

The pattern of scattered radiation is called the diffraction pattern and was first interpreted by Bragg. Bragg showed that the distribution of scattered radiation could be understood by considering that the diffracted beams behave as if they were reflected from planes passing through the crystal lattice. Figure 4 schematically shows x-rays diffracted from a crystal lattice. If the diffracted radiation is viewed as a wave, then the two rays A and B will reinforce each other only if their path lengths differ by one wavelength ($\lambda$).

$$n\lambda = 2d \sin \theta$$

This equation is the Bragg equation and states that an integer times the wavelength ($\lambda$) must equal twice the distance ($d$) between planes times the sine of the angle of incidence. Thus for a single crystal and monochromatic x-rays, diffraction maxima will only be observed for certain values of the angle of incidence ($\theta$). If the crystal is rotated in the x-ray beam, diffraction will occur only at certain rotation angles. The Bragg equation does not determine the intensity of the diffracted radiation. This is determined by the electron density of the atoms in the plane causing the diffraction.

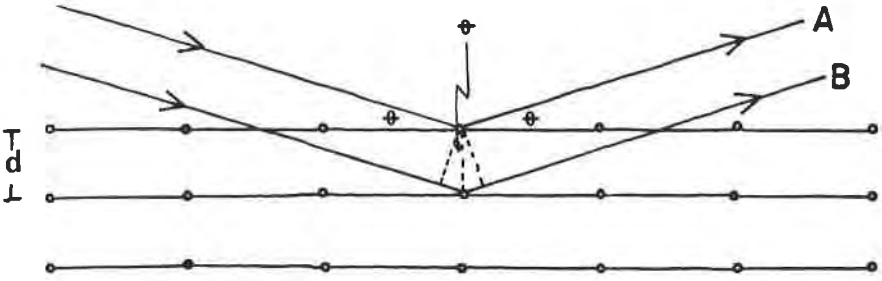


**FIGURE 4.** X-Rays diffracted from a crystal lattice with spacing $d$ between the planes and a diffraction angle of $\theta$.

### *2. Experimental Measurements*

The determination of the crystal structure requires the determination of the unit-cell dimensions and the intensities of a large fraction of the diffracted beams from the crystal.

The first step is selection of a suitable crystal. Crystals should be examined under a microscope and separated into groups according to external morphology or crystal habit. For a complete study, each crystal of a completely different external morphology should be examined.

Once the crystals have been separated according to shape, the best crystal of the first group should be mounted on a goniometer head with an adhesive such as glue (Figure 5).

The unit-cell dimensions are then determined by photographing the mounted crystal on either a Weissenberg or precession camera. Figure 6 shows a precession camera, and Figure 7 shows a precession photograph.

The unit-cell parameters are determined from the precession photograph by measuring the distance between the rows and columns of spots and the angle between a given row and column. This is done for three different orientations of the crystal, thus allowing determination of $a,b,c,\alpha$, $\beta$, and $\gamma$.

The intensities of the diffracted radiation are most conveniently measured using an automated diffractometer, which is a computer-controlled device that automatically records the intensities and background intensities of the diffracted beams on a magnetic tape. In this device, the diffracted beam is intercepted by a detector, and the intensity is recorded electronically. Figure 8 shows an automated diffractometer.

### *3. Space Groups and Symmetry*

It is possible to determine the unit-cell type from the x-ray diffraction pattern of a crystal. In addition, the symmetry of this pattern can be used to determine the space group. There are 230 possible space groups that

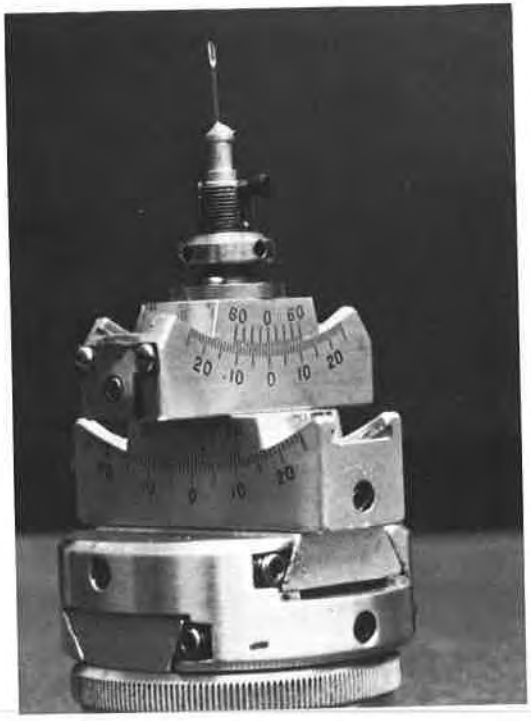

**FIGURE 5.** A goniometer head with a mounted crystal.

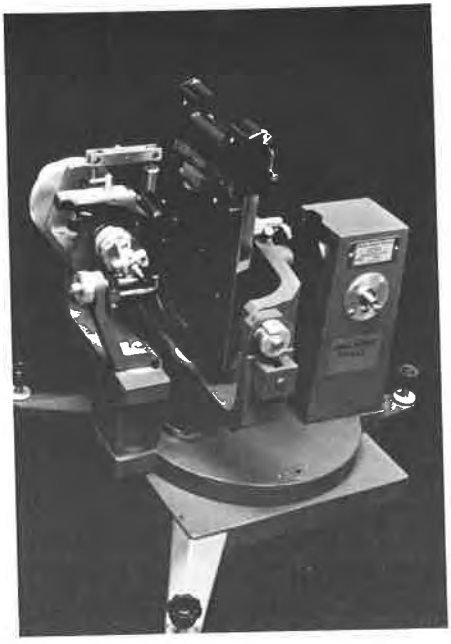

**FIGURE 6.** A precession camera.

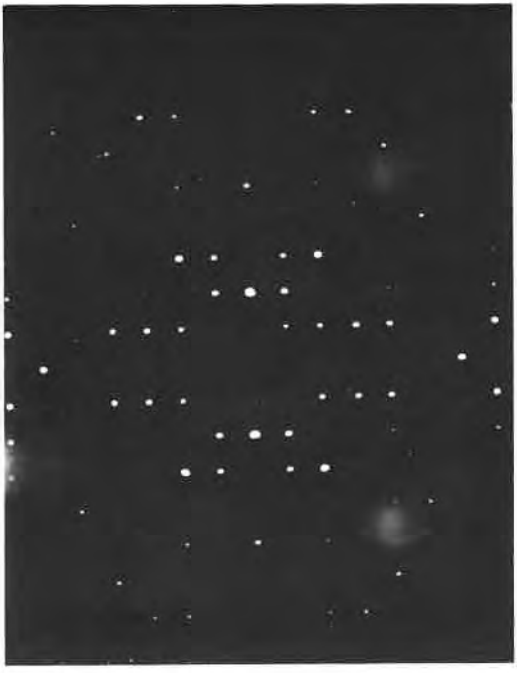

**FIGURE 7.** A precession photograph.

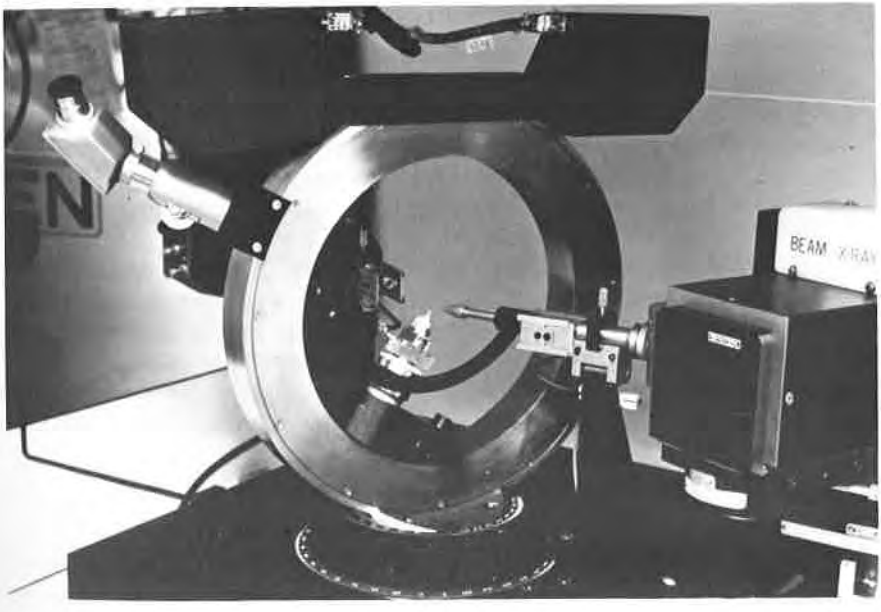


**FIGURE 8.** The chi circle of an automated x-ray diffractometer.

represent all of the distinct ways of arranging identical objects in one of the seven unit cells.

A knowledge of the space group can simplify the analysis of the diffraction pattern and may reveal an important symmetry element or elements within the unit cell. For example, a recent determination of a space group in our laboratory revealed that the synthetic procedure used to prepare the compound involved a racemization step, since the crystals belonged to a space group that required the presence of both *d* and *l* isomers.

The following symmetry elements are involved in defining the space group.

*Rotation axes.* When rotation of 360°/*n* results in the same structure, then the crystal contains an *n*-fold rotation axis. For crystals, *n* is restricted to 1, 2, 3, 4, and 6.

*Rotatory-inversion axes.* An *n*-fold rotatory-inversion axis exists when a rotation of 360°/*n* followed by inversion results in the same structure.

*Mirror planes.* A mirror plane exists when a reflection through that plane results in the same structure.

*Screw axes.* An *n*-fold screw axis exists when a rotation of 360°/*n* followed by a translation parallel to the axis of rotation brings the structure into coincidence.

*Glide planes.* A glide plane exists when reflection through a mirror plane followed by translation brings the structure into concidence.

All of the 230 possible space groups, their symmetries, and the symmetries of their diffraction patterns are compiled in "International Tables for X-Ray Crystallography."

### *4. Structure Determination*

The problem that must be solved to convert the experimentally determined intensities of the diffracted rays into a structure of the crystal is termed the *phase problem.*

The phase problem can best be understood in terms of equations. In order to convert the experimentally determined intensities into an image of the atoms in the unit cell one performs, by definition, a three-dimensional Fourier summation. This summation can be mathematically written as

$$\rho(xyz) = \frac{1}{V} \sum_h \sum_k \sum_l F(hkl) \exp[-2\pi i(hx + ky + lz)]$$

where $\rho$ is the electron density at point $x, y, z$; $V$ is the volume of the unit cell; $h$, $k$, and $l$ are the Miller indices; and $F(hkl)$ is the structure factor.

The structure factor depends on both the intensity and the phase of the diffracted radiation. While the intensities are easily determined, there is no experimental method to determine the phases. Thus the determination of crystal structures requires that a nonmeasurable quantity be determined. As might be expected, rather complex and elaborate methods have evolved for determining crystal structures.

The most widely used methods are the so-called direct methods along with the heavy-atom method and the isomorphous replacement method. The heavy-atom and isomorphous replacement methods will not be discussed here, because direct methods are normally used to determine the crystal structures of drugs. The heavy-atom method is used to determine the structures of inorganic and organic crystals containing heavy atoms (atoms with atomic weight $>17$). The isomorphous replacement method is used for the determination of the crystal structures of proteins.

The direct method is based on the fact that it is possible to derive relationships among the phases of different reflections. These relations predict the phases of these reflections and also provide a probability that the phase is correct. They are normally determined on a computer, and often several electron-density maps are calculated and inspected until the correct or most reasonable structure is found.

Once the atomic positions are determined from the electron-density maps, the structure is refined by least-squares minimization of the difference between the calculated intensities and the observed intensities. In this refinement, the atomic positions and the temperature factors are varied. As with the structure determination, the least-squares refinement is carried out on a high-speed computer.

The atomic positions obtained can then be used to construct drawings of the molecule and/or the contents of the unit cell or several unit cells. These drawings provide a visual picture of any unusual structural features of the molecule. In addition, drawings of the contents of several unit cells allow a visual examination of the intermolecular interactions among molecules in the crystal. These intermolecular interactions are often responsible for the solid-state chemistry of drugs.

#### *5. Determination of the Miller Indices of the Faces—Optical Goniometry*

The crystal structure describes the position of the atoms of the molecule relative to the unit cell. However, it is often important to know the relationship of the orientation of the unit cell relative to the faces of the crystal. Figure 3, shown earlier, describes two habits of the same crystal and shows how the unit cell is related to the faces of the crystal. For these

**FIGURE 9.** An optical goniometer.

two habits it is possible to determine the indices of the faces by inspection. For an unknown crystal, one must use the interfacial angles determined from optical goniometry and the law of rational indices to determine the Miller indices of the faces. Figure 9 shows an optical goniometer.

The typical optical goniometer consists of a light source, a crystal support system, a microscope/telescope for observing the crystal or reflected light, and two circles perpendicular to each other that allow observation of all faces of the crystal (other than those near the point of attachment). These two circles thus allow all faces to be set in a position in which their normals bisect the angle between the light source and the telescope. In such a position the crystal face reflects the light.

These reflections are then observed and the angle recorded. Usually a crystal 0.2 to 0.5 mm on a side is used for these measurements, although slightly smaller crystals can also be studied. The best approach to determination of the interfacial angles is to use the axes of the goniometer head to adjust the crystal so that a zone of faces is parallel to the spindle axis. For example, the crystal should be adjusted so that all of the faces on the sides of the crystal are in reflecting position as the crystal is rotated about the spindle axis. Then the angles between the faces in this zone are mea-

**FIGURE 10.** A crystal misaligned with respect to the spindle axis of an optical goniometer.

sured. Next, the angle between this zone and another zone is measured and the process repeated until all of the interfacial angles have been measured. This process is illustrated in Figures 10 and 11. The alignment of the crystal shown in Figure 10 is accomplished by adjusting the arcs until the situation in Figure 11 occurs.

Once all the interfacial angles are determined, the crystal is transferred to the precession camera and an x-ray photograph is taken with the x-rays normal to one of the faces. The photograph is examined to see whether it contains spots, which give cell parameters and symmetries corresponding to two of the unit-cell parameters. If this is so, then the face is parallel to these axes and thus perpendicular to the third axis (in the orthorhombic crystal system). Thus if the precession photograph contains the $a$ and $c$ axes, then the face is parallel to $a$ and $c$ and perpendicular to $b$ and has Miller indices 010. Once the indices of one of the faces are determined by this procedure, a trial-and-error procedure can be used to determine the indices of the other faces using the following formulas.

$$\begin{aligned}\cos\phi = (D_1)(D_2)[&(S_{11})(h_1)(h_2) + (S_{22})(k_1)(k_2) + (S_{33})(l_1)(l_2) \\ &+ S_{23}[(k_1)(l_2) + (k_2)(l_1)] + S_{13}[(l_1)(h_2) + (l_2)(h_1)] \\ &+ S_{12}[(h_1)(k_2) + (h_2)(k_1)]],\end{aligned}$$

where

$$D_1 = 1/[S_{11}(h_1)^2 + (S_{22})(k_1)^2 + (S_{33})(l_1)^2 + 2(S_{12})(h_1)(k_1) + 2(S_{23})(k_1)(l_1) + 2(S_{13})(h_1)(l_1)]^{-1/2}$$

$D_2$ = corresponding expression for $h_2$, $k_2$, $l_2$

$$S_{11} = (b)^2(c)^2(\sin\alpha)^2$$
$$S_{12} = (a)(b)(c)^2(\cos\alpha\ \cos\beta - \cos\gamma)$$
$$S_{13} = (a)(b)^2(c)(\cos\gamma\ \cos\alpha - \cos\beta)$$
$$S_{22} = (a)^2(c)^2(\sin\beta)^2$$
$$S_{23} = (a)^2(b)(c)(\cos\beta\ \cos\gamma - \cos\alpha)$$
$$S_{33} = (a)^2(b)^2(\sin\gamma)^2$$

In these expressions, $\phi$ is the interfacial angle, $h$, $k$, and $l$ are the Miller indices, and $a$, $b$, $c$, $\alpha$, $\beta$, $\gamma$ are the unit-cell parameters.

A knowledge of the Miller indices is also crucial for the construction of packing drawings, discussed next.

## C. CRYSTAL-PACKING DRAWINGS

Photomicrographic study of crystals sometimes shows that the crystal behaves anisotropically during a solid-state reaction. For example, during

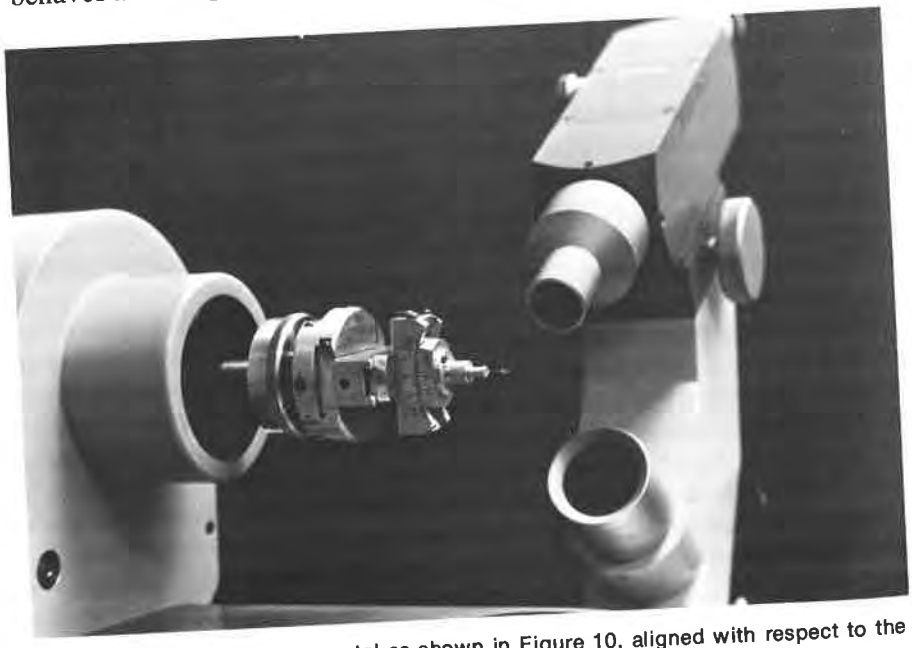

**FIGURE 11.** The same crystal as shown in Figure 10, aligned with respect to the spindle axis.

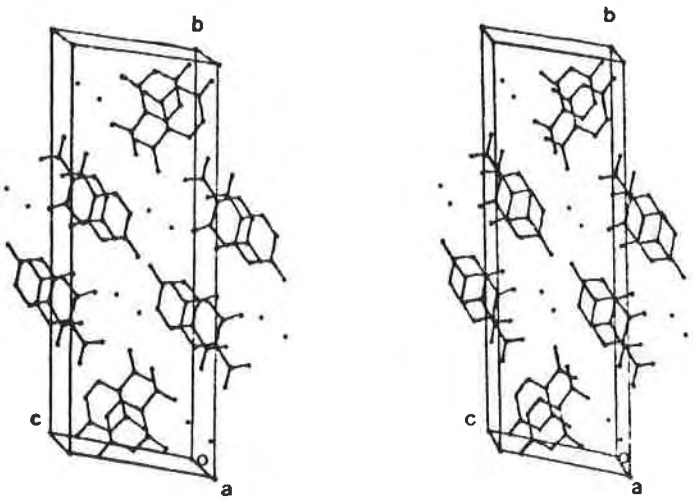


**FIGURE 12.** Stereoscopic packing drawing of 5-nitrouracil viewed down the *a* crystallographic axis.

desolvation some crystals show the anisotropic advancement of an opaque zone through the crystal (see Chapter 6).

When anisotropic behavior is observed, it is often useful to examine crystal-packing drawings viewed from a direction perpendicular to the faces of the crystal. Such drawings require a knowledge of the crystal structure and the Miller indices of the crystal faces. Since the crystal structure gives the location of the atoms relative to the unit cell and the Miller indices describe the orientation of the unit cell relative to the crystal faces, it is only a routine geometric problem to view the molecules from a direction perpendicular to any crystal face.

A crystal-packing drawing is thus constructed from a view perpendicular to all crystal faces, and attempts are made to explain the anisotropic behavior in terms of the crystal packing.

Figure 12 shows a crystal-packing drawing of 5-nitrouracil viewed perpendicular to the *bc* crystal plane.

## D. THE POWDER DIFFRACTION METHOD

In some cases it is necessary and helpful to determine the x-ray diffraction pattern of drug powders prepared by grinding the crystals with a mortar and pestle. This method is particularly useful for the study of solid-state reactions where a single crystal often reacts to give polycrystalline product.

The method that is usually used is called the Debye–Scherrer method (Shoemaker and Garland, 1962). The specimen is mounted on a fiber and placed in the Debye–Scherrer powder camera, shown in Figure 13. This camera consists of an incident-beam collimator, a beam stop, and a circular plate against which the film is placed. During the recording of the photograph, the specimen is rotated in the beam. Because the crystallites are randomly oriented, at any given Bragg angle a few particles will be in diffracting position and will produce a powder line whose intensity is related to the electron density in that set of planes.

This method, along with precession photography, can be used to determine whether a pair of crystals are polymorphs or crystal habits. To measure a powder pattern of a crystal or crystals on a Debye–Scherrer camera, one grinds the sample to a uniform size (200–300 mesh). The sample is then placed in a 0.1- to 0.5-mm-diameter glass capillary tube made of lead-free glass. Commercially made capillary tubes with flared ends are available for this purpose. The capillary tube is placed on a brass

**FIGURE 13.** A Debye–Scherrer powder camera.

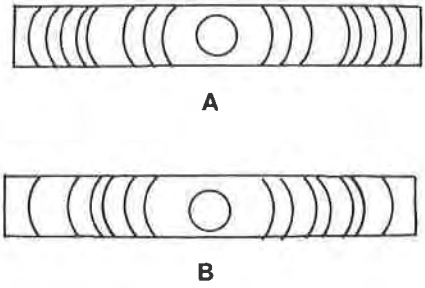


**FIGURE 14.** A schematic representation of the powder pattern of two polymorphs or hydrocortisone *tert*-butylacetate.

pin and inserted into the pin-holder in a cylindrical Debye–Scherrer powder camera. The capillary tube is aligned so that the powdered sample remains in the x-ray beam for a 360° rotation. Film is then placed in the camera, and the sample is exposed to $CuK_\alpha$ x-rays. The film is then developed and the pattern is compared to the pattern from other crystals of the same substance. If the patterns are identical the crystals have the same internal structure. If the patterns are different, then the crystals have a different internal structure and are polymorphs.

Figure 14 shows a schematic representation of the powder pattern of two polymorphs of hydrocortisone *tert*-butylacetate.

## II. Microscopy and Photomicrography

This method of analysis involves the observation of the behavior of a crystal on a microscope (Kuhuert-Brandstatter, 1971). Crystals are usually placed on a microscope slide and covered with a cover slip. However, sometimes a steel ring with input and output tubes is used to control the atmosphere.

The microscope slide is often placed on a "hot stage," a commercially available device for heating crystals while allowing observation with a microscope. The heating rate of crystals on a hot stage is usually constant and controlled with the help of a temperature programmer.

Crystals are often photographed during heating. Photography is helpful because for solid-state reactions taking weeks to complete it is sometimes difficult to remember the appearance of a crystal during the entire reaction. Obviously, photography permanently preserves the details of the reaction. A microscope equipped with a hot stage and a camera is shown in Figure 15.

The following types of behavior are of particular interest to the solid-state chemist:

1. The loss of solvent of crystallization, as shown in Chapter 6.
2. Sublimation of the crystal—the crystal slowly disappears and condenses on the cover slip.
3. Melting and resolidification, indicating a phase change (polymorphic transformation) or solid-state reaction.
4. Chemical reaction characterized by a visible change in the appearance of the crystal.

The detection of loss of solvent of crystallization and phase or polymorphic transformations is important to the solid-state chemist, since crystals exhibiting this behavior can have different reactivity and different bioavailability. Sublimation, while not a solid-state reaction, can cause confusion if one is unaware that it can occur. A chemical reaction is of particular interest to the solid-state chemist.

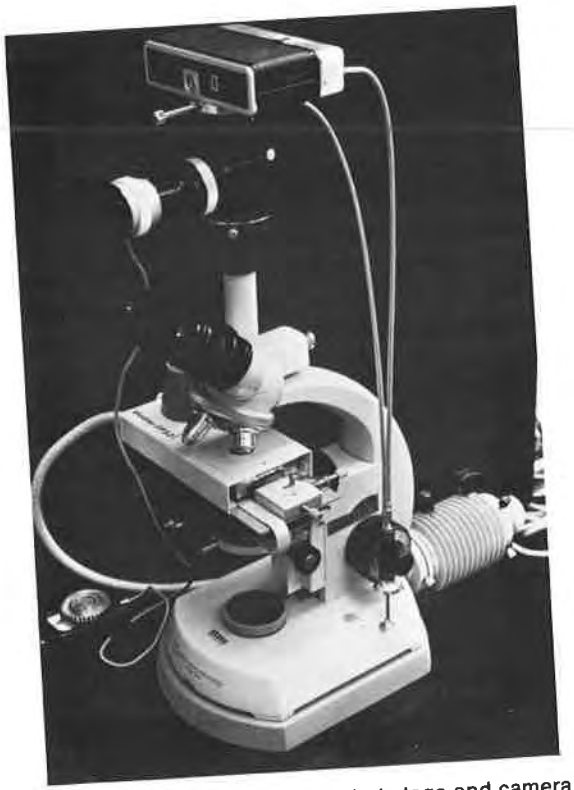

**FIGURE 15.** A microscope equipped with a hot stage and camera for photographing crystals during reaction.

## III. Thermal Methods of Analysis

*Thermal analysis* generally refers to any method involving heating the sample and measuring the change in some physical property. The most important thermal methods for the study of solid-state chemistry are thermogravimetric analysis (TGA) and differential thermal analysis (DTA). *Thermogravimetric analysis* involves measuring the change in the mass of the sample as the temperature is changed. *Differential thermal analysis* involves measuring the difference between the temperature of the sample and a reference compound as the temperature is changed, and provides information on the enthalpy change of various solid-state processes. Thermal methods of analysis are widely accepted analytical methods, and there are two journals devoted to publications in this area.

### A. THERMOGRAVIMETRIC ANALYSIS (TGA)

This method involves the measurement of the change in mass with temperature and is often used to study the loss of solvent of crystallization or other solid → solid + gas reactions. A typical TGA trace is shown in Figure 16.

In studies of solid-state chemistry, TGA is usually performed in one of two modes: isothermal or dynamic. In the isothermal mode the temperature is constant, while in the dynamic mode the temperature is raised at a constant rate.

There are a number of factors or conditions that affect TGA curves, including the heating, atmosphere, particle size of the sample, nature of the reaction, treatment of the sample, and thermal conductivity of the sample.

The affect of the heating rate has been extensively studied (Wendlandt, 1974). In general, as the heating rate is increased, the starting temperature

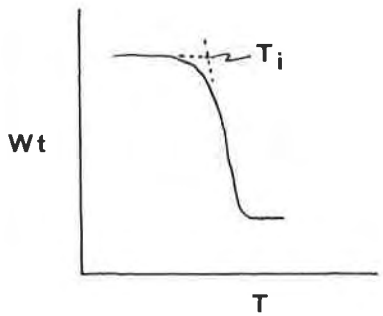


**FIGURE 16.** A typical TGA trace with $T_i$ (the transition temperature) marked. This is a trace for the dehydration of cytosine hydrate.

of the thermal event ($T_i$) increases. However, this condition can sometimes be corrected by decreasing the sample size.

The atmosphere can have a dramatic effect on the TGA curve. For example, an atmosphere containing the product gas can increase $T_i$ or stop the reaction completely. In addition, the atmosphere can change the course of the reaction, particularly if the atmospheric gas reacts with either the products or the reactant.

In general, the particle size of the sample has a predictable effect on the TGA curve. The smaller the particle size, the faster the reaction and the lower the value of $T_i$. This is because the smaller particle sizes have larger surface areas, and more rapid escape of the product gas is allowed.

Obviously, the nature of the reaction effects $T_i$. The $T_i$ will be lower for the more facile reactions. In addition, the treatment of the sample and in particular the extent of compression of the sample will obviously affect the $T_i$. For example, increased compression will increase $T_i$ since the product gas will have fewer opportunities to escape.

Finally, the thermal conductivity of the sample will influence $T_i$ and could lead to anomalous effects if the temperature of the sample is not uniform.

The rates of reactions of the type solid → solid + gas can be determined using TGA. Obviously, isothermal TGA traces can be used to determine the rate of the reaction and the rate law governing the reaction.

Dynamic TGA has also been used to determine the rates of solid → solid + gas reactions. However, in general, the kinetic data obtained should be substantiated by other data before it is considered absolutely correct. It should be noted that the use of dynamic TGA to study kinetics has been criticized.

Isothermal thermogravimetric analysis has been used extensively in our laboratory to study the desolvation of crystal solvates. Figure 16 shows the TGA trace for desolvation of crystals of cytosine hydrate.

## B. DIFFERENTIAL THERMAL ANALYSIS (DTA)

As mentioned, DTA is a method in which the temperature of the sample ($T_s$) is compared to the temperature of a reference compound ($T_r$) as a function of increasing temperature. Thus a DTA thermogram is a plot of $\Delta T = T_s - T_r$ (temperature difference) versus $T$. Figure 17 shows a schematic diagram of a DTA cell. Figure 18 shows an idealized DTA thermogram. The endotherms represent processes in which heat is absorbed, such as phase transitions and melting. The exotherms represent processes such as chemical reactions where heat is evolved. In addition, the area under a peak is proportional to the heat change involved. Thus

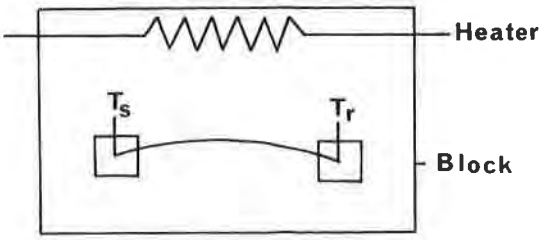


**FIGURE 17.** A schematic diagram of a DTA cell.

this method with proper calibration can be used to determine the heats ($\Delta H$) of the various processes. the temperatures of processes such as melting, $T_m$, can be used as an accurate measure of the melting point.

There are a number of factors that can affect the DTA curve, including heating rate, atmosphere, the sample holder and thermocouple location, and the particle size and sample packing. In general, the greater the heating rate the greater the transition temperature (i.e., $T_m$). An increased heating rate also usually causes the endotherms and exotherms to become sharper. The atmosphere of the sample affects the DTA curve in much the same way it affects the TGA curve. If the atmosphere is one of the reaction products, then increases in its partial pressure would slow down the reaction. The shape of the sample holder and the thermocouple locations can also affect the DTA trace. Thus it is a good idea to only compare data measured under nearly identical conditions. As with TGA, the particle size and packing of the sample has an important influence on all reactions of the type solid → solid + gas. In such reactions, increased particle size (thus decreased surface area) usually decreases the rate of the reaction and increases the transition temperature.

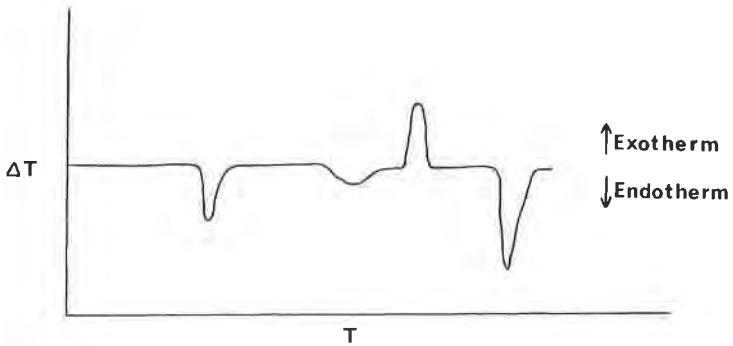


**FIGURE 18.** A DTA thermogram showing the changes that occur upon heating the compound H1.

DTA has been used to study the kinetics of solid-state reactions but, like the TGA methods, this approach has been criticized and results of kinetic studies by DTA should probably be checked by other methods before they are considered reliable.

An important branch of differential thermal analysis is differential scanning calorimetry (DSC). *Differential Scanning Calorimetry* refers to a method very similar to DTA in which the $\Delta H$ of the reactions and phase transformations can be accurately measured. A DSC trace looks very similar to a DTA trace, and in a DSC trace the area under the curve is directly proportional to the enthalpy change. Thus this method can be used to determine the enthalpies of various processes.

Figure 18 shows the usefulness of DTA in the study of solid-state chemical reactions. In this particular example, the thermogram shows an initial endotherm at about 124°C associated with partial melting of H1. This changes suddenly to an exotherm, which corresponds to reaction to form a mixture of H2 and H3. The second broad exotherm corresponds to conversion of the remaining H2 to H3. The final endotherm corresponds to melting (Curtin *et al.*, 1969).

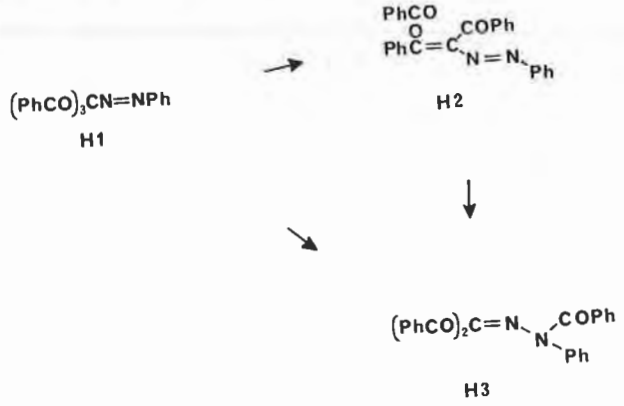


## IV. Electron Microscopy

Electron microscopy is a powerful tool for studying the surface properties of crystals. High-resolution election microscopy can be used to visualize lattice fringes in inorganic compounds, but its usefulness for visualization of lattice fringes in organic compounds is so far unproven. Nevertheless, electron micrographs of organic crystals allow the examination of the crystal surface during reaction. Electron microscopy is par-

ticularly useful for studying the affects of structural imperfections and dislocations on solid-state organic reactions. For example, the surface photooxidation of anthracene is obvious from electron micrographs taken at a magnification of 10,000 (Thomas, 1974). Even more interesting is the use of electron microscopy, sometimes in conjunction with optical microscopy, to study the effects of dislocations and various kinds of defects on the nucleation of product phase during a solid state reaction.

Electron microscopy is also quite useful for the studies of the effect of crystal size on desolvation reactions. Electron micrographs have significantly more depth of field than optical micrographs, so that the average crystal size can be more easily determined using them.

## V. Infrared Spectroscopy of Solids

Infrared spectroscopy is a quite useful method for the analysis of solids since it can be performed without dissolution of the sample. The method involves grinding the sample and suspending it in Nujol or grinding the sample with KBr and pressing this mixture into a disc. This preparation is then placed in the sample beam and the spectrum is recorded.

The infrared spectrum is extremely sensitive to the structure and conformation of the compound and thus can be used to compare the structure and conformation of the compound in different solids or in solid and solution.

Curtin and Byrn (1969) used infrared spectroscopy to investigate the hydrogen bonding in the yellow and white crystals of dimethyl 3,6-dichloro-2,5-dihydroxyterephthalate (**1**, **2**). The yellow crystals (Y1)

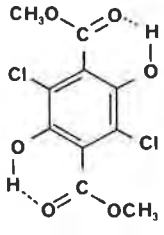

Y1

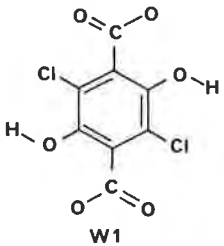

W1

showed a C=O stretching frequency at 1680 $cm^{-1}$, indicating OH···O=C hydrogen bonding, while the white crystals (W1) showed a carbonyl stretch at 1720 $cm^{-1}$, which indicates little or no OH···O=C hydrogen bonding. Subsequent single crystal x-ray studies showed that crystals of Y1 had strong intramolecular hydrogen bonds while crystals of W1 had

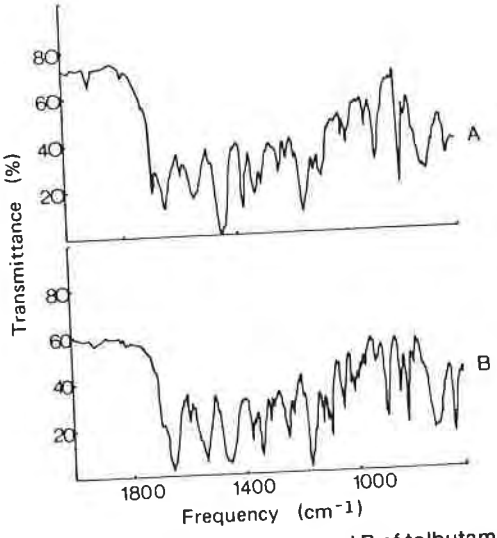


**FIGURE 19.** Infrared spectra of polymorphs A and B of tolbutamide (Simmons *et al.*, 1972).

weak intermolecular hydrogen bonds. These experiments clearly show the usefulness of infrared spectroscopy for studies of hydrogen bonding.

Infrared spectroscopy is also useful for the investigation of polymorphs of some drugs in the solid state. For example, polymorphs A and B of tolbutamide (3) give different infrared spectra (Simmons *et al.*, 1972).

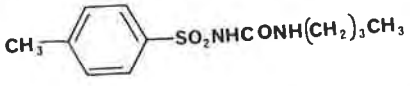


3

These spectra are shown in Figure 19. It is clear from this figure that there are significant differences between the spectra of the polymorphs. Unfortunately, it is not clear whether these differences in spectra are due to different crystal packing or to the presence of different conformers in polymorphs A and B.

## VI. Analytical Methods Requiring Dissolution of the Sample

While in some cases it is necessary to analyze the products of a solid-state reaction in the solid without dissolution, many of the most popular analytical methods of analysis require dissolution of the sample. These

methods are useful for solid-state reactions if the reactants and products are stable in solution. For example, for solid-state reactions induced by heat or light, it is convenient to remove the heat or light, dissolve the sample, and analyze the products. In this section several important methods are reviewed and examples of their use in solid-state chemistry is discussed.

## A. ULTRAVIOLET SPECTROSCOPY

Ultraviolet spectroscopy is very useful for studying the rates of solid-state reactions. Such studies require that the amount of reactant or product be measured quantitatively. Quantitative analysis by ultraviolet spectroscopy is based on Beer's law, $A = \epsilon bc$, where $A$ is the absorbance, $\epsilon$ the molar extinction coefficient, $b$ the cell pathlength, and $c$ the molar concentration. This equation predicts that a plot of absorption versus concentration will give a straight line. Usually a concentration range can be found where this equation holds; however, several factors can cause deviations from this law. The most common reasons for deviation from Beer's law are (*a*) effects resulting from too wide a spectral band width in the spectrometer, (*b*) effects resulting from stray light, and (*c*) effects occurring at very high concentrations.

However, assuming that a concentration range where Beer's law holds can be found, this method is quite useful for measuring the concentrations of reactant and product. In this procedure, a plot of absorbance versus concentration is made. It is generally best to choose a wavelength for this graph to give a line with the largest slope. This wavelength, in the absence of other interfering conditions, is the wavelength of maximum absorbance. The plot, which is often termed a calibration curve, is then used to determine the concentrations of the unknown.

The limit of detection using ultraviolet spectroscopy depends upon the value of $\epsilon$, the molar extinction coefficient. However, for a favorable case, $\epsilon$ may approach $10^5$. With a 1-cm cell this means that a $10^{-5}$ M solution will have an absorbance of 1.

In the discussion presented thus far, we have assumed that ultraviolet spectroscopy is being used to analyze one component. However, in practice this is usually not the case. Nevertheless, ultraviolet spectroscopy can in principle be used on multicomponent systems. For a two-component system with concentrations $C_1$ and $C_2$, of the two components, the following two equations can be written for the absorbances at two wavelengths $\lambda_A$ and $\lambda_B$:

$$A_{\lambda_A} = \epsilon_{1\lambda_A} C_1 + \epsilon_{2\lambda_A} C_2$$

$$A_{\lambda_B} = \epsilon_{1\lambda_B} C_1 + \epsilon_{2\lambda_B} C_2$$

Since the E values can be measured on the pure components and $A_{\lambda_A}$ and $A_{\lambda_B}$ can be measured from the mixture, these two equations can be solved for the two unknowns $C_1$ and $C_2$. For three components, three equations can in principal be written and solved.

Pendergrass *et al.* (1974) developed an ultraviolet method for the analysis of the solid-state thermal reaction of azotribenzoylmethane. In this reaction, the yellow (H1) thermally rearranges to the red (H2) and white (H3) forms in the solid state. All three compounds (H1, H2, and H3) have

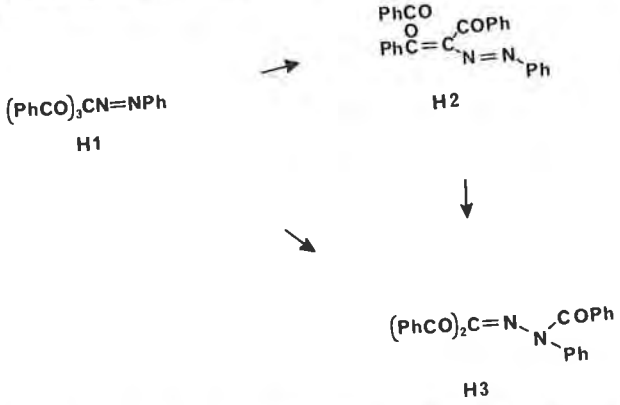


different chromophores, so that this reaction is amenable to analysis by ultraviolet spectroscopy. Pendergrass developed a matrix-algebra method for analyzing multicomponent mixtures by ultraviolet spectroscopy and used it to analyze the rate of the solid-state reaction under various conditions.

## B. NUCLEAR MAGNETIC RESONANCE (NMR) SPECTROSCOPY

The observation of NMR spectra requires that the sample be placed in a magnetic field where the normally degenerate nuclear energy levels are split. The energy of transition between these levels is then measured. In general, the proton magnetic resonance spectra are measured for quantitative analysis, although the spectra of other nuclei are also sometimes measured.

There are three important quantities measured in NMR spectroscopy: the chemical shift; the spin–spin coupling constant, and the area of the peak. The chemical shift is related to the energy of the transition between nuclei, the spin–spin coupling constant is related to the magnetic interaction between nuclei, and the area of the peak is related to the number of

nuclei responsible for the peak. It is the area of the peak that is of interest in quantitative NMR analysis.

The ratio of the areas of the various peaks in proton NMR spectroscopy is equal to the ratio of protons responsible for these peaks. For multicomponent mixtures, the ratios of areas of peaks from each component are proportional both to the number of protons responsible for the peak and to the amount of the component. Thus, the addition of a known concentration of an internal standard allows the determination of the concentrations of the species present. Unfortunately, area measurement is subject to several errors and the accuracy of this method is seldom better than 1 to 2%. For cases where the ratio of starting material and product is desired it is not necessary to add an internal standard. For example, Lin (1980) used proton NMR spectroscopy to study the rate of the solid-state photochemical oxidation of hydrocortisone 21-*tert*-butylacetate·0.9 $C_2H_5OH$ (**4**) to cortisone 21-*tert*-butylacetate (**5**). In this reaction, the

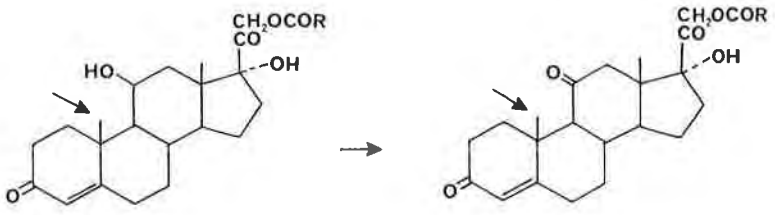


**4** **5**

chemical shift of the angular methyl group denoted by the arrow changes during the reaction. Thus measurement of the ratio of areas of this methyl group in the spectra of reacted mixtures of cortisone and hydrocortisone times the initial concentration of hydrocortisone gives the concentrations of starting material and product, and thus allows determination of the rate of this solid-state reaction.

## C. POLAROGRAPHY

Polarography is a special type of voltammetry that uses a dropping mercury electrode. In this experiment an electrochemical reaction is allowed to proceed at a given potential at the electrode and the current flow is measured. The current flow is proportional to the amount of species present. This proportionality is reflected in the well-known Ilkovic equation. Since different compounds undergo reactions at different potentials, polarography, at least in favorable cases, allows the quantative analysis of one species in the presence of others. However, the "resolution" of

polarography is significantly less than other methods such as ultraviolet or NMR spectroscopy. This is because members of one functional class of compounds (i.e., the substituted quinones) undergo electrochemical reaction at potentials close enough that significant overlap between their polarograms occurs. Polarography is sensitive to concentrations down to $10^{-5}$ to $10^{-6}$ M, depending on the functional group undergoing electrochemical reaction.

The polarographic experiment must be performed in the absence of dissolved oxygen. This is because oxygen reduction will produce a wave that obscures the reduction of most materials of interest. With water solutions, 5 min of nitrogen bubbling is usually sufficient to remove dissolved oxygen; however, organic solvents often require longer bubbling.

Clay (1980) used polarography to study the solid-state oxidation of dialuric acid (**6**) to alloxantin (**7**). In this case, dialuric acid was signifi-

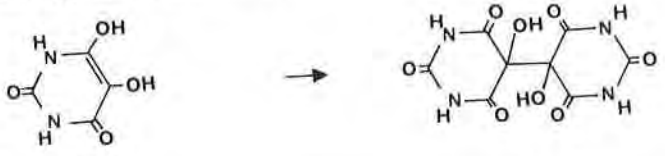

6 7

cantly more electroactive than alloxantin. Calibration curves of mixtures of dialuric acid and alloxantin showed that polarography could be used to analyze such mixtures and thus determine the rate of the solid-state oxidation of dialuric acid to alloxantin. It is important to note that deoxygenation of the water solvent was the key to analysis of this reaction by polarography. Preliminary experiments showed that dialuric acid had a half-life of 45 sec in aqueous solution. Even when care was taken to deoxygenate the solution, simple transfer of the solution to ultraviolet cuvettes resulted in the oxidation of dialuric acid. This extreme sensitivity of dialuric acid to oxygen in solution made the much slower solid-state oxidation almost impossible to study by normal solution methods. However, dissolution of the solid sample in the polarographic sample holder, which had been deoxygenated, and analysis under nitrogen resulted in no air oxidation of the dialuric acid and provided reproducible results.

## D. GAS CHROMATOGRAPHY

Gas chromatography is sometimes used to study the rates and/or course of a solid state reaction. However, because the method involves both dissolving and heating the sample it has inherent drawbacks. Obviously it cannot be used to study solid-state thermal reactions, since the

reaction would occur during analysis in the gas chromatograph. Gas chromatography, however, is well suited for studying thermally stable materials and has found use in the study of solid-state photochemical reactions as well as desolvations and solid-state hydrolysis reactions. Gas chromatography is rapid, with a typical analysis requiring 5–30 min, and is sensitive. The sensitivity can be greatly enhanced by using a mass spectrometer as a detector.

A typical analysis proceeds in the following steps:

*Step 1.* A suitable stationary phase (column) is selected.
*Step 2.* The optimum column temperature, flow rate, and column length are selected.
*Step 3.* The best detector is chosen.
*Step 4.* A number of known samples are analyzed, a calibration curve is constructed, and the unknowns are analyzed.

In our laboratory, gas chromatography has been used to study several solid-state reactions. Lin (1979) used gas chromatography to measure the rate of loss of ethanol from crystals of hydrocortisone 21-*tert*-butylacetate·0.9 $C_2H_5OH$. In this analysis, the crystals were dissolved in anhydrous DMSO and injected onto a 3% OV–17 column. A flame ionization detector was used to detect the ethanol. Popke (1978) used gas chromatography and derivatization to study the rate of hydrolysis of aspirin by water vapor. In this analysis, the crystals were dissolved in solvent and silylated using common procedures. Again, a 3% OV–17 column with flame ionization detector was used.

## E. HIGH-PRESSURE LIQUID CHROMATOGRAPHY (HPLC)

High-pressure liquid chromatography is probably the most widely used analytical method in the pharmaceutical industry. However, because it is a relatively new method (1965–1970), only a few examples of its use for the study of solid-state reactions are available.

In some ways, a high-pressure liquid chromatograph resembles a gas chromatograph in that it has an injector, a column, and a detector. However, in high-pressure liquid chromatography it is not necessary to heat the column or sample, making this technique useful for the analysis of heat sensitive materials. In addition, a wide range of column materials are available, ranging from silica to the so-called reversed-phase columns (which are effectively nonpolar columns). As with gas chromatography, several detectors are available. The variable-wavelength ultraviolet detector is particularly useful for pharmaceuticals and for studying the solid-

state reactions of drugs, since most drugs and their reaction products absorb in the ultraviolet range. In addition, extremely sensitive fluorescence and electrochemical detectors are also available.

A typical analysis by HPLC proceeds in the following manner:

*Step 1.* Selection of column and detector—these selections are usually based on the physical properties of the reactant and the product.

*Step 2.* Optimization of flow rate and column length to obtain the best separation.

*Step 3.* Analysis of known mixtures of reactant and product and construction of a calibration curve.

In our laboratory, HPLC has been used to follow the course of several solid-state reactions. Clay (1980) used HPLC to follow the degradation of the dye FD&C Yellow No. 5 (tartrazine, **8**) and sulfanilic acid (**9**). Stewart (1978) used HPLC to follow the solid-state oxidation of vitamin $D_2$ (**10**).

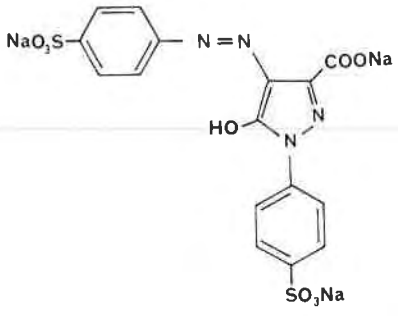


8


9

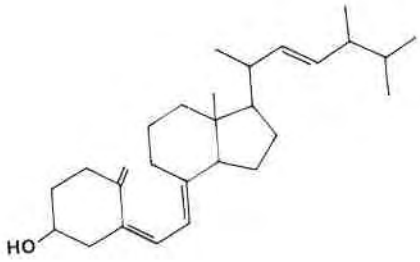


10

## F. THIN-LAYER CHROMATOGRAPHY

Thin-layer chromatography (TLC) provides a very simple and efficient method of separation. Only minimal equipment is required for TLC, and

very good separations can often be achieved. In general, it is difficult to quantitate TLC, so it is usually used as a method for separation of compounds.

A typical investigation of a solid-state reaction with TLC proceeds as follows:

*Step 1.* The adsorbent (stationary phase) is selected and plates either purchased or prepared. Usually silica gel or alumina are used.

*Step 2.* The sample and controls, such as unreacted starting material, are spotted near the bottom of the plate and developed in several solvents until the best separation is discovered.

This procedure then gives the researcher a good idea of the number of products formed. Based on these preliminary studies, an efficient preparative separation of the products and reactant can often by designed and carried out.

Stewart (1978) used TLC to separate the products of the solid state reaction of vitamin $D_2$. This separation allowed conclusive identification of one of the products and provided insight into the probable structure of two other products.

## VII. Summary

In this chapter, methods of analysis particularly useful for the analysis of solid-state reactions were reviewed and discussed. These included: (*a*) x-ray crystallographic methods involving the analysis of single crystals and a determination of their structure; (*b*) determination of the Miller indices of the faces of a crystal; (*c*) generation of crystal-packing diagrams; (*d*) application of powder diffraction to solid-state problems; (*e*) microscopy—both optical and electron; (*f*) thermal methods of analysis; (*g*) solid-state infrared spectroscopy; and (*h*) analytical methods involving dissolution of the sample.

The reader should now have enough background, particularly in crystallography, to understand the rest of this book.

The methods reviewed are best used in combination, since a single method has inherent drawbacks. Thus the complete study of a solid-state reaction should probably involve the application of several of these methods.

## Bibliography

Glusker, J. P., and Trueblood, K. N. (1972). "Crystal Structure Analysis." Oxford University Press, New York.
Shoemaker, D. P., and Garland, C. W. (1962). "Experiments in Physical Chemistry." McGraw-Hill Book Company, Inc., New York.
Stout, G. H., and Jensen, L. H. (1968). "X-Ray Structure Determination." Macmillan, New York.

## References

Clay, R. J. (1980). Ph.D. Thesis, Purdue University.
Curtin, D. Y., and Byrn, S. R. (1969). *J. Am. Chem. Soc.* **91,** 1965.
Curtin, D. Y., Byrn, S. R., and Pendergrass, D. B., Jr. (1969). *J. Org. Chem.* **34,** 3345.
Kuhnert-Brandstatter, M. (1971). "Thermomicroscopy in the Analysis of Pharmaceuticals." Pergamon, New York.
Lin, C. T. (1980). Unpublished results, Purdue University.
Pendergrass, D. B. Jr., Curtin, D. Y., and Paul, I. C. (1972). *J. Am. Chem. Soc.* **94,** 8722.
Popke, S. (1978). Unpublished results, Purdue University.
Simmons, D. L., Ranz, R. J., Gyanchandani, N. D., and Picotte, P. (1972). *Can. J. Pharm. Sci.* **7,** 121.
Stewart, B. S. (1978). M.S. Thesis, Purdue University.
Thomas, J. M. (1974). Phil. Trans. R. Soc. *London, Ser. A* **277,** 251.
Wendlandt, W. (1974). "Thermal Methods of Analysis," 2nd ed., p. 9. John Wiley and Sons, New York.

# 3 Kinetics of Solid-State Reactions

The subject of kinetics of solid-state reactions of drugs and of solid-state reactions in general is not well understood. Solid-state reactions show complex rate behavior that is not easily understood and cannot be easily fitted to a single kinetic equation. With this in mind, this chapter discusses the kinetic laws governing solid-state reactions and a few pharmaceutical examples of the study of solid-state kinetics.

The kinetics of the solid-state decomposition reactions of pharmaceuticals have been extensively studied, because this data is used to make shelf-life predictions and arrive at preliminary expiration dates (see Chapter 1). The aim of most of these studies is to obtain an equation that provides an adequate fit for plots of rate versus time. Most of these studies have not aimed at elucidating the molecular details of the solid-state reaction. For this reason, most solid-state decompositions of pharmaceuticals have been analyzed in terms of zero-order and first-order kinetics (Carstensen, 1974), although the Prout–Tompkins equation has also been used (Horikoshi and Himuro, 1966).

# I. Theoretical Description of Solid-State Reactions and Their Kinetics

## A. INTRODUCTION

In this section we will deal only with reactions of a single substance, solid–solid reactions will not be discussed.

The kinetics of a large number of reactions of inorganic hydrates and carbonates have been studied, as well as the kinetics of the solid-state reactions of ceramic materials. Explosives and related compounds have also been extensively studied (Bawn, 1955; Ubbelohde, 1955).

Usually a kinetic study of a solid-state reaction begins by plotting the *fraction decomposed*, $\alpha$, versus *time*, $t$. Figure 1 shows two typical curves of $\alpha$ versus time. These curves are sigmoid and are thus in some respects characteristic of an autocatalytic reaction. In the next sections, several kinetic equations for analyzing plots of $\alpha$ versus $t$ are presented. In all of these equations, $\alpha$ refers to the fraction decomposed, $t$ refers to the time, and $k$ refers to the rate constant.

## B. REACTIONS INVOLVING NUCLEATION

In this section, two common equations for the kinetics of reactions involving nucleation are discussed.

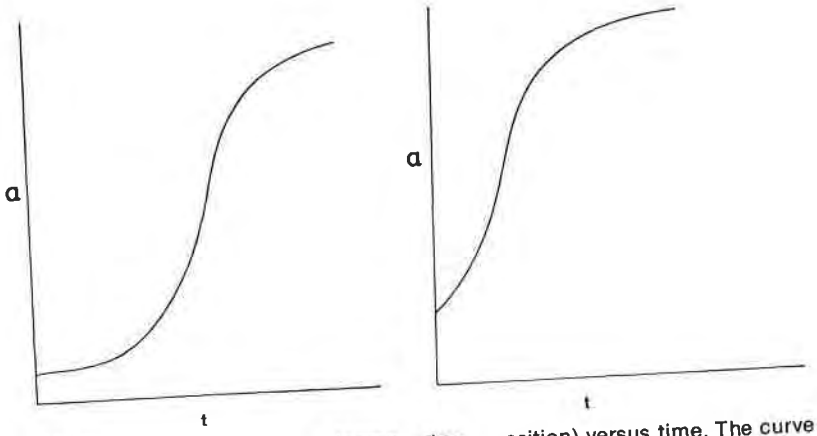


**FIGURE 1.** Typical curves of $\alpha$ (percent decomposition) versus time. The curve on the left has a noticible induction period, while the curve on the right has virtually no induction period.

*1. The Prout–Tompkins Equation*

If the rate of a solid-state reaction is assumed to be controlled by linearly growing nuclei that branch into chains and are terminated according to the number of nucleii present, then the Prout–Tompkins equation (1) can be derived.

$$\ln\left(\frac{1}{1-\alpha}\right) = kt \tag{1}$$

This equation has been successfully applied to several inorganic solid-state reactions, including the reactions of mercury fulminate, lead oxalate, and nickel formate (Prout and Tompkins, 1944).

*2. The Avrami–Erofeev Equation*

If the rate of a solid-state reaction is assumed to be governed by random nuclei that grow in three dimensions and ingest other nuclei, then the Avrami–Erofeev equation (2) can be derived (Avrami, 1939, 1940, 1941; Erofeev, 1946).

$$[-\ln(1-\alpha)]^n = kt \tag{2}$$

where the value of $n = \frac{1}{4}, \frac{1}{3}, \frac{1}{2}, \frac{2}{3}$, and 1.

The Avrami–Erofeev equation, like the Prout–Tompkins equation, has been used to analyze the kinetics of several solid-state reactions of inorganic compounds.

## C. REACTIONS CONTROLLED BY PHASE BOUNDARIES—CONTRACTING GEOMETRIES

If the solid-state reaction is assumed to be controlled not by the formation of nuclei but rather by the advancement of phase boundaries from the outside of a crystal inward, then a different series of equations can be derived.

*1. One-Dimensional Advancement of a Phase Boundary*

If a crystal is assumed to react along one direction, then the rate is a function of time only and thus a zero-order rate equation applies:

$$1 - \alpha = kt \tag{3}$$

*2. Two-Dimensional Advancement of a Phase Boundary*

If the reaction is assumed to proceed from the surface of a circular disk or cylinder inward, then Eq. (4) can be derived (Sharp *et al.*, 1966):

$$1 - (1-\alpha)^{1/2} = kt \tag{4}$$

#### 3. Three-Dimensional Advancement of a Phase Boundary

If the reaction is assumed to proceed from the surface of a sphere inward in three dimensions, then Eq. (5) can be derived (Sharp *et al.*, 1966):

$$1 - (1 - \alpha)^{1/3} = kt \tag{5}$$

## D. DIFFUSION-CONTROLLED REACTIONS

If diffusion controls the rate of the reaction, instead of nucleation or phase-boundary advancement, then another set of equations closely related to the phase-boundary equations can be derived. Obviously, only reactions involving gaseous starting materials or products should be treated as diffusion-controlled reactions.

#### 1. One-Dimensional Diffusion

If the rate of the reaction is controlled by a one-dimensional diffusional process, then Eq. (6) can be derived (Sharp *et al.*, 1966):

$$\alpha^2 = kt \tag{6}$$

This equation is the same as the power law [Eq. (10)] with $n = 2$.

#### 2. Two-Dimensional Diffusion

If the rate of the reaction is controlled by two-dimensional diffusion from the surface of a circular disk or cylinder, then Eq. (7) can be derived (Holt *et al.*, 1962):

$$(1 - \alpha) \ln(1 - \alpha) + \alpha = kt \tag{7}$$

#### 3. Three-Dimensional Diffusion

If the reaction is assumed to be controlled by diffusion from the surface of a spherical particle, then Eq. (8) can be derived (Ginstling and Braunshtein, 1950; Valensi, 1936; Carter, 1961a,b):

$$1 - \tfrac{2}{3}\alpha - (1 - \alpha)^{2/3} = kt \tag{8}$$

A simplified version of Eq. (8) is known as the Jander equation:

$$[1 - (1 - \alpha)^{1/3}]^2 = kt \tag{9}$$

## E. OTHER EQUATIONS

In addition to the preceding equations, which were each derived on the basis of some model for the progress of the reaction through the crystal,

there are other equations that are sometimes used to treat solid-state rate data. These other equations are of two types: the power-law equations, and the equations based on the concept of order of the reaction.

*1. Power-Law Equations*

In general, the power-law equation [Eq. (10)] has no theoretical basis, but it has been used to analyze solid-state rate data:

$$\alpha^n = kt \tag{10}$$

where $n = \frac{1}{4}, \frac{1}{3}, \frac{1}{2}$, and 1.

*2. Equations Based on the Concept of Order of the Reaction*

Solution reactions are routinely analyzed in terms of equations based on the concept of order, and often the order of a reaction is used to gain insight into the molecularity of a reaction. The *order* of a reaction is the sum of the exponents of the concentration terms in the rate law. Since the concept of molecularity of a reaction is not as well defined for solid-state reactions, kinetic equations based on order are not as widely used. Nevertheless, sometimes data are analyzed in their terms. Equation (11) is for zero-order reactions (sum of exponents is zero), Eq. (12) for first-order reactions (sum of exponents is one), and Eq. (13) for second-order (sum of exponents is two) reactions.

$$1 - \alpha = kt \tag{11}$$

$$\ln(\alpha) = kt \tag{12}$$

$$1/(1 - \alpha) = kt \tag{13}$$

## F. REACTIONS INVOLVING PARTIAL LIQUEFACTION

Some solid-state reactions of drugs involve partial melting or reaction in a liquid layer. In these cases, it is necessary to treat the rate of the reaction as determined by a sum of the rates in the liquid and solid phases. If first-order kinetics are assumed for both the liquid- and solid-phase reaction, then the overall rate of change of the product versus time for a reaction of the type

$$\underset{1-x}{\text{A}} \rightarrow \underset{x}{\text{B}} + \text{gaseous products}$$

is $dx/dt = k_s(1 - x - xs) + k_l(xs)$, where $k_s$ and $k_l$ are the rate constants for reaction in the solid and liquid phases, and $s$ is the molecular solubility of the reactant crystal in the liquid phase.

Solution of this equation gives Eq. (14) (Bawn, 1955; Carstensen, 1974).

$$x = \frac{1}{k_1 s - k_s s - k_s} \exp[(k_1 s - k_s s - k_s) k_s t - 1] \tag{14}$$

This equation is of the same form as the first-order equation (12), as might be expected.

## G. A COMPUTER PROGRAM FOR ANALYZING SOLID-STATE KINETIC DATA

Perrier (1980) has written a computer program for treatment of $\alpha$ versus $t$ data according to Eqs. (1)–(13). This program simply calculates the various quantities on the left side of Eqs. (1)–(13) and plots them against time. It then calculates the least-squares line through these points and reports the slope, intercept, and correlation coefficient.

A consideration of the application of this program to the $\alpha$ versus $t$ data for the dehydration of cytosine monohydrate illustrates the usefulness of this program, as well as the problems faced by solid-state chemists.

**TABLE I**

*Results of Application of Equations (1)–(13) to Data from the Dehydration of Cytosine Monohydrate*[a]

| Equation | Slope | Intercept | Correlation |
|---|---|---|---|
| Prout–Tompkins (1) | 0.692 | −1.495 | .995 |
| Avrami–Erofeev (2), $n = \frac{1}{4}$ | 0.0837 | .739 | .982 |
| Avrami–Erofeev (2), $n = \frac{1}{3}$ | .116 | .649 | .991 |
| Avrami–Erofeev (2), $n = \frac{1}{2}$ | .192 | .452 | .999 |
| Avrami–Erofeev (2), $n = \frac{2}{3}$ | .286 | .221 | .997 |
| Avrami–Erofeev (2), $n = 1$ | .558 | −.426 | .968 |
| Two-dimensional phase boundary (4) | .0866 | .147 | .970 |
| Three-dimensional phase boundary (5) | .0814 | .640 | .995 |
| Diffusion-controlled—two-dimensional (7) | .106 | .00723 | .969 |
| Diffusion-controlled—three-dimensional (8) | .0344 | −.151 | .986 |
| Jander equation (9) | .0776 | −.0992 | .971 |
| Power law (10), $n = \frac{1}{4}$ | .0284 | .769 | .740 |
| Power law (10), $n = \frac{1}{3}$ | .0361 | .707 | .754 |
| Power law (10), $n = \frac{1}{2}$ | .0492 | .597 | .781 |
| Power law (10), $n = 1$ | .0761 | .363 | .845 |
| Power law (10), $n = 2$ (one-dimensional diffusion) | .101 | .118 | .912 |
| Zero-order (one-dimensional phase boundary) (11) | −.0762 | .637 | .845 |
| First-order (12) | −.558 | .426 | .968 |
| Second-order (13) | 24.15 | −69.6 | .490 |

[a] The slope, intercept, and correlation coefficient for the best line obtained by plotting the quantity on the left side of Eqs. (1)–(13) versus time are shown. A good correlation coefficient is .99 (Perrier, 1980).

Batches of crystals of cytosine monohydrate were decomposed at 58.5°C and the data were plotted according to Eq. (1)–(13). Table I shows the slope intercept and correlation coefficient for the least-squares analysis of the data.

It is clear from this table that several kinetic equations give good fits to the data. Obviously the fact that more than one equation fits the data indicates that solid-state kinetic data cannot be used to prove the mechanism of a solid-state reaction. Nevertheless it is important for determination of the activation energy to select the proper kinetic equation. The following approach is suggested. The equations that give good fits to the data (correlation greater than .990) are initially selected. Then other data, including the kinetics and mechanism of the reaction in solution and the behavior of reacting single crystals on the microscope, are used to provide further insight into the mechanism. For example, if front movement is observed under the microscope, the three-dimensional advancement of a phase boundary can be ruled out. If several possible kinetic equations still remain, the theoretical basis for these equations should be considered in choosing the best equation.

## II. Examples of Solid-State Kinetic Studies

In this section, several examples of studies of the kinetics of solid-state reactions are discussed. This discussion will illustrate the usefulness as well as the difficulties associated with solid-state kinetic studies.

### A. THE PHASE TRANSFORMATION OF *p*-DICHLOROBENZENE

The phase transformation of *p*-dichlorobenzene begins at observable defects and proceeds through the crystal via nearly linear advancement of the reaction front (Kitaigorodskii *et al.*, 1965). By the use of diagrams, Kitaigorodskii *et al.* (1965) clearly showed that the rate of volume transformation of such crystals depends on a set of random factors. Figure 2(*a*) obviously shows that for a given rate of front advancement the number of nuclei can greatly influence the rate of conversion of reactant to product. Figure 2(*b*) shows that the orientation of the nucleus with respect to the rate of front advancement can influence the rate of conversion of reactant to product. Figure 2(*c*) shows how the location of the nucleus can affect the rate of transformation of reactant to product, and Figure 2(*d*) illustrates the effect of crystal size on the rate of volume transformation. Although with a sufficiently large number of crystals these effects are

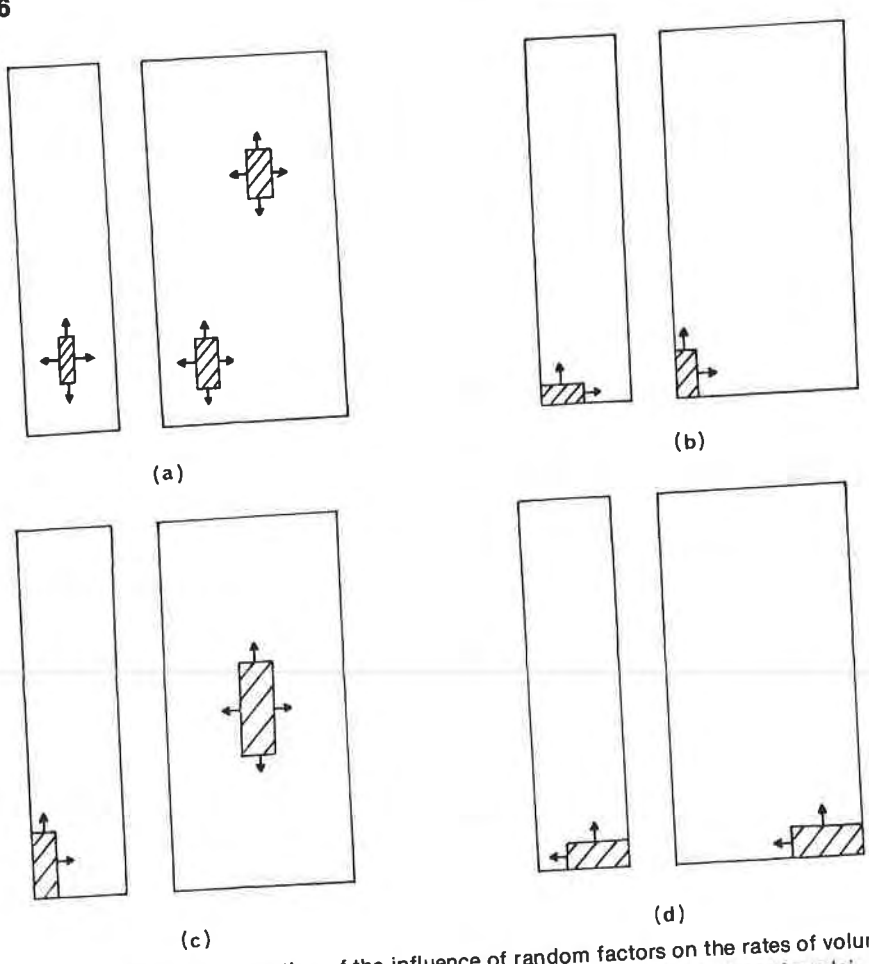


**FIGURE 2.** An illustration of the influence of random factors on the rates of volume transformation of crystals reacting in fronts. (*a*) The effect of the number of nuclei. (*b*) The effect of the orientation of the nuclei. (*c*) The effect of the location of the nucleus. (*d*) The effect of crystal size and shape. (Data from Kitaigorodskii *et al.*, 1965.)

averaged, with a few crystals these effects could cause major errors in kinetic studies. For this reason, Kitaigorodskii *et al.* measured the advancement of the reaction front through the crystal. The front advanced linearly and thus obeyed zero-order kinetics.

## B. THE KINETICS OF DESOLVATION OF CYTOSINE MONOHYDRATE

The rate of desolvation of batches of cytosine monohydrate made up of "large" crystals and "small" crystals were measured at five temperatures

ranging from 58.5 to 39.1°C (Perrier, 1980). The results for 58.4°C for the small crystals have been shown in Table I. It is obvious that at least four rate equations give a good fit to the data, since their correlation coefficient is greater than .99. Analysis of the rate data at other temperatures gives similar results; however, the Avrami–Erofeev equation ($n = \frac{2}{3}$) gives the best fit to the data at all five temperatures. The rate constant from this equation was then plotted versus $1/T$ in the usual manner. The activation energy ($E_A$) was then determined from this plot according to the classical equation $k = Ae^{(E_A/RT)}$, where $k$ is the rate constant, $A$ is the preexponential factor, and $E_A$ is the activation energy. The $E_A$ value for the "small" crystals is 25.9 kcal/mole.

The rate of desolvation of the "large" crystals was also measured at five temperatures and analyzed using the computer program described above. In this case, the Prout–Tompkins equation gives the best fit to the data at all temperatures. The activation energy was determined from the rate constants obtained from the Prout–Tompkins equation in the usual way, and is 25.4 kcal/mole.

While the results of one set of experiments using different sizes of crystals are not enough to lead to any definite conclusions, it is interesting to note that the rate constants from two different equations gave essentially the same activation energy. Further studies are needed to establish whether the activation energy of desolvation reactions is independent of the kinetic equation used to analyze the data.

## C. THE DECOMPOSITION OF DIBENZOYL PEROXIDE

Dibenzoyl peroxide decomposes below its melting point to form phenylbenzoate and carbon dioxide in almost quantative yield (Morsi *et al.*, 1975). The rate of this reaction was measured gravimetrically and gave a good fit to the Avrami–Erofeev equation ($n = \frac{1}{2}$) for $\alpha = 0$ to $\alpha = 0.1$ ($\alpha$ = fraction decomposed). For $\alpha > 0.1$, the data give a good fit to the equation for three-dimensional advancement of a phase boundary (5). Activation energies were determined for both the $\alpha = 0$ to $\alpha = 0.1$ stage of the reaction and the $\alpha > 0.1$ stage of the reaction, and are 45 kJ/mole and 72.0 kJ/mole, respectively. This approach of using more than one equation to fit kinetic data from the same compound is analogous to the treatment of solution reactions by two different kinetic equations presumably resulting from a change in mechanism of the reaction. Thus the concept of using more than one equation to treat solid-state kinetic data makes an already confused situation even more complex. Nevertheless, using two equations to treat solid-state rate data is a valid and useful kinetic approach that cannot be discarded.

In summary, this study along with previous discussions in this chapter shows that the same set of solid-state kinetic data can sometimes fit several different single equations, as well as combinations of these equations. A detailed comparison of the activation energies obtained from these various equations is needed.

## D. THE SOLID-STATE RACEMIZATION OF BINAPHTHYL

Upon crystallization of 1,1′-binaphthyl (**1**), two polymorphs are formed. Single crystals of one polymorph contain both *R* and *S* molecules

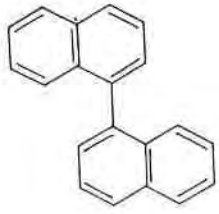

**1**

of **1** and are achiral, while a single crystal of the other polymorph contains either *R* or *S* molecules and is therefore chiral. Heating the achiral (or racemic) polymorph of **1** causes it to transform to the chiral polymorph (Wilson and Pincock, 1977). The rate of this reaction (which results in a change in the optical rotation of batches of crystals) was determined. The rate data were fitted to both the Avrami–Erofeev equation (2) and the Prout–Tompkins equation (1) and give good fits; however, the best fit of the data was obtained with the Prout–Tompkins equation. Determination of the rate constant at several temperatures was accomplished using the Prout–Tompkins equation. The activation energy was then determined and found to be about 60 kcal/mole.

This large activation energy is consistent with similar measurements for other phase transformations and was suggested to be related to the energy required to remove a molecule from the center of the crystal to the vapor state. This suggestion is consistent with the fact that the solid-state reaction is much slower than the corresponding solution reaction (Wilson and Pincock, 1977).

## E. THE DECARBOXYLATION OF MALONIC ACID

The decarboxylation of malonic acid (**2**) (mp 134°C) marks one of the first kinetic studies of solid-state organic reactions other than reactions

$$\underset{2}{HOOCCH_2COOH} \longrightarrow CH_3COOH + CO_2$$

involving explosives (Bawn, 1955). This reaction was studied in both the solid state and the supercooled liquid. In both states, first-order kinetics were obeyed. Table II reports the rates and the rate ratios for this reaction at the temperatures shown. These data give activation energies (and preexponential factors) of 32.4 kcal/mole (log $A$ = 13.6) for the liquid reaction and 60.4 kcal/mole (log $A$ = 28.0) for the solid reaction.

## F. THE REARRANGEMENT OF PHENYLAZOTRIBENZOYLMETHANE

Phenylazotribenzoylmethane (**3**) rearranges to **4** and **5** in the solid state (Pendergrass *et al.*, 1972). The rate of disappearance of **3** was measured by

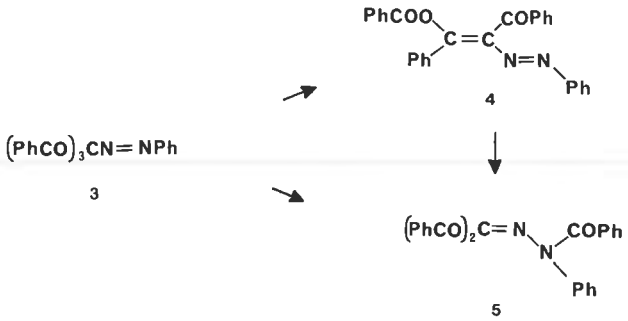


immersing a flask containing crystals of **3** in an oil bath and rotating it constantly to assure that all crystals were heated evenly. The data obey first-order kinetics after a brief induction period. The results of these studies on both an unsolvated and a solvated form are shown in Table III. It is obvious from this table that the rates of reaction of all of the crystals

**TABLE II**
*A Comparison of the Rates of Decarboxylation of Malonic Acid at Different Temperatures and in Different States*[a]

| Temperature | Solid state, $k_s$ (min$^{-1}$) | Super-cooled liquid $k_l$(min$^{-1}$) | Ratio, $k_l/k_s$ |
|---|---|---|---|
| 126.3 | $2.5 \times 10^{-4}$ | $20.7 \times 10^{-4}$ | 8 |
| 125.5 | $2.2 \times 10^{-4}$ | $19.2 \times 10^{-4}$ | 9 |
| 117.3 | $4.1 \times 10^{-5}$ | $8.7 \times 10^{-4}$ | 21 |
| 110.8 | $2.1 \times 10^{-5}$ | $4.7 \times 10^{-4}$ | 39 |

[a] Data from Bawn (1955).

**TABLE III**
*Rates of Rearrangement of Solid Phenylazotribenzoylmethane* **(3)** *at 90°C*

| Sample | $k \times 10^6 (sec^{-1})$ |
|---|---|
| Form I (from xylene–hexane) | |
| Crystals | 25.0 |
| Crushed crystals | 14.6 |
| Form II (ether solvate) | |
| Habit I: pointed crystals | 324 |
| Habit II: blunt crystals | 50 |
| Crushed crystals | 12.8 |

except the pointed habit of the etherate are approximately the same. It is interesting to note that desolvation preceeds reaction and yet the reaction is not accelerated. This is probably because soon after desolvation the unsolvated form, form I, crystallizes. It is also interesting to note that crushing the sample does not accelerate the reaction, even though this process should greatly increase the types of certain nuclei.

## G. DEGRADATION OF BACITRACIN

In some cases it is impossible to distinguish between zero-order and first-order solid-state reactions. For example, the degradation of bacitracin fits both first-order and zero-order kinetic equations, as shown in Figure 3.

## H. DEHYDRATION OF THEOPHYLLINE MONOHYDRATE

The dehydration of theophylline hydrate was studied using x-ray crystallography (Shefter and Kmack, 1967). The data for desolvation at both 40° and 50°C followed good first-order kinetics. It is interesting to note that the dehydration of cytosine monohydrate also gave a somewhat reasonable fit to the first-order equation with the correlation coefficient being .968, but the cytosine data gave a much better fit to several other equations.

## I. DEGRADATION OF VITAMINS A, $B_1$, AND C IN MULTIVITAMIN TABLETS

In a study of the rates of degradation of vitamins A, $B_1$, and C in multivitamin tablets, Tardif (1965) found that in the temperature range 50° to 60°C the decompositions of all three vitamins obeyed first-order kine-

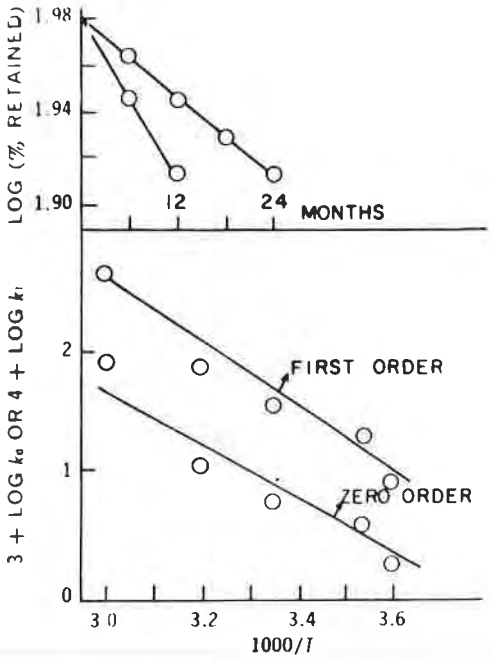


**FIGURE 3.** Plots showing the treatment of data for the decomposition of bacitracin by both a zero- and a first-order equation (Carstensen, 1974). These data appear to indicate that either equation fits the data. (Reproduced with permission of the copyright owner.)

tics (see, for example, Figure 4). In addition, he was able to use these rates to predict the stability of these vitamins in tablets at room temperature, and the observed stability was quite close to the predicted stability.

## J. DECOMPOSITIONS TREATED AS A COMBINED SOLID AND SOLUTION REACTION

The kinetics of a number of decompositions of pharmaceuticals have been treated according to Eq. (14), which assumes that the pharmaceutical is decomposing in parallel first-order reactions in the solid state and solution. While it is dangerous to apply an equation such as Eq. (14) to a set of data and then argue that if it fits the data the mechanism is established, there is often other evidence to indicate that the decomposition is proceeding by parallel reactions in the liquid and solid states.

Kornblum and Sciarrone (1964) studied the rate of decarboxylation of *p*-aminosalicylic acid (**3**) at various temperatures and vapor pressures of water.

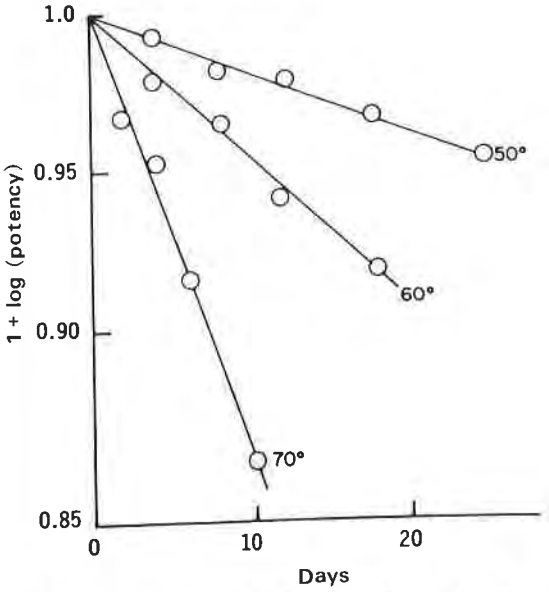


**FIGURE 4.** Treatment of the data for the decomposition of vitamin C according to a first-order equation (Tardif, 1965). (Reproduced with permission of the copyright owner.)

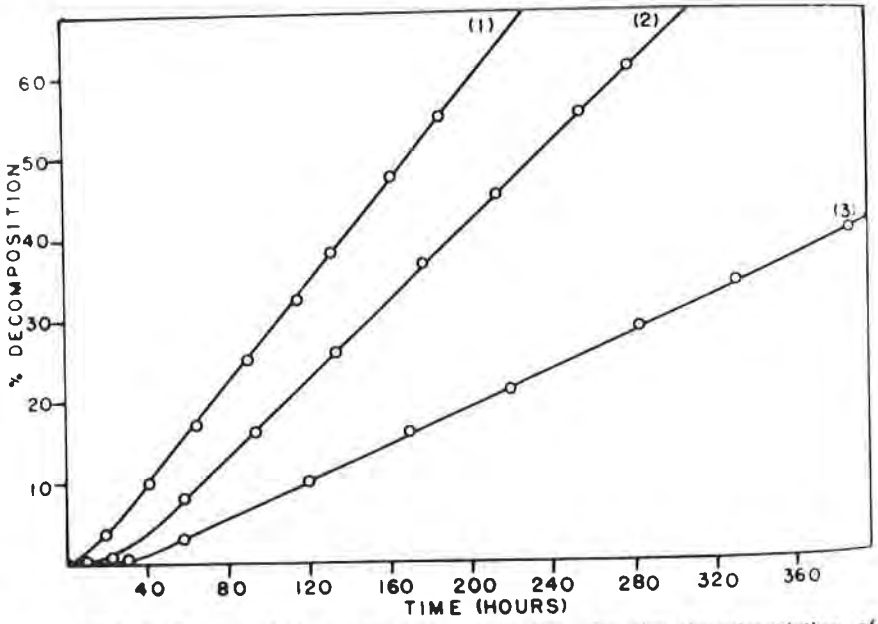


**FIGURE 5.** Curves of decomposition versus time for the decarboxylation of *p*-aminosalicylic acid at 70°C at an aqueous tension of: (1) 144.0 mmHg; (2) 118.4 mmHg; (3) 52.3 mmHg (Kornblum and Sciarrone, 1964). (Reproduced with permission of the copyright owner.)

In the dry state, a sigmoid plot of percentage decomposition versus time is obtained at 70°C. This data was not analyzed further, but it is clear that one of Eqs. (1)–(13) would fit the data and that a solid-state reaction in the absence of moisture does occur.

In humid conditions, different results are obtained, as shown in Figure 5. It is clear from this figure that under these conditions, essentially zero-order kinetics is observed. It is also clear that moisture accelerates the reaction, perhaps by forming a layer on the solid.

More recently, Pothisiri and Carstensen (1975) have studied the decompositions of a series of crystalline *p*-substituted salicylic acids. All of the curves of percentage decomposition versus time for these compounds in dry atmosphere have a sigmoid shape, just like that for *p*-aminosalicylic acid (Kornblum and Sciarrone, 1964). These data were analyzed using Eq. (14), and the liquid- and solid-state rate constants were obtained. Unfortunately, attempts were not made to fit these data to other equations. In another study, Carstensen and Kothari (1980) fitted the percentage decomposition versus time data for the decarboxylation of 5-tetradecyloxy-2-furoic acid to Eq. (14). Again, both the solid and liquid rate constants were obtained and analyzed.

The kinetics of the decomposition of aspirin in the solid state has been studied by Leeson and Mattocks (1958). The curve of percentage decomposition versus time followed sigmoid kinetics and was treated according to a first-order solution reaction, which occurs in a sorbed moisture layer. A reasonably good fit of the data was obtained (see Figure 6).

Carstensen (1974) has replotted these data according to Eq. (14) and also obtained a reasonably good fit (Figure 7).

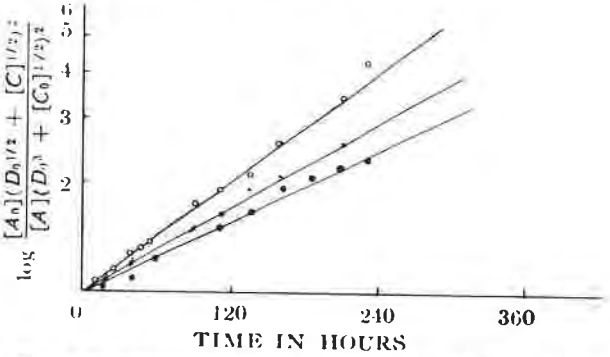


**FIGURE 6.** The decomposition of aspirin, treated according to a reaction occurring in a sorbed moisture layer: ○—vapor pressure of water (232 mm); x—vapor pressure of water (199.5 mm); and ●—vapor pressure of water (181.0 mm) (Leeson and Mattocks, 1958). (Reproduced with permission of the copyright owner.)

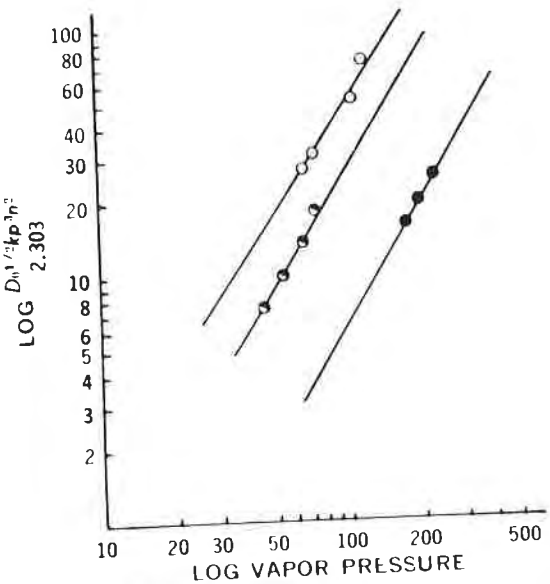


**FIGURE 7.** Aspirin decomposition in the presence of 232 mm water (○); 199.5 mm water (●); and 181.0 mm water (●); replotted using Eq. (14), the equation for a reaction in a partial solution. Note that the data are the same as those used for Figure 6 (Carstensen, 1974). (Reproduced with permission of the copyright owner.)

It is clear that a good fit is obtained for both plots. In the absence of further data it is impossible to use the kinetic data to prove the mechanism of the aspirin decomposition.

## III. Summary

In this chapter, the various kinetic equations for solid-state reactions were presented, along with a computer program for analysis of solid-state reactions in terms of these equations. Several studies of the kinetics of solid-state reactions were presented and discussed.

It should be clear that the area of solid-state kinetics is quite complex and that, as in any kinetic study, it is not advisable to argue that if a set of data obeys certain kinetics then the mechanism of the reaction is established.

## References

Avrami, J. (1939). *J. Chem. Phys.* **7**, 1103.
Avrami, M. (1940). *J. Chem. Phys.* **8**, 212.

Avrami, M. (1941). *J. Chem. Phys.* **9,** 177.
Bawn, C. H. E. (1955). In "Chemistry of the Solid State" (W. E. Garner, ed.), pp. 254, 262. Butterworths, London.
Carstensen, J. T. (1974). *J. Pharm. Sci.* **63,** 1.
Carstensen, J. T., and Kothari, P. (1980). *J. Pharm. Sci.* **69,** 123.
Carter, R. E. (1961a). *J. Chem. Phys.* **34,** 2010.
Carter, R. E. (1961b). *J. Chem. Phys.* **34,** 1137.
Erofeev, B. V. (1946). *C. R. Acad. Sci., USSR* **52,** 511.
Ginstling, A. M., and Braunshtein, B. I. (1950). *J. Appl. Chem. USSR* **23,** 1327.
Holt, J. B., Cutler, I. B., and Wadsworth, M. E. (1962). *J. Am. Ceramic Soc.* **45,** 133.
Horikoshi, I., and Himuro, I. (1966). *J. Pharm. Soc. Jap.* **86,** 319, 324, 353, 356.
Kitaigorodskii, A. E., Mnyukh, Y. V., and Asadov, Y. G. (1965). *J. Phys. Chem. Solids* **26,** 463.
Kornblum, S. S., and Sciarrone, B. J. (1964). *J. Pharm. Sci.* **53,** 935.
Leeson, L. J., and Mattocks, A. M. (1958). *J. Am. Pharm. Assoc.* **47,** 329.
Morsi, S. E., Thomas, J. M., and Williams, J. O. (1975). *J. Chem. Soc., Faraday Trans. 1,* 1857.
Pendergrass, D. B. Jr., Curtin, D. Y., and Paul, I. C. (1972). *J. Am. Chem. Soc.* **94,** 8722.
Perrier, P. (1980). Unpublished results, Purdue University.
Pothisiri, P., and Carstensen, J. T. (1975). *J. Pharm. Sci.* **64,** 1931.
Prout, E., and Tompkins, F. (1944). *Trans. Faraday Soc.* **40,** 448.
Sharp, J. H., Brindley, G. W., and Narahariachar, B. N. (1966). *J. Am. Ceramic Soc.* **49,** 379.
Shefter, E., and Kmack, G. (1967). *J. Pharm. Sci.* **56,** 1028.
Tardif, R. (1965). *J. Pharm. Sci.* **54,** 281.
Ubbelohde, A. R. (1955). In "Chemistry of the Solid State" (W. E. Garner, ed.), p. 268. Butterworths, London.
Valensi, G. (1936). *Compt. Rend.* **202,** 309.
Wilson, K. R., and Pincock, R. E. (1977). *Can. J. Chem.* **55,** 889.

II

# Physical Transformations

# 4 Polymorphism of Drugs

## I. General Review of Polymorphism

Compounds that crystallize in polymorphs can show a wide range of physical and chemical properties, including different melting points and spectral properties. Polymorphism is particularly important for pharmaceuticals, where the polymorph present can alter the dissolution rate, bioavailability, chemical stability, and physical stability.

The existence of polymorphs is best established by x-ray crystallographic examination. The clearest indication of the existence of polymorphs comes from the examination of single crystals of the various forms. If these crystals belong to a different space group or have different unit-cell parameters (beyond experimental error), then they are polymorphs. Often, x-ray powder diffraction is also used to establish the existence of polymorphs. Polymorphs can differ in their solubility, melting point, density, hardness, and crystal shape. While some compounds exist in two polymorphs, many compounds exist in many polymorphs, such as progesterone with five and water with eight or nine.

Enantiotropic and monotropic polymorphs have been defined (Kuhnert-Brandstatter, 1971). Enantiotropic polymorphs can be interconverted below the melting point of either polymorph, while monotropic

polymorphs cannot. Thus for a monotropic polymorphic pair, one form is stable throughout the temperature range.

The determination of the crystal polymorphs, solvates, and habits in which a drug crystallizes and the use of this knowledge can lead to a dramatic improvement in stability and/or bioavailability.

## A. SELECTED EXAMPLES OF POLYMORPHISM

### *1. Polymorphism of* p-*Chlorophenol*

The crystal structure of both the stable ($\alpha$) and unstable ($\beta$) forms of *p*-chlorophenol (**1**) have been determined (Perrin and Michel, 1973). Both

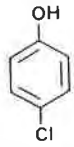


1

forms belong to the same space group ($P2_1/c$) and have the same number of molecules per unit cell ($Z = 8$) but different cell parameters (Table I). The crystal packing of the $\beta$ form is shown in Figure 1. The packing consists of tetramers connected by hydrogen bonds. The crystal structure of the $\beta$ form projected on the 100 plane is shown in Figure 2. Again, the packing consists of tetramers of molecules connected by hydrogen bonding. However, the arrangement of the rings is slightly different in these two polymorphs. Although the $\beta$ form is less stable than the $\alpha$ form, no detailed studies of this transformation have been reported.

### *2. Polymorphism of 1,2,5,6-Dibenzanthracene*

In an early study of polymorphism, the crystal structures of forms I and II of 1,2,5,6-dibenzanthracene (**2**) have been determined (Robertson and

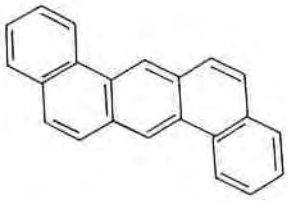

2

White, 1947, 1956). The forms belong to different space groups (Table II) but have nearly the same density.

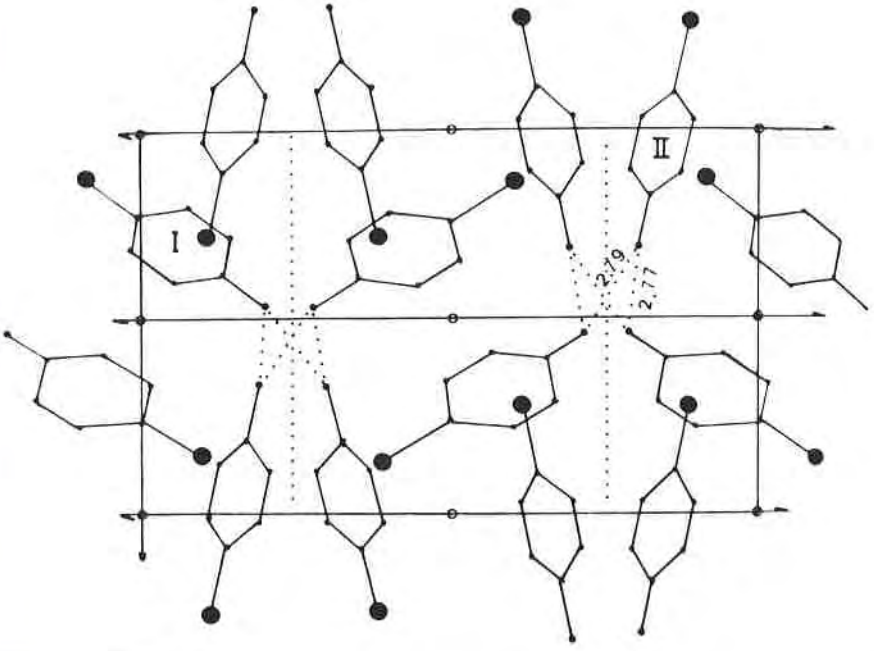


**FIGURE 1.** Projection of the crystal structure of the $\beta$-polymorph of *p*-chlorophenol on the *ab* crystal plane. In the drawing *a* is vertical, *b* is horizontal, and *c* is out of the plane (Perrin and Michel, 1973).

The conformation of 1,2,5,6-dibenzanthracene is the same in both forms; however, the crystal packing is quite different. The packing of the orthorhombic form is shown in Figure 3. In this form, there is some overlap of molecules. In the monoclinic form shown in Figure 4 there is also overlap of a slightly different kind.

### *3. Polymorphism of Acridine*

Acridine (**3**) crystallizes in five polymorphs as shown in Table III (Herbstein and Schmidt, 1955).

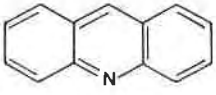


3

The crystal structures of the $\alpha$ and $\epsilon$ forms have been determined and are shown in Figures 5 and 6.

**TABLE I**
*Crystallographic Parameters for the Two Polymorphs of p-Chlorophenol*

| Parameter | $\alpha$ Form | $\beta$ Form |
|---|---|---|
| $a$ (Å) | 8.84 | 4.14 |
| $b$ (Å) | 15.726 | 12.85 |
| $c$ (Å) | 8.790 | 23.20 |
| $\beta$ | 92.61° | 93.0° |
| Space group | $P2_1/c$ | $P2_1/c$ |
| $\rho_{calc}$ (gm/cm$^3$) | 1.40 | 1.38 |
| Volume (Å$^3$) | 1220.7 | 1232.5 |

**TABLE II**
*Crystallographic Parameters for the Two Polymorphs of 1,2,5,6-Dibenzanthracene*

| Parameter | Form I | Form II |
|---|---|---|
| $a$ (Å) | 8.22 | 6.59 |
| $b$ (Å) | 11.39 | 7.84 |
| $c$ (Å) | 15.14 | 14.17 |
| $\beta$ | — | 103.5° |
| $Z$ | 4 | 2 |
| $\rho_{calc}$ (gm/cm$^3$) | 1.29 | 1.288 |
| Space group | $Pcab$ | $P2_1$ |
| Volume (Å$^3$) | 1417.5 | 711.9 |
| Volume/molecule | 354.4 | 355.9 |

**TABLE III**
*Crystal Parameters of the Various Polymorphs of Acridine* (3)

| | Form | | | | |
|---|---|---|---|---|---|
| | $\alpha$ | $\beta$ | $\gamma$ | $\delta$ | $\epsilon$ |
| $a$ (Å) | 16.18 | 16.37 | 17.45 | 15.61 | 11.375 |
| $b$ (Å) | 18.88 | 5.95 | 8.89 | 6.22 | 5.988 |
| $c$ (Å) | 6.08 | 30.01 | 26.37 | 29.34 | 13.647 |
| $\beta$ | 95°40′ | 141°20′ | — | — | 98°58′ |
| $Z$ | 8 | 8 | 16 | 12 | 4 |
| $\rho_{calc}$ (gm/cm$^3$) | 1.27 | 1.29 | 1.15 | 1.24 | 1.29 |
| Space group | $P2_1/a$ | $Aa$ | $Pnab$ | $P2_12_12_1$ | $P2_1/n$ |
| Habit | Needles | Plates | Laths | Laths | Prismatic |
| Volume (Å$^3$) | 1848.2 | 1826.3 | 4090.8 | 2848.7 | 918.2 |
| Volume/molecule | 231.0 | 228.3 | 255.7 | 237.4 | 229.5 |

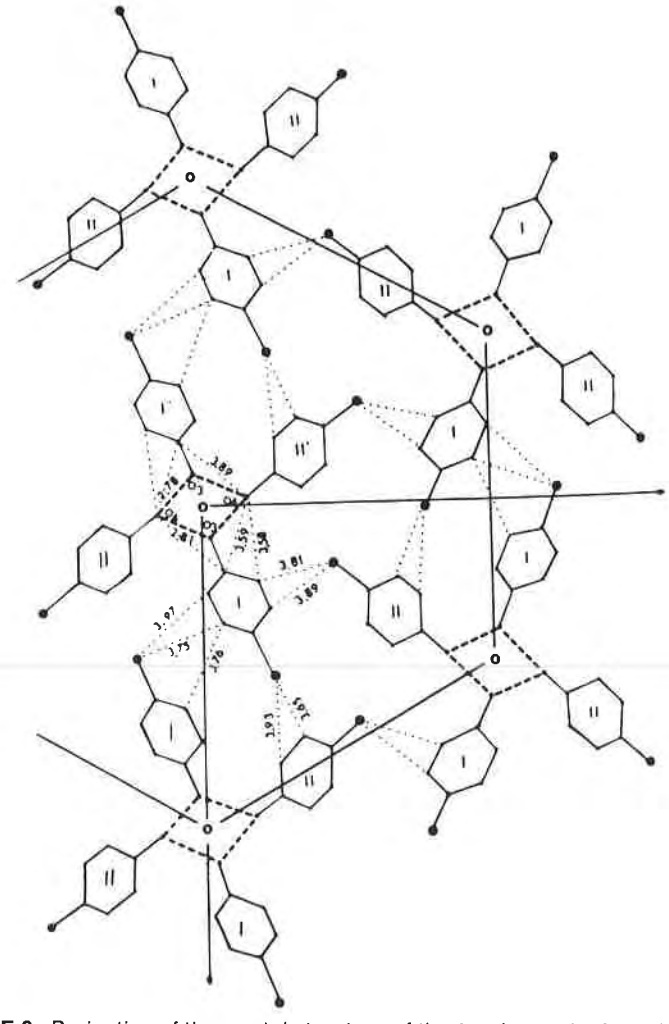

**FIGURE 2.** Projection of the crystal structure of the $\beta$-polymorph of *p*-chlorophenol on the *bc* crystal plane. The origin is in the center with *c* across, *b* down, and *a* out of the plane of the paper (Perrin and Michel, 1973).

The crystal packing of these forms appears to be quite similar, although the cell parameters are obviously different.

## B. POLYMORPHS THAT INTERCONVERT

In this section, organic polymorphs known to interconvert are reviewed. Of particular interest is the carefully studied equilibration of the two forms of *p*-dichlorobenzene.

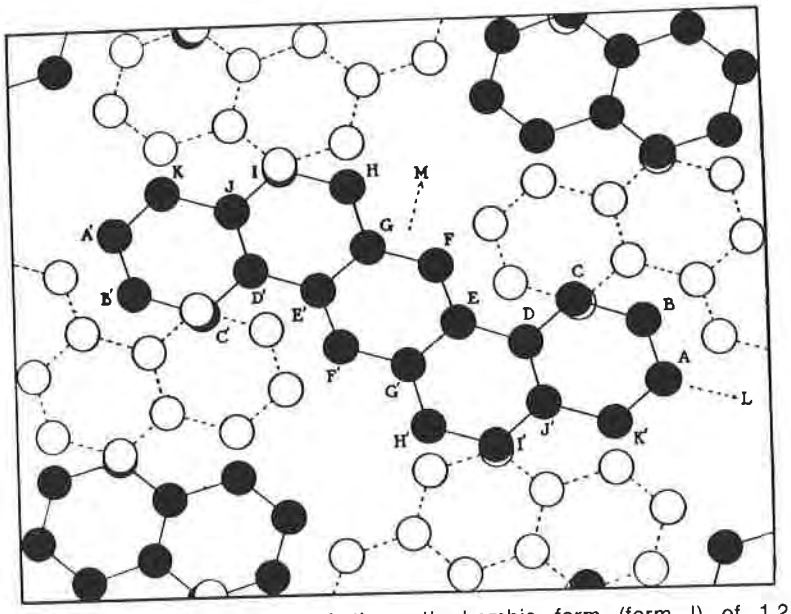


**FIGURE 3.** Crystal packing of the orthorhombic form (form I) of 1,2,5,6-dibenzanthracene. The origin is at the lower left, with *c* across and *b* up (Robertson and White, 1947).

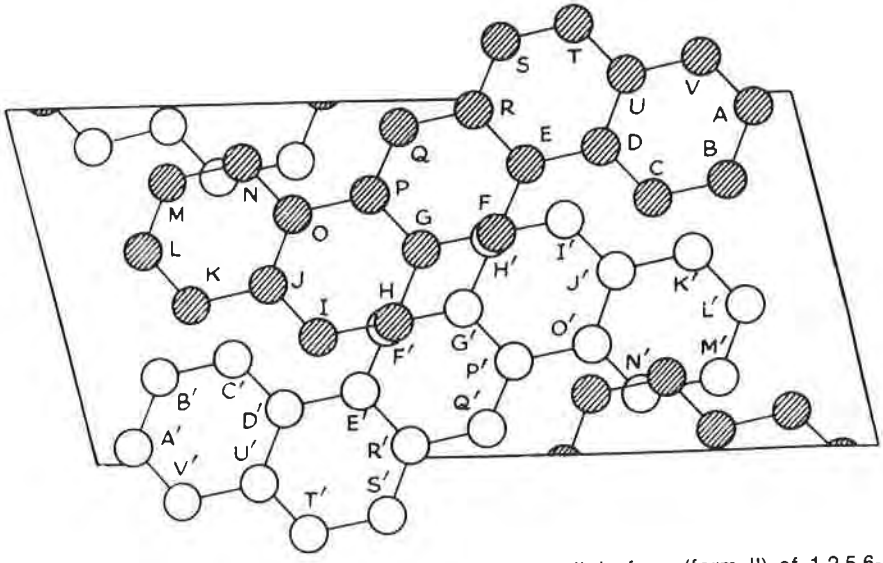


**FIGURE 4.** Crystal-packing drawing of the monoclinic form (form II) of 1,2,5,6-dibenzanthracene. The origin is at the lower right, with *a* across and *c* up (Robertson and White, 1956).

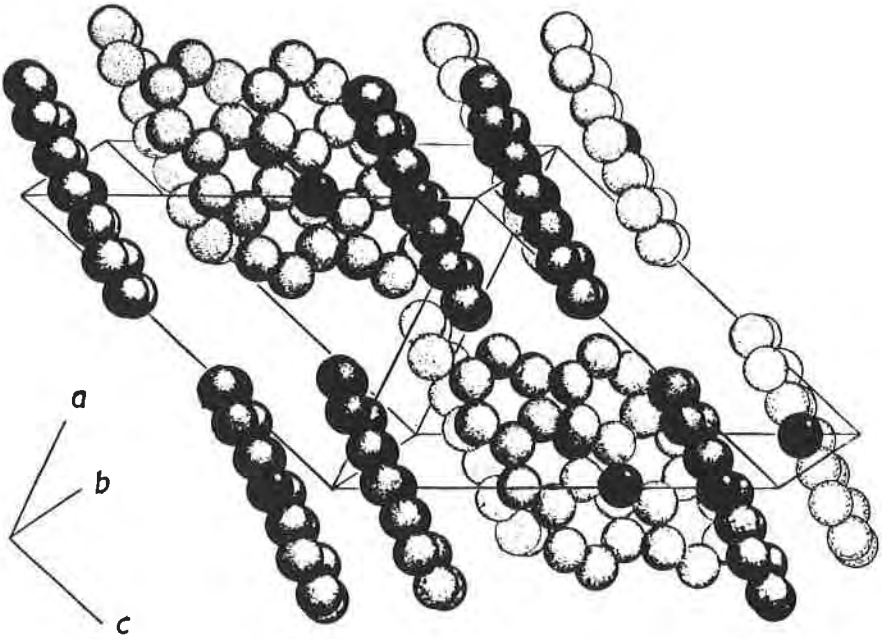


**FIGURE 5.** Projection of the structure of the $\alpha$-polymorph of acridine on the *ac* plane (Phillips, 1956).

### *1. Polymorphism of p-Dichlorobenzene*

The polymorphic transformation of $\alpha \rightleftarrows \beta$-*p*-dichlorobenzene (**4**) has been carefully studied. While only *p*-dichlorobenzene was examined in


4

detail, the results are suggested to have more general significance (Kitaigorodskii *et al.*, 1965).

The phase transformation was studied microscopically and crystallographically, showing that the reaction occurred by the growth of one crystal in the other. In general, there appears to be a great deal of similarity between the growth of one phase in the other and the growth of a crystal from solution. During the solid-state interconversion, a crystal of the $\alpha$ form grows in a crystal of the $\beta$ form or vice versa, showing front advancement in much the same way that *p*-dichlorobenzene crystals grow

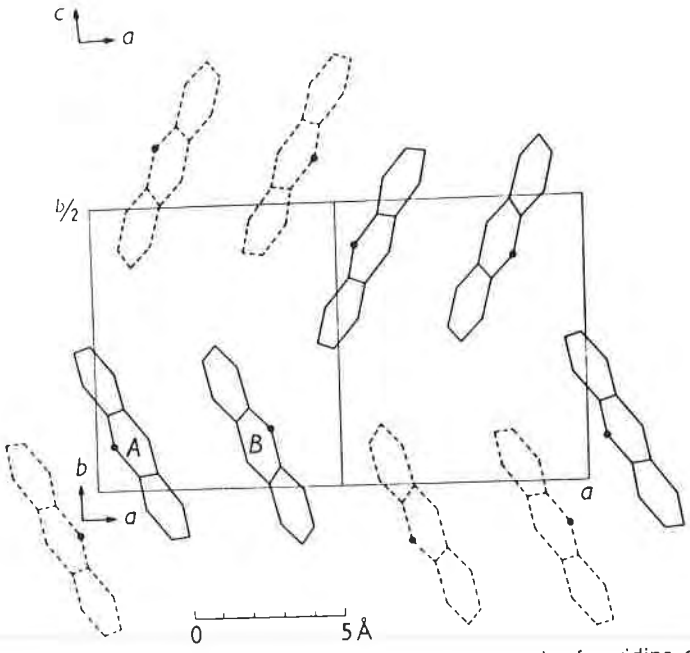


**FIGURE 6.** Projection of the structure of the γ-polymorph of acridine on the *ab* crystallographic plane (Phillips *et al.*, 1960).

from solution. In addition, the growth direction of the product crystal could be reversed by merely raising (or lowering) the temperature.

Crystallographic studies showed that there is no relationship between the orientation of the product crystal and the starting crystal. These crystallographic studies also showed that if the transformations are nucleated at a single site they are single-crystal-to-single-crystal transformations, while if they are nucleated at $n$ sites, then $n$ crystals of different orientation are formed. In addition, it was impossible to predict which crystals would nucleate at single sites and which at multiple sites. It was also found that in some cases, even if the phase transformation nucleated at one site, the product crystal contained microcrystallites of arbitrary relative orientation. In these cases, stresses and defects that occur during reaction are thought to induce the crystallization of many orientations of the product phases.

Studies of the nucleation process showed that in perfect crystals it was often impossible to induce a phase transformation, and these crystals simply melted at the melting point of the respective initial phase. However, with less perfect crystals it was often possible to induce the phase transformation by artificial creation of a defect, using a pin.

Studies of repeated transformations, $\alpha \rightarrow \beta \rightarrow \alpha \rightarrow \beta$, showed that when the transformation of a crystal began at one site it always began at that site, whether it was a $\beta \rightarrow \alpha$ or an $\alpha \rightarrow \beta$ transformation. Thus the crystal seemed to remember its nucleation site. This memory effect is explained by the conservation of the nucleation site at crystal defects. Thus repeated transformation does not destroy the nucleation site for this transformation.

The rates of the $\alpha \rightarrow \beta$ and $\beta \rightarrow \alpha$ polymorphic transformations were best studied by measuring the rate of advancement of the phase boundary or front under a microscope during heating. Each rate was determined by measuring the volume of the crystal transformed per unit time and was shown to be dependent on the location of the nucleus in the crystal as well as the crystal shape. For example, if the nucleus is in the center of the crystal and the reaction expands symmetrically, after a fixed time more crystal will be reacted than if the reaction started on the end. This is illustrated in Figure 2 of Chapter 3. For the nucleus in the center of the crystal, twice as much crystal is reacted as for an identical reaction from a nucleus on the end. Thus the rate of volume transformation depends on noncrystallographic factors and is therefore not a true measure of the absolute rate. This observation probably explains partially why there is great variation in the measured rates of solid-state reactions when measurements depend on the volume transformed (amount transformed) and not the rate of front advancement. Based on these observations, the rates were measured by determining the rate of advancement of the front in crystals which nucleated at a single site. Even with these measurements the rates of transformation of apparently similar crystals differed by a factor of 6. The rates were determined at different temperatures, and this data was used to calculate the activation energy of the process. The activation energy for the $\alpha \rightarrow \beta$ reaction was 17.4 ± 2.5 kcal/mole, while that for the $\beta \rightarrow \alpha$ process was 17.1 ± 2.5 kcal/mole. Thus, these measurements indicate the $\alpha$ and $\beta$ phases are within 1 kcal/mole of each other in energy.

### *2. Polymorphism and Phase Transformation of 5-Methyl-1-thia-5-azacyclooctane-1-oxide*

5-Methyl-1-thia-5-azacyclooctane-1-oxide (**5**) crystallizes in an $\alpha$ and a $\beta$ form wth the crystal parameters shown in Table IV (Paul and Go, 1969).

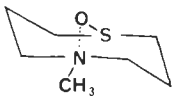


5

**TABLE IV**
*Crystal Parameters of the Two Polymorphs of 5-Methyl-1-thia-5-azacyclooctane-1-oxide*

| | Form | |
|---|---|---|
| | $\alpha$ | $\beta$ |
| $a$ (Å) | 9.87 | 20.10 |
| $b$ (Å) | 8.78 | 8.89 |
| $c$ (Å) | 13.26 | 6.67 |
| $\beta$ | 97°54′ | 97°48′ |
| Space group | $P2_1/c$ | $P2_1/a$ |
| Volume (Å$^3$) | 1138.2 | 1180.8 |

The crystal structures of both forms have been determined and are shown in Figure 7. The transformation can be explained in terms of either a ring-flipping mechanism or slipping of layers. This reaction is discussed in more detail in a subsequent chapter; however, regardless of the mechanism, the transformation is reversible and occurs upon cooling the $\beta$ form (which is stable at 25°C) to 3°C, at which point the $\alpha$ form is generated. Raising the temperature reverses this process. Interestingly, this is one of the few examples of a single-crystal-to-single-crystal transformation.

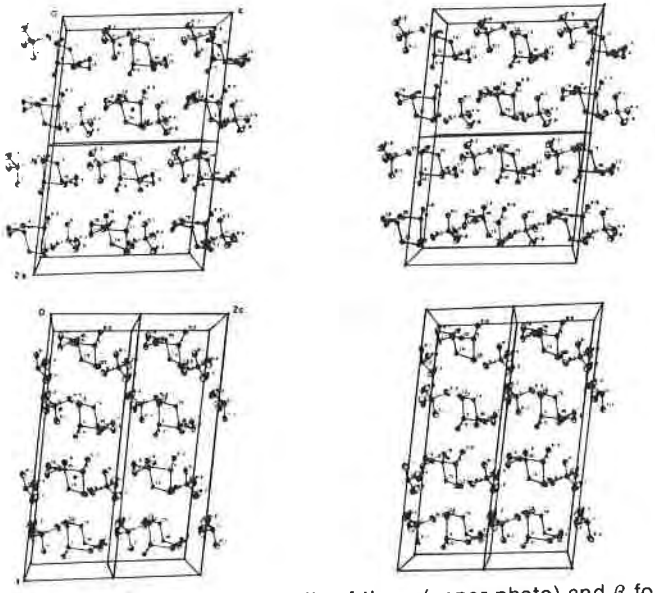

**FIGURE 7.** Stereo view of two unit cells of the $\alpha$ (upper photo) and $\beta$ form (lower photo) of 5-methyl-1-thia-5-azacyclooctane-1-oxide (Paul and Go, 1969).

### 3. Polymorphism and Phase Transformation of Resorcinol

Resorcinol (**6**) exists in two polymorphs, $\alpha$ and $\beta$ (Robertson and Ubbelohde, 1936). The $\alpha$ form is more stable than the $\beta$ form at room temp-

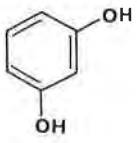


6

erature; however, it is less dense than the $\beta$ form. Resorcinol is one of the few substances known for which the denser polymorph is the metastable polymorph at room temperature. This situation is unusual, since normally the densest polymorph is the most stable form at room temperature.

Careful studies showed that upon transformation to the high-temperature $\beta$ polymorph there is (*a*) a contraction in volume, (*b*) no change in crystal symmetry, and (*c*) transition heat not exceeding 5% of the heat of fusion. In addition, the temperature factors show that the thermal motion in $\alpha$- and $\beta$-resorcinol is nearly the same.

A comparison of the crystal structure of the $\alpha$ and $\beta$ forms provides an explanation for the fact that the less dense $\alpha$ form is more stable at room temperature. The $\alpha$ form has significantly shorter hydrogen bonds than the $\beta$ form: thus the energy of the $\alpha$ form that is lost by being less dense is compensated for by the stronger hydrogen bonds. The hydrogen-bonding energy overcomes the loss in packing energy and renders the $\alpha$ form more stable than the $\beta$ form. This explanation is also consistent with the three experimental observations mentioned above.

### 4. Polymorphism and Phase Transformation of p-Nitrophenol

The phase transformation of $\beta$- to $\alpha$-*p*-nitrophenol (**7**) has been carefully studied and resembles, in many respects, the behavior of


7

**TABLE V**
*Crystal Parameters of the Two Polymorphs of p-Nitrophenol*

| Parameter | Form α | Form β |
|---|---|---|
| a (Å) | 14.8 | 15.40 |
| b (Å) | 8.9 | 11.12 |
| c (Å) | 6.17 | 3.79 |
| β | 130°25′ | 107°6′ |
| Space group | $P2_1/a$ | $P2_1/a$ |
| $\rho_{calc}$ (g/cm³) | 1.51 | 1.49 |
| Volume (Å³) | 618.8 | 620.3 |

*p*-dichlorobenzene (Cohen *et al.*, 1964). The crystallographic properties of these polymorphs are shown in Table V.

The crystal structures of both polymorphs are similar, and in both polymorphs the molecules are linked into infinite chains parallel to [100] by head-to-tail hydrogen bonding.

The $\beta \rightarrow \alpha$ phase transformation occurs upon heating a crystal of the $\beta$ form. During this transformation, the crystals retain their original shape and the product crystal consists of one or a small number of single crystals. This is quite similar to the behavior of *p*-dichlorobenzene. In addition, experiments with thin films showed that the orientation of the product crystal was not dependent upon the orientation of the starting one, again in marked similarity to the behavior of *p*-dichlorobenzene. Similar experiments with single crystals show that the orientation of the product crystal(s) was not related to the starting crystal.

### *5. The Induction of Phase Transformations by Stresses*

Phase transformations can be stress-induced (Thomas, 1974). Usual methods for introducing stresses in the crystal include mechanical deformations with a pin or cutting with a razor blade. For example, 1,8-dichloro-10-methylanthracene (**8**) undergoes a stress-induced phase trans-

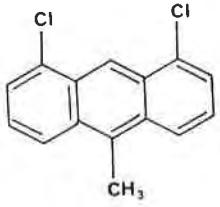


8

formation. In addition, the orientation of the product crystal is related to the starting crystal. Thus for this compound the generalizations of Mnyukh and Kitaigorodskii based on *p*-dichlorobenzene do not seem to apply.

It is interesting to note that 1,8-dichloro-9-methylanthracene, unlike the 10-isomer, does not undergo a phase transformation, but merely conformational twinning.

### *6. Phase Transformations of Racemic to Chiral Crystals*

A number of chiral organic compounds—including amino acids, drugs, and tartaric acid—crystallize in both racemic and chiral crystals. In the racemic crystals, both *R* and *S* isomers are present in the unit cell, and thus an individual crystal contains both isomers. In the chiral crystals, an individual crystal contains only the *R* or the *S* isomer.

A third class of compounds, including 1,1′-binaphthyl (**9**), belongs to a special group of compounds that exist in rapidly equilibrating isomers that

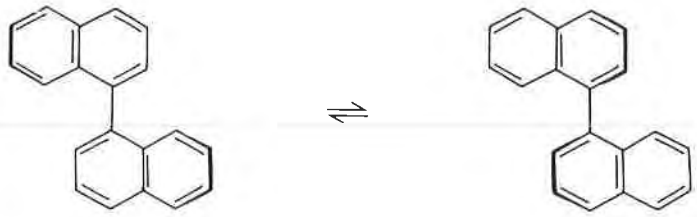

R-9 S-9

are individually chiral. Upon crystallization, two polymorphs are found. One polymorph contains chiral molecules (either *R* or *S*), while the other contains both *R* and *S* isomers and is thus the racemic crystal. In this second case, separation of crystals cannot lead to a resolution, while in the first case separation of the crystals leads to a resolution in the same way that tartaric acid was resolved by Pasteur.

Surprisingly, for binaphthyl the chiral crystals that contain either the *R* or *S* isomers have a melting point of 158°C and are more stable than the racemic crystals. Heating the racemic polymorph causes a transformation to the chiral crystals. The kinetics of this transformation have been studied by measuring the optical rotation of batches of crystals during heating (Wilson and Pincock, 1977). Grinding seemed to accelerate the transformation but to a lower overall optical rotation. Storage of partially reacted samples resulted in higher final rotations. These observations can be explained as follows. During heating, the racemic crystals are seeded and either the *R* or *S* chiral crystals grow from the racemic crystal until com-

plete conversion is attained. However, in the ground crystals many more seeds and nucleii are formed due to the mechanical stress, and the conversion of racemic crystals to chiral crystals leads to a larger number of $R$ and $S$ crystals and thus a closer approach to the statistically expected 1 : 1 ratio of $R$ and $S$ crystals. Thus ground crystals lead to a lower optical rotation. In contrast, storage allows annealing, which leads to fewer crystals and thus on the average a higher overall rotation. These reactions are quite similar to those of $p$-dichlorobenzene, where the product contains one or a few single crystals and mechanical defects lead to seeds at which the transformation begins.

The kinetic data were also fitted to both the Avrami–Erofeev equation $[-\log(1 - y) = (kt)^n]$ and the Prout–Tompkins equation $(\log[y/(1 - y)] = kt)$. The Prout–Tompkins plot gave a straight line with an average activation energy of approximately 60 kcal/mole. This large activation energy is consistent with similar measurements for some other phase transformations and may be related to the energy required to remove a molecule from the center of the crystal to the vapor state. This implies that this reaction may proceed via a mechanism that involves vaporization of a few molecules, isomerization, and crystallization—a suggestion consistent with the rate of the solid-state reaction, which is much slower than the solution- or gas-phase isomerization. Since only a small percentage of the molecules are vaporized at any given time the effective concentration of the reactant is very small; thus, such a reaction should be much slower than the same reaction in solution or the gas phase.

In contrast, the activation energy for phase transformation for $p$-dichlorobenzene was much smaller (~17 kcal/mole). More research is needed to explain this large difference in activation energy between $p$-dichlorobenzene and binaphthyl.

## C. CONFORMATIONAL POLYMORPHISM

### *1. p-(N-Chlorobenzylidene)-p-chloroaniline*

The Schiff's base $p$-($N$-chlorobenzylidene)-$p$-chloroaniline (**10**) crystallizes in two polymorphs (Bernstein and Hagler, 1978). The stable form belongs to the triclinic crystal system, and the unstable form belongs to the orthorhombic crystal system. Both polymorphs are disordered, but

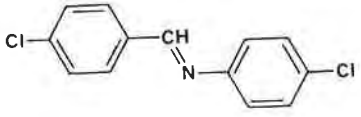


10

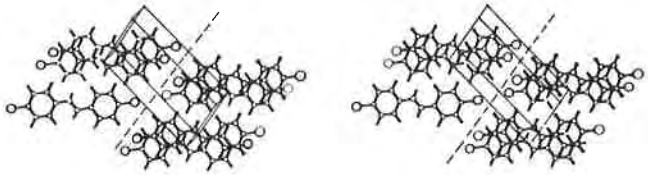

**FIGURE 8.** Stereo view of the triclinic polymorph of the Schiff's base **10.** The origin is at the lower top corner, with the *b* axis out of the plane of the paper (Bernstein and Hagler, 1978). (Reprinted with permission from J. Bernstein and A. T. Hagler [1978]. Copyright 1978 American Chemical Society.)

the conformation of the molecule is strikingly different in the two polymorphs. Thus these forms can be termed conformational polymorphs.

In the triclinic form, the molecules are planar, while in the orthorhombic form the phenyl rings are rotated by equal but opposite amounts (24.8°) about the N–phenyl and CH–phenyl bonds. The crystal packing of these two forms is shown in Figures 8 and 9.

Molecular orbital and lattice energy calculations were used to analyze the reasons for conformational polymorphism of **10** (Bernstein and Hagler, 1978). The quantum-mechanical calculations showed that the nonplanar form of the molecule was energetically favored by perhaps 0.5 to 1.5 kcal/mole. The lattice-energy calculations were performed using semiempirical potential functions and showed that the planar structure (triclinic) gave a lower lattice energy. These calculations explain why the triclinic polymorph is the stable polymorph (by about 1 kcal/mole) and why the less stable planar conformer is present in the most stable crystal polymorph.

A more recent study was aimed at explaining why the lowest energy conformer of **10** was not observed in the crystal. In this study, the predicted lowest energy conformation was found to be the crystalline conformation in crystals of **11** where both chlorine atoms are replaced by methyl groups. The torsion angles of **11** are 41.7° about the N–phenyl bond and −3° about the C–phenyl bond. Using the lattice-energy calcula-

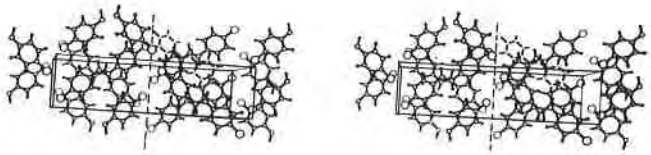

**FIGURE 9.** Stereo view of the orthorhombic polymorph of **10.** The origin is the upper left-hand corner, with *a* across, *b* down, and *c* into the paper (Bernstein and Hagler, 1978). (Reprinted with permission from J. Bernstein and A. T. Hagler [1978]. Copyright 1978 American Chemical Society.)

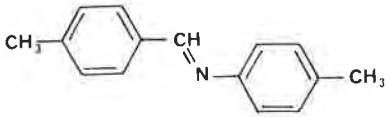

11

tions, the dichloro compound was put into this lattice and its energy was calculated. These calculations showed that such a crystal is less stable than the orthorhombic form by 1.5 kcal/mole and less stable than the triclinic form by 2.5 kcal/mole. This explains why the most stable conformation of **10** is not observed in the solid state.

In conclusion, this study explains in some detail the factors that control the crystalline conformation of a drug. These factors include crystal packing and the stable conformation of the drug.

### *2. Tri-α-naphthylboronamine*

Brown and Sujishi (1948) reported an early example of conformational polymorphism. The data supporting conformational polymorphism are as follows:

1. Two crystalline forms of tri-α-naphthylboronamine (**12**) are found.
2. The metastable form is converted to the stable form slowly at room temperature and rapidly above 100°C.
3. The dissociation pressure of the metastable form is higher than the stable form.
4. Removal of $NH_3$ from either form gives identical samples of tri-α-naphthylboron.

Based on these results, the two forms were suggested to have structures **12a** and **12b.** In these two forms the conformation of the tri-α-

12a 12b

naphthylboron is the same except that the $NH_3$ is connected on the more hindered side for the unstable form and the less hindered side for the stable form. Thus these structures explain the difference in dissociation

pressures of the two forms and the fact that removal of $NH_3$ gives the same conformer of tri-$\alpha$-naphthylboron. These structures also explain why the unstable form can be converted to the stable form, since it is the more sterically hindered form.

Unfortunately, while this was one of the first suggestions of conformational polymorphism it was never confirmed by x-ray crystallographic analysis. Clearly this is a case where further studies are needed.

*3. 1,10-Diphenyl-1,3,5,7,9-decapentane*

The polyene 1,10-diphenyl-1,3,5,7,9-decapentane (**13**) crystallizes in two crystalline forms (Drenth and Wiebenga, 1954). One form belongs to

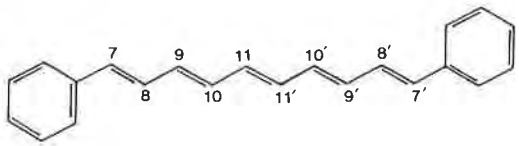


13

the monoclinic crystal system, while the other belongs to the orthorhombic system (See Table VI).

The molecules have slightly different conformations in the two forms. In the monoclinic form there is very little twist of the phenyl ring out of the plane determined by C9′, C10′, and C11′, while in the orthorhombic form this twist is 7.5°. The conformation of the two forms is shown in Figure 10. The crystal packing of these two forms is also different and is shown in Figure 11. While this example involves only a slight twist of a phenyl group, it clearly illustrates that conformational polymorphism can involve small as well as large conformational differences. In addition,

**TABLE VI**
*Cell Parameters for the Polymorphs of the Polyene* (*13*)

| Parameter | $\alpha$, Monoclinic | $\beta$, Orthorhombic |
|---|---|---|
| $a$ (Å) | 6.23 | 10.06 |
| $b$ (Å) | 7.45 | 7.57 |
| $c$ (Å) | 17.91 | 22.03 |
| $\beta$ | 83°3′ | — |
| $\rho_{calc}$ (gm/cm³) | 1.145 | 1.126 |
| $Z$ | 2 | 4 |
| Space group | $P2_1/a$ | $Pcab$ |
| Volume (Å³) | 825.2 | 1677.7 |
| Volume/molecule | 412.6 | 419.4 |

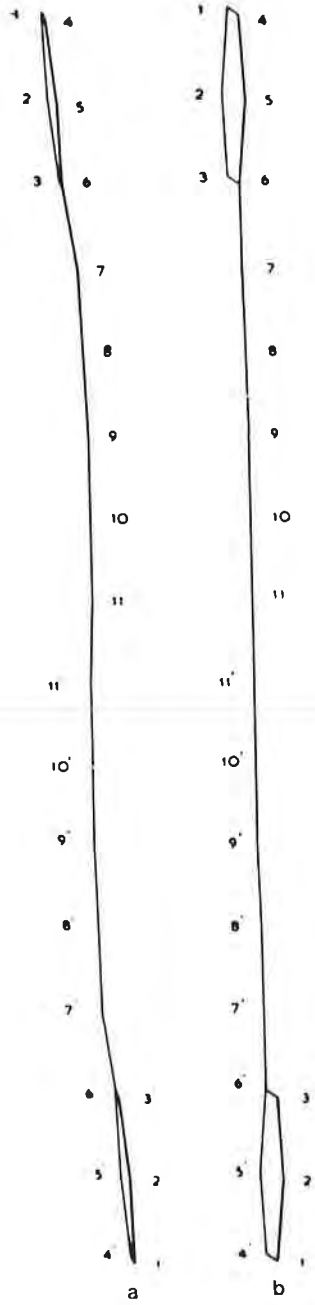


**FIGURE 10.** Shape of 1,10-diphenyl-1,3,5,7,9-decapentane in (*a*) the monoclinic polymorph and (*b*) the orthorhombic polymorph (Drenth and Wiebenga, 1954).

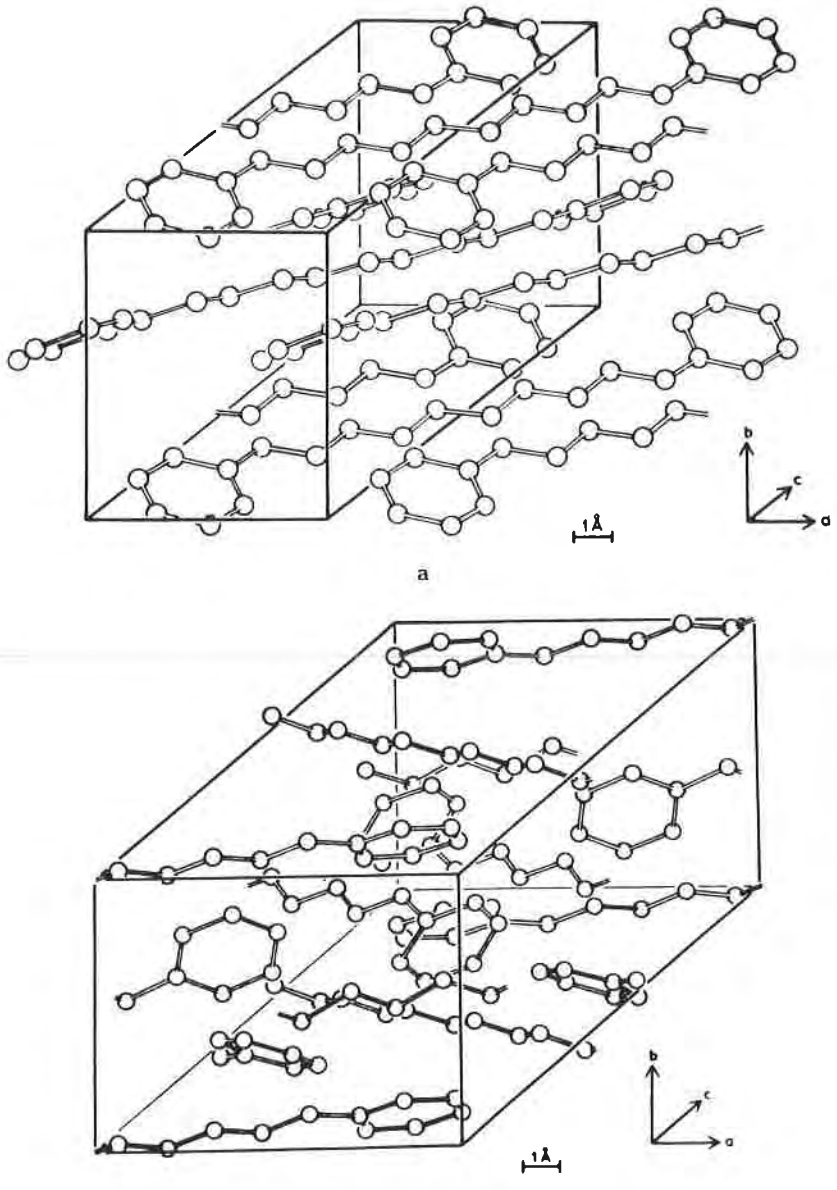


**FIGURE 11.** The crystal packing of (*a*) the monoclinic polymorph and (*b*) the orthorhombic polymorph of 1,10-diphenyl-1,3,5,7,9-decapentane (Drenth and Wiebenga, 1954).

Drenth and Wiebenga (1954) showed that the monoclinic form could be transformed into the orthorhombic form at 160° to 180°C.

### 4. 3-Oxo-3H-2,1-benzoxiodol-1-yl m-Chlorobenzoate

As part of their extensive study of the crystal chemistry of iodoperoxides, Gougoutas and Lessinger (1974) determined the crystal structure of two polymorphs of 3-oxo-3*H*-2,1-benzoxiodol-1-yl *m*-chlorobenzoate (**14**). This compound crystallizes in $\alpha$ and $\beta$ forms that both belong to the monoclinic crystal system (Table VII).

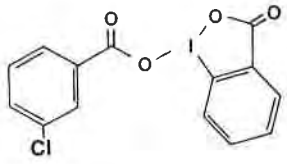


14

The $\alpha$ form is essentially planar in the crystal, while in the $\beta$ form the two phenyl rings make an angle of approximately 55° with each other. The crystal packing of the two forms is also different as shown in Figures 12 and 13. Even more interesting is the fact that these two forms have different solid-state infrared spectra (Figure 14). This suggests that infrared spectroscopy might be used to determine whether conformational polymorphs exist.

In this regard it is interesting to note that infrared spectroscopy may be a useful tool to investigate polymorphism. However, if the conformation of the compound is identical in the different polymorphs, it is expected that the infrared spectra would be nearly identical. Further studies are needed on systems where the crystal structure is known before conclusions concerning the usefulness of infrared spectra to investigate conformational polymorphism and polymorphism in general can be drawn.

**TABLE VII**
*Crystallographic Unit Cell Parameters for the Chlorobenzoate* (**14**)

| Parameter | $\alpha$ Form | $\beta$ Form |
|---|---|---|
| *a* (Å) | 6.376 | 5.057 |
| *b* (Å) | 10.547 | 13.035 |
| *c* (Å) | 20.066 | 10.339 |
| $\beta$ | 92.0° | 99.5° |
| Volume (Å$^3$) | 1348.6 | 672.2 |

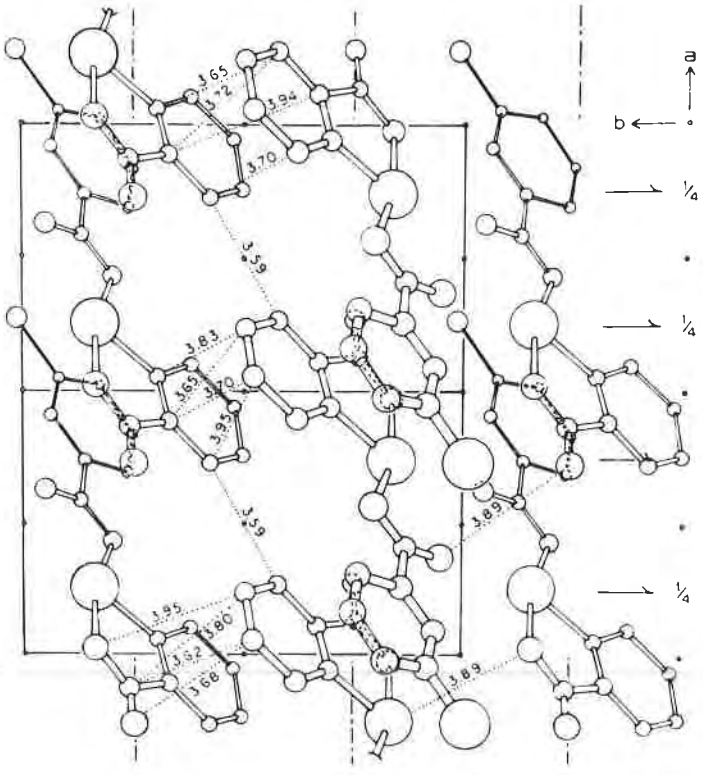


**FIGURE 12.** The crystal packing of the $\alpha$ form of 3-oxo-3H-2,1-benzoxiodol-1-yl *m*-chlorobenzoate (Gougoutas and Lessinger, 1974).

## D. CONFIGURATIONAL POLYMORPHISM

### *1. Ethyl β-Benzylaminocrotonate* (15)

Infrared studies (Dabrowski, 1963; Dabrowski and Dabrowski, 1968; Schad, 1955) and NMR studies (Dudek and Volpp, 1963) indicate that the Schiff's base **15** exists in configurational polymorphs, with the low-

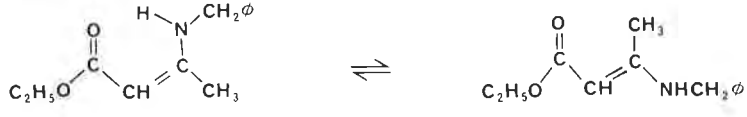


15a 15b

melting form (mp 23°C) having the cis or *Z* structure **15a** and the high-melting form (mp 75–80°C) having the trans or *E* structure **15b.** These

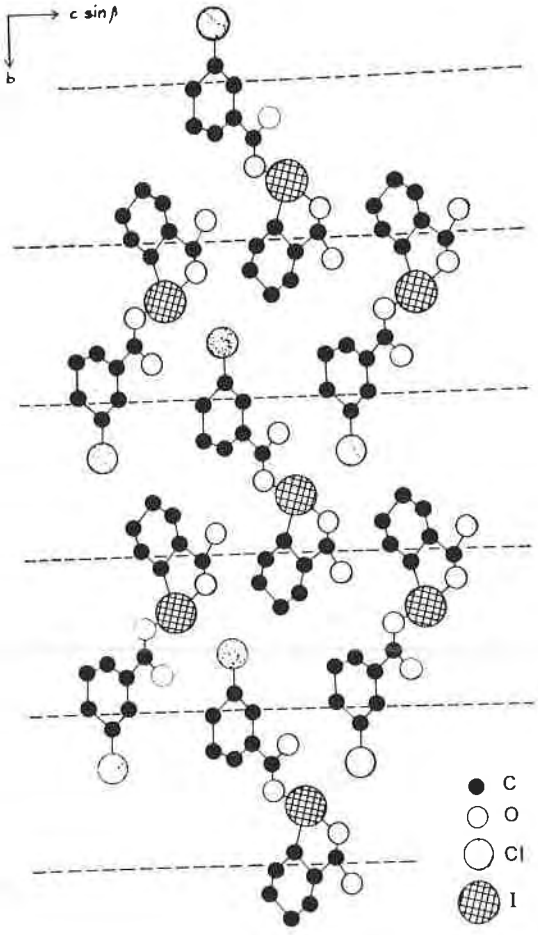


**FIGURE 13.** The crystal packing of the $\beta$ polymorph of 3-oxo-3H-2,1-benzoxiodol-1-yl *m*-chlorobenzoate projected along (100) Gougoutas and Lessinger, 1974).

isomers equilibrate in solution, but upon crystallization the configurations shown are "frozen" out.

The crystal structure of isomer **15b** has been determined in our laboratory. Crystals of **15b** belong to space group $P2_12_12_1$ with $a = 19.655$, $b = 5.778$, and $c = 10.632$ Å. Figure 15 shows the structure of this isomer, and indeed it has the structure **15b** suggested based on spectroscopic evidence (Dudek and Volpp, 1963).

The NMR and IR spectra of **15** are completely consistent with this

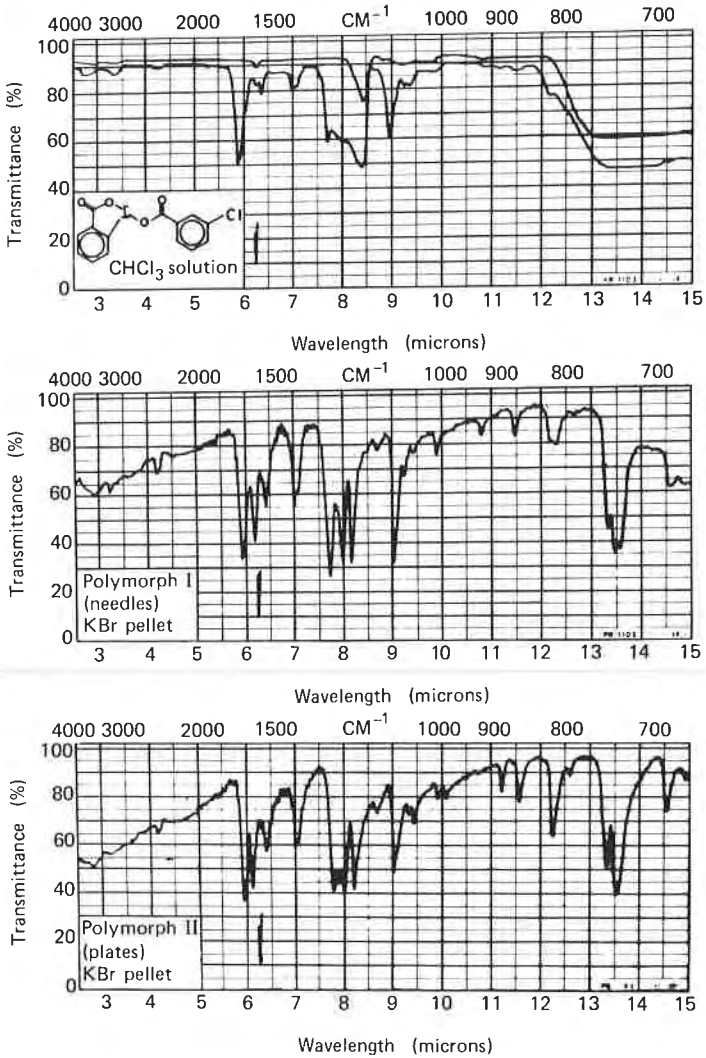


**FIGURE 14.** The infrared spectra of 3-oxo-3*H*-2,1-benzoziodol-1-yl *m*-chlorobenzoate. Top: chloroform solution (with base line). Middle: the $\alpha$ polymorph (KBr pellet). Bottom: the $\beta$ polymorph. (Gougoutas and Lessinger, 1974).

assignment. The NMR spectrum of a solution prepared by dissolving crystals of **15a** at low temperature indicates that **15a** has the structure shown (Dudek and Volpp, 1963). In this experiment the isomer present in the solid state predominates in solution because of the low temperature. In

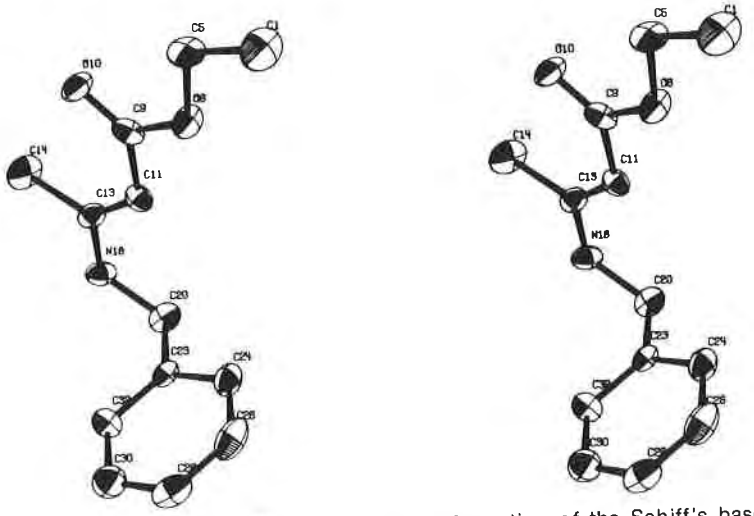


**FIGURE 15.** A stereoscopic view of the conformation of the Schiff's base ethyl $\beta$-benzylaminocrotonate (**15b**) in the high-melting crystalline form.

our laboratory we have studied the rate of isomerization of **15a** to **15b** at ambient temperature. In DMSO the rate of isomerization of **15a** to **15b** is relatively rapid. Measurement of the rate of this reaction at various temperatures gives an activation energy of 13.6 kcal/mole.

The energies in kcal/mole of a number of rotamers of **15a** and **15b** have been calculated using the CAMSEQ program (Weintraub and Hopfinger, 1975). This program uses semiempirical potential functions such as the Lennard–Jones 6–12 potential and an electrostatic function to calculate the energies of each rotamer. Because semiempirical functions are used, this program is much faster than quantum-mechanical programs. These calculations indicate that the x-ray conformation of **15b** is one of the lowest energy conformations. These calculations also indicate that isomers **15a** and **15b** have nearly the same energy in vacuum.

### *2. Configurational Polymorphism due to Tautomers: Tautomerizational Polymorphism*

Schulenberg (1968) has reported the crystallization of the keto and enol tautomers of **16.** Compound **16** crystallized in two forms. One form had a melting point of 93°–99°C and upon dissolution in $CDCl_3$ gave NMR spectra consistent with **16a.** The other form had a melting point of 110°–122°C and upon dissolution gave NMR spectra consistent with the enol form **16b.** Addition of triethylamine to either solution gave an equilibrium mixture containing 70% **16a** and 30% **16b.**

Although the crystal structures of **16a** and **16b** have not been deter-

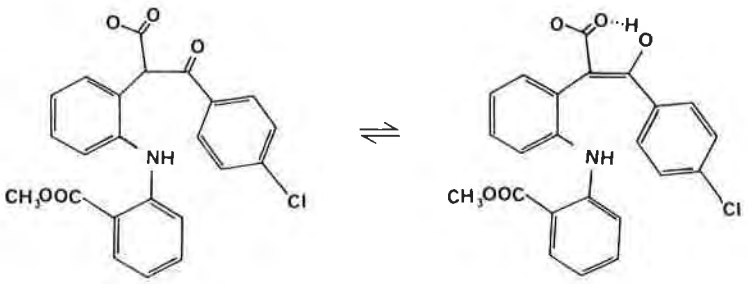


16a 16b

mined, this study illustrates a case where two different crystalline forms exist each containing an individual tautomer. This situation could be termed tautomerizational polymorphism.

*3. Conclusion*

Note that several other cases of configurational polymorphism exist. For example, **17** crystallizes in two forms. One form contains **17a** and the


17a 17b

other contains **17b** (Eistert *et al.*, 1952). In addition, there are numerous examples of the crystallization process freezing one configurational isomer or tautomer out of solution. These cases are reviewed by Curtin and Engelmann (1972).

## II. Polymorphism of Sulfonamides

The polymorphism of sulfonamides has been investigated and reviewed by Kuhnert-Brandstatter using a Kofler hot stage. Sulfonamides exhibited behavior expected of polymorphs, including successive melting points as the temperature is raised and changes in color under crossed Nicols. Table VIII summarizes the results of Kuhnert-Brandstatter's (1971) studies on these compounds. It should be noted that these studies

**TABLE VIII**
*Polymorphism of Sulfonamides and Related Compounds*[a]

| Compound | Melting point of form (°C) | | | | | | |
|---|---|---|---|---|---|---|---|
| | I | II | III | IV | V | VI | VII |
| Acetazolamide | 258–260 | 248–250 | | | | | |
| Acetylsulfisoxazole | 190–195 | 176–177 | 173–174 | | | | |
| Chlortalidone | 212–224 | 188–189 | | | | | |
| Clofenamide | 210–215 | 203–207 | 183–185 | 168–170 | | | |
| Diphenylmethane-4,4′-disulfonamide | 185–187 | 172–174 | | | | | |
| Mafenide hydrochloride | 250–260 | 235–240 | 220–225 | 210–212 | | | |
| *N′*-Methyl-*N*⁴-sulfanilylsulfanilamide | 148–151 | 144–146 | | | | | |
| Phthalylsulfathiazole | 260–274 | 230 | | | | | |
| Sulfachlorpyridazine | 196–197 | 178–181 | | | | | |
| Sulfadichramide | 176–180 | 174–176 | | | | | |
| Sulfadimidine | 206–208 | 199 | 178 | ~175 | | | |
| Sulfaethidole | 188 | 181 | 149 | | | | |
| Sulfafurazole | 190–195 | 131–133 | | | | | |
| Sulfaguanidine | 187–191 | 174–176 | 143–145 | | | | |
| Sulfamerizine | 235–238 | 228 | | | | | |
| Sulfameline | 210–212 | 197–199 | 181–183 | 179–181 | 176–177 | 155 | |
| Sulfamethizole | 209 | 193 | | | | | |
| Sulfamethaoxazole | 169 | 168 | 166 | | | | |
| Sulfamethoxypyridazine | 180–182 | 158–159 | 153–154 | | | | |
| Sulfamoxole | 200–204 | 188–195 | 177–180 | | | | |
| 4′-Sulfamoyl-2,4-diaminoazobenzeze | 224–228 | 217–219 | 212 | | | | |
| Sulfanilamide | 165 | 156 | 153 | | | | |
| *N*-Sulfanilyl-3,4-xylamide | 215–218 | 208 | 203 | 196 | | | |
| Sulfapyridine | 192 | 185 | 179 | 176 | 174 | 167 | 149 |
| Sulfathiazole | 202 | 175 | 162 | 158 | | | |
| Sulfathiourea | 178–180 | 168–171 | | | | | |
| Sulfatriazine | 158–166 | 132–135 | | | | | |
| Sulfametoxin | 194–198 | 176–177 | 156–158 | | | | |
| Tolbutamide | 127 | 117 | 106 | | | | |
| Vesulong | 182–185 | 176–178 | | | | | |

[a] This table shows the melting points of the polymorphic forms of the various drugs. (Data from Kuhnert-Brandstatter, 1971).

have not been confirmed by crystallographic studies and should be considered tentative.

The crystal structures of several polymorphs of sulfonamides have been determined and will be discussed next. In general, the conformations of the drug are similar in the different polymorphs. Thus differences in crystal packing are mainly responsible for polymorphism.

## A. POLYMORPHISM OF SULFANILAMIDE

Sulfanilamide (**18**) exists in three crystalline forms, which have the crystallographic parameters shown in Table IX. The $\alpha$ form has the crystal

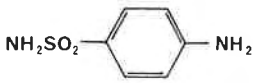


18

packing shown in Figure 16 (O'Connor and Maslen, 1965). The crystal packing of this form contains layers of phenyl rings and sulfonamide groups. In each stack there is an amino group, an amino group, a sulfonamide group, a sulfonamide group, an amino group, etc.

The crystal packing of the $\beta$ form is shown in Figure 17 and is quite different from the $\alpha$ form (Alleaume and Decap, 1965). There are again layers of phenyl rings and sulfonamide groups. However, in the layers the order of groups is sulfonamide, amino group, sulfonamide, amino group, etc.

The crystal packing of the $\gamma$ form is shown in Figure 18 and in general appears to be similar to the $\alpha$ form with layers of phenyl rings and sulfonamide amino groups. In these layers the stacking is amino group, sulfonamide, amino group, sulfonamide, etc. (Alleaume and Decap, 1966).

Since the density of the $\beta$ form is greatest, the principle of closest packing would predict that it is the most stable form; however no studies of the interconversion of these forms have been reported. It is interesting to note that the conformation of the sulfanilamide group is similar in all forms, with the nitrogen atom being the atom furthest out of the plane of the phenyl ring.

A fourth form of sulfonanilamide has been reported with cell param-

**TABLE IX**
*Crystallographic Data for the Polymorphs of Sulfanilamide*

| | Crystal form | | |
|---|---|---|---|
| Parameter | $\alpha$ | $\beta$ | $\gamma$ |
| $a$ (Å) | 5.65 | 8.975 | 7.95 |
| $b$ (Å) | 18.509 | 9.005 | 12.945 |
| $c$ (Å) | 14.794 | 10.039 | 7.79 |
| $\beta$ | — | 111°26′ | 106°30′ |
| $Z$ | 8 | 4 | 4 |
| Space group | *Pbca* | $P2_1/c$ | $P2_1/c$ |
| Volume (Å$^3$) | 1547.1 | 755.2 | 768.7 |
| $\rho_{calc}$ (gm/cm$^3$) | 1.47 | 1.514 | 1.486 |

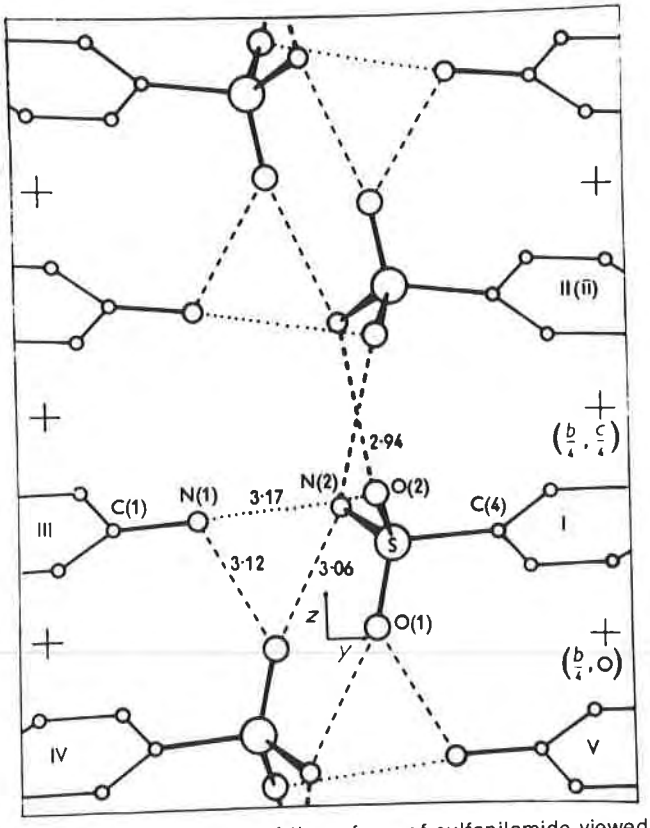


**FIGURE 16.** Molecular packing of the $\alpha$ form of sulfanilamide viewed from the a crystallographic direction. The symbols I, II, III, IV, V refer to molecules at $(x, y, z)$; $(-\frac{1}{2} + x, y, \frac{1}{2} - z)$; $(\frac{1}{2} - x, -\frac{1}{2} + y, z)$; $(-x, -y, -z)$; and $(\frac{1}{2} + x, \frac{1}{2} - y, -z)$ (O'Connor and Maslen, 1965).

eters $a = 14.81$, $b = 5.65$, and $c = 18.46$ Å (Lin *et al.*, 1974). This form belongs to the orthorhombic system and is probably identical to the $\alpha$ form, since the cell parameters are nearly identical.

## B. POLYMORPHISM OF SULFATHIAZOLE

Sulfathiazole (**19**) exists in three polymorphs as shown in Table X. Form I is the least stable of the three forms. Forms II and III are of nearly

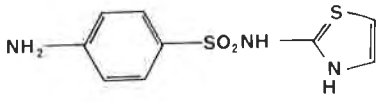


19

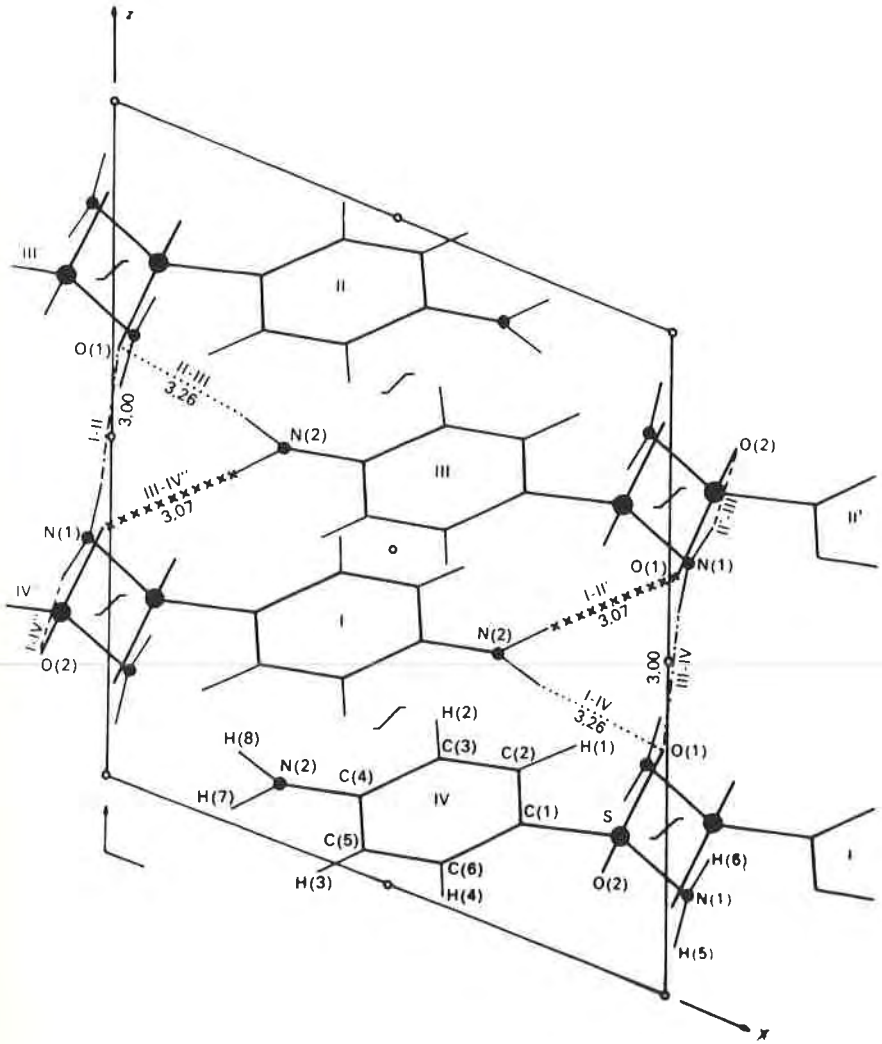


**FIGURE 17.** The crystal packing of the $\beta$ form of sulfanilamide projected on the *xz* plane (Alleaume and Decap, 1965).

equal stability. This order of stability is consistent with the measured and calculated densities.

Figures 19–21 show packing drawings of all three polymorphs. It is obvious that the N atom of the sulfonamide group is the atom that is the greatest distance from the plane of the phenyl ring. This is in marked similarity to sulfanilamide. In addition, the conformation of the molecule

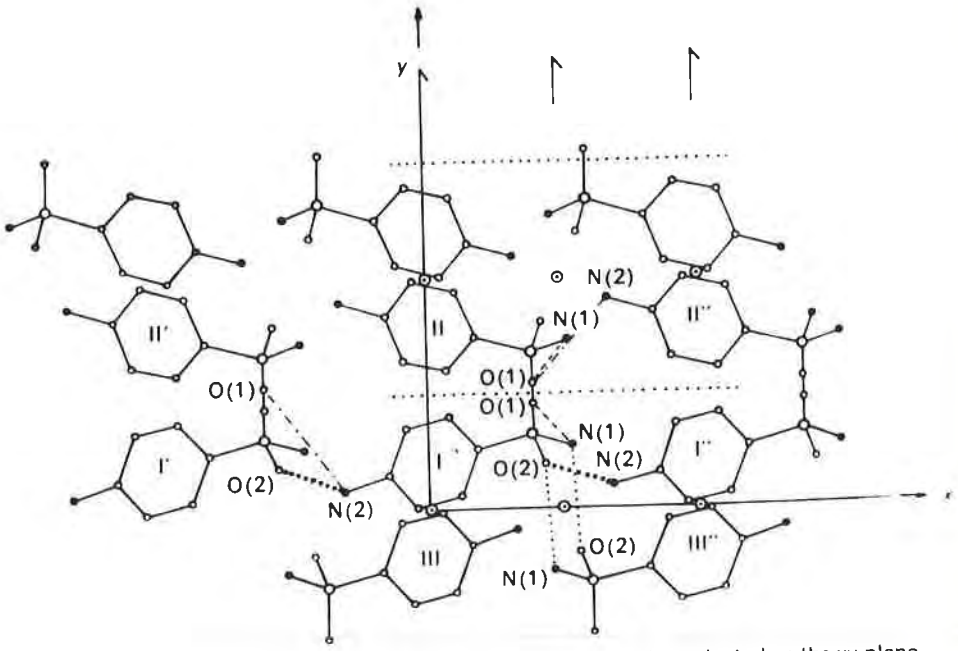


**FIGURE 18.** Crystal packing of the γ form of sulfanilamide projected on the *xy* plane (Alleaume and Decap, 1966).

**TABLE X**
*Crystallographic Parameters for the Polymorphs of Sulfathiazole* (**19**)

| Parameter | Forms | | |
|---|---|---|---|
| | I | II | III |
| Melting point | 200–202 | 200–202 | 173–175 (or 200–202) |
| Transition point | — | 173–175 | 173–175 |
| Habit | Rods | Hexogonal prisms | Hexagonal plates |
| Space group | $P2_1/c$ | $P2_1/c$ | $P2_1/c$ |
| *a* (Å) | 10.554 | 8.235 | 17.570 |
| *b* (Å) | 13.220 | 8.550 | 8.574 |
| *c* (Å) | 17.050 | 15.558 | 15.583 |
| $\beta$ | 108.06° | 93.67° | 112.93° |
| *Z* | 8 | 4 | 8 |
| Volume (Å$^3$) | 2261.7 | 1093.2 | 2162.0 |
| $\rho_{meas}$ (gm/cm$^3$) | 1.50 | 1.55 | 1.57 |
| $\rho_{calc}$ (gm/cm$^3$) | 1.50 | 1.55 | 1.57 |

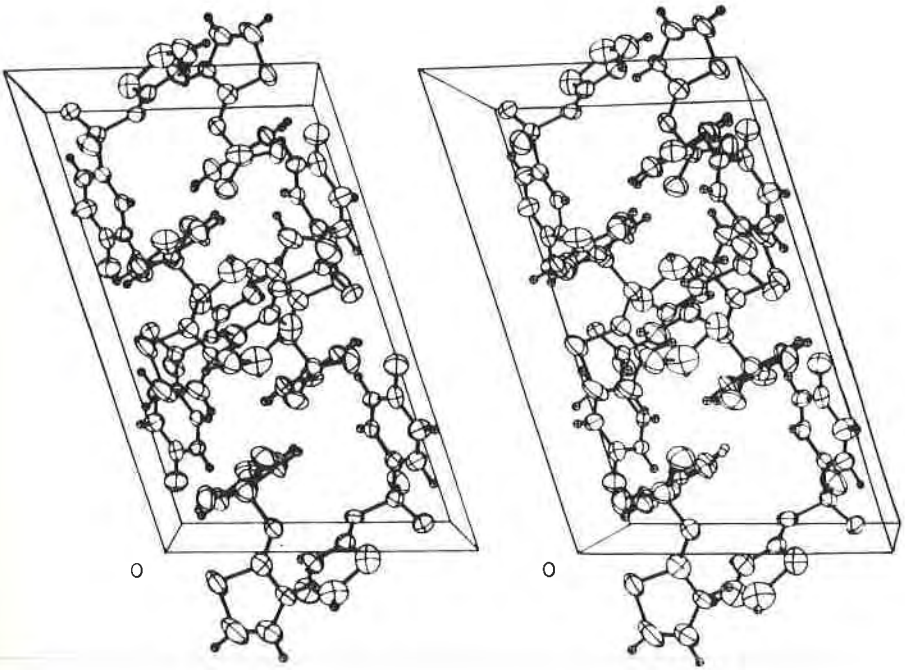

**FIGURE 19.** A stereopair view of the crystal packing of polymorph I of sulfathiazole. The view is along the *b* axis, with the *a* axis horizontal (Kruger and Gafner, 1972).

in all three forms is very similar. The major crystallographic difference between these forms is the nature and type of hydrogen bonds.

The crystallographic data clearly establishes the existence of at least three polymorphs of sulfathiazole; however, at this point it is worthwhile to review studies of the polymorphism of this drug using other techniques. As reported earlier in this chapter, Kuhnert-Brandstatter reported that sulfathiazole has four polymorphs based on hot stage microscopy. In the 1960s, three groups of workers—Milosovich (1964), Guillory (1962), and Higuchi *et al.* (1967)—reported that sulfathiazole existed in only two polymorphs. Differential scanning calorimetry also indicated the existence of only two polymorphs (Shenouda, 1970). More recent studies by Mesley (1971) using infrared spectroscopy, differential scanning calorimetry, and x-ray powder diffractometry showed that there were three polymorphs of sulfathiazole. He suggested that most of the earlier workers had been dealing with mixtures of the three polymorphic forms.

Future studies of polymorphism should involve separation of similar habits under a microscope and then crystallographic studies of single

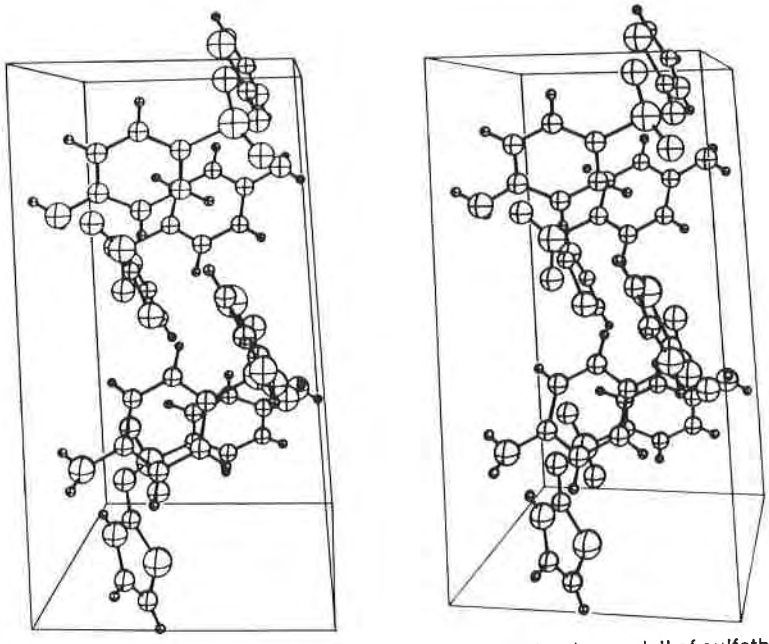

**FIGURE 20.** A stereopair view of the crystal packing of polymorph II of sulfathiazole (Kruger and Gafner, 1971).

crystals of each habit to determine its unit-cell parameters and space group. This approach would make sure that mixtures of polymorphs are not involved.

The physical properties of forms I and II of sulfathiazole have been

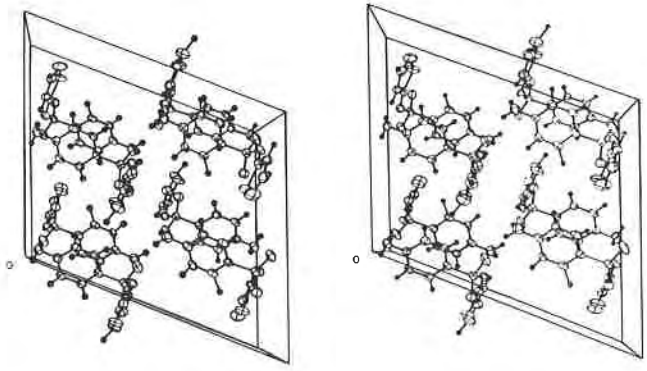

**FIGURE 21.** A stereopair view of the crystal packing of polymorph III of sulfathiazole. The view is along the *b* axis, with the *c* axis vertical (Kruger and Gafner, 1972).

**TABLE XI**
*Dissolution Rate and Solubility of Forms I and II of Sulfathiazole*

| | Dissolution rate (mg $cm^{-2}sec^{-1}$) | | Solubility (gm/1000 gm solvent) | |
|---|---|---|---|---|
| Temperature (°C) | Form I | Form II | Form I | Form II |
| 59.1 | .185 | .239 | 31.5 | 40.7 |
| 48.8 | .102 | .145 | 19.8 | 28.1 |
| 39.4 | .0598 | .0913 | 14.0 | 21.4 |
| 29.6 | .0355 | .0597 | 9.93 | 16.7 |
| 24.1 | .0237 | .0413 | 8.15 | 14.2 |
| 20.4 | .0201 | .0371 | 7.10 | 13.1 |

studied (Sunwoo and Eisen, 1971; Milosovich, 1964). These studies involved measurement of the dissolution rate, and care was usually taken to avoid a solution-mediated phase transformation of form II to form I. The experiments used a 300-rpm stirrer and a specially constructed apparatus that allowed measurement of dissolution rate by measuring the change in absorbance per second using a spectrometer and flow cell. The results of these studies are shown in Table XI. These studies clearly show that form II has a significantly higher dissolution rate and solubility than form I. This indicates that in the absence of a solvent-mediated conversion of form II to form I, form II should have the higher bioavailability, other things being equal.

## C. POLYMORPHISM OF SULFAMETHOXYDIAZINE

Sulfamethoxydiazine (**20**) exists in at least six different forms (Moustafa *et al.*, 1971). Form I is obtained from boiling water or by heating any other

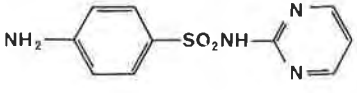


20

form to 150°C. Form II is prepared by rapid cooling of a saturated ethanol solution. Form III is obtained from a number of solutions including methanol, isopropanol, and ethanol. Forms IV and V are probably solvates and are obtained from dioxane and chloroform, respectively. An amorphous form is also known.

These forms were characterized by their infrared spectra, which were

all slightly different, particularly in the 800–875, 900–970, 1550–1600, and 3000–3500 $cm^{-1}$ regions of the spectrum. The powder diffraction patterns of these forms are also significantly different.

The forms can be interconverted by heating or grinding. Surprisingly, heating converts all forms to form I, while grinding or suspension in water converts all forms to form III. This behavior is summarized in Scheme I.

The dissolution rates of these forms have been measured as a means of estimating their bioavailability. The results of these measurements are shown in Figure 22 (Moustafa *et al.*, 1971). Obviously, form II and the amorphous form dissolve most rapidly. Form III has the slowest dissolution rate, about half that of form II. It is also very interesting to note that form II has a faster dissolution rate than the amorphous form, suggesting that the amorphous form may in fact be crystalline or that the surface area of form II is much larger than the amorphous form.

Commercial preparations were also studied and in general contained form I or mixtures of forms I and III. These forms are the most stable and the slowest dissolving. Thus these preparations have low bioavailability.

The kinetics of the phase transformations of sulfamethoxydiazine have also been studied using infrared spectroscopy (Moustafa *et al.*, 1972). The rates of conversion of form II to form I and form II to form III were determined. A plot of the absorbance ratio ($A_{950\,cm^{-1}}/A_{1595\,cm^{-1}}$) versus the concentration ratio ($C_I/C_{II}$) gave curved but well-behaved lines that allowed the measurement of the amount of form I in II. The rate of conversion of form II to form I was studied at 100°, 105°, and 110°C. The rate of conversion of form II to form III was studied in water suspension at 20°, 25°, 30°, and 37°C. Plots of $\log(C_{II})$ versus time were linear for both the reaction in the solid state and in suspension. They indicate the reactions follow first-order kinetics. Analysis of these kinetic data gave an activation energy of about 100 kcal/mole for the solid-state conversion of form II

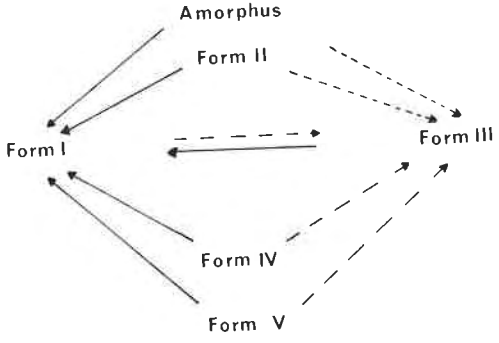

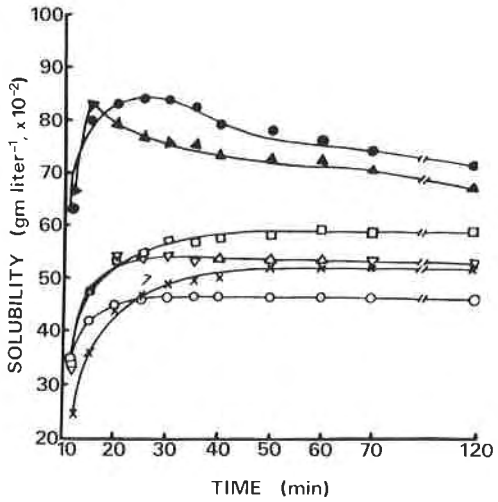


**FIGURE 22.** Dissolution rates of the different crystalline forms of sulfamethoxydiazine: x-form I; ●-form II; ○-form III, □-form IV; △-form V; ▲-amorphous form (Moustafa *et al.*, 1971).

to form I and an activation energy of about 20 kcal/mole for the conversion of form II to form III in suspension. These differences in rate and activation energy are no doubt due to the fact that the phase transformation in suspension is water-mediated. Thus the conversion in water suspension is actually a dissolution–recrystallization process as described by McCrone (1965) for other compounds. However, a mechanism involving a solid-state transformation mediated by water is also possible. Forms I and III are of nearly equal energy, ruling out any explanation of the differences in rate of the solid state and suspension reaction based on differences in energies of the products. That is, since the products and the reactants are of nearly equal energy for the two reactions, any differences in activation energy must be due to actual differences in the height of the barrier.

## D. POLYMORPHISM OF OTHER SULFONAMIDES

In addition to the three sulfonamides already discussed, a number of other sulfonamides exhibit polymorphism. Many of these sulfonamide studies have been carried out in order to determine whether these compounds might undergo metastable to stable transformations during storage and result in the caking of a suspension or a change in drug bioavailability. The major analytical methods used for these studies were differential thermal analysis and x-ray powder diffraction.

*1. Sulfabenzamide*

Sulfabenzamide (**21**) exists in four polymorphs and three solvates (Yang and Guillory, 1972). Form III can be transformed to form I by

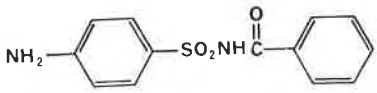

21

trituration, and form IV can be transformed to form III and then form I by heating. Desolvation of two of the solvates yielded form II.

*2. Sulfaguanidine*

Sulfaguanidine (**22**) exists in three crystalline forms and one solvate (Yang and Guillory, 1972). Extensive differential thermal analytical stud-

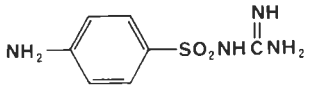

22

ies and infrared studies were used to identify these forms; however, their existence has not been confirmed by x-ray crystallograhic studies.

*3. Sulfapyridine*

Sulfapyridine (**23**) exists in at least four polymorphs and one amorphous form (Yang and Guillory, 1972). The infrared spectra of two of these

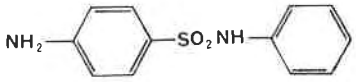

23

forms are identical, but their x-ray diffraction patterns are completely different. In addition, hot-stage experiments indicated that sulfapyridine (**23**) crystallized in at least seven forms (Kuhnert-Brandstatter, 1971).

*4. Sulfamethoxypyridiazine*

Sulfamethoxypyridiazine (**24**) exists in three crystalline forms (Yang and Guillory, 1972). Form II can be transformed to form I at 154°C.

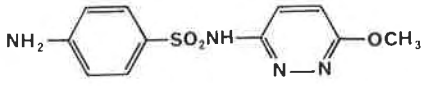

24

*5. Sulfamethoxazole*

Sulfamethoxazole (**25**) exists in three polymorphs and form II can be converted to form I at 164°C (Yang and Guillory, 1972). These studies are

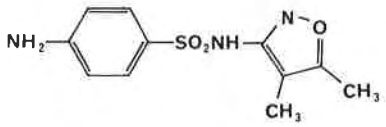

25

in agreement with Kuhnert-Brandstatter (1971), who also showed there were three polymorphs of **25.**

*6. Chlorpropamide*

Chlorpropamide (**26**) exists in three polymorphs that have different diffraction patterns (Simmons *et al.*, 1973). Form I is obtained from

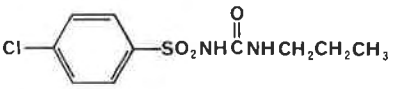

26

alcohol–water, form II from benzene, and form III by heating form I or II at 110°C. The infrared spectra of all three forms are slightly different, and the x-ray powder patterns of all three forms are significantly different. It is interesting to note that the DTA thermograms of the three forms are essentially the same, indicating that in this case DTA is not a good method for studying polymorphs.

The three forms of **26** have different dissolution rates. The dissolution rates of forms I and III in water are identical, while form II dissolves about half as fast. However, in beagle dogs the serum levels following peroral administration are identical for all three forms (Simmons *et al.*, 1973). Further single-crystal studies are necessary to completely characterize these forms and explain these results.

*7. Tolbutamide*

Tolbutamide (**27**) crystallizes in two forms (Simmons *et al.*, 1972). Form I is obtained from benzene–hexane, and the crystals are prismatic

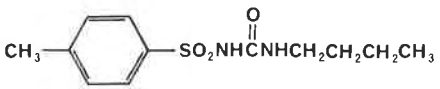

27

with mp 127–128°C. Form II is obtained from alcohol–water and the crystals are plates with mp 126–128°C. Both the infrared spectra and the DTA thermograms of forms I and II are slightly different. The DTA of form II shows an endotherm at 113°C that is not present in form I. This endotherm apparently corresponds to the conversion of form II to form I. The dissolution rates of forms I and II are the same in waater at pH 5.5 and 7.3. The serum levels of these two forms are also identical. One explanation of this data is that upon exposure to liquid, form II is converted to form I by a solution-mediated phase transformation.

### E. CONCLUSION

This section shows the extent of polymorphism in the sulfonamides. The fact that polymorphism of these drugs is so widespread is probably due to (*a*) the availability of a variety of hydrogen-bonding schemes and (*b*) the occurrence of a number of ring–ring stacking modes.

Further study of the polymorphism of these compounds using single-crystal x-ray techniques should no doubt lead to a better understanding of their polymorphism.

## III. Polymorphism of Steroids

Steroids exhibit widespread polymorphism that affects their stability as well as their bioavailability. Thus polymorphism of these compounds can have an important effect on their pharmaceutical and biological properties. In this section we review the polymorphism of steroids and the properties of these polymorphs. A few examples of the polymorphism of steroids have been discussed in preceding chapters.

Kuhnert-Brandstatter (1971) has studied the polymorphism of steroids using a Kofler hot stage, and the results of her studies are summarized in Table XII.

This table clearly shows the extent of polymorphism in this important class of compounds. It should be noted that these studies are based only on hot-stage results and should be considered unconfirmed until other methods verify the existence of these polymorphs.

### A. POLYMORPHISM OF ESTRONE

As indicated in Table XII, estrone (**28**) exists in three polymorphs, and the existence of these forms has been confirmed by x-ray crystallographic

**TABLE XII**

*Melting Points of Polymorphic Steroids*[a]

| Compound | Forms | | | | |
|---|---|---|---|---|---|
| | I | II | III | IV | V |
| Allopregnane-3$\beta$,20$\alpha$-diol | 215–219 | 162–168 | | | |
| Allopregnane-3,20-dione | 202–206 | 198–203 | | | |
| Androstane-3$\beta$,17$\beta$-diol | 168–169 | 163–164 | 158–161 | 146–147 | |
| Androstane-3,17-dione | 132–134 | 128–130 | | | |
| Androstanolone | 182 | 168 | | | |
| $\Delta^5$-Androstene-3$\beta$,17$\alpha$-diol | 202–205 | 180–195 | | | |
| $\Delta^5$-Androstene-3$\beta$,17$\beta$-diol | 181–185 | 177–180 | 155–158 | | |
| $\Delta^4$-Androstene-3,17-dione | 170–174 | 142–145 | | | |
| Corticosterone | 180–186 | 175–179 | 162–168 | 155–160 | |
| Cortisone enanthate | 138–140 | 135–137 | 129–132 | | |
| Dehydroepiandrosterone | 149–153 | 139–141 | 137–140 | 130–136 | |
| Dehydroepiandrosterone acetate | 170–172 | 132–135 | 94–96 | 65–69 | |
| Epiandosterone | 174–176 | 167–169 | | | |
| Etiocholane-3$\alpha$-ol-17-one | 150–152 | 141–143 | 133 | | |
| Etiocholane-17$\beta$-ol-3-one | 141–143 | 103 | | | |
| Fluorocortisone trimethylacetate | 192–198 | 184–190 | | | |
| 9$\alpha$-Fluorohydrocortisone acetate | 225–233 | 208–212 | 205–208 | | |
| Hydrocortisone hemisuccinate | 198–205 | 182–188 | 168–172 | | |
| Methandriol | 205–208 | 202–205 | 196–198 | | |
| Methandriol dipropionate | 83–86 | 74–75 | | | |
| 17$\alpha$-Methandrostane-3$\beta$,17$\beta$-diol | 213 | 205 | | | |
| 1-Methylandrostenolone acetate | 143 | 106 | | | |
| 17$\alpha$-Methylestradiol | 190–194 | 188 | | | |
| 6-$\alpha$-Methylprednisolone acetate | 225–229 | 208–212 | 205–210 | | |
| 17-Norethisterone | 200–207 | 199 | | | |
| $\beta$-Estradiol | 178 | 169 | | | |
| $\alpha$-Estradiol | 225 | 223 | | | |
| Estradiol benzoate | 188–195 | 177.5 | 176 | | |
| Estradiol dipropionate | 107 | 97 | 82 | | |
| Estradiol 17-propionate | 198–200 | 154–156 | | | |
| Estrone | 260–263 | 256 | 254 | | |
| Estrone methyl ether | 172–174 | 123–126 | 88–92 | | |
| Prednisolone | 218–234 | 215 | | | |
| Prednisolone acetate | 232–241 | 225–228 | 217–220 | | |
| Progesterone | 131 | 123 | 111 | 106 | 100 |
| Testosterone | 155 | 148 | 144 | 143 | |
| Testosterone isobutyrate | 131–133 | 88–90 | | | |
| Testosterone nicotinate | 194–196 | 185–188 | | | |
| Testosterone Propionate | 122 | 74 | | | |

[a] Data from Kuhnert-Brandstatter (1971).

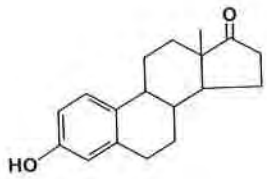


28

studies; these crystal parameters are shown in Table XIII (Busetta *et al.*, 1973). The crystal structures of all three polymorphs have been determined (Busetta *et al.*, 1973). The conformation of the estrone molecule is similar in all three polymorphs. The crystal packing of these three forms is shown in Figures 23, 24, and 25. Form I contains layers of estrone molecules but no obvious stacks of estrone molecules. Form III contains both layers and stacks of estrone molecules. Form II has a herringbone arrangement of estrone molecules. The crystal packing of form I appears to be controlled by H–H contacts of 2.26 and 2.26 Å as shown; the crystal packing of form III appears to be controlled by C–C contacts of 3.35 Å.

No transformations or interconversions of these forms have been reported; however, it is likely that the densest form, form II, is the most stable.

## B. POLYMORPHISM OF 5α-ANDROSTAN-3,17-DIONE

The steroid 5α-androstan-3,17-dione (**29**) crystallizes in three polymorphs (Bouche *et al.*, 1977; Coiro *et al.*, 1973). The crystal structure

**TABLE XIII**
*Crystallographic Parameters of the Three Polymorphs of Estrone* (**28**)

| | Forms | | |
|---|---|---|---|
| Parameters | I | II | III |
| Source | Sublimation | Acetone | Sublimation |
| Space group | $P2_12_12_1$ | $P2_12_12_1$ | $P2_1$ |
| $Z$ | 4 | 4 | 4 |
| $a$ (Å) | 12.188 | 10.043 | 9.271 |
| $b$ (Å) | 16.301 | 18.424 | 22.285 |
| $c$ (Å) | 7.463 | 7.787 | 7.610 |
| $\beta$ | — | — | 111.45° |
| Volume (Å$^3$) | 1481 | 1440 | 1461 |

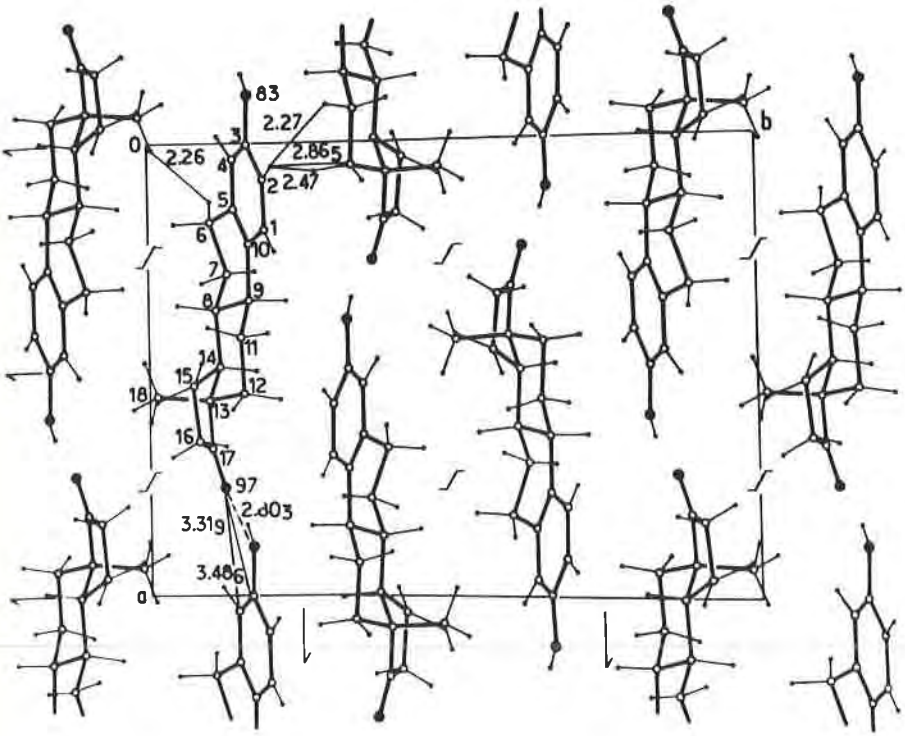


**FIGURE 23.** Projection of the crystal structure of form I of estrone on the *xy* plane (Busetta *et al.*, 1973).

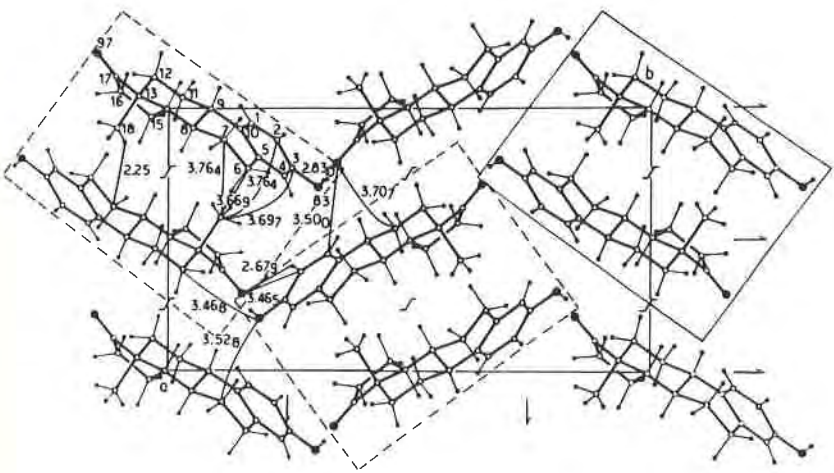


**FIGURE 24.** Projection of form II of estrone on the *xy* plane (Busetta *et al.*, 1973).

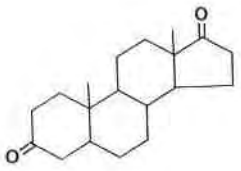

29

of form I has been determined. Form I belongs to space group $C2$ with $a = 12.70, b = 6.19$, and $c = 21.34$ Å, and $\beta = 91°16'$. Figures 26 and 27 show the crystal packing of form I. Form II is unstable, and form III is a

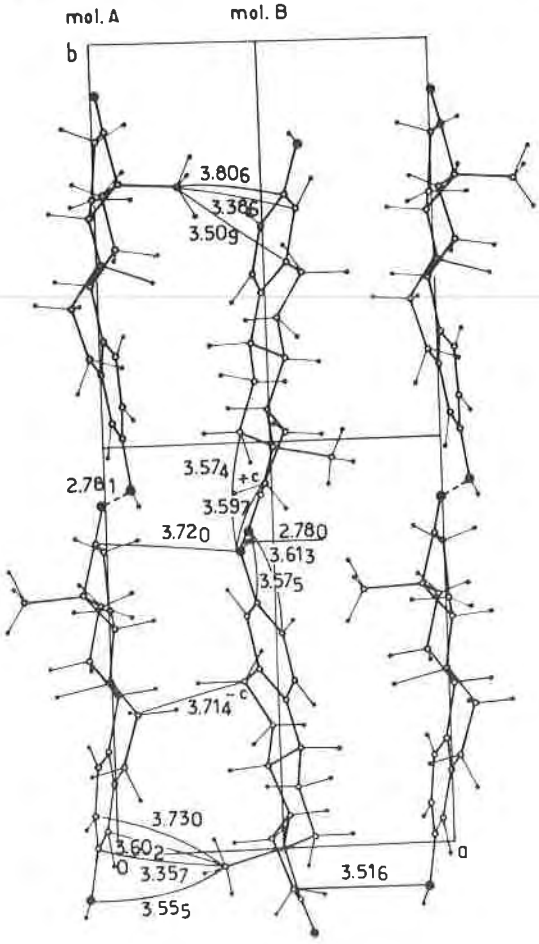


**FIGURE 25.** Projection of the structure of form III of estrone on the *xy* plane (Busetta *et al.*, 1973).

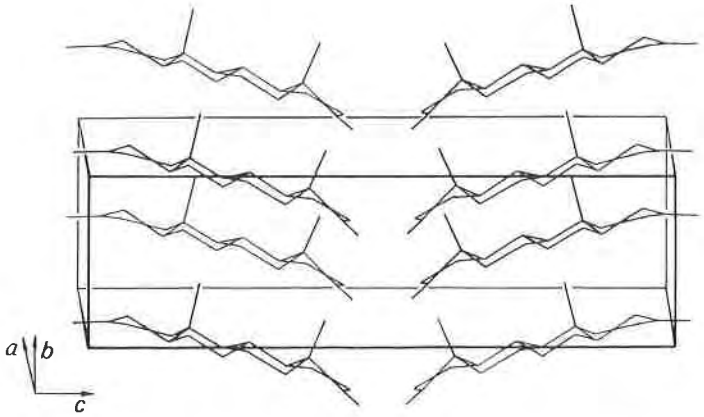


**FIGURE 26.** Molecular packing of crystals of 5α-androstan-3,17-dione viewed along the *a* axis (Coiro *et al.*, 1973).

solvate containing four molecules of water. Unfortunately, the crystal structures of forms II and III have not been determined.

## C. POLYMORPHISM AND BIOAVAILABILITY OF METHYLPREDNISOLONE

Methylprednisolone (**30**) exists in two polymorphs. Form I can be prepared by recrystallization from acetone, and form II can be prepared by sublimation at 190°C (Hamlin *et al.*, 1962). Pellets of these two forms were

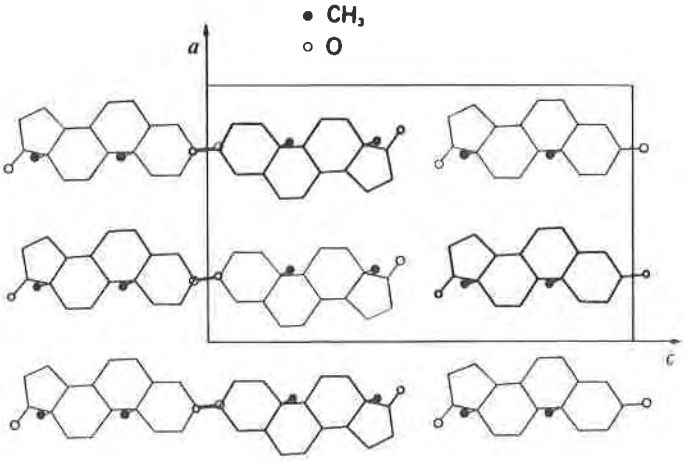


**FIGURE 27.** Molecular packing of 5α-androstan-3,17-dione viewed along the *b* axis. (Coiro *et al.*, 1973).

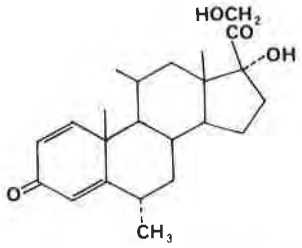


30

prepared and their dissolution rates were studied under varying conditions of agitation. Under all conditions except the most rapid agitation, form II has a faster dissolution rate than form I. *In vivo* tests of the rate of dissolution of forms I and II using the pellet implant method, which involves implanting the pellets in rats, showed that form II has a faster dissolution rate than form I. Studies of the dissolution rate of crystalline samples of forms I and II also showed that form II has a faster dissolution rate (Higuchi *et al.*, 1967).

Studies of the dissolution rates of forms I and II using the rotating disk method also showed that form II has a faster dissolution rate than form I. At increased stirring rates, forms I and II had more similar dissolution rates. These studies also indicated that low agitation rates give data that correlate with the pellet-implant *in vivo* data, while higher agitation rates are required to give results that correlate with gastrointestinal data (Levy and Procknal, 1964).

Infrared attenuated reflectance (ATR) spectra showed that the surfaces of pellets of form II revert to form I in water even after only a 2-min exposure. This appears to be a water-mediated phase transformation of the type discussed by Haleblian and McCrone (1969). This observation also explains the slower than expected dissolution rates of form II in water (Higuchi *et al.*, 1969).

## D. POLYMORPHISM OF HYDROCORTISONE 21-*tert*-BUTYLACETATE

Hydrocortisone 21-*tert*-butylacetate (**31**) crystallizes in three crystalline forms (Biles, 1963). X-Ray diffraction studies in our laboratory indicate that there are actually four different forms, and elemental analysis shows that two of these forms contain varying amounts of ethanol. The results of these studies are shown in Table XIV. Recently a fifth crystal form has been isolated from pyridine.

During recrystallization from ethanol a mixture of crystal forms I, II, and III often formed, but a pure single form could be obtained under

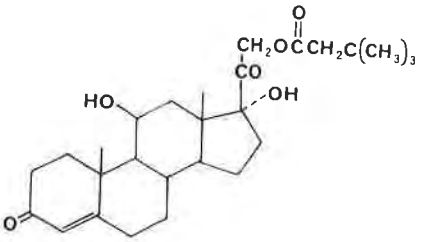

31

certain conditions. A new form designated form IV was produced when forms I, II, and III were heated at 120°C. Forms I and II underwent desolvation and phase transformation to form IV, while form III changed from one phase to another. All crystal forms except form I were inert to irradiation with ultraviolet light.

Form I was oxidized to **32** upon irradiation with ultraviolet light in air.

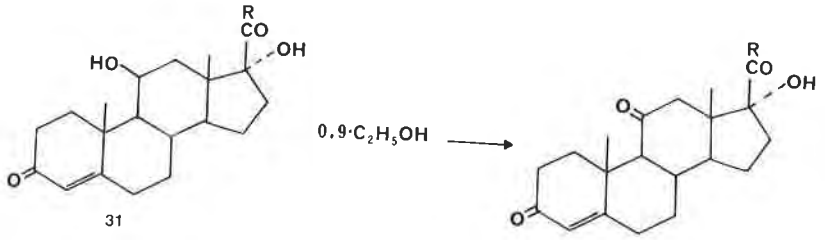

31 32

$R = CH_2OCOCH_2C(CH_3)_3$

A known weight of crystals was put in vials and irradiated at 30°C. The formation of **31** was determined by the change in the NMR chemical shift of the C-18 methyl signal, and the content of ethanol was measured by gas

**TABLE XIV**

*Crystal Forms of Hydrocortisone 21-tert-Butylacetate*

| Crystal form | Ethanol content (mole ratio) | Oxidation in ultraviolet light | mp[a] (°C) |
|---|---|---|---|
| I | 0.9 | Reaction | 170–180 |
| II | 1.0 | No Reaction | 110–120[b] |
| III | 0 | No Reaction | 123–126[c] |
| IV | 0 | No Reaction | 234–238 |

[a] The exact melting temperature may vary from one crystal to another.
[b] Opaque at this temperature range with final melting at 234°–238°C.
[c] After melting, the melt resolidified as the temperature was increasing and finally remelted at 234–238°C.

**TABLE XV**
*Desolvation and Oxidation of Crystalline Hydrocortisone 21-tert-Butylacetate 0.9 Ethanol (Form I) upon Exposure to Ultraviolet Light*

| Days | % Cortisone (**32**) formed | % Ethanol lost |
|---|---|---|
| 1 | 20.0 | 43.3 |
| 2 | 38.9 | 75.6 |
| 3 | 50.0 | 83.3 |
| 6 | 52.9 | 88.9 |
| 10 | 56.3 | 93.3 |
| 14 | 66.7 | 95.6 |
| 21 | 71.4 | 96.7 |

chromatography. The percent desolvation and oxidation of the hydrocortisone ester **31** to the cortisone ester **32** are shown in Table XV. Apparently the loss of ethanol is faster than oxidation. However, this behavior is different from that of dihydrophenylalanine hydrate, in which water loss almost completely preceded the oxidation (Lin and Byrn, 1976). In addition, ethanol loss does not occur from crystals stored in the dark, indicating that oxidation is required for ethanol loss to begin. Further studies of this interesting reaction are in order.

### E. CONCLUSION

The steroids exhibit a wide range of polymorphic behavior, which appears to affect both the bioavailability and stability of these compounds. Of particular interest are the cases where one form is reactive in the solid state while the others are stable. Further studies on these compounds are definitely in order.

## IV. Polymorphism of Barbiturates

Barbiturates are another class of drugs in which widespread polymorphism exists. As in the discussions of the polymorphism of sulfonamides and steroids just presented, this section begins with a table describing the results of hot-stage experiments on barbiturates. Then two detailed studies of the polymorphism of barbiturates are discussed.

Kuhnert-Brandstatter (1971) reported the results of her extensive studies on barbiturate polymorphism. These studies were made using a Kofler hot stage and should be considered tentative until confirmed by other experiments (Table XVI).

**TABLE XVI**
*Melting Points of Polymorphs of Barbiturates*[a]

| Compound | Melting point of form (°C) | | | | | | |
|---|---|---|---|---|---|---|---|
| | I | II | III | IV | V | VI | VII |
| Allobarbital | 173 | 122 | | | | | |
| 5-Allyl-5-(2-Cyclopentenyl-1-yl)-barbituric acid | 148 | 126 | 124 | 125 | | | |
| 5-Allyl-5-phenylbarbituric acid | 159 | 133 | 130 | 129 | 128 | 126 | |
| Amobarbital | 157 | 151 | | | | | |
| Aprobarbital | 141 | 139 | 133 | 130 | 116 | 95 | |
| Barbital | 190 | 184 | 183 | 181 | 176 | 159 | |
| Butalloylonal | 131 | 128 | 104 | | | | |
| Buthalitone | 149 | 117 | 95 | | | | |
| 5-Crotyl-5-ethylbarbituric acid | 117 | 90 | | | | | |
| Cyclobarbital | 173 | 161 | | | | | |
| 5,5-Dipropylbarbituric acid | 148 | 146 | 126 | 120 | 110 | 105 | 85 |
| Dormouit | 171 | 146 | | | | | |
| Ethallobarbital | 160 | 149 | 137 | 129 | 117 | 108 | |
| 5-Ethyl-5-(1-piperidyl)-barbituric acid | 217 | 210 | 204 | | | | |
| Heptabarbital | 174 (VIII—100) | 150 | 145 | 143 | 141 | 137 | 127 |
| 5-Methyl-5-phenylbarbituric acid | 226 | 226 | 200 | | | | |
| Pentobarbital | 176 (VIII—141; IX—133; X—126; XI—112) | 174 | 167 | 163 | 160 | 157 | 153 |
| Propallonal | 184 | 180 | 179 | 127 | 123 | | |
| Thiothyr | 146 | 125 | | | | | |
| Vinbarbital | 166 | 129 | 106 | | | | |

[a] Data from Kuhnert-Brandstatter (1971).

## A. POLYMORPHISM OF AMOBARBITAL

Craven and co-workers have examined the crystal structures of a number of barbiturates. Among these studies is the determination of the crystal structures of the two polymorphs of amobarbital (**33**) (Craven and

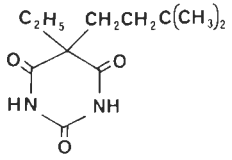


**33**

Vizzini, 1969). These studies showed that amobarbital exists in two crystalline forms, and these results are consistent with those reported in Table XV. The two forms have the cell parameters shown in Table XVII.

**TABLE XVII**
*Crystallographic Parameters for the Two Forms of Amobarbital*

| Parameter | Form I | Form II |
|---|---|---|
| Melting point (°C) | 154–156 | 160–162 |
| $a$ (Å) | 21.480 | 10.281 |
| $b$ (Å) | 11.590 | 22.061 |
| $c$ (Å) | 10.370 | 11.679 |
| $\beta$ | 97°4′ | 109°6′ |
| $Z$ | 8 | 8 |
| Space group | $C2/c$ | $P2_1/c$ |
| Volume (Å$^3$) | 2562.0 | 2503.1 |
| $\rho_{calc}$ (gm/cm$^3$) | 1.171 | 1.178 |
| Crystal habit | Plates developed on 100 | Needles elongated along $b$ |

The conformation of amobarbital is virtually identical in the two polymorphs but the crystal packing is different. Figures 28 and 29 show this packing. Both forms show the so-called double-ribbon arrangement; however, in form I there is no interaction between the sheets while in form II an interlocking structure is present. The slightly higher density of form II is consistent with the interlocking structure of this form, which would seem to indicate tighter crystal packing.

## B. POLYMORPHISM OF PHENOBARBITAL

Phenobarbital (5-ethyl-5-phenylbarbituric acid), **34,** has been reported to crystallize in as many as 13 modifications. Single-crystal studies of

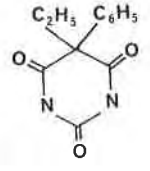


34

these polymorphs revealed at least four distinct anhydrous forms and one hydrate (Table XVIII).

The crystal structures of the hydrate (form XIII) and of form III have been determined (Williams, 1973, 1974). The conformations of phenobarbital, including the angle between the two rings, are slightly different in

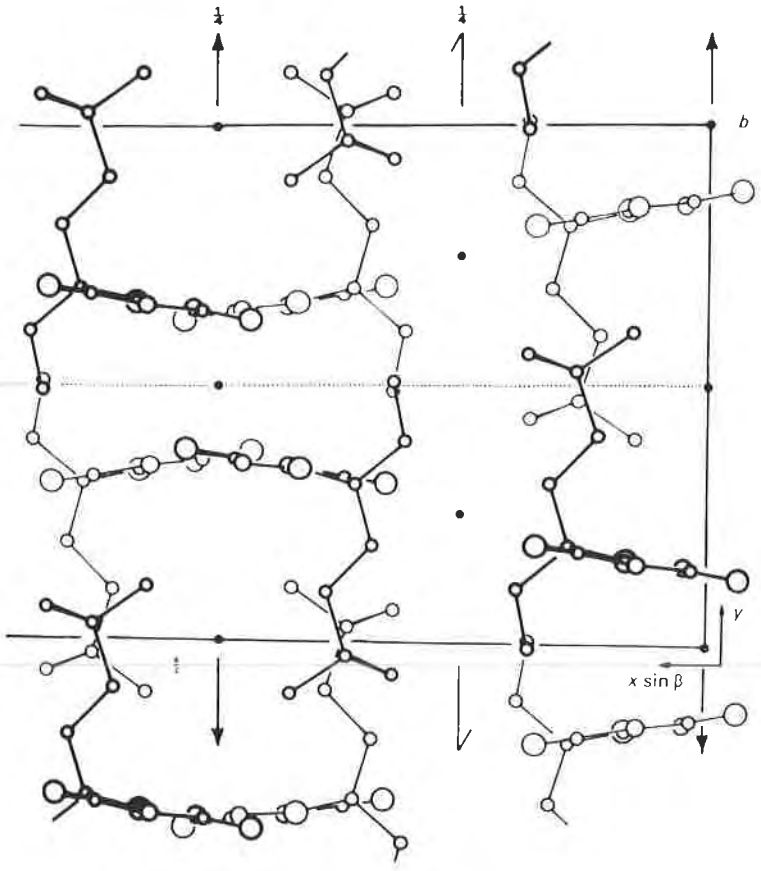


(*b*)

**FIGURE 28.** The crystal structure of form I of amobarbital viewed down the *c* axis (Craven and Vizzini, 1969).

these two forms, and they might be considered conformational polymorphs. If the normal to the planar part of the pyrimidine ring is defined as the base vector of a spherical coordinate system, then the coordinates of the normal to the phenyl ring in form III are $\phi = 80.8°$ and $\theta = 38.4°$. The same coordinates in form XIII are $\phi = 86.0°$ and $\theta = 13.8°$. In these calculations $\phi$ is defined as the rotation of the median plane of the phenyl ring toward C-2 of the pyrimidine ring. The crystal packing of these two forms is shown in Figures 30 and 31. The packing of these two forms is somewhat different; however, both forms contain layers of phenyl rings and layers of hydrogen-bonded pyrimidine rings.

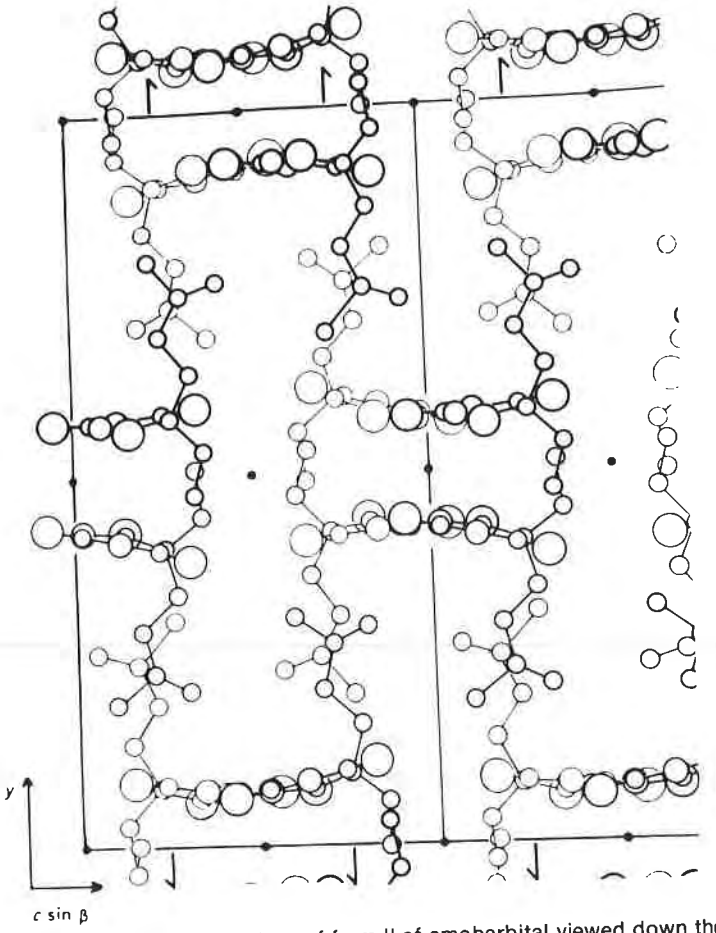


**FIGURE 29.** The crystal structure of form II of amobarbital viewed down the *a* axis (Craven and Vizzini, 1969).

## V. Polymorhism of Other Drugs

In this section the polymorphic properties of several other drugs are reviewed. While this review is not exhaustive, it illustrates the widespread existence of polymorphism in pharmaceuticals.

### A. POLYMORPHISM OF PROMEDAL ALCOHOL

DeCamp and Ahmed (1972a,b) have determined the crystal structures of both the monoclinic and rhombohedral forms of ±-β-promedal alcohol,

**TABLE XVIII**

*Crystallographic Parameters for the Crystal Forms of Phenobarbital* (**34**)

| Parameter | Form | | | | |
|---|---|---|---|---|---|
| | I | II | III | V | XIII (hydrate) |
| $a$ (Å) | 6.800 | 6.784 | 9.534 | 12.66 | 7.157 |
| $b$ (Å) | 47.174 | 23.537 | 11.855 | 6.75 | 30.879 |
| $c$ (Å) | 10.695 | 10.741 | 10.794 | 27.69 | 10.87 |
| $\alpha$ | 90° | 91.89° | 90° | 90° | 90° |
| $\beta$ | 94.18° | 94.43° | 111.56° | 106.9° | 90° |
| $\gamma$ | 90° | 89.03° | 90° | 90° | 90° |
| Space group | $P2_1/n$ | $P\bar{1}$ | $P2_1/c$ | $P2_1/c$ | $Pbca$ |
| $Z$ | 12 | 6 | 4 | 8 | 8 |
| Volume (Å$^3$) | 3421.7 | 1708.8 | 1134.6 | 2264.1 | 2402.3 |
| $\rho_{calc}$ (gm/cm$^3$) | 1.352 | 1.354 | 1.360 | 1.362 | 1.384 |

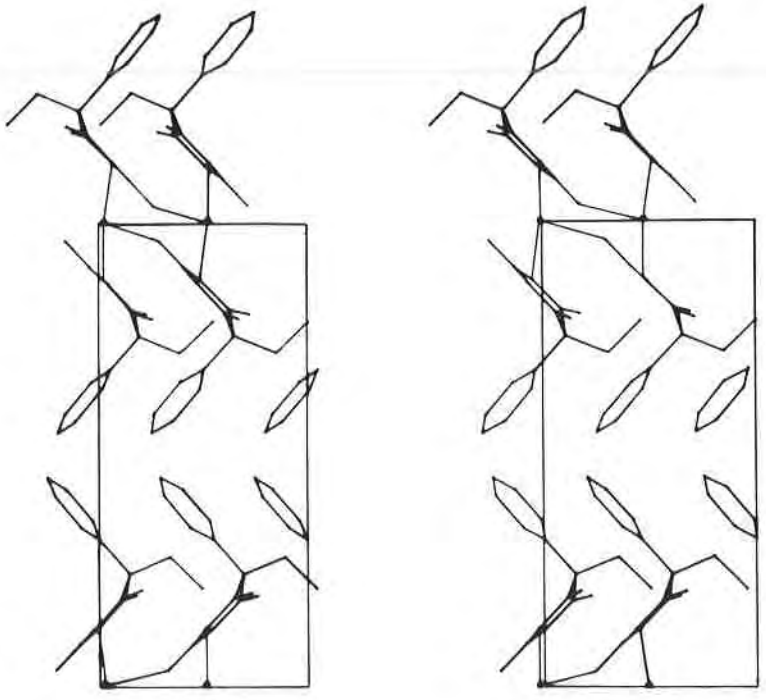

**FIGURE 30.** The crystal packing of the hydrate of phenobarbital (form XIII) viewed down the $z$ axis (Williams, 1973).

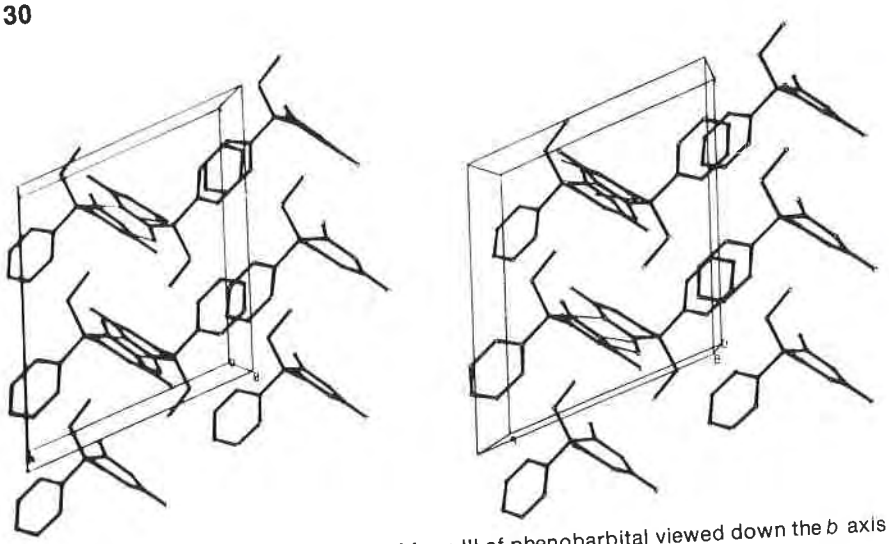

**FIGURE 31.** The crystal packing of form III of phenobarbital viewed down the *b* axis (Williams, 1974).

**35** (see Table XIX). The conformation of β-promedal is the same in both forms, but the crystal packing differs. In the monoclinic form, OH···N

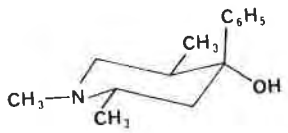


35

hydrogen bonds link molecules of the same chirality to form chains. In the rhombohedral form there are also OH···N hydrogen bonds; however, these link molecules of alternating chirality into hexameric rings. The

**TABLE XIX**
*Crystallographic Parameters for the Two Forms of Promedal Alcohol* (**35**)

| | Form | |
|---|---|---|
| Parameter | Monoclinic | Rhombohedral |
| *a* (Å) | 13.298 | 29.754 |
| *b* (Å) | 7.721 | — |
| *c* (Å) | 12.776 | 7.713 |
| β | 90.09° | — |
| *Z* | 4 | 18 |
| Volume (Å$^3$) | 1311.8 | 5913.5 |
| $\rho_{calc}$ (gm/cm$^3$) | 1.109 | 1.110 |

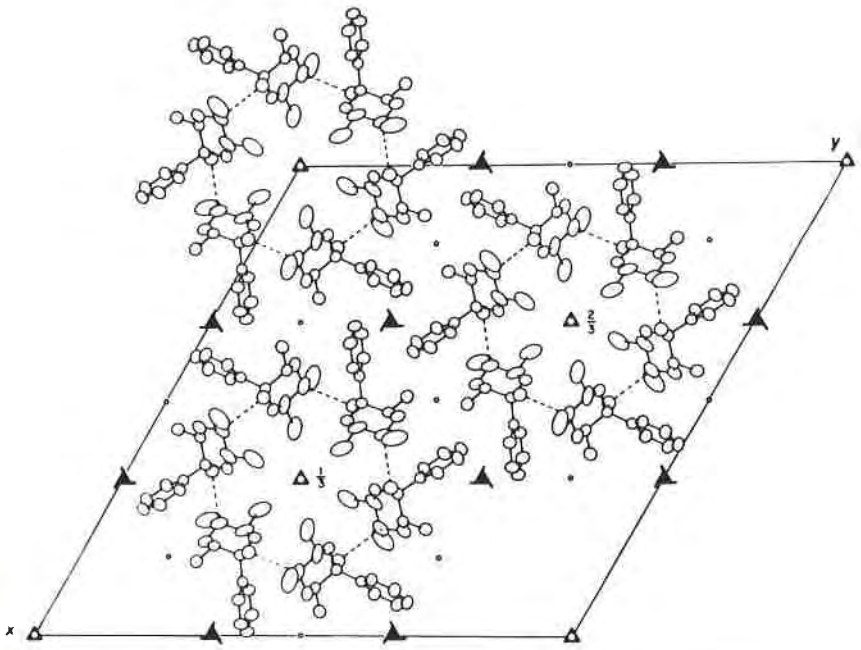


**FIGURE 32.** Crystal packing of the rhombohedral form of $\beta$-promedal alcohol viewed down the $c$ axis (DeCamp and Ahmed, 1972b).

crystal packing of these two forms is shown in Figures 32 and 33. Despite the differences in crystal packing, the monoclinic and rhombohedral crystals have almost the same density. The melting point of the rhombohedral form is 104.5° to 105°C, and the melting point of the monoclinic form is 90.5° to 91°C. This difference in melting point is probably not related to differences in hydrogen bonding, since the OH···N distances are approximately the same in the two forms. In addition, the densities indicate that the two forms have nearly equal packing energies. Thus DeCamp and Ahmed (1972b) suggested that since the rhombohedral form contains rings of molecules of alternating chirality while the monoclinic form contains stacks of molecules of the same chirality, the monoclinic form is more ordered. This increased ordering results in an entropy difference that results in a lower melting point for the monoclinic form. Similar arguments were also advanced by Krigbaum and Wildman (1971).

## B. POLYMORPHISM AND COLOR DIMORPHISM OF 14-HYDROXYMORPHINONE

The phenolic $\alpha,\beta$-unsaturated ketone 14-hydroxymorphinone (**36**) exists in two crystallline modifications (see Table XX), which are inter-

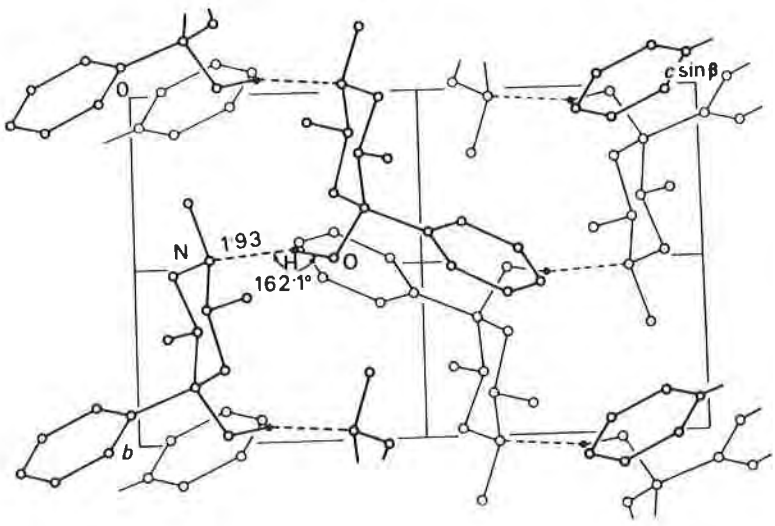


**FIGURE 33.** Crystal packing of the monoclinic form of β-promedol alcohol viewed down the *x* axis (DeCamp and Ahmed, 1972a).

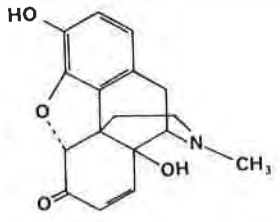


36

convertible by dissolution and recrystallization (Chiang *et al.*, 1978). Recrystallization from polar solvents (ethanol) yields yellow crystals (**36Y**), while crystallization from benzene gives colorless crystals (**36W**). Both forms are stable indefinitely in the solid state.

Infrared spectra show that **36Y** has carbonyl absorption at 1685 $cm^{-1}$ while **36W** has a carbonyl absorption at 1660 $cm^{-1}$. Since both forms have a carbonyl absorption, neither form contains an enol tautomer.

Crystallographic studies show that the conformation of **36** in the two forms is similar; however, the yellow form contains an intermolecular OH···O hydrogen bond, while the white form contains an intramolecular OH···O hydrogen bond. The crystal packing of these two forms is shown in Figure 34.

The color of **36Y** may, in part, result from the intermolecular OH···O hydrogen bond since a similar effect was found for dimethyl-3,6-

**TABLE XX**

*Crystallographic Parameters for the Two Forms of the Morphine Derivative* ***36***

| | Form | |
|---|---|---|
| Parameter | **36-W** | **36-Y** |
| *a* (Å) | 12.918 | 13.150 |
| *b* (Å) | 14.074 | 13.508 |
| *c* (Å) | 8.035 | 7.837 |
| *Z* | 4 | 4 |
| Volume (Å$^3$) | 1460.8 | 1392.1 |
| $\rho_{calc}$ (gm/cm$^3$) | 1.36 | 1.428 |
| Space group | $P2_12_12_1$ | $P2_12_12_1$ |

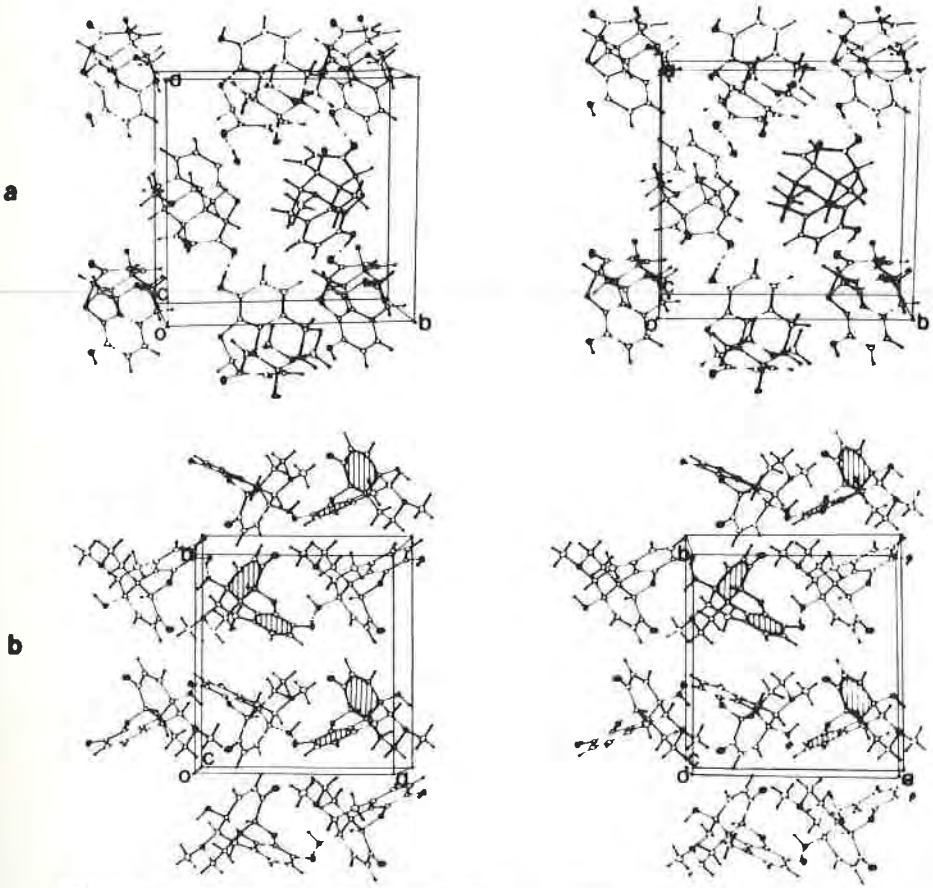


**FIGURE 34.** Stereoscopic view of the molecular packing of (*a*) **35Y** looking in the *c* direction and (*b*) **35W** looking in the *c* direction (Chiang *et al.*, 1978). (Reprinted with permission from C. C. Chiang, W. H. DeCamp, D. Y. Curtin, I. C. Paul, S. Shifrin, and U. Weiss [1978]. Copyright 1978 American Chemical Society.)

dichloro-2,5-dihydroxyterephthalate (Byrn *et al.*, 1972). An alternative explanation is that there is a weak charge-transfer interaction between the C═O group and an adjacent phenyl ring in the yellow form but not in the colorless or white form. A clear distinction between these two explanations is not possible.

Numerous other reports of color dimorphism have been published for compounds that are not drugs. These reports are briefly reviewed by Chiang *et al.* (1978), Byrn *et al.* (1972), and Desiraju *et al.* (1977), and will not be discussed further in this chapter. Color dimorphism of at least one other biologically important compound has been reported (Small and Meitzner, 1933). Reduction of thebaine gave a compound named metathebanone, assigned structure **37.** Final neutralization of a solution of

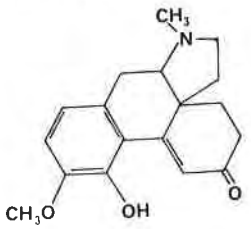


37

metathebanone with sodium bicarbonate and recrystallization gave yellow crystals, while neutralization with NaOH or $NH_3$ and recrystallization gave colorless crystals. Both crystals had the same melting point and both gave a yellow solution in ethanol or water and a colorless solution in benzene. Unfortunately no structural explanations of these differences in color and no investigation of differences in polymorphism of these compounds have been reported.

## C. POLYMORPHISM OF CARBOHYDRATES

Numerous carbohydrates exhibit polymorphism; however, relatively few studies of these compounds have been reported.

Mannitol exists in three forms, and *p*-methoxyphenyl-β-D-glucopyranoside exists in two forms (I and II). Each form has a distinct powder pattern, and form II can be converted to form I at 161°C (Shafizadeh and Susott, 1973). Phenyl-2-acetamidotri-*O*-acetyl-β-D-glucopyranoside also exists in two polymorphs that have different powder patterns. Form II can be converted to form I at 185°C. (Shafizadeh and Susott, 1973).

*p*-Methoxy-2-acetamidotri-*O*-acetyl-β-D-glucopyranoside exists in four forms, which have different powder patterns. Form IV is converted to form III at 158°C, form III can be converted to form II at 177°C, and form II can be converted to the least stable form, form I, at 183°C. Form I melts

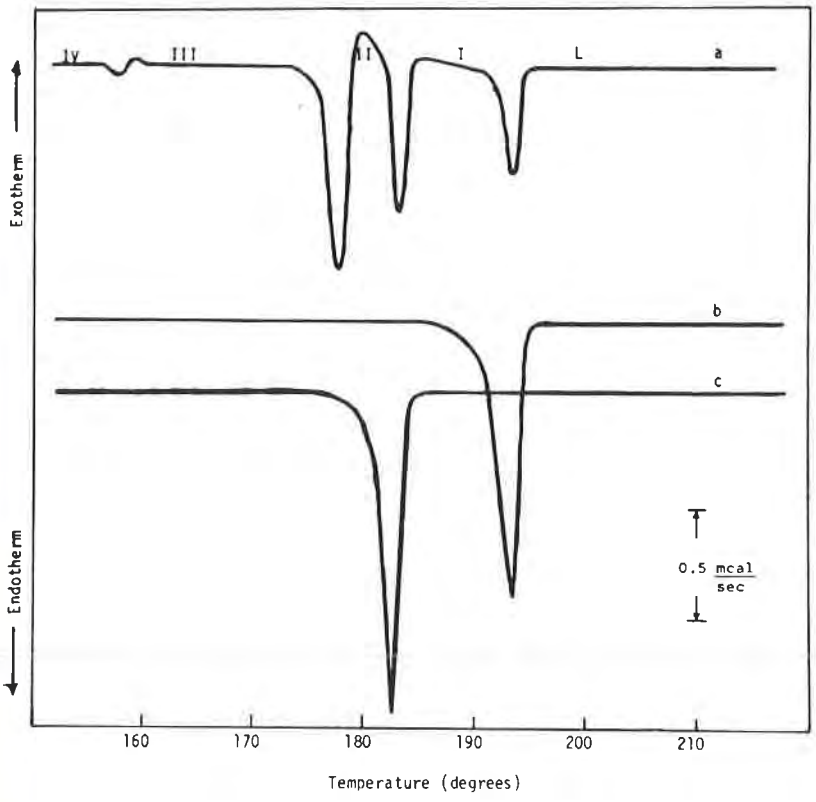


**FIGURE 35.** Differential-scanning calorimetric trace of *p*-methoxyphenyl-2-acetamidotri-*o*-acetyl-2-deoxy-β-D-glucopyranoside. Trace (*a*): complete tracing of form II. Trace (*b*) DSC of form I produced by heating form II at 183°C. Trace (*c*) DSC of phase II formed by heating form I to 192°C. (Shafizadeh and Susott, 1973). (Reprinted with permission from F. Shafizadeh and R. A. Susott [1973]. Copyright 1973 American Chemical Society.)

at 192°C. Figure 35 shows the differential scanning calorimetric traces of this process and illustrates how DSC can be used to characterize polymorphs. Unfortunately, DSC requires more than one crystal for a measurement; unless crystals are sorted it is possible that mixtures of crystals could be present so that the observed behavior would simply be the sum of the behaviors of the individual crystals.

Some carbohydrates also exist in hydrates as well as anhydrous crystalline forms. For example, 1,6-anhydro-β-D-altrropyranose exists in three anhydrous forms, a monohydrate, and a plastic (i.e., glass-like) crystalline form. Two of the anhydrous forms can be converted to the plastic crystalline form at 110° to 115°C, and the monohydrate is converted to one of the anhydrous forms at 62°C.

## D. POLYMORPHISM OF PHENYLBUTAZONE

As mentioned earlier in this chapter, different polymorphs possess different physical properties. From a practical point of view, solubility, surface tension, and bioavailability could depend on the polymorph present. In addition, it is possible that high pressure such as that attained in a tableting machine could induce a polymorphic transformation. Studies of phenylbutazone (**38**) illustrate several of the practical consequences of

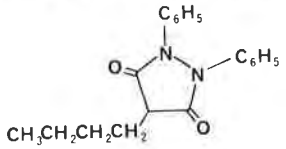


38

polymorphism. Ibrahim *et al.* (1977) prepared four batches of crystals of phenylbutazone by crystallization; form I, from *i*-butanol; form II, from cyclohexane; form III, from *n*-heptane; and form IV, from 2-propanol–water. The x-ray powder patterns and infrared spectra of these four forms were different; thus, these workers concluded that four polymorphs were present. However, it is possible that some batches of crystals contained mixtures of forms. Single-crystal x-ray diffraction studies of these forms are in order, to show that there are actually four polymorphs present. Studies of the dissolution rates of these four forms show that the crystals from cyclohexane have the slowest dissolution rate and that the other three batches have nearly equal dissolution rates. These differences were attributed to differences in surface area; however, it is quite reasonable to expect that a solution-mediated phase transformation could have converted all three forms to the same form.

All four batches of crystals were compressed into discs using a die and a press at 1590 to 2040 kg of pressure. This treatment caused form III to transform to form IV and forms I and II to transform to a fifth phase. Grinding forms I, II, and III produced similar changes.

In conclusion, these studies appear to indicate that high pressure can cause polymorphic transformations. This suggestion is consistent with the studies reported next (Ibrahim *et al.*, 1977).

## E. EFFECT OF PRESSURE ON THE POLYMORPHIC TRANSITIONS OF SUCCINYLSULFATHIAZOLE

As mentioned in the previous section, the studies on phenylbutazone indicate that pressure could cause a polymorphic transformation. This suggestion is consistent with Rankell's (1969) studies on the polymorphism of

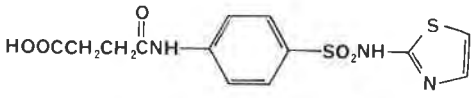

39

succinylsulfathiazole (**39**). Succinylsulfathiazole exists in two hydrates and an anhydrous form. These forms were subjected to compression forces produced by a tablet punch and die placed in a hydraulic press. Under pressure, the structures of the two crystal hydrates were altered as measured by DSC and TGA but the anhydrous form seems to be unaffected. In addition, the extent of the change was related to the compression force.

Grinding also alters both the water content and the crystal structure of the two hydrates but has little effect on the anhydrous form. This may indicate that grinding accelerates solid-state transformations because it increases the number of defects. Grinding also causes the DTA thermograms of the compressed hydrate forms to revert to those of the ground, uncompressed material. In addition, the dissolution rates of the tablets were found to depend upon the compression force. This was probably the result of harder tablets rather than the result of polymorphic transformation.

In conclusion, these studies show that compression can cause phase transformations that could result in changes in dissolution rates and solubilities.

## F. SOLUTION-MEDIATED PHASE TRANSFORMATIONS OF DRUGS

The solution-phase method of studying the transformation of one crystalline form of a drug to another has been used to clarify the apparently anomalous dissolution rates of a new hypertensive agent (Lin and Lachman, 1969). This agent gave a dissolution profile depicted in Figure 36. Such a profile is characteristic of phase transformation to a more stable form during dissolution. Investigation of this process under a microscope showed that this transformation appears to be an *in situ* crystalline transformation in which crystals of the more soluble polymorph (hexagonal crystals) transform into crystals of the less soluble polymorph (rod-shaped crystals). This transformation is closely related to McCrone's solution-phase transformation experiments (Haleblian and McCrone, 1969), in which the more stable crystals grow and the less stable crystals disappear. The most notable feature of the solution-mediated phase transformation of this antihypertensive agent is that it is rapid, nearing completion in 30 min.

These studies indicate that the fact that many polymorphs appear to

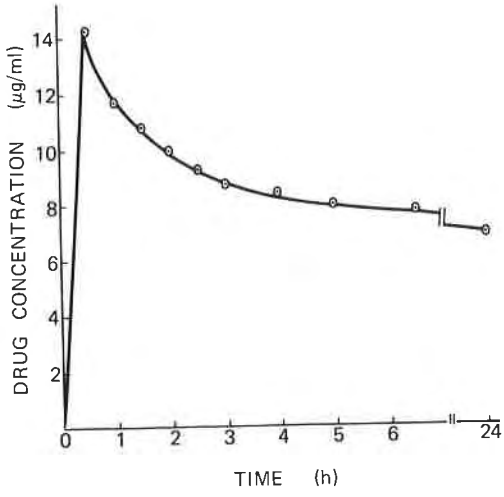


**FIGURE 36.** Dissolution rate of a new hypertensive drug in 0.1 *N* HCl (Lin and Lachman, 1969). (Reproduced with permission of the copyright owner.)

have the same dissolution rate might actually be due to solution-mediated phase transformations. In cases where the rate of solution-mediated phase transformation is comparable to the dissolution rate, one would expect to see anomalous dissolution curves such as that shown in Figure 36.

## G. POLYMORPHS OF ANTIBIOTICS

Antibiotics exhibit polymorphism which could affect their stability and bioavailability. In particular, important studies of the cephalosporin and polyene antibiotics have been reported.

Pfeiffer *et al.* (1970) reported that cephaloglycin (**40**) and cephalexin (**41**) crystallize in a number of solvates. Cephaloglycin crystallizes in the

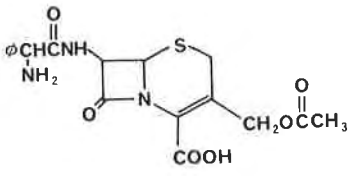


40

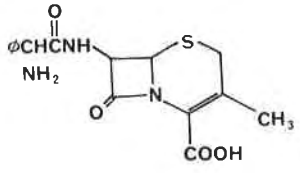


41

following solvates: 2 $H_2O$; formamide; methanol · $H_2O$; acetonitrile; acetic acid · $H_2O$; 2 acetic acid; acetic acid · methanol; ethanol · $H_2O$; and *N*-methylformamide. Cephalexin crystallizes in the following solvates: $2H_2O$; $H_2O$; formamide; methanol; 2 acetonitrile; acetonitrile · $H_2O$; *N*-methylformamide; and *N*-ethylformamide. The crystal solvates of

cephaloglycin or cephalexin can be desolvated and resolvated without a change in the crystal lattice. For example, cephalexin·2 acetonitrile can be desolvated by drying. The desolvated crystal has the same crystal structure as the solvate as evidenced by the powder pattern. The desolvated crystal can take up limited amounts of water from the atmosphere. In addition, exposure of the desolvated crystal to other vapors results in formation of the corresponding solvate, and exposure of the desolvated crystal to acetonitrile results in the formation of the original crystal solvate. As mentioned, all these transformations are reversible and occur without changes in the crystal lattice, as evidenced by the lack of change of the powder pattern.

These experiments indicate that improper drying or storage of these antibiotics can result in changes in the solvate present. Thus care must be taken to ensure which drug form is marketed and its bioavailability. Crystals should probably be isolated free from mother liquor and dried by blotting rather than exposure to vacuum. The products should be stored in well-sealed containers with a minimum of void space. Exposure of these antibiotics to other solvents and temperature changes should be avoided.

For the polyene antibiotics mepartricin and nystatin, different conditions of crystallization have resulted in products with different activity and acute toxicity. Careful studies showed that crystal size did not explain the different activities and toxicities of the different crystals (Ghielmetti *et al.*, 1976).

Studies of mepatricin showed that crystallization from methylene chloride–methanol (9 : 1) at room temperature and evaporation to dryness gave an oil. This oil crystallized upon standing to form a solid which had one-fourth the oral activity and between one-sixth and one-tenth the $LD_{50}$ (for mice) compared to the solid obtained by cooling an acetone–water–ether solution.

Studies of nystatin showed that crystals obtained by crystallization of a water–methyl ethyl ketone solution had approximately the same activity against microorganisms but half the solubility and half to one-tenth the $LD_{50}$ of crystals obtained from chloroform–methanol–ammonia. While the existence of nystatin polymorphs has not been proved by x-ray powder diffraction or other experimental techniques, it is likely that the differences in activity of the different crystals are due to differences in solubility and solution rate, which are in turn due to differences in the polymorph.

## H. POLYMORPHISM OF VITAMIN A ACID

Vitamin A acid (**42**) crystallizes in a triclinic and a monoclinic crystal form (Stam and MacGillaury, 1963). The monoclinic crystals are metastable and transform irreversibly to the triclinic form at 120°C. The triclinic

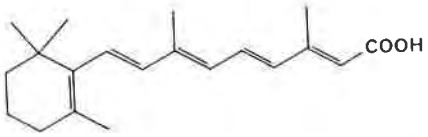


42

form has the following cell parameters: $a = 8.04$ Å, $b = 28.49$ Å, $c = 5.996$ Å, $\alpha = 50°58'$, $\beta = 71°38'$, $\gamma = 95°7'$, and $Z = 2$. The side-chain in the triclinic form is markedly curved due to the methyl groups, and the structure is made up of dimers. The crystal structure of the monoclinic form has not been determined.

## VI. Polymorphism and Its Pharmaceutical Application

Because polymorphs have different physical properties it is often advantageous to choose the proper polymorph for the desired pharmaceutical application. In general, the pharmaceutical applications of polymorphism depends on the answers to the following questions (*a*) what are the solubilities of each form, (*b*) can pure, stable crystals of each form be prepared, and (*c*) will the form survive processing, micronizing, and tableting? Furthermore, several more basic questions about polymorphs also need to be answered: (*a*) how many polymorphs exist, (*b*) what is the chemical and physical stability of each of these polymorphs, and (*c*) can the metastable states be stabilized?

These basic questions can be answered as follows: The number of polymorphs can be determined by microscopic examination and by subsequent x-ray powder and single crystal x-ray studies. The physical stability of each form can be determined using the solution phase transformation method. This method involves placing two polymorphs in a drop of saturated solution under the microscope. Under these conditions the crystals of less stable form will dissolve and crystals of the more stable form will grow until only the most stable form remains. Comparison of the relative stabilities of pairs of forms in succession gives the order of stability of the various forms. This method can also be used to prepare metastable forms. In this case, the temperature is increased or decreased to the temperature where the metastable form is most stable and then the experiment repeated.

There are numerous activities in the pharmaceutical industry that require consideration of polymorphism; these have been reviewed by Haleblian and McCrone (1969). Tableting behavior depends upon the

polymorph present. For example, Simmons *et al.* (1972) showed that tolbutamide exists in forms A and B. Form B is platelike and causes powder bridging in the hopper and capping problems during tableting. Form A, which is not platelike, showed no problems during tableting.

The behavior of suspensions also depends upon the polymorph present. If the wrong polymorph of a drug is used, a phase transformation to a more stable polymorph may occur, producing a change in crystal size and possibly caking. A change in particle size is often undesirable as it may cause serious caking problems as well as changes in the syringeability of the suspension. In addition, the new polymorph may have altered dissolution properties and thus bioavailability. Caking is a particularly serious problem since a caked suspension cannot be resuspended upon shaking. For example, oxyclozanide upon standing in quiescent suspension undergoes an increase in particle size (Pearson and Varney, 1969). This is due to a solvent-mediated phase transformation between two polymorphs. As discussed earlier, under these conditons crystals of the more stable form grow and those of the less stable form dissolve. This produces cakes that cannot be resuspended by shaking.

Polymorphic transformations can also affect the properties of creams. If the wrong polymorph is used, a phase transformation can occur, resulting in crystal growth of the new phase. The cream can then become gritty and cosmetically unacceptable. Thus it is usually best to select the polymorph that is least susceptible to phase transformations and crystal growth. This is the most stable polymorph and thus least soluble in the cream base. When a metastable polymorph with high solubility in the cream base is used, there is a high risk that nucleation and crystallization of a more stable form can occur. On the other hand, some metastable polymorphs may transform sufficiently slowly that they could be used in the preparation of creams. This situation is particularly attractive since metastable polymorphs by virtue of their higher solubility often have better bioavailability.

Phase transformations can also occur in suppositories, resulting in products with altered melting characteristics that could result in either premature melting during storage or failure to melt after administration.

## A. POLYMORPHISM AND CHEMICAL STABILITY

Because polymorphs have different properties, including different melting points, densities, and crystal structures, it is not surprising that polymorphs have different chemical stabilities.

Perhaps the most striking effect of polymorphism on chemical reactiv-

ity is seen in the polymorphs of *o*-ethoxy-*trans*-cinnamic acid (Scheme I, compound 1) (Cohen and Green, 1973). Irradiation of this compound in solution produces trans to cis isomerization but no dimerization. Crystallization of this cinnamic acid yields three polymorphs $\alpha$, $\beta$, and $\gamma$. The $\alpha$ polymorph is obtained from ethyl acetate, ether, or acetone. The $\beta$ polymorph is obtained from benzene or petroleum ether and the $\gamma$ polymorph from aqueous ethanol. Irradiation of the $\alpha$ polymorph gives the centrosymmetric dimer, irradiation of the $\beta$ polymorph gives the minor symmetric dimer, and irradiation of the $\gamma$ form produces no reaction. These reactions are summarized in Scheme II. Numerous examples of similar behavior have been found in other cinnamic acid derivatives and in anthracene dimerizations.

A number of pharmaceutical examples of different stabilities of polymorphs are also known. For example, methylprednisolone crystallizes in two forms. One form is stable while the other is reactive when exposed to heat, ultraviolet light, or high humidity (Munshi and Simonelli, 1970).

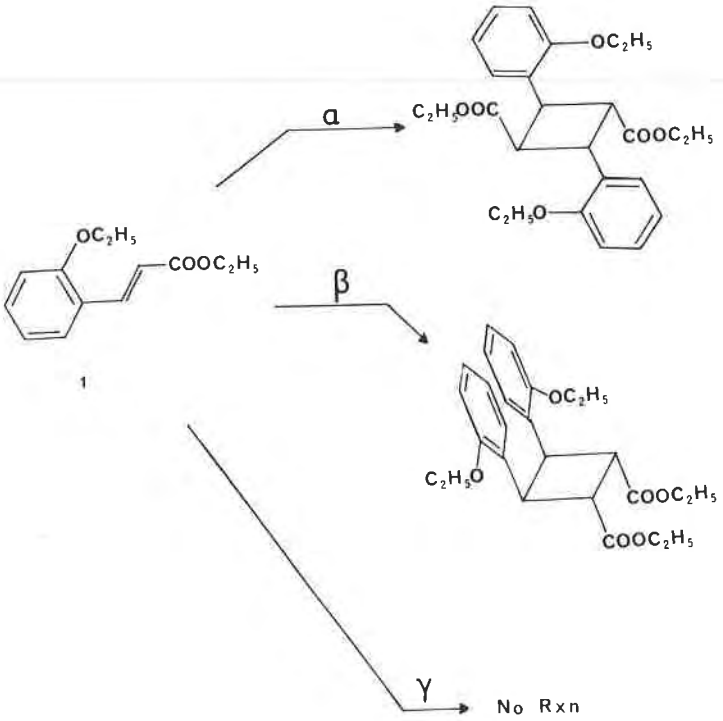


**SCHEME I.** Summary of the reactivities of the $\alpha$, $\beta$, and $\gamma$ crystalline forms of ethoxycinnamic acid upon exposure to ultraviolet light.

In our laboratory we have reinvestigated the behavior of the various polymorphs of hydrocortisone 21-*tert*-butylacetate. This steroid crystallizes from ethanol in three polymorphs, one anhydrous and two solvates. When exposed to light, one of the solvates is reactive while the other two forms are stable. In addition, there are numerous cases where amorphous forms are much more reactive than the crystalline form (see the novobiocin discussion earlier). In another example, Macek (1965) has reported that the amorphous forms of sodium and potassium penicillin G are significantly less stable than the crystalline forms. Crystals of the potassium salt can withstand heating for several hours, while identical treatment of the amorphous form results in a significant loss of activity.

This discussion clearly shows that in cases where chemical stability is a problem, there is a need for careful control of the polymorph marketed and stored.

## B. POLYMORPHISM AND BIOAVAILABILITY

The rate of absorption of a drug is dependent upon the dissolution rate. The dissolution rate and rate of absorption will either increase or decrease depending upon the polymorph present. The most stable polymorph will have the lowest solubility and in many cases the slowest dissolution rate. Other less stable polymorphs will usually have higher dissolution rates. Thus if polymorphism is ignored, significant dose-to-dose variations can occur (Haleblian and McCrone, 1969).

In a particularly striking example, a suspension of chloramphenicol palmitate containing various ratios of polymorphs A and B showed significant variations in bioavailability (i.e., blood levels) (Aguiar *et al.*, 1967).

Figure 37 shows a comparison of mean blood serum levels of suspensions containing varying ratios of polymorphs A and B. Clearly the maximum blood levels are quite different, ranging from 3 to 22 $\mu$g/ml or by approximately a factor of 7. Interestingly, a plot of peak blood levels versus % form B gave a straight line, as shown in Figure 38. These data show that bioavailability is influenced by the type and concentration of the polymorph present. Obviously if products are manufactured containing polymorph A they will be largely inactive, while products containing polymorph B will show activity.

Although the bioavailability of other polymorphs has not been directly determined, the dissolution rates of several polymorphic drugs have been determined. For example, fluprednisolone crystallizes in three polymorphs and two solvates. These forms were pressed into pellets and implanted into rats, and their *in vivo* dissolution rates were measured

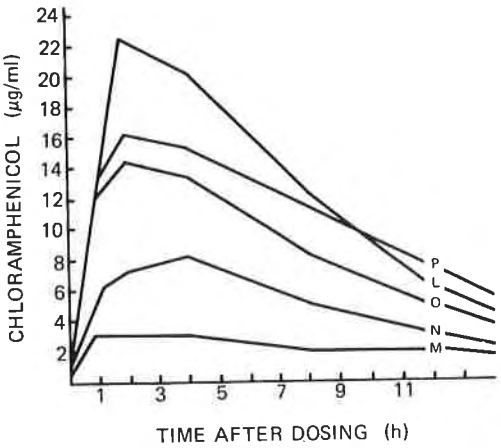


**FIGURE 37.** Comparison of the mean serum levels obtained with chloramphenicol palmitate suspensions containing varying ratios of the A and B polymorphs following a single oral dose equivalent to 1.5 gm of chloramphenicol. As the blood level increases, the percent polymorph B increases. The lowest curve corresponds to 0% B, the next 25% B, the next 50%, then 75% B, and the highest 100% B (Haleblian and McCrone, 1969). (Reproduced with permission of the copyright owner.)

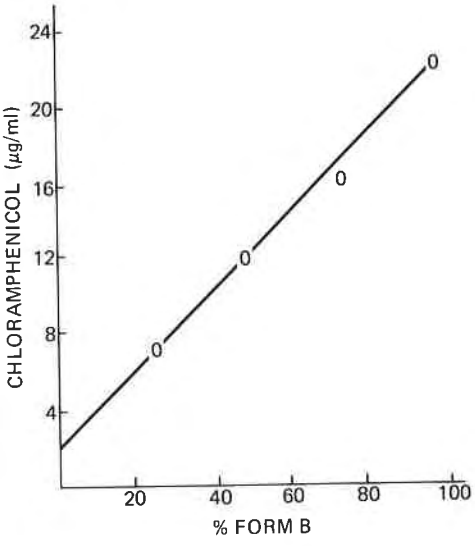


**FIGURE 38.** Plot of the peak chloramphenicol blood levels (as plotted in Figure 2) versus the percent of polymorph B (Haleblian and McCrone, 1969). (Reproduced with permission of the copyright owner.)

**TABLE XXI**
*Blood Levels for Various Suspensions of Chloramphenicol Palmitate*[a]

| Suspension used | Hours after feeding | | | |
|---|---|---|---|---|
| | 2 | 4 | 6 | 8 |
| In Children | | | | |
| Amorphous | 1018 | 604 | 417 | 263 |
| Polymorph A | 344 | 347 | 567 | 234 |
| In rhesus monkeys | | | | |
| Amorphous | 675 | 389 | 183 | |
| Polymorph A | 223 | 173 | 170 | |

[a] Data from Banerjee *et al.* (1971).

(Haleblian and McCrone, 1969). The dissolution rates showed the following order and value: form I (0.237 mg $cm^{-2}$ $M^{-1}$) > form III (0.209 mg $cm^{-2}$ $M^{-1}$) > form II (0.186 mg $cm^{-2}$ $M^{-1}$) > $\beta$-monohydrate (0.162 mg $cm^{-2}$ $M^{-1}$) > $\alpha$-monohydrate (0.147 mg $cm^{-2}$ $M^{-1}$). Thus the variation in dissolution rate is approximately a factor of 1.6 when comparing form I to the $\alpha$-monohydrate.

In a more recent study, serum levels of the amorphous form and polymorph A of chloramphenicol palmitate have been compared in both children and Rhesus monkeys. Table XXI shows the results of these studies (Banerjie *et al.*, 1971). These data show that the amorphous form has greater bioavailability than polymorph A.

The examples discussed in this section clearly show that the polymorph present can dramatically affect the bioavailability and thus the therapeutic effect of a drug.

## VII. Summary

1. *Definition of Polymorphism*—Polymorphs exist when different crystal habits have different crystallographic unit cells and/or space groups. Thus polymorphs give different powder diffraction patterns.
2. Properties of polymorphs
   a. Polymorphs have different physical properties.
   b. Polymorphs can be interconverted by a solvent-mediated process.
   c. Polymorphs can be interconverted by phase transformations, which can be single-crystal-to-single-crystal processes.

d. Phase transformations can be solvent-mediated, heat-induced, or stress-induced.
e. The conformation of the compound can be different in different polymorphs, resulting in conformational polymorphism.
f. Compounds can have different colors in different polymorphs, thereby resulting in color polymorphism.

3. Polymorphs can best be studied by x-ray crystallography and optical microscopy, although other methods, including infrared spectroscopy and thermal analysis, have been used.
4. Different polymorphs have different chemical and physical stability.
5. Different polymorphs can have different dissolution rates and bioavailability.
6. No rules exist that allow the prediction of whether a compound will exhibit polymorphism; however, polymorphism is widespread in pharmaceuticals, particularly steroids, sulfonamides, and barbiturates.

## References


Alleaume, P. M., and Decap, J. (1965). *Acta Cryst.* **18,** 731.
Alleaume, P. M., and Decap, J. (1966). *Acta Cryst.* **19,** 934.
Aguiar, A. J., Krc, J., Jr., Kinkel, A. W., and Samyn, J. C. (1967). *J. Pharm. Sci.* **56,** 847.
Banerjee, S., Bandyopadnyay, A., Bhattacharjee, R. C., Mukherjee, A. K., and Halder, A. K. (1971). *J. Pharm. Sci.* **60,** 153.
Bernstein, J., and Hagler, A. T. (1978). *J. Am. Chem. Soc.* **100,** 673.
Biles, J. A. (1963). *J. Pharm. Sci.* **52,** 1066.
Bouche, R., Draguet-Brughmans, M., and DeRauter, C. (1977). *Microchim. Acta* **1,** 511.
Brown, H. C., and Sujishi, S. (1948). *J. Am. Chem. Soc.* **70,** 2793.
Busetta, P., Courseille, C., and Hospital, M. (1973). *Acta Cryst.* **B29,** 298.
Byrn, S. R., Curtin, D. Y., and Paul, I. C. (1972). *J. Am. Chem. Soc.* **94,** 890.
Chiang, C. C., DeCamp, W. H., Curtin, D. Y., Paul, I. C., Shifrin, S., and Weiss, U. (1978). *J. Am. Chem. Soc.* **100,** 6195.
Cohen, M. D., and Green, B. S. (1973). *Chem. Br.* **9,** 490.
Cohen, M. D., Coppens, P., and Schmidt, G. M. J. (1964). *J. Phys. Chem. Solids* **25,** 258.
Coiro, V. M., Giglio, E., Lucano, A., and Puliti, R. (1973). *Acta Cryst.* **B29,** 1404.
Craven, B. M., and Vizzini, E. A. (1969). *Acta Cryst.* **B25,** 1993.
Curtin, D. Y., and Englemann, J. H. (1972). *J. Org. Chem.* **37,** 3439.
Dabroswki, J. (1963). *Spectrochim Acta* **19,** 475.
Dabrowski, J., and Dabrowski, U. (1958). *Rocz. Chem.* **32,** 821.
Desiraju, G. R., Paul, I. C., and Curtin, D. Y. (1977). *J. Am. Chem. Soc.* **99,** 1594.
DeCamp, W. H., and Ahmed, F. R. (1972a). *Acta Cryst.* **B28,** 1796.
DeCamp, W. H., and Ahmed, F. R. (1972b). *Acta Cryst.* **B28,** 3484.
Drenth, W., and Wiebenga, F. H. (1954). *Recl. Trav. Chim. Pays-Bas* **73,** 218.
Dudek, G. O., and Volpp, G. P. (1963). *J. Am. Chem. Soc.* **85,** 2697.
Eistert, B., Weygand, F., and Csendes, E. (1952). *Chem. Ber.* **85,** 164.

Ghielmetti, G., Bruzzese, T., Bianchi, C., and Recusani, F. (1976). *J. Pharm. Sci.* **65,** 905.
Gougoutas, J. Z., and Lessinger, L. (1974). *J. Solid State Chem.* **9,** 155.
Guillory, J. K. (1967). *J. Pharm. Sci.* **56,** 72.
Haleblian, J., and McCrone, W. C. (1969). *J. Pharm. Sci.* **58,** 911.
Hamlin, W. E., Nelson, E., Ballard, B. E., and Wagner, J. G. (1962). *J. Pharm. Sci.* **51,** 432.
Herbstein, F. H., and Schmidt, G. M. J. (1955). *Acta Cryst.* **8,** 399.
Higuchi, W. I., Bernardo, P. D., and Mehta, S. C. (1967). *J. Pharm. Sci.* **56,** 200.
Higuchi, W. I., Hamlin, W. E., and Mehta, S. C. (1969). *J. Pharm. Sci.* **58,** 1145.
Ibrahim, H. G., Pisano, F., and Bruno, A. (1977). *J. Pharm. Sci.* **66,** 669.
Kitaigorodskii, A. I., Mnyukh, Y. V., and Asadov, Y. G. (1965). *J. Phys. Chem. Solids* **26,** 463.
Kornblum, S. S. (1970). *Drug Cosmet. Ind.*, April, p. 42.
Krigbaum, W. R., and Wildman, C. C. (1971). *Acta Cryst.* **B27,** 2353.
Kruger, G. J., and Gafner, G. (1971). *Acta Cryst.* **B27,** 326.
Kruger, G. J., and Gafner, G. (1972). *Acta Cryst.* **B28,** 272.
Kuhnert-Brandstatter, M. (1971). "Thermomicroscopy in the Analysis of Pharmaceuticals." Pergamon Press, New York.
Levy, G., and Procknal, J. A. (1964). *J. Pharm. Sci.* **53,** 657.
Lin, C. T., and Byrn, S. R. (1976). *J. Am. Chem. Soc.* **98,** 4004.
Lin, H. O., Baenziger, N. C., and Guillory, J. K. (1974). *J. Pharm. Sci.* **63,** 145.
Lin, S. L., and Lachman, L. (1969). *J. Pharm. Sci.* **58,** 377.
O'Connor, B. H., and Maslen, E. N. (1965). *Acta Cryst.* **18,** 363.
Macek, T. J. (1965). *Am. J. Pharm.* **137,** 217.
Mesley, R. J. (1971). *J. Pharm. Pharmacol.* **23,** 687.
McCrone, W. C. (1965). *In* "Physics and Chemistry of the Organic Solid State," Vol. II (D. Fox, M. M. Labes, and A. Weissberger, eds.), pp. 725–767. Interscience, New York.
Milosovich, G. (1964). *J. Pharm. Sci.* **53,** 484.
Moustafa, M. A., Ebian, A. R., Khalil, S. A., and Motawi, M. M. (1971). *J. Pharm. Pharmacol.* **23,** 868.
Moustafa, M. A., Khalil, S. A., Ebian, A. R., and Motawi, M. M. (1972). *J. Pharm. Pharmacol.* **24,** 921.
Munshi, M., and Simonelli, A. (1970). *Abstr. Am. Pharm. Assoc.*(Acadamy of Pharmaceutical Sciences), Washington, D.C., April 12, 1970.
Paul, I. C., and Go, K. T. (1969). *J. Chem. Soc.* **13,** 33.
Pearson, J., and Varney, G. (1969). *J. Pharm. Pharmacol.* **21,** 60S.
Perrin, P. M. and Michel, P. (1973). *Acta Cryst.* **B29,** 253, 258.
Pfeiffer, R. R., Yang, K. S., and Tucker, M. A. (1970). *J. Pharm. Sci.* **59,** 1809.
Phillips, D. C. (1956). *Acta Cryst.* **9,** 237.
Phillips, D. C., Ahmed, F. R., and Barnes, W. H. (1960). *Acta Cryst.* **13,** 365.
Rankell, A. S. (1969). Ph.D. Thesis, University of Wisconsin, Madison, Wisconsin.
Robertson, J. M., and White, J. G. (1947). *J. Chem. Soc.*, 1001.
Robertson, J. M., and White, J. G. (1956). *J. Chem. Soc.*, 925.
Robertson, J. M., and Ubbelohde, A. R. (1936). *Proc. R. Soc. London, Ser. A.* **167,** 136.
Schad, H. P. (1955). *Helv. Chim. Acta* **38,** 1117.
Schulenberg, J. W. (1968). *J. Am. Chem. Soc.* **90,** 7008.
Shafizadeh, F., and Susott, R. A. (1973). *J. Org. Chem.* **38,** 3710.
Shenouda, L. S. (1970). *J. Pharm. Sci.* **59,** 785.
Simmons, D., Ranz, R., Gyanchandani, N., and Picotte, D. (1972). *Can. J. Pharm. Sci.* **7,** 121.
Simmons, D. L., Ranz, R. J., and Gyanchandani, N. D. (1973). *Can. J. Pharm. Sci.* **8,** 125.

Small, L. F., and Meitzner, E. (1933). *J. Am. Chem. Soc.* **55,** 4602.
Stam, C. H., and MacGillaury, C. H. (1963). *Acta Cryst.* **16,** 62.
Sunwoo, C., and Eisen, H. (1971). *J. Pharm. Sci.* **60,** 238.
Thomas, J. M. (1974). *Phil. Trans. R. Soc., Ser.* **A277,** 1268.
Weintraub, H. J. R., and Hopfinger, A. J. (1975). *Int. J. Quantum Chem.* **QBS2,** 201.
Williams, P. P. (1973). *Acta Cryst.* **B29,** 1572.
Williams, P. P. (1974). *Acta Cryst.* **B30,** 12.
Wilson, K. R., and Pincock, R. E. (1977). *Can. J. Chem.* **55,** 889.
Yang, S. S., and Guillory, J. K. (1972). *J. Pharm. Sci.* **61,** 26.

# 5 Loss of Solvent of Crystallization

The appearance of water of hydration is common in crystals of both organic and inorganic compounds. A review of "Molecular Structures and Dimensions" (Kennard and Watson, 1962–1978) indicates that more than 1000 crystal structures of solvates have been determined. In addition, Clark (1963) has reviewed crystallographic studies of hydrated organic crystals up to 1963. In general, this review shows that water molecules in these crystals are almost always involved in hydrogen bonds, and that these hydrogen bonds often contribute to the coherence of the crystal structure.

A large number of drugs and biologically important compounds crystallize with solvent of crystallization. Table I lists some of these. There are more than 90 hydrates listed in the "United States Pharmacopeia."

## I. Loss of Solvent of Crystallization

### A. GENERAL OVERVIEW

The desolvation of crystals is a widespread phenomenon in pharmaceuticals. Numerous methods have been used to study these pro-

**TABLE I**
*A Partial Listing of Drugs That Form Solvates*

| Drug | Reference |
|---|---|
| Estradiol | Kuhnert-Brandstatter and Gasser (1971) |
| Hydrocortisone acetate | Shell (1955) |
| Cortisone acetate | Carless *et al.* (1966) |
| Fluprednisolone | Haleblian *et al.* (1971) |
| *t*-Butylacetylprednisolone | Biles (1963) |
| *t*-Butylacetylhydrocortisone acetate | Biles (1963) |
| Fluorohydrocortisone acetate | Shefter and Higuchi (1963) |
| Cholesterol | Shefter and Higuchi(1963) |
| Erythromycin | Rose *et al.* (1953) |
| Gramicidin | Olesen and Szabo (1959) |
| Nitrofurmethone | Borka *et al.* (1972) |
| Ampicillin | Austin *et al.* (1965) |
| Cephaloridine | Chapman *et al.* (1968) and Pfeiffer *et al.* (1970) |
| Chloramphenicol | Himuro *et al.* (1971) |
| Griseofulvin | Sekiguchi *et al.* (1968) |
| Sulfanilamide | Lin (1972) |
| Sulfabenzamide | Yang and Guillory (1972) |
| Sulfaguanidine | Yang and Guillory (1972) |
| Succinylsulfathiazole | Shefter and Higuchi (1963) |
| Sulfameter | Moustafa *et al.* (1971) |

cesses, including thermomicroscopy, differential scanning calorimetry, differential thermal analysis, x-ray crystallography, and analysis of gases. The results of all of these methods will be discussed in this chapter. Special emphasis will be placed on the results of thermomicroscopic and x-ray crystallographic studies of these reactions.

In an extensive study, Kuhnert-Brandstatter (1971) has characterized the behavior of solvates of pharmaceuticals using thermomicroscopy, reported in Table II. Many of the hydrates listed in this table show unusual behavior that may be caused by dehydration prior to melting. These are marked with an asterisk(*). In addition, many of these crystals are reported to become opaque, and opaque crystals would appear dark when viewed by transmitted light as do the photomicrographs of crystals shown later in this chapter. Some of these hydrates crack and "jump" during dehydration. This behavior is characteristic of rapid solid-state reactions that have gaseous products.

In addition to these compounds, several carbohydrates have been shown to dehydrate before melting (Shafizadeh and Susott, 1973). These

**TABLE II**

*Thermomicroscopic Characterization of Solvates of Pharmaceuticals*[a]

| Compound[b] | mp (°C) | Remarks |
|---|---|---|
| 1. L-Ephedrine<br>$C_{10}H_{15}NO \cdot H_2O$ | 38–40 | |
| 2. Cyclophosphamide<br>$C_7H_{15}Cl_2N_2O_2P \cdot H_2O$ | 40–47 | Melts as hydrate |
| 3. Atroscine<br>$C_{17}H_{21}NO_4 \cdot H_2O$ | 54–56 | |
| 4. Cocaine nitrate<br>$C_{17}H_{21}NO_4 + HNO_3 + 2H_2O$ | 55–59 | Needles of decomposition product appear |
| 5. Lidocaine hydrochloride<br>$C_{14}H_{22}N_2O \cdot HCl \cdot H_2O$ | 65–78 | |
| 6. Levisoprenaline bitartrate<br>$C_{11}H_{17}NO_3 \cdot C_4H_6O_6 \cdot 2H_2O$ | 74–78 | |
| 7. Cetylpyridinium chloride<br>$C_{21}H_{38}ClN \cdot H_2O$ | 78–80 | |
| 8. Oxyphenbutazone<br>$C_{19}H_{20}N_2O_3 \cdot H_2O$ | 65–85 | |
| 9. $\alpha$-Rhamnose<br>$C_6H_{12}O_5 \cdot H_2O$ | 70–95 | |
| 10. Pholcodine<br>$C_{23}H_{30}N_2O_4 \cdot H_2O$ | 98–99 | |
| 11. Chlorbutanol<br>$C_4H_7Cl_3O \cdot \frac{1}{2}H_2O$ | 99.5 | |
| 12. Levacterenol bitartrate<br>$C_8H_{11}NO_3 \cdot C_4H_6O_6 \cdot H_2O$ | 93–103 | |
| *13. Terpin hydrate<br>$C_{10}H_{20}O_2 \cdot H_2O$ | 105.5 | Transforms to anhydrous form at 65°–70°C |
| 14. Procaine benzylpenicillin<br>$C_{16}H_{18}N_2O_4S \cdot C_{13}H_{20}N_2O_2 \cdot H_2O$ | 93–107 | |
| 15. Benzathine penicillin V<br>$(C_{16}H_{18}N_2O_5S)_2 \cdot C_{16}H_{20}N_2 \cdot 4H_2O$ | 102–103 | |
| *16. Pyridoxine phosphate<br>$C_8H_{11}NO_3 \cdot H_3PO_4 \cdot H_2O$ | 122–124 | Turbidity from 65°C |
| 17. Isoprenaline sulfate<br>$(C_{11}H_{17}NO_3)_2 \cdot H_2SO_4 \cdot H_2O$ | 120–128 | |
| *18. Sparteine sulfate<br>$C_{15}H_{26}N_2 \cdot H_2SO_4 \cdot 5H_2O$ | 100–130 | Turbidity with loss of water at 60°–80° |
| 19. Dihydrocodeinone bitartrate<br>$C_{18}H_{21}NO_3 \cdot C_4H_6O_6 \cdot 2.5H_2O$ | 115–130 | |
| *20. Pyrogallol<br>$C_6H_6O_3 \cdot 0.25H_2O$ | 133 | Turbidity |
| *21. Raffinose<br>$C_{18}H_{32}O_{16} \cdot 5H_2O$ | 132–135 | Transforms to anhydrous form at 78°–80°C |
| *22. Droperidole<br>$C_{22}H_{22}FN_3O_2 \cdot H_2O$ | 143–147 | Transforms to anhydrous form at 120°–125°C |
| *32. 5,5-Dipropyl barbituric acid<br>$C_{10}H_{16}N_2O_3 \cdot xH_2O$ | 148 | Commercial product partly dehydrated and turbid |

**TABLE II** (*continued*)

| Compound[b] | mp (°C) | Remarks |
|---|---|---|
| *24. Quinine hydrobromide<br>$C_{20}H_{24}N_2O_2 \cdot NBr \cdot H_2O$<br>(same with hydrochloride) | 145–152 | Water evolved at 90°C |
| 25. Aesculin<br>$C_{15}H_{16}O_9 \cdot 1.5H_2O$ | 146–152 | Transforms at 125°–130°C, resolidifies and melts at 200°–205°C |
| *26. Sulphacarbamide<br>$C_7H_9N_3O_3S \cdot H_2O$ | 150–154 | Turbidity from 80°C |
| 27. Ergometrine tartrate<br>$(C_{19}H_{23}N_3O_2)_2 \cdot C_4H_6O_6 \cdot H_2O$ | 145–155 | Loss of birefringence at 120°–125°C |
| 28. Ethylmorphine hydrochloride<br>$C_{19}H_{23}NO_3 \cdot HCl \cdot 2H_2O$ | 148–155 | Loss of birefringence at 110°–130°C |
| *29. Citric acid<br>$C_6H_8O_7 \cdot H_2O$ | 152–155 | Loss of $H_2O$ and turbidity at 60°–70°C |
| *30. Hyoscyamine hydrochloride<br>$C_{17}H_{23}NO_3 \cdot HCl \cdot H_2O$ | 152–155 | Turbidity with loss of water during heating |
| 31. Codeine<br>$C_{18}H_{21}NO_3 \cdot H_2O$ | 156 | Loss of water with turbidity at 70°C |
| *32. Quinine bisulfate<br>$C_{20}H_{24}N_2O_2 \cdot H_2SO_4 \cdot 7H_2O$ | 155–160 | Turbidity at 60°C |
| 33. Prothipendyl hydrochloride<br>$C_{16}H_{19}N_3S \cdot HCl \cdot H_2O$ | 158–160 | Melts with loss of water at 80°–90°C |
| *34. Benzethonium chloride<br>$C_{27}H_{42}ClNO_2 \cdot H_2O$ | 160–162 | Turbidity at 105°C |
| *35. Arecoline hydrochloride<br>$C_8H_{13}NO_2 \cdot HCl \cdot H_2O$ | 163 | Melts with loss of water from 155°C |
| 36. Brucine sulfate<br>$(C_{23}H_{26}N_2O_4)_2 \cdot H_2SO_4 \cdot 7H_2O$ | 130–165 | Gradual loss of water from 140°C |
| 37. Stigmasterol<br>$C_{29}H_{48}O \cdot H_2O$ | 167 | Microcrystalline transformation of folicate crystals from 90°C |
| 38. Narceine<br>$C_{23}H_{27}NO_8 \cdot 3H_2O$ | 165–170 | |
| *39. Amdricaine hydrochloride<br>$C_{16}H_{26}N_2O_2 \cdot HCl \cdot 2H_2O$ | 171 | Loss of water with turbidity from 80°C |
| *40. Fosylchloramide sodium<br>$C_7H_7ClNNaO_2S \cdot 3H_2O$ | 171–174 | Loss of water with turbidity from 55°C |
| 41. Histidine monohydrochloride<br>$C_6H_9N_3O_2 \cdot HCl \cdot H_2O$ | 155–176 | |
| 42. Methylarbutin<br>$C_{13}H_{18}O_7 \cdot H_2O$ | 176 | |
| *43. Brucine<br>$C_{23}H_{26}N_2O_4 \cdot 4H_2O$ | 170 | Crystals are rarely clear and usually partially dehydrated |
| *44. Amodiaquine hydrochloride<br>$C_{20}H_{22}ClN_3O \cdot 2HCl \cdot 2H_2O$ | 172–180 | Loses gas from 155°C |

**TABLE II** (*continued*)

| Compound[b] | mp (°C) | Remarks |
|---|---|---|
| *45. Ouabain<br>$C_{29}H_{44}O_{12} \cdot 8H_2O$ | 178–184 | Loses $H_2O$ from 90°C |
| *46. Acoine<br>$C_{23}H_{25}N_3O_3 \cdot HCl \cdot H_2O$ | 165–185 | Loses $H_2O$ and becomes turbid from 70°C |
| 47. Pecazine hydrochloride<br>$C_{19}H_{22}N_2S \cdot HCl \cdot H_2O$ | 170–186 | |
| 48. Methicillin sodium<br>$C_{17}H_{19}N_2NaO_6S \cdot H_2O$ | 182–186 | Loss of birefringence from 170°C |
| 49. Berberine hydrochloride<br>$C_{20}H_{18}NO_4Cl \cdot 2H_2O$ | 182–188 | |
| *50. 7-Hydroxy-4-methylcoumarin<br>$C_{10}H_8O_3 \cdot H_2O$ | 188 | Turbidity of crystals from 70°C with loss of water |
| *51. Sulphaguanidine<br>$C_7H_{10}N_4O_2S \cdot H_2O$ | 187–191 | From 90°C loss of water with turbidity |
| 52. Hexamethonium tartrate<br>$C_{20}H_{40}N_2O_{12} \cdot xH_2O$ | 182–192 | |
| *53. Cotarnine chloride<br>$C_{12}H_{14}ClNO_3 \cdot 2H_2O$ | 184–192 | The yellow compound becomes turbid at 70°–90°C with loss of water |
| 54. Atropine sulfate<br>$(C_{17}H_{23}NO_3)_2 \cdot H_2SO_4 \cdot H_2O$ | 190–193 | Substance partially dehydrated |
| 55. Succinylsulphathiazole<br>$C_{13}H_{13}N_3O_5S_2 \cdot H_2O$ | 190–193 | |
| 56. Phenacaine hydrochloride<br>$C_{16}H_{22}N_2O_2 \cdot HCl \cdot H_2O$ | 190–194 | Original substance already partially dehydrated; from 80°C, loss of $H_2O$ with turbidity |
| 57. Methenamine sulphosalicytate<br>$C_{13}H_{18}N_4O_6S \cdot H_2O$ | 180–195 | |
| *58. Thebaine hydrochloride<br>$C_{19}H_{21}NO_3 \cdot HCl \cdot H_2O$ | 185–195 | Crystals jump during heating |
| 59. Rutoside<br>$C_{27}H_{30}O_{16} \cdot 3H_2O$ | 190–195 | |
| 60. Noscapine hydrochloride<br>$C_{22}H_{23}NO_7 \cdot HCl \cdot H_2O$ | 190–198 | |
| *61. Arbutin<br>$C_{12}H_{16}O_7$ | 200 | From 65°C, turbidity |
| 62. Narceine hydrochloride<br>$C_{23}H_{27}NO_8 \cdot HCl \cdot 3H_2O$ | 180–202 | |
| *63. L-Thyroxine sodium<br>$C_{15}H_{10}I_4NNaO_4 \cdot 5H_2O$ | 195–202 | From 70°C, effervescence with jumping |
| 64. Benzoylecgonine<br>$C_{16}H_{19}NO_4 \cdot 4H_2O$ | 200–203 | From 70°C, partial melting |
| *65. Suxamethonium chloride<br>$C_{14}H_{30}Cl_2N_2O_4 \cdot 2H_2O$ | 198–204 | From 130°C, turbidity |
| *66. Hyoscine hydrochloride<br>$C_{17}H_{21}NO_4 \cdot HCl \cdot 2H_2O$ | 195–205 | From 70°C, turbidity |

**TABLE II** (*continued*)

| Compound[b] | mp (°C) | Remarks |
|---|---|---|
| *67. Hydrocortisone hemisuccinate $C_{25}H_{34}O_8 \cdot H_2O$ | 198–205 | From 85°C, loss of water with turbidity |
| 68. Hyoscyamine sulfate $(C_{17}H_{23}NO_3)_2 \cdot H_2SO_4 \cdot 2H_2O$ | 200–205 | From 130°C, transformation |
| *69. Cinchonidine sulfate $(C_{19}H_{22}N_2O)_2 \cdot H_2SO_4 \cdot 3H_2O$ | 200–298 | From 40°C, turbidity with loss of water |
| 70. Quinidine sulfate $(C_{20}H_{24}N_2O_2)_2 \cdot H_2SO_4 \cdot 2H_2O$ | 205–210 | |
| *71. Quinidine tartrate $(C_{20}H_{24}N_2O_2)_2C_4H_6O_6 \cdot 2H_2O$ | 205–210 | From 180°C, turbidity with loss of water |
| 72. Chloroquine sulfate $C_{18}H_{26}ClN_3 \cdot H_2SO_4 \cdot H_2O$ | 209–213 | |
| 73. Emetine hydrochloride $C_{29}H_{40}N_2O_4 \cdot 2HCl \cdot xH_2O$ | 205–215 | |
| 74. Lactose $C_{12}H_{22}O_{11} \cdot H_2O$ | 205–216 | |
| *75. Cinchonine hydrochloride $C_{19}H_{22}N_2O \cdot HCl \cdot 2H_2O$ | 208–216 | From 50°C, turbidity |
| *76. Bamipine hydrochloride $C_{19}H_{24}N_2 \cdot HCl \cdot H_2O$ | 214–217 | From 60°C, loss of water |
| *77. Mephentermine sulfate $(C_{11}H_{17}N)_2 \cdot H_2SO_4 \cdot 2H_2O$ | 190–220 | From 120°C, transforms with turbidity |
| *78. Phloroglucinol $C_6H_6O_3 \cdot 2H_2O$ | 218–220 | At 55°–90°C, turbidity with loss of water |
| *79. Quinine sulfate $(C_{20}H_{24}N_2O_2)_2 \cdot H_2SO_4 \cdot 2H_2O$ | 219–223 | At 70°–105°C, turbidity with loss of water |
| *80. Reserpine hydrochloride $C_{33}H_{40}N_2O_9 \cdot HCl \cdot H_2O$ | 125–225 | From 180°C, turbidity of crystals |
| *81. Sodium methane sulfate noramidopyrine $C_{13}H_{16}N_3NaO_4S \cdot H_2O$ | 224–228 | From 105°C, decrepitation with loss of water |
| *82. Heroine hydrochloride $C_{21}H_{23}NO_5 \cdot HCl \cdot H_2O$ | 218–232 | Turbidity of crystals from 115°–120° |
| 83. Adenosine $C_{10}H_{13}N_5O_4 \cdot 1.5H_2O$ | 234–236 | |
| 84. Codeine phosphate $C_{18}H_{21}NO_3 \cdot H_3PO_4 \cdot 1.5H_2O$ | 225–240 | |
| 85. Morphine sulfate $(C_{17}H_{19}NO_3)_2 \cdot H_2SO_4 \cdot 5H_2O$ | 230–240 | |
| 86. Brucine nitrate $C_{23}H_{26}N_2O_4 \cdot HNO_3 \cdot 2H_2O$ | 225–245 | |
| 87. Ethacridine lactate $C_{15}H_{15}N_3O \cdot C_3H_6O_3 \cdot H_2O$ | 225–250 | |
| *88. Mescaline sulfate $(C_{11}H_{17}NO_3)_2 \cdot H_2SO_4 \cdot 2H_2O$ | 230–250 | From 125°C, water escapes with turbidity |
| *89. Morphine $C_{17}H_{19}NO_3 \cdot H_2O$ | 245–255 | At 115°–140°C, loss of water with turbidity |

**TABLE II** (*continued*)

| Compound[b] | mp (°C) | Remarks |
|---|---|---|
| 90. Apomorphine hydrochloride $C_{17}H_{17}NO_2 \cdot HCl \cdot 0.5H_2O$ | 220–260 | From 220°C, turbidity and carbonization |
| 91. Mepacrine hydrochloride $C_{23}H_{30}ClN_3O \cdot 2HCl \cdot 2H_2O$ | 245–260 | |
| *92. Oxycodone hydrochloride $C_{18}H_{21}NO_4 \cdot HCl \cdot 3H_2O$ | 245–260 | From 70°C, loss of water with turbidity |
| *93. Quinidine hydrochloride $C_{20}H_{24}N_2O_2 \cdot HCl \cdot H_2O$ | 262–265 | From 90°C, loss of water and turbidity from the crystals |
| *94. Theophylline $C_7H_8N_4O_2 \cdot H_2O$ | 274 | At 70°–80°C, loss of water with turbidity |
| 95. Codeine hydrochloride $C_{18}H_{21}NO_3 \cdot HCl \cdot 2H_2O$ | 260–275 | |
| 96. Aminophylline $(C_7H_8N_4O_2)_2 \cdot C_2H_8N_2 \cdot 2H_2O$ | 274 | |
| *97. Meconic acid $C_7H_4O_7 \cdot 3H_2O$ | 275–285 | At 90°–110°C, water escapes |
| *98. Morphine hydrochloride $C_{17}H_{19}NO_3 \cdot HCl \cdot 3H_2O$ | 285–310 | From 80°C, loss of water with turbidity |
| *99. Strychnine hydrochloride $C_{21}H_{22}N_2O_2 \cdot HCl \cdot H_2O$ | 290–310 | From 70°C, loss of water with turbidity |
| 100. Quercetin $C_{15}H_{10}O_7 \cdot 2H_2O$ | 300–320 | |
| 101. Mercaptopurine $C_5H_4N_4S \cdot H_2O$ | 300–325 | From 160°C, turbidity of crystals |

[a] Data from Kuhnert-Brandstatter (1971).

[b] Compounds marked with asterisk show unusual behavior that may be caused by dehydration prior to melting.

include β-D-glycopyranoside, phenyl-2-amino-2-deoxy-β-D-glucopyranoside, and *p*-amino-phenyl-β-D-glucopyranoside.

In our laboratory we have examined a number of solvates and characterized their behavior. In general, their behavior has been observed on a hot stage mounted on a microscope. The temperature is adjusted so that the desolvation takes a reasonable length of time—4 hr to several days. The behavior of the crystal during desolvation is then photographed. These photographs often depict anisotropic behavior such as desolvation from the ends of the crystal. If anisotropic behavior is observed and the crystal structure is known, then the crystal is mounted on an optical goniometer and the Miller indices of the crystal faces are determined as described in Chaper 2.

This information (the Miller indices and the crystal structure) is then

used to construct a crystal-packing drawing viewed from the same direction as the microscope.

The crystal packing is then used to attempt to interpret the observed behavior of the crystals on the microscope.

## B. SPECIFIC STUDIES OF DESOLVATION REACTIONS

### *1. Caffeine Hydrate*

Crystals of caffeine hydrate (**1**) effervesce and are rapidly dehydrated at room temperature. Studies using precision photography to determine the

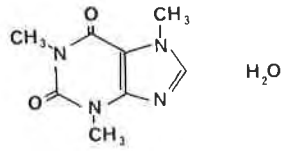


**1**

orientation of the crystal axis relative to the crystal faces and subsequent photomicrography of crystals during desolvation showed that the desolvation was anisotropic (Figure 1) and proceeded along the *c* crystal axis.

Analysis of the crystal packing of caffeine hydrate (Figure 2) shows that there are water tunnels parallel to the *c* crystal axis. The anisotropic behavior of crystals of caffeine is explained by the preferential escape of the water molecules along these tunnels. Desolvation from other crystal directions would require the water molecules to penetrate the somewhat closely packed layers of nonpolar groups in the other two crystallographic directions. This explanation is given added support because of its similarity to the explanations of the anisotropic behavior of benzoic acid crystals upon reaction with ammonia gas (Miller *et al.*, 1973).

Other caffeine solvates lose solvent of crystallization under relatively mild conditions. Caffeine · $2CH_3COOH$ loses acetic acid upon exposure to air, and caffeine · HCl · $2H_2O$ decomposes at 80° to 100°C with loss of water and HCl ("Merck Index," 1968). This latter observation is particularly interesting because of recent studies of dehydrochlorination of *p*-aminosalicyclic acid hydrochloride (Lin *et al.*, 1978).

### *2. Theophylline Hydrate*

The crystal structure of theophylline hydrate (**2**) is essentially isomorphous with that of caffeine hydrate. Its packing has tunnels filled with water molecules parallel to the *c* axis, and the crystals are elongated

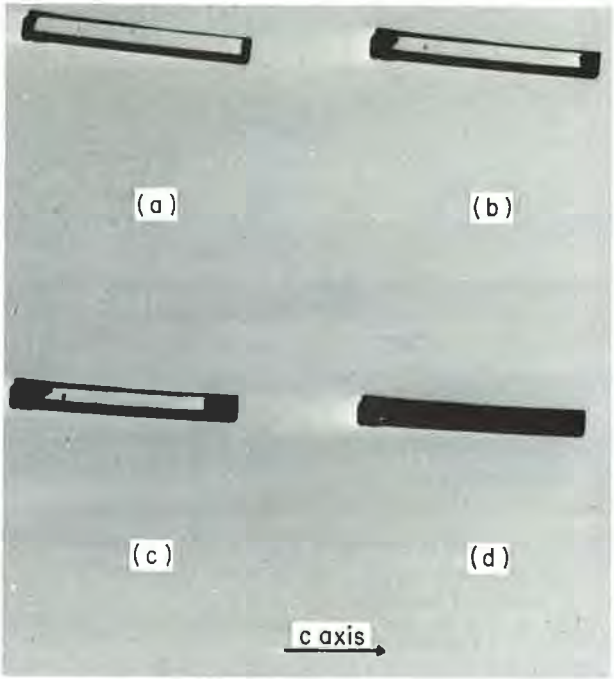


**FIGURE 1.** Behavior of a crystal of caffeine monohydrate in air at room temperature after both ends were cutt off using a razor blade: (*a*) immediately after cutting; (*b*) after 4 hr; (*c*) after 24 hr; and (*d*) after 72 hr.

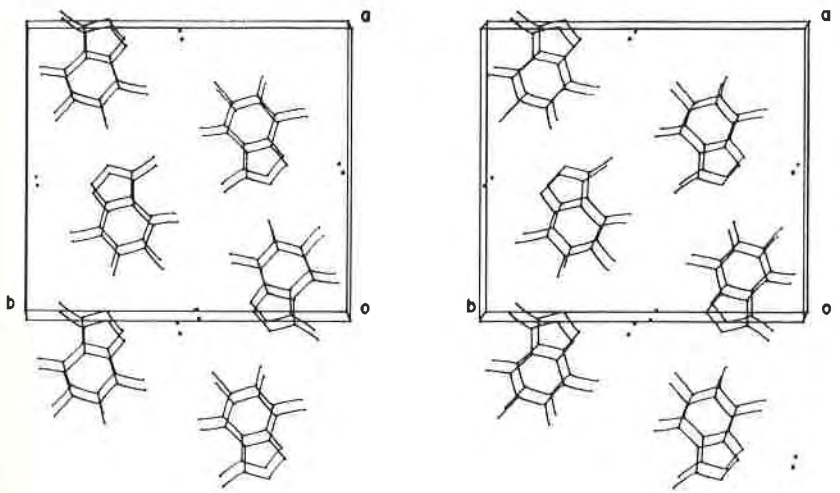


**FIGURE 2.** Stereopair drawing of the crystal packing of caffeine monohydrate viewed perpendicular to the *ab* plane. The oxygen atoms of the water molecules are designated by dots.

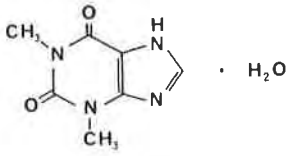

2

along $c$ in marked similarity to caffeine. Surprisingly, crystals of theophylline hydrate did not effervesce, and dehydration only occurred if the crystals were heated to 35°–50°C as illustrated in Figure 3. However, like caffeine hydrate, the desolvation proceeded from the ends of the crystal towards the center. In the latter stages of the reaction, some desolvation occurred from the sides. An important question whose answer might provide information on the factors controlling the rate of desolvation of crystal solvates involves the reasons for the difference in the rate of desolvation of caffeine hydrate and theophylline hydrate, discussed later in this chapter.

### 3. *Thymine Hydrate and Cytosine Hydrate*

Several other dehydrations of crystalline hydrates have been studied in our laboratory, including those of thymine hydrate (**3**) and cytosine hydrate (**4**). Figure 4 shows the behavior of crystals of thymine hydrate upon heating to 40°C, and Figure 5 shows the crystal packing of thymine hydrate.

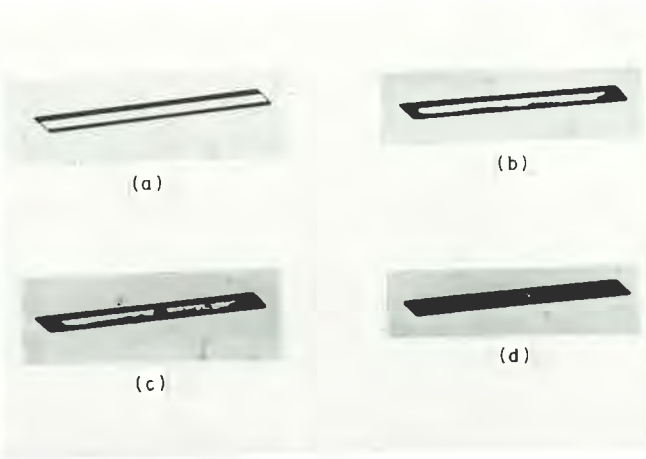


**FIGURE 3.** Behavior of a crystal of theophylline monohydrate in air at 35°C on a Mettler hot stage: (*a*) at start; (*b*) after 24 hr; (*c*) after 48 hr; and (*d*) after 5 days.

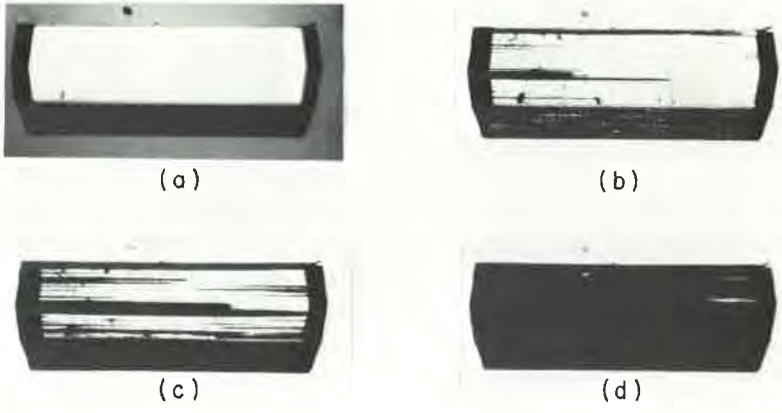


**FIGURE 4.** The behavior of a crystal of thymine hydrate upon heating to 40°C; (*a*) at start; (*b*) after 24 hr; (*c*) after 48 hr; and (*d*) after 5 days. The directions of the crystal axes are *c* across, *b* down, and *a* out of the plane of the paper.

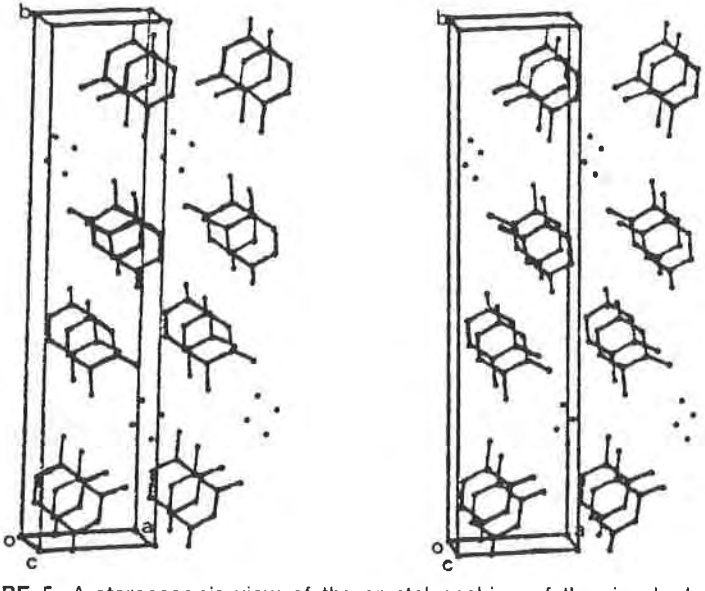


**FIGURE 5.** A stereoscopic view of the crystal packing of thymine hydrate. The directions of the crystal axes are *a* across, *b* vertical, and *c* out of the plane of the paper.

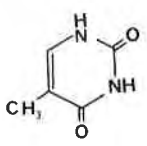

3

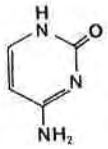

4

The crystals of thymine hydrate are elongated along the *c* crystal axis, and the packing drawing (Figure 5) is viewed along this axis. This diagram shows tunnels of water molecules running parallel to the *c* axis. As with caffeine, the rapid dehydration along the *c* axis (Figure 4) is consistent with the preferential exit of water molecules along the water tunnels (*c* axis).

Figure 6 shows the behavior of crystals of cytosine hydrate upon heating to 65°C. Figure 7 shows its crystal packing viewed down the *b* crystallographic axis. This drawing shows that there are tunnels of water molecules running parallel to the *b* crystal axis, which is the long axis of the crystal. As with thymine and caffeine, the water molecules are preferentially lost out those tunnels. Note that many of these compounds crystallize with their long crystal axis parallel to the water-tunnel direction and with the long axis nearly perpendicular to the rings of the molecules.

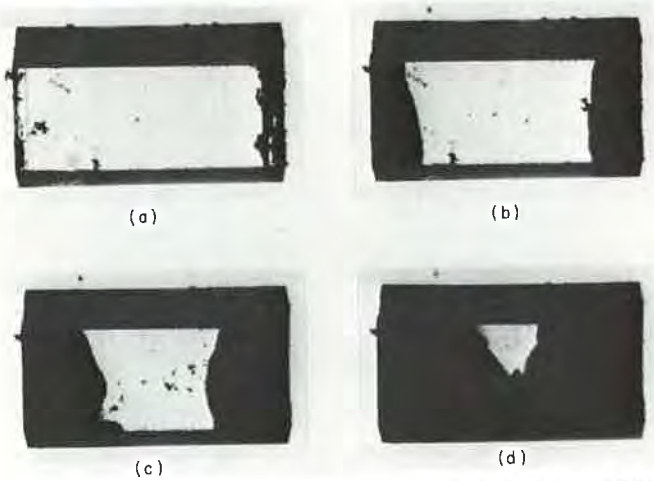


**FIGURE 6.** Behavior of crystals of cytosine hydrate upon heating to 60°C: (*a*) at start; (*b*) after 8 min; (*c*) after 15 min; and (*d*) after 24 min. The end faces were activated by scratching with anhydrous compound. The direction of the crystal axes is *a* into the paper, *b* vertical, and *c* across.

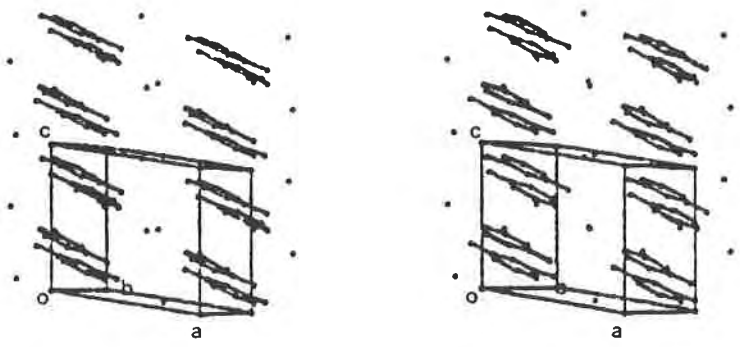


**FIGURE 7.** A stereoscopic view of the crystal packing of cystosine hydrate. The direction of the crystal axes is *a* across, *c* vertical, and *b* out of the plane of the paper.

*4. Dihydrophenylalanine Hydrate*

Crystals of dihydrophenylalanine hydrate (Byrn and Lin, 1976) desolvate during solid-state oxidation.

Crystals of dihydrophenylalanine hydrate (**5**) were prepared by slow evaporation of an 80% ethanol or methanol–ethyl acetate solution under a

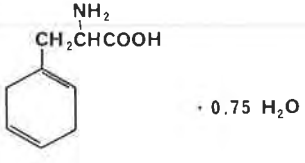


**5**

stream of nitrogen gas. These crystals dehydrated and then oxidized upon standing in air to give phenylalanine. Crystals of the anhydrous form of dihydrophenylalanine prepared by recrystallization from ether were air-stable. Figure 8 shows the behavior of a crystal of **5** that was cut on both ends. Loss of water of crystallization proceeded toward the center in fronts starting from the ends in marked similarity to caffeine. However, the crystals of **5** were much more sensitive to defects than caffeine hydrate crystals. Nearly perfect crystals of dihydrophenylalanine hydrate (**5**) were much more stable than those with observable defects, and cutting the ends off provided nucleation sites that led to the anisotropic behavior of these crystals. If only one end of a crystal was removed, then dehydration proceeded in a front from that end toward the other. A stream of nitrogen gas caused a fivefold to 10-fold increase in the rate of dehydration.

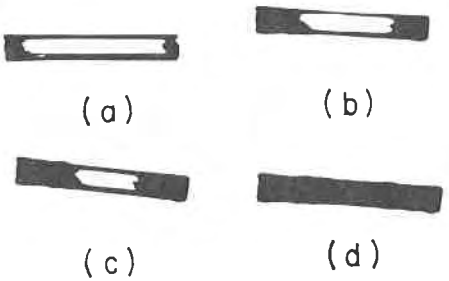


**FIGURE 8.** The dehydration of crystals of dihydrophenylalanine 0.75(hydrate) at room temperature: (*a*) after 0.5 hr; (*b*) after 2 hr; (*c*) after 3 hr; and (*d*) after 5 hr.

The rapid dehydration of **5** has thus far prevented the determination of its crystal structure, since the diffraction intensity of the opaque crystals was very low.

At room temperature in air, dehydration is much faster than the solid-state oxidation of dihydrophenylalanine hydrate. Analysis of a typical batch of opaque crystals showed that in 2 hr only 2.76% phenylalanine was present, in 5 days 8.3%, and in 10 days only 16.73%. This indicates that water loss preceded the oxidation of dihydrophenylalanine. It is interesting to speculate that the oxygen susceptibility of the solvate crystals may be due to the facile desolvation, which leaves the molecules within the desolvated crystal accessible to oxygen.

### 5. *Dialuric Acid Hydrate*

The behavior of dialuric acid hydrate (**6**) is related to that of dihydrophenylalanine hydrate (Clay and Byrn, 1980). At 76°C, dialuric acid

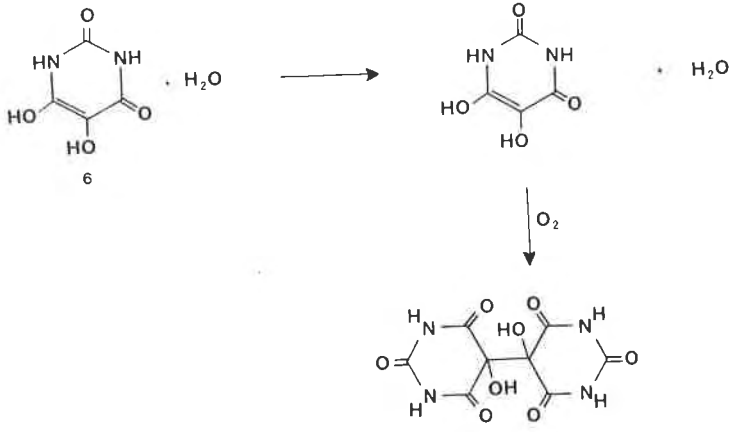

monohydrate loses solvent of crystallization in less than 24 hr to give an anhydrous form. Powder diffraction analysis shows that the anhydrous form has a different crystal structure from the hydrate. Upon prolonged heating (8 to 10 weeks) at 76°C this form then oxidizes to yield alloxantin (7). The oxidation reaction is discussed in more detail in Chapter 8.

*6. Cycloserine*

Studies on the desolvation of cycloserine hydrate (8) illustrate the important influence nucleation sites can have on these reactions (Lin and

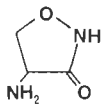


8

Byrn, 1979). Figure 9 shows the behavior of a pair of crystals of cycloserine hydrate upon heating to 40°C. The top crystal is almost completely reacted before the bottom crystal begins to react [Figure 9(*b*)]. Apparently the top crystal contained a nucleation site at which the reaction begins, while in the bottom crystal this site was absent.

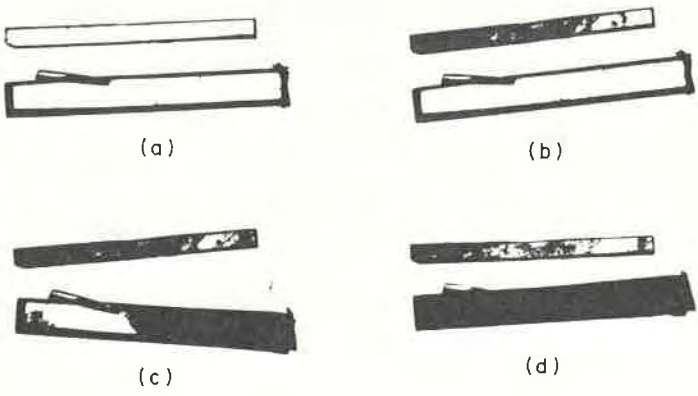


**FIGURE 9.** Desolvation of a pair of crystals of cycloserine monohydrate at 40°C: (*a*) at start; (*b*) after 165 min; (*c*) after 190 min; (*d*) after 200 min.

### 7. *Erythromycin Dihydrate*

The dehydration of erythromycin (**9**) dihydrate and monohydrate illustrates an important point concerning the crystal structures of the product

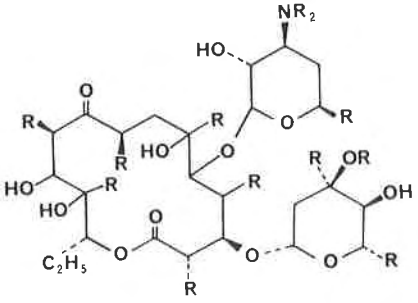

E, 9

crystal (Allen *et al.*, 1978). The dehydration of the dihydrate crystal follows this mechanism:

$$E \cdot 2H_2O(\text{cryst}) \xrightarrow{\sim 120^\circ C} E(\text{cryst}) + 2H_2O(g)$$

$$E(\text{cryst}) \xrightarrow{120^\circ - 135^\circ C} E(\text{amorphous})$$

$$E(\text{amorphous}) \xrightarrow{120^\circ - 190^\circ C} E'(\text{cryst})$$

$$E'(\text{cryst}) \xrightarrow[\text{melt}]{190^\circ - 193^\circ C} E(\text{liq})$$

The monohydrate desolvates via the mechanism:

$$E \cdot H_2O(\text{cryst}) \xrightarrow{\sim 100^\circ C} E(\text{cryst}) + H_2O(g)$$

$$E(\text{cryst}) \xrightarrow{114^\circ - 137^\circ C} E(\text{anhyd})$$

$$E(\text{anhyd}) \xrightarrow{120^\circ - 190^\circ C} E'(\text{cryst})$$

$$E'(\text{cryst}) \xrightarrow{186^\circ - 190^\circ C} E(\text{liq})$$

It is surprising to note that the dihydrate does not dehydrate via the monohydrate.

### 8. *Mercaptopurine Hydrate*

Mercaptopurine (**10**) is an important antitumor agent and crystallizes as the monohydrate.

Differential scanning calorimetry (DSC) shows that mercaptopurine hydrate loses water at 125°C and then melts at above 300°C (Niazi, 1978). The DSC trace is shown in Figure 10.

This DSC trace has also been used to calculate the enthalpy and activa-

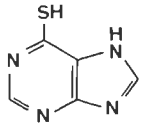


10

tion energy for the dehydration. While DSC has been criticized as a method for determining activation energies (see Chapter 2), the activation energy for this reaction was found to range from 45 to 63 kcal/mole. The enthalpy of dehydration was found to be 8.27 kcal/mole.

X-Ray powder diffraction showed that the anhydrous form has a completely different crystal structure from the hydrate. Solubility studies showed that even though the anhydrous form partially converts to the hydrate in aqueous solution, it has greater solubility and perhaps greater bioavailability.

### *9. Fenoprofen Hydrate*

Fenoprofen (**11**), (±)-methyl-3-phenoxybenzeneacetic acid, is a nonsteroidal antiinflammatory, analgesic, and antipyretic agent (Hirsch *et al.*, 1978).

Fenoprofen salts crystallize as mono- or dihydrates that have surpris-

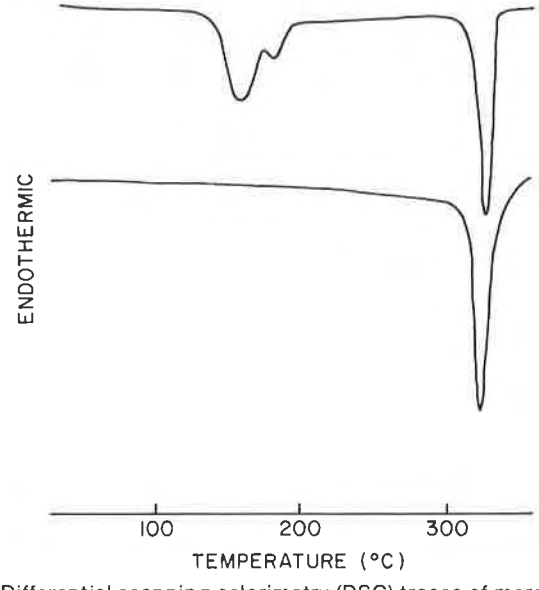


**FIGURE 10.** Differential scanning calorimetry (DSC) traces of mercaptopurine (top) and a heat-treated sample of mercaptopurine (bottom) (Niazi, 1978). (Reproduced with permission of the copyright owner.)

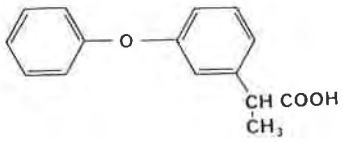


11

ingly different stability. The calcium-salt dihydrate is much more stable than either the sodium-salt dihydrate or the calcium-salt monohydrate (Figure 11). In addition, exposure of these forms to humidities ranging from 1 to 93% at room temperature showed that the sodium dihydrate lost both moles of water at 1% relative humidity and absorbed excessive amounts of water at high humidities. In contrast, the calcium dihydrate was stable under these conditions.

Mixtures of fenoprofen salts with propoxyphene salts showed that a solid–solid reaction occurred with the sodium dihydrate, but that the calcium dihydrate remained unreacted in these mixtures. The reactivity of the sodium dihydrate under these conditions is thought to be related to its ease of desolvation.

### *10. Manganous Formate Dihydrate*

Although the focus of this review is solvates of organic compounds, a relevant study of the dehydration of crystals of manganous formate dihy-

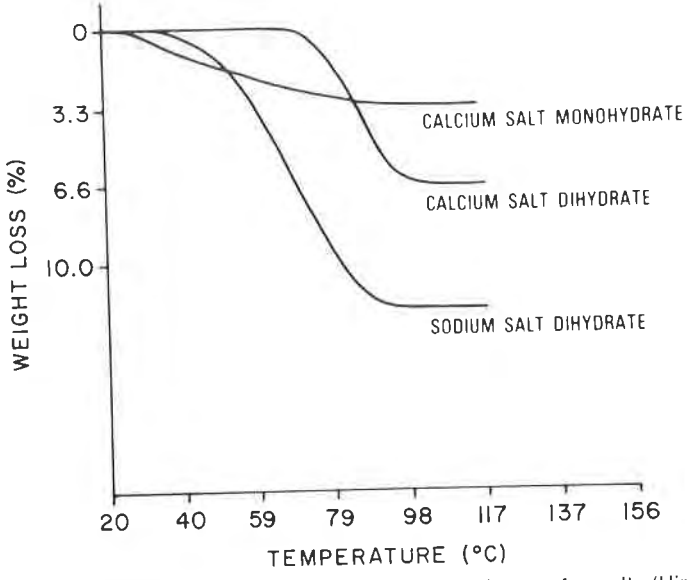


**FIGURE 11.** Thermal gravimetric analysis traces of fenoprofen salts (Hirsch *et al.*, 1978). (Reproduced with permission of the copyright owner.).

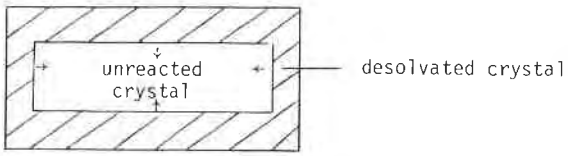


**FIGURE 12.** Diagram of the loss of water from crystals of manganous formate dihydrate.

drate has been carried out (Clark and Thomas, 1969; Eckhardt and Flanagan, 1964). This hydrate lost water from two pairs of crystal faces as shown in Figure 12. This behavior was consistent with the crystal packing. Thus, this study indicates that in cases where the crystal packing is favorable one might be able to observe desolvation of organic hydrates from two pairs of crystal faces.

It was also shown that the rate of dehydration of manganous formate dihydrate could be determined by either thermal gravimetric analysis (TGA) or measuring the rate of interface advancement from photomicrographs. These approaches, which can only be used when suitable crystals are available, provide a convenient method of measuring the rates of solid-state desolvation reactions. It is noteworthy that the rates measured by TGA, which measures the volume transformation, are similar to the rates measured by front advancement. This observation appears to be in contrast to the studies by Mnyukh *et al.* (1966) of *p*-dichlorobenzene, where it was suggested that measurement of rates by measurement of the volume of transformation gives results that depend on a number of random factors.

### *11. Bis(salicylaldehyde)ethylenediimine Cobalt(II) Chloroformate*

Crystals of the chloroform solvate of bis(salicylaldehyde) ethylenediimine cobalt(II) (**12**) lose $CHCl_3$ upon standing and then revers-

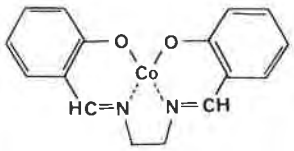


12

ibly bind oxygen after the $CHCl_3$ of solvation has left the crystal (Byrn and Lin, 1979; Schaefer and Marsh, 1969; Vogt *et al.*, 1963). Figure 13 shows the behavior of a crystal of 12 during desolvation. The crystal packing (Figure 14) of this solvate shows that there are tunnels of $CHCl_3$ molecules running parallel to the long axis of the crystal.

Thus the behavior of this chloroformate is quite similar to the behavior

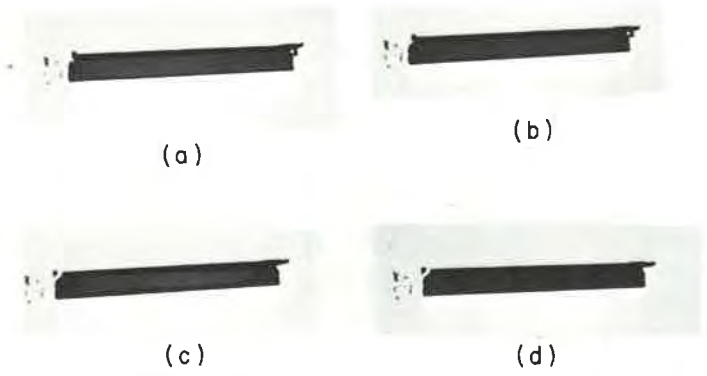


**FIGURE 13.** Desolvation of a crystal of bis(salicylaldehyde)ethylenediimine cobalt(II) chloroformate with its ends removed at room temperature: (*a*) at start; (*b*) after 12 hr; (*c*) after 28 hr; and (*d*) after 48 hr. The long axis of the crystal is the *b* crystallographic axis.

of the crystal hydrates discussed above. Apparently, the chloroform preferentially exits the crystal along the tunnel direction.

### *12. The Acetone Solvate of the Indanetrione*

The acetone solvate of indanetrione 2-(*N*-*p*-*t*-butylbenzoyl)-*N*-phenylhydrazone loses acetone at 45°C to give crystals with a crystal

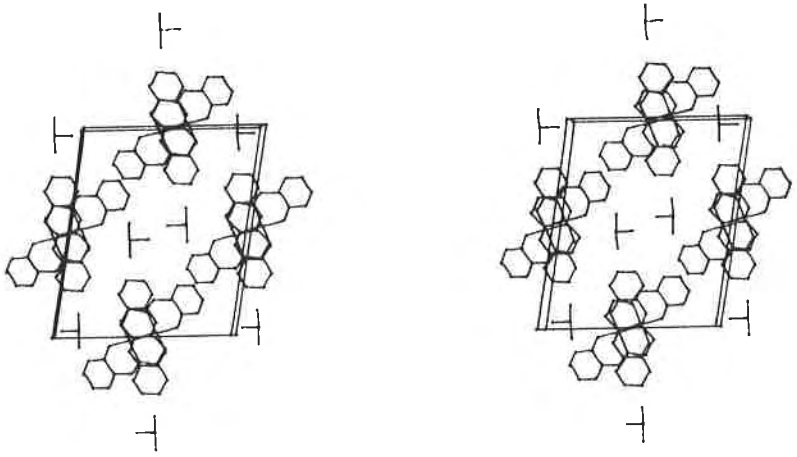

**FIGURE 14.** The crystal packing of bis(salicyaldehyde)ethylenediimine cobalt(II) chloroformate. The view is parallel to the *b* axis.

structure different from crystals obtained without solvent of crystallization (**13**) (Puckett *et al.*, 1976).

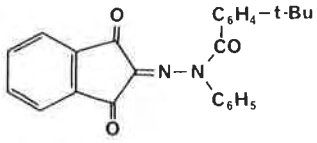

13

Photomicrography and optical goniometry showed that acetone was lost along the *c* crystal axis. The crystal structure of this solvate showed that acetone was in channels of approximately 4 Å diameter that paralleled the *c* crystal axis. These studies further illustrate that solvent of crystallization is lost along the direction of the solvent tunnels.

### *13. Phenylazotribenzoylmethane Etherate*

Phenylazotribenzoylmethane crystallized from diethyl ether as an etherate (McCullough *et al.*, 1970). After standing for a period of days at

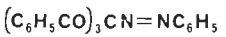

14

room temperature, these crystals lost ether. X-Ray powder photography showed that upon loss of ether the crystals collapsed to microcrystallites with the same internal structure as crystals of phenylazotribenzoylmethane crystallized without ether of solvation. As with the desolvations described above, the loss of ether was anisotropic, started on an edge, and proceeded in a semicircle front to the other side of the crystal.

### *14. Solvates of Cephaloglycine and Cephalexin*

In contrast to the behavior of caffeine, theophylline, and mercaptopurine, the powder patterns of the solvates and unsolvated crystal forms of cephaloglycine (**15**) and cephalexin (**16**) are virtually identical (Pfeiffer

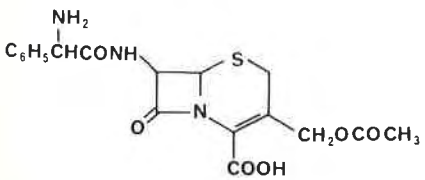

15

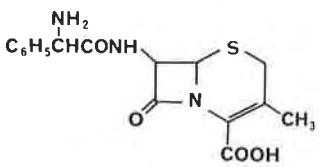

16

*et al.*, 1970). Cephaloglycine forms solvates with water (1 : 2), formamide (1 : 1), methanol–water (1 : 1 : 1), acetonitrile–water (1 : 1 : 1), acetic

acid–water (1 : 1 : 1), acetic acid (1 : 2), acetic acid–methanol (1 : 1 : 1), ethanol–water (1 : 1 : 1), and *N*-methylformamide (1 : 1). Cephalexin forms solvates with water (1 : 2 and 1 : 1), formamide (1 : 1), methanol (1 : 1), acetonitrile (1 : 2), acetonitrile–water (1 : 1 : 1), *N*-methylformamide (1 : 1), *N*-ethylformamide (1 : 1). Drying of many of these solvates under normal conditions reportedly yielded a "desolvated" crystal with a powder pattern very similar to that of the solvated crystal form. Although the powder patterns of the "desolvated" crystals were not identical to the patterns of the solvated forms, only minor differences such as a general loss of diffraction intensity and a change in the intensities at one or two reflections were reported. Exposure of the "desolvated" crystal to solvent vapor yielded the original solvate. This behavior has been termed crystal pseudopolymorphism. It would be interesting to determine the crystal structure of some of these solvates in order to find how the solvent molecules are packed in the lattice and to compare the theoretical powder pattern calculated from the atom positions in the single crystal to that observed.

It is appropriate to mention inclusion compounds (Mendelcorn, 1964) at the conclusion of this section. The behavior and properties of these compounds has been extensively reviewed, and Puckett, Curtin, and Paul provide an excellent overview of this area (Puckett *et al.*, 1976). Organic inclusion compounds have the following properties in common (Puckett *et al.*, 1976): (*a*) the crystal structure collapses to a different one upon loss of solvent; (*b*) the stability of individual crystals depends on their perfection (Byrn and Lin, 1976); and (*c*) the cavity size varies from roughly 4 Å in diameter to a cavity of dimensions 9 × 11 Å.

Clearly, nearly all the compounds discussed except cephaloglycin and cephalexin could tentatively be classified as inclusion compounds.

### *15. Hydrocortisone tert-Butylacetate Ethanolate*

The *tert*-butylacetate ester of hydrocortisone (**17**) crystallizes as an ethanolate and an anhydrous form. Preliminary crystallographic studies

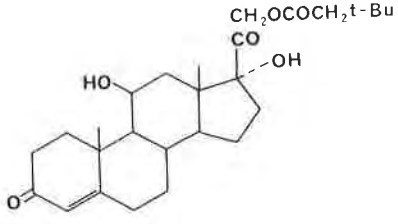


17

indicate that one of the ethanolate forms belongs to the hexagonal space group $P6_1$, and it appears that solvent is lost in a process in which the

crystal remains in space group $P6_1$ with essentially the same crystal structure. Further studies are required to confirm this behavior, but it appears that this ester is unique in that the product of desolvation is a single crystal.

## II. The Mechanism of Desolvation Reactions

Desolvation reactions are influenced by a number of factors including atmosphere, nucleation, crystal packing, and hydrogen bonding. In this section, studies of the influence of these factors on the facility or ease of desolvation and the rate of desolvation are reviewed and used to provide information on the mechanism of this reaction.

### A. INFLUENCE OF ATMOSPHERE

As might be expected, desolvation reactions are greatly dependent on the atmosphere. For example, a stream of dry nitrogen accelerated the dehydration of dihydrophenylalanine hydrate by a factor of 5 to 10. In addition, fenoprofen sodium dihydrate dehydrated at relative humidities $< 1\%$ at room temperature, but was hygroscopic at humidities $> 10\%$. Similarly, dialuric acid dehydrated at room temperature at relative humidities $< 30\%$, but was stable at humidities $> 30\%$.

The cephalosporins cephalexin and cephaloglycin form a crystal structure that allows facile desolvation and resolvation. For example, the hydrate can be desolvated in a dry atmosphere, and subsequent exposure of the crystal to an acetonitrile atmosphere then results in the formation of the acetonitrile solvate.

It should be noted that x-ray crystallographers have for many years prevented dehydration of crystals by mounting them in sealed capillaries with an atmosphere of solvent vapor or by spraying them with varnish.

### B. CRYSTALLOGRAPHIC PROPERTIES OF SOLVATES

In general, desolvation results in two types of crystallographic behavior. Many solvates upon desolvation change crystal structure to form a new polymorph, the anhydrous form. Among these are dialuric acid, caffeine, and mercaptopurine. In all these cases, the powder pattern of the product is different from the starting material and corresponds to that of the anhydrous form, which can be obtained by crystallization from other solvents. However, in some cases the anhydrous form obtained by desolvation has a crystal structure different from that obtained by crystallization.

The second kind of behavior occurs when desolvation does not result in a change in crystal structure. In these cases the solvent is lost but the crystal structure is unchanged, thus resulting in a crystal with voids and cavities. Crystals that exhibit this behavior include the inclusion compounds, cephalosporin hydrate, cephaloridine hydrate, and cephalexin hydrate.

## C. FACTORS THAT COULD INFLUENCE SOLID-STATE DESOLVATION REACTIONS

### *1. Crystal Packing*

In the previous sections we have discussed numerous examples of desolvation reactions. It is quite clear that in many instances the behavior of the crystal when viewed through a microscope can be explained in terms of the crystal packing. This ability to explain the behavior of crystals in terms of the crystal packing is, in principle, related to explanations of the behavior of organic crystals during color changes (Byrn *et al.*, 1972) and the reactions of organic acids and anhydrides with ammonia (Miller *et al.*, 1974) in terms of crystal packing.

In instances where the behavior of the desolvating crystal on a microscope can be explained by crystal packing, the crystal appears to lose its solvent of crystallization along particular crystallographic directions. These directions generally correspond to the direction of solvent tunnels in the crystal. Thus desolvation appears to proceed in the crystallographic direction that offers the least resistance to escape of the solvent molecules.

Other crystal-packing factors may also play a role in hindering the escape of solvent molecules out of the crystal:

1. The tunnel size and the number of tunnels per unit area. For example, it would be easier for solvent to exit a large tunnel than a small tunnel. Thus, this parameter may be approximated by measuring the cross-sectional area of the tunnel. Obviously, the more tunnels per unit area, the greater the facility or case of solvent loss.
2. The compactness of the crystal packing. The more closely packed a crystal, the harder it will be for solvent molecules to escape. Thus the compactness of the packing, the ratio of the volume of the molecules in the unit cell to the volume of the unit cell, may play a role in hindering the escape of solvent molecules, particularly in cases where some of the solvent molecules do not escape out the tunnel direction. The compactness of crystals is calculated using a computer program developed in our laboratory and based on the molecular volume elements suggested by Kitaigorodskii (1961).

3. Several other less important crystal-packing factors may also influence solid-state desolvation reactions. These include the direction of the water chain relative to the main plane of the molecules, the straightness of the water chain, and the coplanarity of the solvent molecules with the molecules of the host compound. All of these factors are reflected in the tunnel cross-sectional area; however, in certain cases they may need to be specifically taken into account. For example, if the tunnel is zig-zag, the cross-sectional area measured by projection on the plane perpendicular to the dehydration direction will be too small and will not accurately reflect the size of the tunnel. The coplanarity of the water molecules with the host molecules will also be reflected in the tunnel cross-sectional area, but if there are constrictions in the tunnel due to the fact that the host molecules exist in planes running through the crystal with the water molecules between these planes, then escape of water out the tunnels is hindered and may occur along other directions.

### 2. *The Influence of Nuclei and Defects*

The impression conveyed in our discussion of solid-state desolvation reactions is that the crystal structure is of major importance in governing the nature and path of chemical change in these reactions. However, nuclei and defects also play a role in these reactions.

Solid-state reactions, particularly desolvation reactions, undoubtedly begin at nuclei and defects. Crystals of caffeine hydrate and dihydrophenylalanine hydrate were quite sensitive to mechanically induced nuclei and defects. For example, crystals with their ends cut off with a razor blade desolvated up to five times faster than undisturbed crystals. However, mechanically induced nuclei did not alter the anisotropic behavior of these solvate crystals. In addition, crystals of the indanetrione(**11**) and manganous formate dihydrate were also sensitive to artificial nucleation (Clark and Thomas, 1969; Mnyukh *et al.*, 1966).

Furthermore, defects rather than crystal packing may control some solid-state photochemical cycloaddition reactions (Desvergne *et al.*, 1974; Thomas, 1974). For example, solid 9-cyanoanthracene yields the trans dimer upon irradiation, rather than the cis dimer expected from crystal packing. Careful optical and electron microscopic studies indicated that these reactions may occur at stacking faults on the (221) planes of the crystal. These faults put the 9-cyanoanthracene molecules in a geometry where the trans dimer could be obtained with a minimum of molecular motion (Desvergne and Thomas, 1973).

Studies of the effect of nucleation sites in anthracene crystals produced by (*a*) compression by tightening a screw holding a crystal between two stainless-steel plates, (*b*) point indentation with a sharp needle, or (*c*)

cutting with a stainless-steel blade showed that the photodimerization occurred at nucleation sites produced by these treatments (Thomas and Williams, 1969).

Microscopic studies of crystals in which these nucleation sites had been produced indicated that compression perpendicular to opposite (010) faces and point indentations on the (001) face produced dislocations that were characterized by etch pits aligned in the (010) direction. On the other hand, cutting with a blade produced different types of dislocations on different crystal faces.

Similar studies on ammonium perchlorate indicated that sublimation (and subsequent decomposition) occurred at dislocations introduced by a pin-prick or by compression (Williams *et al.*, 1971).

Solid–gas reactions also occur at defects. For example, the reaction of ammonia with acenaphthalene-10-carboxylic acid is affected by defects as well as molecular packing (Desvergne and Thomas, 1973), and the decomposition of dibenzoylperoxide also begins at defects where $CO_2$ escapes the crystal (Morsi *et al.*, 1975). It has been shown, for example, that the phase transition of the $\alpha$ form of *p*-dichlorobenzene to the $\beta$ form begins at visually observable defects. Perfect crystals of the $\alpha$ form are resistant to reaction. However, when these crystals are pricked with a pin, the reaction nucleates at this site (Kitaigorodskii *et al.*, 1965; Mnyukh *et al.*, 1966).

Solid-state thermal reactions have also been initiated by inoculation with reaction products (Hartshorne and Roberts, 1951; Patterson and Groshens, 1954), and the desolvation of cytosine hydrate is initiated by inoculation with desolvated material.

It is interesting to note that although the transformation of yellow to white dimethyl 3,6-dichloro-2,5-dihydroxyterephthalate sometimes began at visually observed defects, neither a pin-prick nor inoculation with product initiated this reaction (Byrn *et al.*, 1972).

These studies show that in favorable cases preparation of crystals free of nucleation sites could lead to substantial stabilization of unstable solids and could thus lead to improved shelf-life of drugs. They also imply that crystallization from different solvents might alter the defects and thus stability of drugs.

### *3. Hydrogen Bonding*

Hydrogen bonding has been reviewed and several books on the subject have been written, including the book by Schuster *et al.* (1976) and the review by Allen (1975).

It is possible that hydrogen bonding of water to the organic molecules in the crystal lattice plays an important role in the dehydration of organic

hydrates. This review is divided into four sections: (*a*) methods of calculation of hydrogen-bond energy; (*b*) use of energy calculations to determine sites of solvation of purines and pyrimidines; (*c*) methods of experimental measurement of hydrogen-bond energies; and (*d*) conclusion.

a. Methods of Calculations of Hydrogen-Bond Energy. Allen has reviewed theoretical studies of hydrogen bonding and offered a simplified expression for the energy of dimerization ($E_D$) of a compound containing an A—H · · · B bond [Eq. (1)]. This equation illustrates what numerous workers have suggested, that directionally plays a minor role in determining the hydrogen bond energy. For example,

$$E_D = K\mu_{A-H}\frac{\Delta I}{R} \tag{1}$$

where $\mu_{A-H}$ is the A–H dipole, $\Delta I$ the difference in ionization potential of the electron donor and the noble gas atom in its row, $R$ the A–B distance, and $K$ an energy-scale factor.

Allen stated that a large change in angle corresponds to an energy change of only a few tenths of a kilocalorie (Allen, 1975; Umeyama and Morokuma, 1977). In addition, Clark (1963) and Donohue (1968) observed large bending angles and variations in geometry in hydrogen bonds of amino acids, nucleic acids, purines, and pyrimidines containing water of hydration.

Other useful potential energy functions for determining hydrogen-bond energy have also been developed. Scheraga and co-workers (Momany *et al.*, 1975) have used the function in Eq. (2) to calculate hydrogen-bond interactions for determination of the geometries of amino acids:

$$U_{HB}(r_{H\cdots X}) = \frac{A'_{H\cdots X}}{r^{12}_{H\cdots X}} - \frac{B_{H\cdots X}}{r^{10}_{X\cdots X}} \tag{2}$$

where $A'_{H\cdots X}$ and $B_{H\cdots X}$ are obtained from tables. Hopfinger (1973) used a more complicated function shown in Eq. (3). This function is in operation in the CAMSEQ program (Weintraub and Hopfinger, 1975):

$$E(S,\theta_1,\theta_2) = \frac{-a}{S^6} + \frac{b}{S^{12}} + k\frac{Q_d Q_a}{\epsilon_s} - \frac{G}{S^n} f(\theta_1,\theta_2) \tag{3}$$

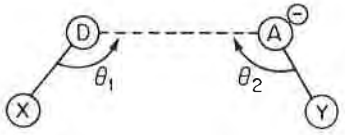


where $S$, $\theta_1$, and $\theta_2$ are defined in this diagram, $a$ and $b$ are from tables, $Q_d$ and $Q_a$ are changes on A and D, and

$$G = b + k\frac{Q_d Q_a}{\epsilon}\frac{S^{11}}{S^{12}} - a\left(\frac{S^6}{2}\right)$$

These functions give several excellent alternatives for determination of the hydrogen-bonding energies in crystals of hydrates.

b. Use of Energy Calculations to Determine the Sites of Solvation of Purines and Pyrimidines. Pullman and co-workers (Port and Pullman, 1972, 1975) have calculated binding energies for the most likely positions of water molecules in the first hydration shells of formamide dimer, nucleic acids, and related compounds.

For the formamide dimer (Port and Pullman, 1972), these workers moved the water molecule to various positions and used the self-consistent field (SCF) method to calculate binding energies.

The hydration sites of adenine, guanine, thymine, and cytosine were calculated using only the electrostatic component of the SCF wave functions (Port and Pullman, 1975). Surprisingly, these workers did not compare the calculated sites of hydration to those observed in the crystal structures of thymine hydrate and cytosine hydrate. The observed hydration sites of cytosine hydrate in the crystal are roughly the same as the lowest energy calculated sites after the areas blocked by neighboring hydrogen bonded bases are eliminated; however, in thymine this does not appear to be the case. Further calculations using a group of molecules in fixed positions and empirical potential functions to determine the hydration sites would appear to be in order.

c. Methods of Experimental Measurement of Heat of Dehydration in Crystals. There are at least two methods available for the determination of the energy of hydration in crystals: calorimetric and differential thermal analysis.

The calorimetric method was used by Eckhardt and Flanagan (1964) in their study of managous formate dihydrate. They measured the heats of solution of both the dihydrate and anhydrous form. The difference between these energies gives the heat of dehydration directly.

A simpler but probably less accurate method (Curtin *et al.*, 1969) involves differential thermal analysis, which has been extensively reviewed (Wendlandt, 1974; Mackenzie, 1977). This method involves heating of a sample and an inert reference at a fixed rate and measuring the temperature difference via thermocouples. By calibration using compounds with known heats of transition, one can directly determine the heats of transition or dehydration with an error of less than 10%.

Differential thermal analysis (DTA) and differential scanning calorimetry (DSC) have been used to determine the heats of dehydration of a number of inorganic hydrates including $MgSO_4 \cdot 7H_2O$ (Rassonshaya,

1969), $ZnSO_4 \cdot 7H_2O$ (Rabbering *et al.*, 1975), $NiSO_4 \cdot 6H_2O$ (Rabbering *et al.*, 1975) and numerous other compounds (Mackenzie, 1977). In all cases, good agreement was found between the heats of dehydration determined by DTA and those determined by DSC.

A potentially useful method for determining heats of dehydration involves the determination of O–H bond stretching frequencies. It has been shown that in solution O–H bond stretching frequencies correlate quite well with the heat of interaction of a donor and acceptor molecule. However, to my knowledge similar correlations have not been made using solid-state data.

Nakamoto, Margoshes, and Rundle have shown (Nakamoto *et al.*, 1955) that the O—H · · · O, N—H · · · O, and O—H · · · N bond lengths correlated with the O–H bond stretching frequencies in a number of crystals, including some hydrates. Since numerous theoretical–experimental studies have shown that distance correlates with energy in hydrogen bonds, there is every indication that a similar correlation could be drawn for hydrates.

d. Conclusion—Possible Role of Hydrogen Bonding in Desolvation Reactions. Obviously, when water leaves the crystal hydrogen bonds are broken. After the solvent leaves the crystal the structure sometimes then collapses to a different crystal structure. Exceptions to this generalization include the solvates of cephaloglycine and cephalexin discussed above. The general overall reaction is:

$$X \cdot H_2O(s) \rightarrow X(s) + H_2O(g) \rightarrow X'(s)$$

If the first step of this reaction is rate-determining and if the transition state resembles the products, then the strength of the hydrogen bond could determine the relative rate of the reaction of two solvates $X \cdot H_2O(s)$ and $Y \cdot H_2O$ if the following additional assumptions hold: (*a*) the energies of the desolvated crystals X(s) and Y(s) are nearly equal, and (*b*) the sole reason for the differences in the energies of the solids $X \cdot H_2O(s)$ and $Y \cdot H_2O(s)$ is due to hydrogen bonding. Because of the assumptions involved, it would be fortuitous if the difference in rates of reaction of crystalline hydrates were due solely to hydrogen-bond strengths. On the other hand, the Bronsted catalysis equation is based on analogous assumptions (Bell, 1941, 1959; Hine, 1962). This equation, which has ample experimental verification, states that there is a linear relationship between the rates of a solution proton-transfer reaction and the acidity or basicity of the reactants. Differences in solvation energy of the starting material and products are assumed to be negligible. Thus this equation states that the rates of proton-transfer reactions depend on the strength of proton binding.

## D. EXPLANATION OF THE THRESHOLD TEMPERATURE OF DESOLVATION IN TERMS OF CRYSTAL PACKING AND HYDROGEN BONDING

In our laboratory, Perrier (1980) has studied the desolvation of thymine hydrate, caffeine hydrate, theophylline hydrate, cytosine hydrate, and deoxyadenosine hydrate. These studies were performed using thermogravimetric analysis (TGA) and analysis of both the crystal packing and the hydrogen bonding. In the TGA studies (6°C/min temperature increase), the temperature at which 2% of the water is lost is taken as the threshold temperature of desolvation. This definition is based on the observation that the hydrates that are unstable at room temperature show a gradual loss of solvent from approximately 40°C to higher temperatures. Table III reports the threshold temperature of dehydration of these compounds, along with several crystal packing parameters and the hydrogen bonding.

Figure 15 shows cross-sectional views of the water tunnels and crystal packing for thymine monohydrate and 5-nitrouracil monohydrate. These figures provide a visual indication of the dramatic difference in the tunnel size in these two hydrates. In general, it is expected that the threshold temperature should be related to the tunnel area and the hydrogen-bond energy, which is in turn related to the length of the hydrogen bonds.

Examination of Table III shows that the hydrates are arranged with the faster reacting hydrates at the top and the slower reacting hydrates at the bottom. In addition, the hydrates with the largest tunnel areas are generally faster reacting, and the hydrates with the shorter and thus stronger hydro-

**TABLE III**
*Crystal-Packing Parameters for Purine and Pyrimidone Hydrates*

| Compound | Tunnel surface area, $S$ (Å$^2$) | Compactness, $C$ | Hydrogen bond (water to compound) | Hydrogen bond length (Å)[a] | Water chain | Dehydration temperature threshold (°C) |
|---|---|---|---|---|---|---|
| Thymine hydrate | 12.48 | 0.56 | 1 | 2.84 | zig-zag | 41.6 |
| Caffeine hydrate | 10.95 | 0.64 | 1 | 2.85 | zig-zag | 44.0 |
| Theophylline hydrate | 9.42 | 0.60 | 1 | 2.89 | zig-zag | 47.3 |
| 5-Nitrouracil hydrate | 1.84 | 0.61 | 2.5 | 3.07, 3.00; 2.94; 2.84 | straight | 54.9 |
| Cytosine hydrate | 2.49 | 0.58 | 3 | 2.97; 2.85; 2.78 | straight | 59.4 |
| 2′-Deoxyadenosine hydrate | 2.48 | 0.64 | 3 | 2.76; 2.73; 2.64 | straight | 88.7 |

[a] Bond is O · · · X where X = O or N.

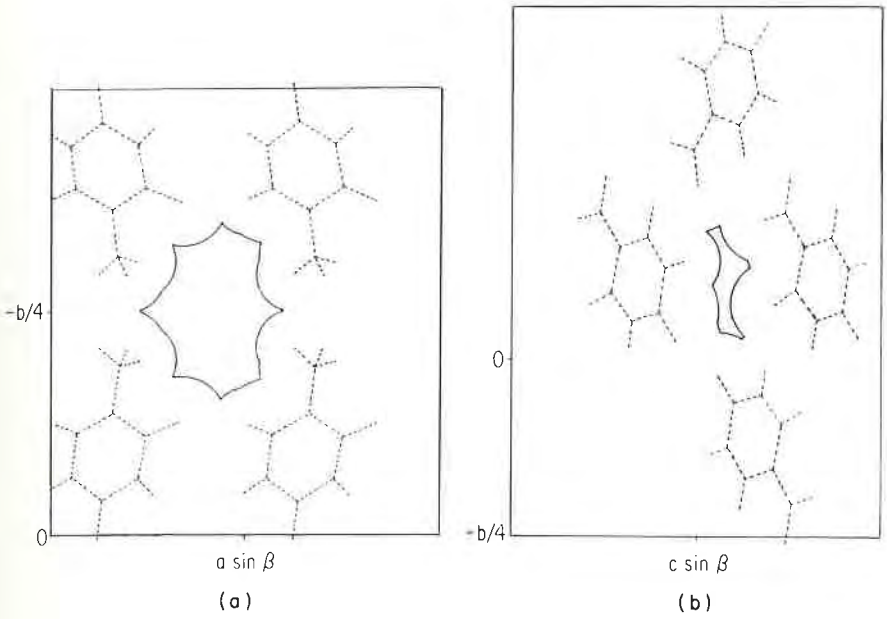


**FIGURE 15.** Projection of the crystal packing of (*a*) thymine hydrate on the *ab* crystallographic plane and (*b*) 5-nitrouracil hydrate on the *bc* plane. The water molecules are not shown, but the water tunnel is outlined in the heavy line and was determined using the van der Waals radii of the atoms lining the tunnel.

gen bonds are slower reacting. In general, this table confirms our expectations that the two most important factors influencing dehydration are tunnel area and hydrogen bonding. Future work in this area will involve more quantitative relationships between the activation energy for dehydration and tunnel area and hydrogen bonding.

## E. MEASUREMENTS OF THE RATES OF SOLID-STATE DEHYDRATION REACTIONS

Rates, activation entropies, and activation enthalpies of solid-state reactions may be composites of initial nucleation processes, intermediate phase transitions, and finally the chemical reaction. Under certain restrictive conditions, Thomas and co-workers have suggested that apparently reliable kinetic data and activation parameters can be obtained (Clark and Thomas, 1969). One indication that rate data are reliable is that the activation parameters for a number of related processes are similar.

For inorganic dehydration reactions of the type $A(s) \rightarrow B(s) + H_2O(g)$, studies of calcium oxalate monohydrate (Manche and Carroll, 1977) and

manganese(II) formate dihydrate (Clark and Thomas, 1969) using TGA have been reported. For manganese formate dihydrate, an activation energy of 18.6 ± 1.8 kcal/mole was obtained by measuring the rate of front movement through an individual single crystal (Clark and Thomas, 1969). The isotope effect for the dehydration of calcium oxalate monohydrate versus monodeuterate was determined to be very small or negligible (Manche and Carroll, 1977). These recent studies may indicate that reliable data can also be obtained for desolvations of organic hydrates.

The rate of desolvation and activation energy for the desolvation of potassium gluconate dihydrate to monohydrate was 4.3 kcal/mole, and the activation energy for the transformation of the monohydrate to anhydrous form was 18.5 kcal/mole (Horikoshi and Himuro, 1976).

The activation energies and rate constants discussed have been interpreted to mean that the rate-determining step in the reaction is loss of water from the crystal surface (Manche and Carroll, 1977) and that the rate of front movement determines the rate of the process (Clark and Thomas, 1969). It was also pointed out that the activation energy for the dehydration of calcium oxalate monohydrate was nearly equal to the enthalpy of the reaction (Manche and Carroll, 1977), suggesting that hydrogen-bond energy could play an important role in these reactions. Further interpretation of activation parameters must await studies of a related series of compounds.

In an interesting related study, Morsi, Thomas, and Williams showed that it was possible to reproducibly determine activation energies for solid-state reactions involving bond breakage (Morsi *et al.*, 1975). They found that the activation energy for decomposition of solid benzoyl peroxide was reproducible and consistent with the solution activation energy. They concluded that the rate-determining step of the solid-state reaction was O–O bond breakage. It is interesting to note that they found that the activation enthalpy for deliberately deformed crystals was the same as that for the as-grown crystals, but the activation entropy was different.

In contrast to these studies, which indicated that reliable activation parameters can be obtained using either thermogravimetric analysis or measurement of front advancement for desolvations and molecular reactions, Mnyukh (1978) has recently shown that both of those methods fail to give reproducible results for polymorphic transitions. Mnyukh has suggested that activation parameters reflect the concentration of defects rather than the energetics of the process.

One possible explanation of this conflict is that the energy required for polymorphic transition is usually small relative to that required for desolvation or molecular reaction, so that the data for desolvations and molecu-

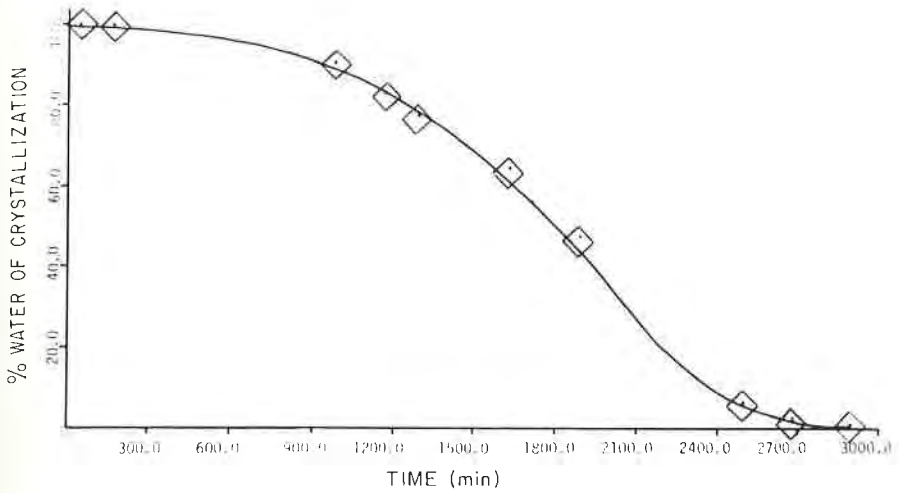


**FIGURE 16.** Dehydration of a single crystal 5-nitrouracil hydrate at 40°C.

lar reactions are representative of the rate-determining step. However, further studies are required to completely clarify this apparent conflict.

Perrier (1980) has studied the dehydration kinetics of single crystals of 5-nitrouracil hydrate, cytosine hydrate, and barbituric acid dihydrate. The plots of percent of water of crystallization versus time are shown in Figures 16, 17, and 18. This data was analyzed using the computer program discussed in Chapter 3, and the best fit of the data was provided with the

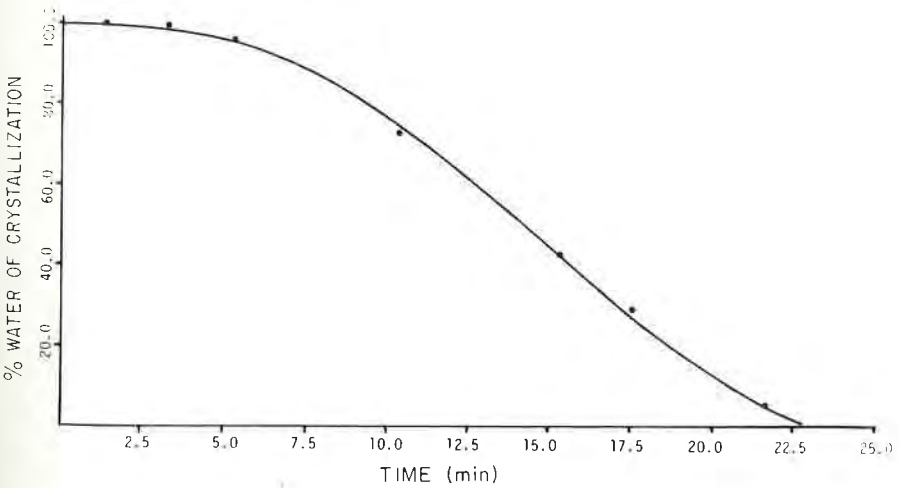


**FIGURE 17.** Dehydration of a single crystal of cytosine hydrate at 60°C.

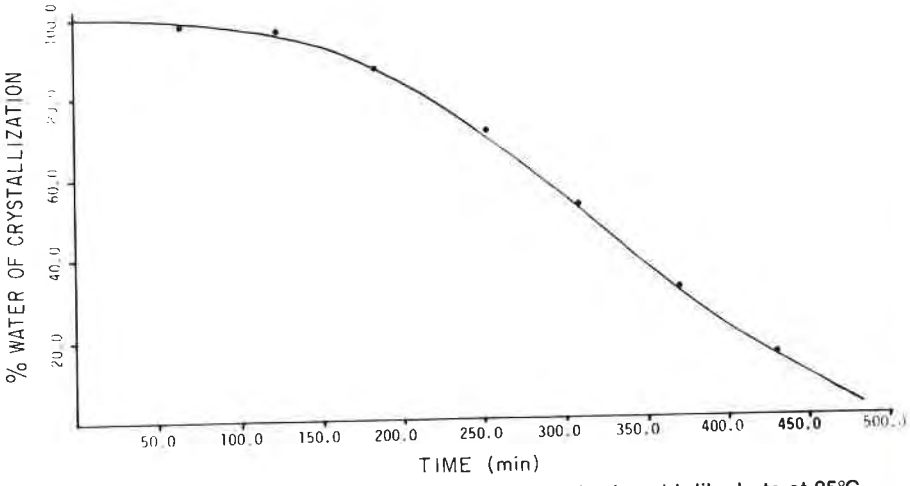


**FIGURE 18.** Dehydration of a single crystal of barbituric acid dihydrate at 25°C.

Avrami–Erofeev equation ($n = \frac{1}{4}$), $[-\ln(1 - \alpha)]^{\frac{1}{4}} = kt$. Table IV summarizes the results of this study.

It is interesting to note that the Avrami–Erofeev equation is derived for reactions governed by a nucleation mechanism, yet visual examination of the crystals indicates that the reaction occurs via a diffusion mechanism or a phase-boundary mechanism. However, attempts to fit all data to either nucleation equations or phase boundary equations gives a much poorer fit, with correlation coefficients in the 0.8 to 0.9 range.

Barbituric acid dihydrate was also crystallized in much smaller crystals, which were often stuck together and resembled a powder. These crystals were used to study the effect of humidity on the rate of desolvation reactions. The results of these studies are shown in Table V. It is clear from this table that dehydration of these smaller crystals follows a zero-order kinetic law. Recall that large crystals follow the Avrami–Erofeev

**TABLE IV**
*Slope and Correlation Coefficient Corresponding to the Avrami–Erofeev Equation ($n = \frac{1}{4}$) for the Dehydration of Different Single-Crystal Compounds*

| Compounds | Slope | Correlation coefficient | Temperature (°C) |
|---|---|---|---|
| 5-Nitrouracil hydrate | $4.5908 \times 10^{-4}$ | 0.993 | 40 |
| Cytosine hydrate | $5.3410 \times 10^{-2}$ | 0.995 | 60 |
| Barbituric acid dihydrate | $2.2537 \times 10^{-3}$ | 0.994 | 25 |

**TABLE V**
*Rate Constant of Dehydration for Barbituric Acid Dihydrate at Room Temperature*

| Relative humidity (%) | Rate constant $k$ (zero-order) ($hr^{-1}$) | $n^a$ | Correlation coefficient |
|---|---|---|---|
| 0 | 5.67 | 8 | 0.998 |
| 12.5 | 4.16 | 8 | 0.997 |
| 19.6 | 2.68 | 12 | 0.999 |
| 32.7 | 0.59 | 9 | 0.998 |
| 60.0 | No reaction after 60 days | | |
| 93.0 | No reaction after 60 days | | |

[a] $n$ = number of points used to calculate $k$.

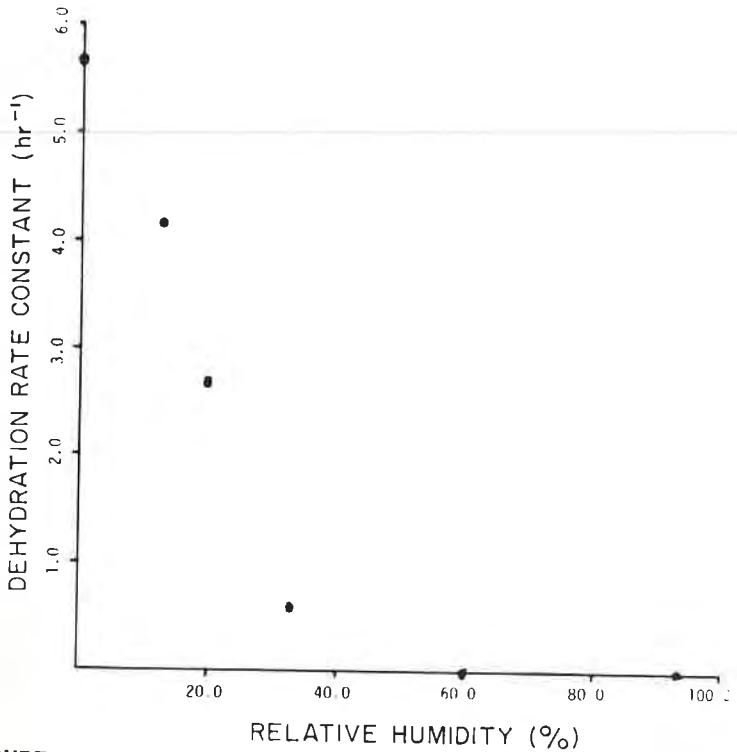


**FIGURE 19.** A plot of the dehydration rate constant of barbituric acid dihydrate versus relative humidity.

equation. Thus changing the size of the crystals used changes the rate law. It is also clear that the rate of the reaction decreases as the humidity increases. This is completely consistent with expectations. Figure 19 shows a plot of the dehydration rate constant versus relative humidity.

In another set of experiments, the kinetics of dehydration of cytosine monohydrate were measured. Single crystals were studied by measuring the rate of front advancement through the crystal. Batches of crystals were studied using weight loss. The data from the single crystals followed Prout–Tompkins kinetics, while the data from batches followed Avrami–Erofeev kinetics.

These results clearly indicate that studies of kinetics of these reactions are difficult because different types of crystals of the same compound give kinetic data which fit different equations; nevertheless, the activation energy of the dehydration of cytosine monohydrate was determined by measuring the rate of the reaction at different temperatures. Table VI summarizes this data, and Figure 20 shows the Arrhenius plots.

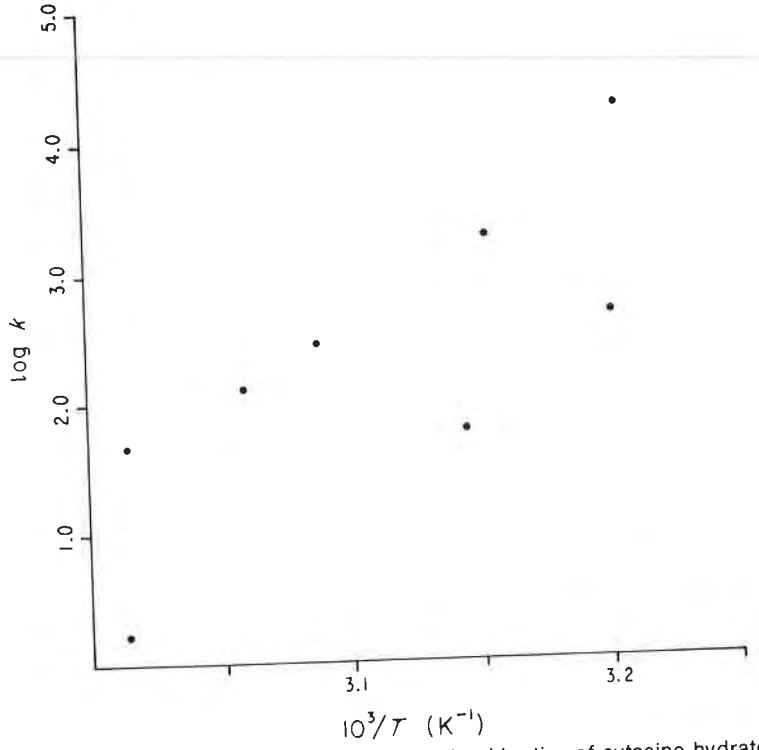


**FIGURE 20.** Arrhenius plots of the dehydration kinetics of cytosine hydrate.

**TABLE VI**
*Dehydration Rate Constant for Cytosine Monohydrate*

Single Crystals: Prout–Tompkins Equation

| $T$ | $10^3 \times (1/T)$ | $k$ | $\ln k$ |
|---|---|---|---|
| 58.54 | 3.014 | .798 | −0.226 |
| 44.95 | 3.144 | .165 | −1.801 |
| 39.36 | 3.200 | .072 | −2.636 |

Batch: Avrami–Erofeev Equation ($n = \frac{1}{2}$)

| $T$ | $10^3 \times T$ | $10^2 \times k$ | $\ln k$ |
|---|---|---|---|
| 58.64 | 3.014 | 19.204 | −1.650 |
| 53.69 | 3.060 | 12.116 | −2.111 |
| 50.67 | 3.088 | 8.494 | −2.466 |
| 44.00 | 3.153 | 3.986 | −3.222 |
| 39.12 | 3.202 | 1.566 | −4.156 |

Different kinetic laws fit the different batches of crystals; however, the activation energy obtained for both types of crystals was 26.0 kcal/mole. This energy is slightly higher than that observed for calcium oxalate monohydrate and manganese formate dihydrate, but in light of the problems involved in determining the proper kinetic law the meaning of these differences is unclear.

## III. Summary

In the first section of this chapter, the desolvation of 15 different crystal solvates was reviewed and discussed. Particular emphasis was placed on the explanation of the observed behavior of crystals of these hydrates in terms of crystal packing. In the second section, mechanistic studies of the desolvation reaction, which is the simplest of the reactions of the type $A(s) \rightarrow B(s) + C(g)$, were discussed. In particular, the influence of crystal packing, crystal compactness, and hydrogen bonding on this reaction were discussed. In addition, the problems involved in the study of the kinetics of these reactions were illustrated.

Both the visual behavior of the solvates and the threshold temperature of desolvation appear to be controlled in part by crystal packing. The studies reviewed in this chapter have the following pharmaceutical implications:

1. The loss of solvent of crystallization can change the dissolution rate, bioavailability and stability of crystals of pharmaceuticals.

2. The threshold temperature of desolvation depends on the crystal packing, on hydrogen bonding, and perhaps on defects within the crystal.
3. Stabilization of solvates could be accomplished by crystallization of a different solvate, protection of the crystal from defects, coating the crystal with glue or other coatings, or storage in an atmosphere of the solvent of crystallization.

## References


Allen, L. C. (1975). *J. Am. Chem. Soc.* **97,** 6921.

Allen, P. V., Rahn, P. D., Sarapu, A. L., and Vanderwielen, A. J. (1978). *J. Pharm. Sci.* **67,** 1087.

Austin, K., Marshall, A. C., and Smith, H. (1965). *Nature (London)* **208,** 999.

Bell, R. P. (1941). "Acid-Base Catalysis," Chapter 8. Oxford University Press, London.

Bell, R. P. (1959). "The Proton in Chemistry," Chapter 10. Cornell University Press, Ithaca, N.Y.

Biles, J. (1963). *J. Pharm. Sci.* **52,** 1066.

Borka, L., Kristiansen, P., and Backe-Hansen, K. (1972). *Acta Pharm. Suec.* **9,** 573.

Byrn, S. R., and Lin, C. T. (1976). *J. Am. Chem. Soc.* **98,** 4004.

Byrn, S. R., Paul, I. C., and Curtin, D. Y. (1972). *J. Am. Chem. Soc.* **94,** 890.

Carless, J., Moustafa, M., and Rapson, H. (1966). *J. Pharm. Pharmacol. Suppl.* **18,** 190S.

Chapman, J., Page J., Parker, A., Rogers, D., Sharp, C. J., and Staniforth, S. E. (1968). *J. Pharm. Pharmacol.* **20,** 418.

Clark, T. A., and Thomas, J. M. (1969). *J. Chem. Soc., Ser. A* 2227.

Clark, J. R. (1963). *Rev. Pure Appl. Chem.* **13,** 50.

Clay, R. J., and Byrn, S. R. (1980). Unpublished results.

Curtin, D. Y., Byrn, S. R., and Pendergrass, D. B., Jr. (1969). *J. Org. Chem.* **34,** 3345.

Desvergne, J. P., and Thomas, J. M. (1973). *Chem. Phys. Lett.* **23,** 343.

Desvergne, J. D., Thomas, J. M., Williams, J. O., and Bouas-Laurent, H. (1974). *J. Chem. Soc., Perkin Trans. 2,* 363.

Donohue, J. (1968). *In* "Structural Chemistry and Molecular Biology" (A. Rich and N. Davidson, eds.).

Eckhardt, R. C., and Flanagan, T. B. (1964). *Trans. Faraday Soc.* **60,** 1289.

Haleblian, J., Koda, R., and Biles, J. (1971). *J. Pharm. Sci.* **60,** 1485.

Hartshorne, N. H., and Roberts, M. H. (1951). *J. Chem. Soc.,* 1097.

Himuro, I., Tsuda, Y., Sekiguchi, K., Horikoshi, I., and Kanke, M. (1971). *Chem. Pharm. Bull.* **19,** 1034.

Hine, J. (1962). "Physical Organic Chemistry," p. 116ff. McGraw-Hill, New York.

Hirsch, C. A., Messenger, R. J., and Brannon, J. L. (1978). *J. Pharm. Sci.,* **67,** 231.

Hopfinger, A. J. (1973). "Conformational Properties of Macromolecules." Academic Press, New York.

Horikoshi, I., and Himuro, I. (1966). *J. Pharm. Sci. Jap.* **86,** 319, 324, 353, 356.

Kennard, O., and Watson, D. G. (1962–1978). "Molecular Structures and Dimensions," Vols. 1–8. Int. Union of Crystallography.

Kitaigorodskii, A. I., Mnyukh, Y. V., and Asadov, Y. G. (1965). *J. Phys. Chem. Solids* **26,** 463.

Kitaigorodskii, A. I. (1961). "Organic Chemical Crystallography." Consultants Bureau, New York.
Kuhnert-Brandstatter, M. (1971). "Thermomicroscopy in the Analysis of Pharmaceuticals." Pergamon Press, New York.
Kuhnert-Brandstatter, M., and Gasser, P. (1971). *Microchem. J.* **16,** 590.
Lin, C. T., and Byrn, S. R. (1979). *Mol. Cryst. Liq. Cryst.* **50,** 99.
Lin, C. T., Siew, P. Y., and Byrn, S. R. (1978). *J. Chem. Soc., Perkin Trans. 2,* 957.
Lin, H. (1972). *Diss. Abstr. Int.* **B31,** 4703B.
Mackenzie, R. C. (1977). "Differential Thermal Analysis." Academic Press, New York.
Manche, E. P., and Carroll, B. (1977). *J. Phys. Chem.* **81,** 2637.
McCullough, J. D., Jr., Curtin, D. Y., Miller, L. L., Paul, I. C., and Pendergrass, D. B., Jr. (1970). *Mol. Cryst. Liq. Cryst.* **11,** 407.
Mendelcorn, L. (ed). (1964). "Non-Stoichiometric Compounds." Academic Press, New York.
"The Merck Index" (1980). 8th ed. Merck Publishing Co., Rahway, N.J.
Miller, R. S., Curtin, D. Y., and Paul, I. C. (1974). *J. Am. Chem. Soc.* **96,** 6329, 6334, 6340.
Mnyukh, Y. V. (1978). *Abst. 5th Int. Meeting on the Organic Solid State,* Brandeis University.
Mnyukh, Y. V., Petrotsavlov, N. N., and Kitaigorodskii, A. I. (1966). *Dokl. Akad. Nauk SSSR* **166,** 80.
Momany, F. A., McGuire, R. F., Burgess, A. W., and Scheraga, H. A. (1975). *J. Phys. Chem.* **79,** 2361.
Morsi, S. E., Thomas, J. M., and Williams, J. O. (1975). *J. Chem. Soc., Faraday Trans. 1,* 1857.
Moustafa, M., Ebian, A., Khalil, S., and Motawi, M. (1971). *J. Pharm. Pharmacology* **23,** 868.
Nakamoto, K., Margoshes, M., and Rundle, R. E. (1955). *J. Am. Chem. Soc.* **77,** 6480.
Niazi, S. (1978). *J. Pharm. Sci.* **67,** 488.
Olesen, P., and Szabo, L. (1959). *Nature (London)* **183,** 749.
Patterson, A. L., and Groshens, B. T. (1954). *Nature* **173,** 398.
Perrier, P. (1980). Unpublished results, Purdue University.
Pfeiffer, R. R., Yang, K. S., and Tucker, M. A. (1970). *J. Pharm. Sci.* **59,** 1809.
Port, G. N. J., and Pullman, A. (1972). *Int. J. Quantum Chem., Quantum Biol. Symp.* **1,** 21.
Port, G. N. J., and Pullman, A. (1975). *F.E.B.S. Lett.* **31,** 70.
Puckett, S. A., Paul, I. C., and Curtin, D. Y. (1976). *J. Chem. Soc., Perkin Trans. 2,* 1873.
Rabbering, G., Wanrooy, J., and Schnijft, A. (1975). *Thermochim Acta* **12,** 57.
Rassonshaya, I. S. (1969). *Proc. 2nd Int. Conf. Thermal Analysis 1968* **2,** 953.
Rose, H. A., Hinch, R. J., and McCrone, W. C. (1952). *Anal. Chem.* **25,** 993.
Schaefer, W. P., and Marsh, R. E. (1969). *Acta Cryst.* **B25,** 1675.
Schuster, P., Zundel, G., and Sanderfy, C. (1976). "The Hydrogen Bond. Recent Developments in Theory and Experiment." North Holland Publishing Co., Amsterdam.
Sekiguchi, K., Horikoshi, I., and Himuro, I. (1968). *Chem. Pharm. Bull.* **16,** 2495.
Shafizadeh, F., and Susott, R. A. (1973). *J. Org. Chem.* **38,** 3710.
Shefter, E., and Higuchi, T. (1963). *J. Pharm. Sci.* **52,** 781.
Shell, J. (1955). *Anal. Chem.* **27,** 1665.
Thomas, J. M. (1974). *Trans. Roy. Soc., Ser. A* **227,** 251.
Thomas, J. M., and Williams, J. O. (1969). *Mol. Cryst. Liq. Cryst.* **9,** 59.
Umeyama, H., and Morokuma, K. (1977). *J. Am. Chem. Soc.* **99,** 1316.

United States Pharmacopeia, XX, (1980), U.S. Pharmacopeial Convention, Inc., Rockville, Md. 20852.
Vogt, L. H., Jr., Faigebaum, H. M., and Wiberley, S. E. (1963). *Chem. Rev.* **63,** 269.
Weintraub, H. J. R., and Hopfinger, A. J. (1975). *Int. J. Quantum Chem., Quantum Biol. Symp.*, **2,** 203.
Wendlandt, W. (1974). "Thermal Methods of Analysis." John Wiley and Sons, New York.
Williams, J. O., Thomas, J. M., Savintsev, Y. P., and Boldyrev, V. V. (1971). *J. Chem. Soc., A*,1757.
Yang, S., and Guillory, J. K. (1972). *J. Pharm. Sci.* **61,** 26.

# III Solid–Gas Reactions

In this section, a number of solid–gas reactions are discussed. These reactions are governed by two general principles: (*a*) solid–gas reactions are very sensitive to crystal packing, and (*b*) solid–gas reactions often begin at crystal defects.

The remarkable sensitivity of these reactions to crystal packing is illustrated by instances in which one crystal form of a compound is reactive while another is stable. The role of defects in these reactions is manifested when solids appear to react in an unpredictable fashion and different crystals crystallized from the same solution under the same conditions react at quite different rates.

This section is divided into three chapters: solid-state oxidations, additions of gases to solids and solid-state hydrolyses, and solid-state decomposition reactions of the type A(solid) → B(solid) + C(gas).

# 6 Solid-State Oxidation Reactions

In this chapter, solid-state oxidation reactions of organic crystals are discussed. Drugs and nondrugs are included. In addition, data from our laboratory is included.

## I. Oxidations of Rubrene and Tetramethylrubrene

Crystals of linear polyacenes (anthracene, **1**; tetracene, **2**; pentacene, **3**; rubrene, **4**; and tetramethylrubrene, **5**) react with $O_2$ upon irradiation with a low-pressure mercury lamp (Hochstrasser and Porter, 1960). However, the reaction of crystals of anthracene and rubrene was confined to the surface, apparently because the crystals were not permeable to oxygen (Hochstrasser, 1959). On the other hand, deep-red crystals of tetramethylrubrene (**5**) gave a good yield of transannular peroxide (**6**) and were completely decolorized upon irradiation in oxygen, as shown in Figure 1. It was suggested that the mechanism of this reaction involves the excited triplet state of the dye (Hochstrasser, 1959); however, it is also possible that this reaction is a singlet oxygen addition to ground-state tetramethylrubrene.

In contrast to Hochstrasser and Porter's studies, Scheffer and Ouchi

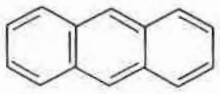

1

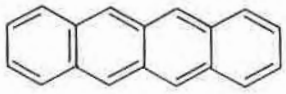

2

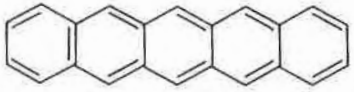

3

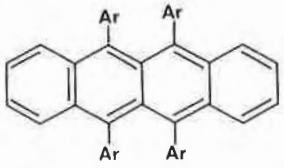


4 Ar = $C_6H_5$
5 Ar = p-$CH_3C_6H_4$

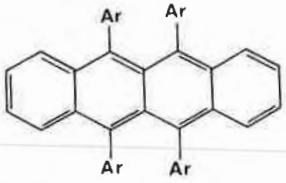


5

Ar = $CH_3C_6H_4$


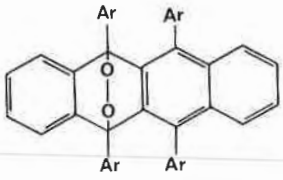


6

(1970) observed that rubrene adsorbed on microcrystalline cellulose or silica gel gave a good yield (> 70%) of the transannular peroxide when exposed to singlet oxygen generated by microwave discharge. These workers also found that under these conditions, 9,10-diphenylanthracene smoothly added singlet oxygen to give a 79% yield of the transannular peroxide. Of the three possible explanations for this apparent discrepancy—(*a*) that crystals are more permeable to singlet oxygen than oxygen, (*b*) that different crystal polymorphs of rubrene are involved, or (*c*) that adsorption on silica gel or cellulose renders the solid more permeable to oxygen, perhaps due to the presence of a noncrystalline amorphous form—(*b*) and (*c*) seem most likely. Three polymorphs of rubrene have been reported: one belonging to space group $P\bar{1}$ (Akopyan *et al.*, 1972), one to $Aba2$ (Henn *et al.*, 1971), and one to $P2_1/n$ (Taylor, 1936). Thus it is possible that the two groups of workers were actually observing different reactivity of different polymorphs. Such an observation would be quite significant and has been a target for study by the Thomas group (Desvergne and Thomas, 1975). Haleblian and McCrone (1969) have reviewed several cases of different reactivity of different polymorphs.

It is interesting to note that Kautsky (1939) carried out solid-state

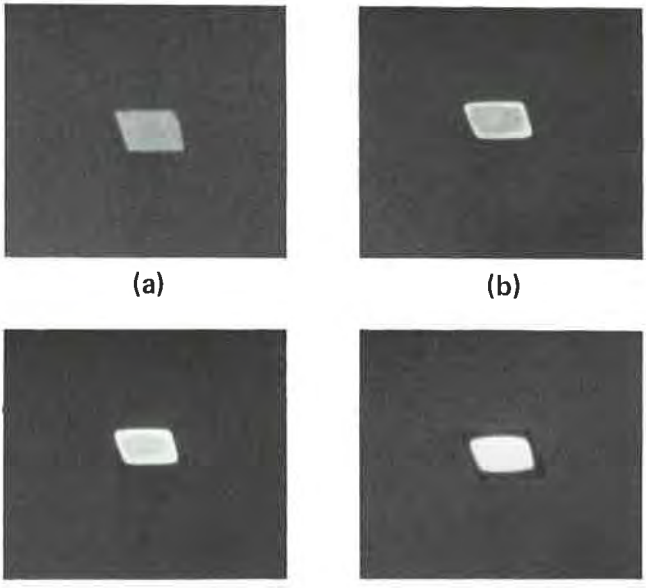


**FIGURE 1.** The behavior of a single crystal of tetramethylrubrene upon exposure to oxygen (ambient atmosphere) and ultraviolet light (Mineralight) (*a*) at start; (*b*) after 5 hr; (*c*) after 7 hr; (*d*) after 8 hr. (C. T. Lin, unpublished results, 1979).

singlet-oxygen reactions by irradiating mixtures of crystals of sensitizer and substance in air.

## II. Solid-State Ozonolysis of Stilbenes

Desvergne and Thomas were searching for systems where they could compare the products and behavior of several polymorphs of stilbene derivatives upon ozonolysis (Desvergne and Thomas, 1975). However, stilbene and diethylstilbesterol existed in only one polymorph.

Irradiation of crystals of stilbenes (**7a**) and (**7b**) in the presence of oxygen gave good yields of the corresponding ketone or aldehyde **8**

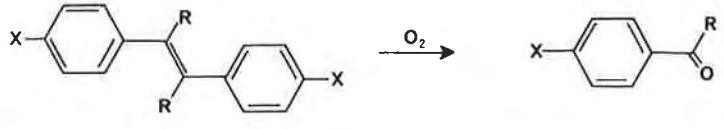


7 a R = H ; X = H
b R = $C_2H_5$ ; X = OH

8

(Desvergne *et al.*, 1974). Since oxidation under similar conditions in solution yielded many products (Desvergne *et al.*, 1974), this reaction illustrates the synthetic advantage solid-state oxidation reactions can have over the corresponding solution reaction. Studies of these reactions using optical microscopy showed that the progress of the reaction through the crystal was controlled by defects.

## III. Reactions of Oxygen with Free Radicals in the Solid State

In the solid state, the triphenylmethyl "radical" has the structure **9**. In solution this radical rapidly dissociates to form the triphenylmethyl radical

9

**10**. Solutions of the equilibrium mixture of **9** $\rightleftharpoons$ **10** react with oxygen to form the peroxide **11**. Crystals of the triphenylmethyl radical also react

10 11

with oxygen, however, the reaction stops when the surface of the crystal is coated with product (Tschitschibabin, 1907). Apparently crystals of the radical **10** are not permeable to oxygen.

In a related study, the reactivity of triphenylmethyl radicals with oxygen in a solid lattice has been investigated (Janzen *et al.*, 1967). Triphenylmethyl radicals were formed by $\gamma$-irradiation of crystals of $(C_6H_5)_3CCOH$, $(C_6H_5)_3CBr$, $(C_6H_5)_3CCl$, $(C_6H_5)_3CCOO^-Na^+$, and $(C_6H_5)_3CCOO^-Ag^+$ and were allowed to react with oxygen to form the peroxy radical **12**. The reactivity of the radicals in these crystals with

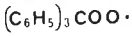

12

oxygen follows the order $(C_6H_5)_3CCOOH > (C_6H_5)_3CBr > (C_6H_5)_3CCl > (C_6H_5)_3CCOO^-Na^+ \gg (C_6H_5)_3CCOO^-Ag^+$. The order of reactivity may reflect differences in crystal packing. Thus, the different crystals would have a different permeability to oxygen. Unfortunately, systematic study of the crystal packing of these compounds has not been completed.

Adler (1972) has studied the reaction of gases with amide radicals pro-

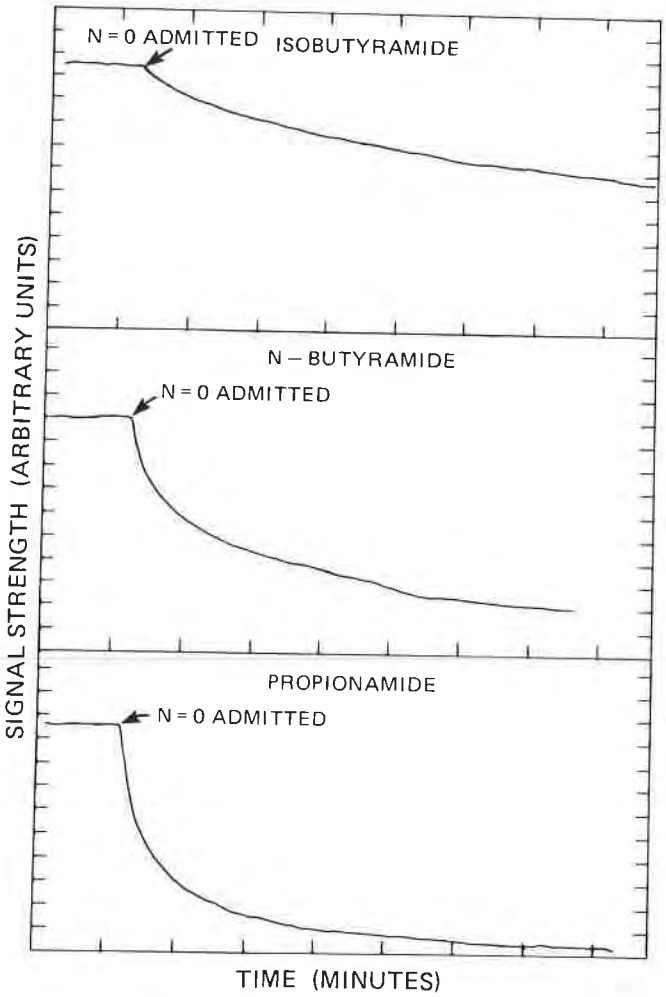


**FIGURE 2.** Decay of the free radicals of the compounds indicated in the presence of nitric oxide (Adler, 1972).

duced by irradiating amides with Co-60 $\gamma$ rays. These amides crystallize in a bilayer structure. The radicals are produced on the $\alpha$-carbon atom near the polar layer. The rate of reaction of gases such as $O_2$ or nitric oxide with these radicals depends on the hydrocarbon chain as illustrated in Figure 2, indicating that $O_2$ penetrates the crystal at the interlayer spacing. For example, the longer the hydrocarbon chain, the slower the reaction. This is to be expected, since the longer the hydrocarbon chain the longer it would take oxygen to

diffuse to the radical and thus the slower the reaction. Furthermore, stearamide reacts slower than oleoamide, as might be expected since stearamide has a linear hydrocarbon chain that packs more closely than oleoamide, which has a cis double bond in its hydrocarbon chain.

It is interesting to note (Adler, 1972) that these crystals bear a resemblance to the bilayer structure of membranes. Their reaction with gases may give us an idea of the mechanism of diffusion of gases into membranes.

## IV. Oxidation of Vitamin $D_2$

Vitamin $D_2$ (13) has an extensive series of solution, photochemical, and thermal reactions (Pfoertner and Weber, 1972; Hoffman and Woodward,

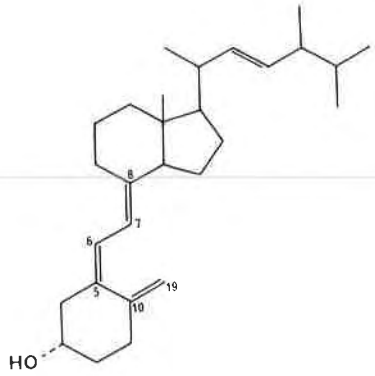


13

1970). Crystalline vitamin $D_2$ is light-, air-, and heat-sensitive and gives a number of products whose structures have not been determined (Kanzaewa and Kotaku, 1953; Keuning, 1965). Furthermore, although crystalline vitamin $D_2$ is unstable and was deemed unsuitable for crystallographic studies, crystals of the 3,20-bisethylenedioxy derivative (Hodgkin *et al.*, 1957) and the 4-iodo-5-nitrobenzoate derivative (Knobler, 1972) of vitamin $D_2$ are more stable and their crystal structures have been determined.

We have found that crystalline vitamin $D_2$ ($C_{28}H_{44}O$, MW = 396.6, calculated elemental analysis C 84.8%, H 11.2%) is completely decomposed to a yellow powder (mp 58°–100°C) after 6 months of exposure to room temperature and fluorescent light in air. The vitamin $D_2$ "crystals" retain their original shape during reaction. Thin-layer chromatography shows that at least five products are formed. Elemental analysis of this

powder indicates extensive oxidation: observed, C, 66.0%, H, 7.7%; calculated for $C_{28}H_{44}O_8$, C, 66.12%, H, 8.72%. Mass spectra indicated degradation, since the highest molecular ion observed had a mass of 322. We also have found that crystals of vitamin $D_2$ decompose and eventually melt when heated at 80°C in air in the presence and absence of fluorescent light. Titrimetric assays showed that 1 molecule of vitamin $D_2$ decomposed to give 0.2 molecules of peroxides and 0.75 molecules of acids. Elemental analysis of these melts indicated oxidation. Crystals of vitamin $D_2$ were stable when heated for 1 week at 80°C in the absence of oxygen.

These thermal and photochemical solid-state reactions in air apparently do not involve formation of cyclized vitamin $D_2$ derivatives such as ergosterol, lumisterol, or suprasterols. Furthermore, the mass spectral data indicate that vitamin $D_2$ does not undergo photochemical dimerization in the solid state. This is consistent with the crystal packing of the bisethylenedioxy derivatives of vitamin $D_2$ (Hodgkin *et al.*, 1957). The only intermolecular contacts less than 5.5 Å between atoms in the triene functionality involve only atom, C(19). Topochemically controlled dimerization reactions do not seem possible. A topochemically controlled polymerization of bisethylenedioxy vitamin $D_2$ involving successive linkage of C(19) to C(6) is possible but is not consistent with the melting-point and mass-spectral studies discussed above. An intramolecular photocyclization of vitamin $D_2$ to suprasterol is possible, but if it is occurring, its rate must be substantially slower than the air oxidation.

Analysis of the neutral oxidation products indicate that the ketone **14** is formed in a yield of greater than 20% (Stewart, 1978). Minor neutral

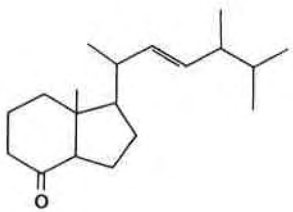


14

oxidation products have also been isolated (Stewart, 1978). Elemental and mass-spectral analysis indicates that these products may actually be a mixture of ketone–alcohols of **14** containing one hydroxy group, perhaps in the six-membered ring. The oxidation of vitamin $D_2$ may proceed by a mechanism quite similar to stilbene ozonolysis, since in both reactions the products correspond to ozone addition followed by cleavage to form the ketone.

## V. Oxidation of Vitamin A

Crystalline esters of vitamin A (including the succinate half-ester, the nicotinate ester, and the 3,4,5-trimethoxybenzoate ester) decompose by both polymerization and oxidation pathways (GUillory and Higuchi, 1962; Baxter and Robeson, 1942). Vitamin A (**15**) exposed to air at room tem-

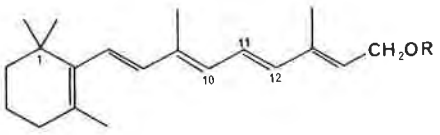


15

perature for several years or heated at 100°C for 5 hr gave at least five ketones on TLC plates treated with 2,4-dinitrophenylhydrazine (Dobrucki, 1971). We have found that vitamin A is a gummy yellow solid after 5 months of exposure to room light, temperature, and air. Elemental analysis indicated that each molecule of vitamin A took up six oxygen atoms, and mass-spectral studies indicated extensive degradation and the presence of many products.

$\beta$-Carotene (**16**) autooxidizes in the solid state in air at 25° and 35°C (Funkelstein *et al.*, 1974). The rate of this oxidation depends on oxygen

$$RH \longrightarrow 2R\cdot$$

$$RH \xrightarrow{O_2} 2R\cdot$$

$$R\cdot + O_2 \longrightarrow RO_2\cdot$$

$$RO_2\cdot + RH \longrightarrow R\cdot$$

$$R\cdot + RH \longrightarrow R\cdot$$

$$R\cdot + RO_2\cdot \longrightarrow \text{Products}$$

$$R\cdot + R\cdot \longrightarrow \text{Products}$$

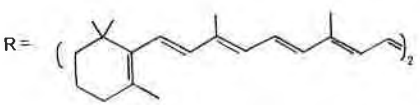


16

pressure and temperature; a free-radical mechanism was proposed (Funkelstein *et al.*, 1974).

Diluents with antioxidant properties stabilize vitamin A palmitate in vitamin preparations (Bhattacharayen, 1969). Aluminum salts of fatty acids such as stearic acid stabilize vitamin A, as does combination with gelatin and dextrin, which probably contain reducing sugars (Leszczynska *et al.*, 1970). In solution, vitamin A and its derivatives undergo several oxidation and isomerization reactions. For example, cobalt(II) stearate oxidized vitamin A to an epoxide with the postulated structure **17**. A

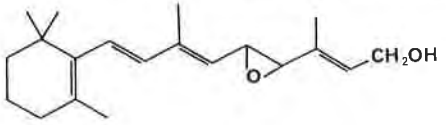


17

hexane solution of vitamin A acetate was converted to peroxides in hexane in the prsence of oxygen (Leszczynska *et al.*, 1970). Vitamin A (**18**) gave 35% of the peroxide **19** upon irradiation of the hexane solution (Lerner *et al.*, 1970) and a 50% yield of **21** when irradiated in methanol in

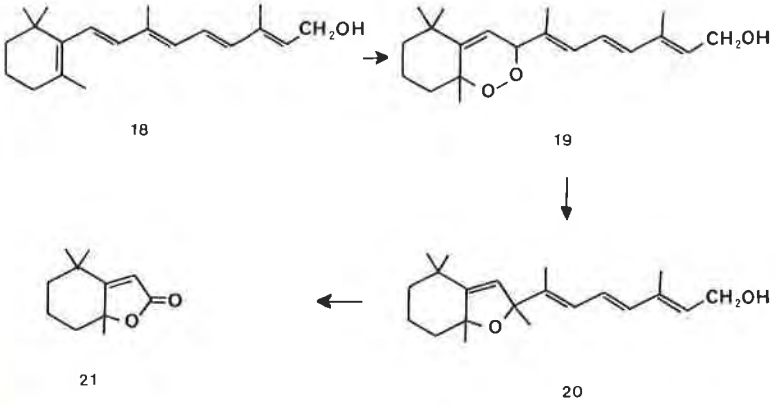


18 19 20 21

the presence of rose bengal (a singlet-oxygen sensitizer) (Canet *et al.*, 1966).

It is impossible to predict the products of the solid-state oxidation on the basis of the solution studies discussed above. It appears likely that these oxidation products can result from singlet-oxygen reactions, free-radical reactions, and perhaps even excited states of vitamin A. In this regard the polymerization of vitamin A in the solid could possibly be topochemically controlled. However, from the packing of vitamin A acetate in the solid state it is clear that there are no stacks of molecules that

could undergo topochemically controlled polymerization. There are two molecules that have the C(11)–C(12) double bond parallel (dihedral angle = 0.0°) and related by a center of symmetry, but they are 5.41 Å apart, which is probably too far for dimerization, according to Schmidt's (1971) topochemical potulate.

An interesting correlation of the melting points of the vitamin A esters with their zero-order rate of solid-state decomposition has been observed (Guillory and Higuchi, 1962). As the melting point increased, the rate of decomposition decreased as shown in Figure 3. The rates of decomposition of these esters in solution were virtually identical. These results were interpreted in terms of crystal lattice energy. It was argued that the higher melting esters had more crystal lattice energy and thus were more stable to the solid–gas oxidation reaction. A much better measure of lattice energy in a series of compounds is the heat of sublimation (Kitaigorodskii, 1973). If the melting point is proportional to the heat of sublimation in this series, then the higher the melting point the more efficient the packing and, conceivably, the less permeable the crystal is to reacting gas. Another approach would be to determine the unit-cell parameters, then calculate the crystal compactness (see Chapter 5) and attempt to correlate crystal

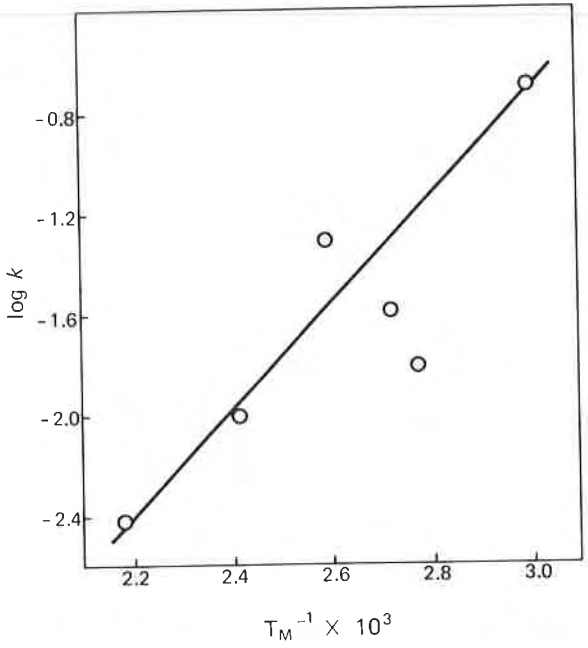


**FIGURE 3.** Relationship between the zero order rate of decomposition of vitamin A derivatives and their melting point (Guillory and Higuchi, 1962). (Reproduced with permission of the copyright owner.)

compartness with reactivity. It is interesting to note that the rates of reaction of acid crystals with ammonia do not correlate with the melting point of the acid (Miller *et al.*, 1971). Whether this failure is due to the fact that melting point does not correlate with the heat of sublimation or other factors is not known.

## VI. Oxidation of Vitamin C (Ascorbic Acid) in Tablets

Vitamin C, like vitamins A and D, is an important pharmaceutical product, and its stability and oxidation in tablets is an important topic. Wilk (1975) suggested that vitamin C degraded during storage and that this degradation could be a threat to the public health. Most of his conclusions were based on infrared spectroscopic studies.

In 1976, Rubin *et al.* reported an extensive study of vitamin C stability using a number of methods including titration with iodine, differential pulse polarography, fluorometry, and thin-layer chromatography. In contrast to Wilk, their results showed that ascorbic acid in various commercial tablets was stable for many years in closed bottles. Even storage of 100-mg tablets in open dishes for 20 weeks at room temperature resulted in only a small amount of degradation.

More careful studies by Rubin *et al.* (1976) and other researchers showed that vitamin C (**22**) degrades in tablets via the following reaction

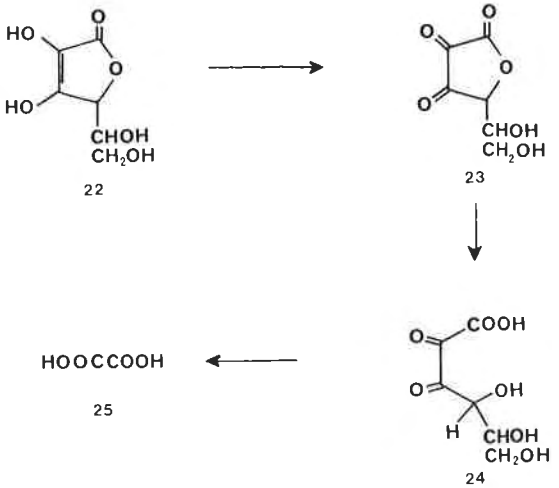


scheme. Table I summarizes the results of these later studies. It is clear that at room temperature vitamin C does not extensively degrade.

**TABLE I**
*Stability of Vitamin C under Various Conditions*

| Storage conditions | Time | Initial assay (% claim) | Dehydroascorbic acid (%) | Diketogluonic acid (%) | Oxalic acid % |
|---|---|---|---|---|---|
| Closed containers at 25°C | 103 months | 110 | 0.4 | 1 | 0.5 |
| Open dish at 25°C | 12 weeks | 100 | 2.9 | — | Not detectable |
| Solution at 45°C | 11 days | 100 | 5.1 | 10 | 20 |

Because of the reports by Wilk, Rubin *et al.* made an effort to validate their methods of analysis in order to rule out the possibility that these studies were subject to errors due to the method of analysis. Their studies indicated that direct titration following the "United States Pharmacopeia" was suitable for determination of vitamin C. In addition, they found that pulsed polargraphy was also suitable for determination of vitamin C, that TLC was suitable for detection of diketogulonic acid and oxalic acid, and that fluorometry was suitable for the detection of dehydroascorbic acid. They suggested that because of band overlap, infrared spectroscopy was impractical as a quantitative tool for studying ascorbic acid degradation. Finally, Rubin *et al.* (1976) also pointed out that degradation of vitamin C did not pose a threat to public health.

## VII. Oxidation of Polyene Antibiotics

A number of polyene antibiotics, including pimaricin (Kekher and Ark, 1949), filipin (Tingstad and Garrett, 1960; Emery and Wright, 1954), and fumagillin, are also oxidized in the solid state. For example, fumagillin (**26**) undergoes both solution and solid-state photochemical oxidation and

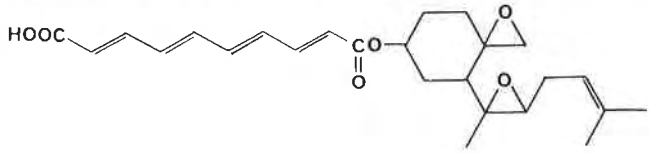


26

the solid decomposes thermally (Garrett and Eble, 1954; Garrett, 1954; Eble and Garrett, 1954). Irradiation of fumagillin with an Atlas fadeometer (light about twice as intense as sunlight) in ethanol solution yielded neofumagillin (structure unknown). The rate and products of this reaction

were the same whether the reaction was run in air or nitrogen. Experiments using filters indicated that the photoreaction of fumagillin ($\lambda_{max}$ 351 and 336 nm, shoulder at 315 nm) required light of wavelength greater than 280 nm.

Although the structure of neofumagillin is unknown, Garrett and Eble suggested that the polyene sidechain of fumagillin might cyclize to yield the cyclohexadiene species (**27**) (Garrett and Eble, 1954; Garrett, 1954;

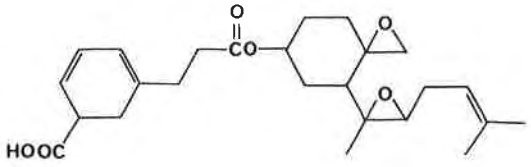


27

Eble and Garrett, 1954). These workers also indicated that neofumagillin was photolabile and decomposed shortly after formation. It was also suggested that neofumagillin solvolytically rearranged, apparently hampering any further attempts to determine its structure.

The solid-state photolysis of fumagillin depends upon the atmosphere. In the presence of air, an oxidized product is obtained upon photolysis in an Atlas fadeometer; in the absence of air, an oxygen-sensitive product is obtained. The first-order rate constant of the solid-state photolysis in air after the first 5 hr is of the same order of magnitude as the solution photolysis (0.14 $hr^{-1}$). During the first 5 hr, the reaction is definitely not first-order and may involve a kinetically important intermediate. The relationship between products of the solid-state and the solution reactions has not been studied, but some of the products of both reactions are probably the same (Garrett and Eble, 1954; Garrett, 1954; Eble and Garrett, 1954).

The solid-state thermal reaction of fumagillin proceeds by different but unknown mechanisms in the presence or absence of air (Garrett and Eble, 1954; Garrett, 1954; Eble and Garrett, 1954). The reaction in the presence of air was interpreted as a thermally induced oxidation. The solid-state thermal reaction is poorly understood, but is slower than the photolytic reaction (bimolecular rate constant of 0.025 at 60°C) and should not interfere with photolytic studies. Fumagillin is thermally stable in ethanol solution.

There are interesting unanswered questions concerning the solid-state and solution behavior of fumagillin: (*a*) Are the products of the photolysis the same in the solid state and in solution? (*b*) The suggested structure of neofumagillin requires a two-step reaction. First a cis–trans isomerization is needed, and then a cyclization. Does neofumagillin have the structure

suggested and is it the product of the solid-state photolysis? If so, what is the extent of the disruption of the crystal lattice required to allow a cis–trans isomerization and is this isomerization similar to the cis–trans isomerization in the cinnamic acids? What are the structures of the products of the solid-state photolysis in the presence and absence of air? Also, why is fumagillin thermally stable in solution but thermally labile in the solid state?

## VIII. Oxidation of Reserpine

The alkaloid reserpine (**28**) is unstable in solution and in the solid state (Wright and Tang, 1972). Irradiation of a chloroform solution gave 3,4-dehydroreserpine (**29**) and finally 3,4,5,6-tetradehydroreserpine (**30**).

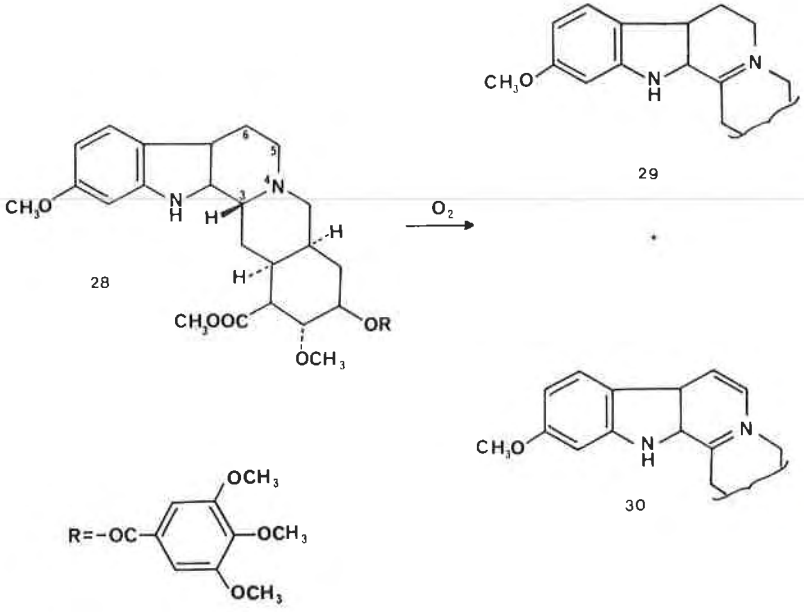


Commercially available tablets of reserpine were found to contain 3,4-dehydroreserpine and 3-isoreserpine in amounts ranging from traces to about 5% (Wright and Tang, 1972). In a separate study, one group of stored tablets was oxidized to the extent of 35% after storage for 4.5 years (Hakkesteegt, 1970). It is interesting to consider the role that the oxidation products of reserpine may play in the recently discovered carcinogenicity of this drug.

## IX. Photooxidation of Dyes Used in Coating Tablets

The solid-state photooxidation of dyes is well known (Gilmour, 1963) and will not be extensively reviewed here. However, the photooxidation of tablet coatings is particularly important to the pharmaceutical industry since discoloration of tablets may cause reduced shelf life.

Tablets were coated with the following dyes: F, D and C Red No. 1; F, D and C Red No. 3; F, D and C Green No. 5; F, D and C Green No. 3; F, D and C Blue No. 2; F, D and C Blue No. 1; F, D and C Yellow No. 5; F, D and C Yellow No. 10; F, D and C Orange No. 3; and F, D and C Violet No. 1. The tablets were then exposed to light in air. The dye erythrosine (**31**)

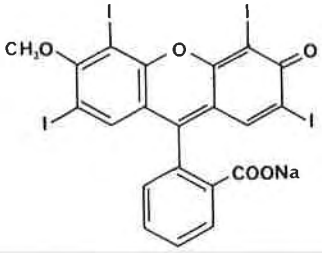


31

(F, D and C Red No. 3) was the most reactive (Lachman *et al.*, 1960; Everhard and Goodhard, 1963). The decomposition of these dyes probably involves photochemical solid–oxygen reactions. Such an explanation is supported by the observation that in solution erythrosine undergoes oxidative bleaching (Usui *et al.*, 1965). Also, the triplet state of fluorescein is reported to react with oxygen to yield a semioxidized dye (Kasche and Lindquist, 1964).

The solid-state oxidation of these dyes may be mechanistically related to the photochemical oxidation of tetramethylrubrene (Section I of this chapter) and could involve addition of oxygen to an excited state of the dye. A plausible alternative explanation is that these reactions involve singlet-oxygen addition to ground-state dye molecules. In this regard it is interesting to note that rose bengal and eosin are fluorescein derivatives and are used as photosensitizers for the production of singlet oxygen in solution (House, 1972). As for tetramethylrubrene and rubrene, different derivatives of fluorescein had different reactivities. A third mechanism involving free-radical-initiated oxidation, similar to that postulated for $\beta$-carotene, cannot be ruled out.

Indigo and triphenylmethane dyes are also oxidized in the solid state.

Brilliant indigo 4B (**32**) is oxidized and dehalogenated to give bromoisatin (**33**) (Iwamoto, 1935), while F, D and C Blue No. 2 (**34**) decomposes in the presence of light and reducing agents to a leuco form (**35**) (Kuramoto *et*

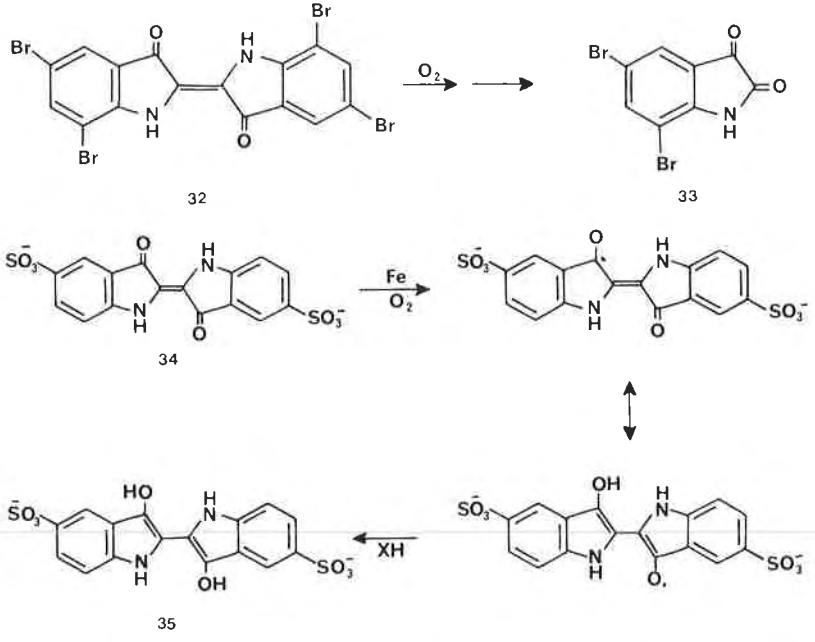


*al.*, 1958). In the presence of tablet excipients containing reducing sugars, this reaction is facile (Kuramoto *et al.*, 1958) and may proceed by a mechanism similar to the one shown in the next section, a mechanism that was proposed for the corresponding solution reaction.

## X. Solid-State Oxidation Reactions Preceded by Loss of Solvent

Although not extensively studied, there are several solid-state oxidation reactions that are preceded by and may indeed require prior loss of solvent of crystallization.

### A. DESOLVATION AND SUBSEQUENT OXIDATION OF DIHYDROPHENYLALANINE

Crystallization of dihydrophenylalanine (**36**), a phenylalanine antagonist, from a dilute 80% ethanol solution yielded stable prisms (mp

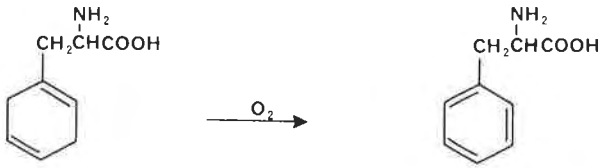


36 37

235–236°C), while crystallization from a saturated 80% ethanol solution or methanol–ethyl acetate yielded unstable needles. After 10 min at 100°C, these unstable needles contained 70% phenylalanine (**37**). In aqueous solution, the dihydrophenylalanine was recovered unchanged after 5 hr at 100°C. Elemental analysis and nuclear magnetic resonance studies showed that the unstable crystals were hydrates (3 water molecules : 4 molecules of **36**). The stable prisms, however, contained no solvent of crystallization. Studies by Ressler (1972) and in our laboratory (Lin and Byrn, 1976) have shown that the oxidation is preceded by loss of the water of crystallization.

A reasonable but untested explanation of this data is that: (*a*) desolvation leaves channels that give oxygen access to the dihydrophenylalanine; (*b*) the crystals without solvent of crystallization are impermeable to oxygen, as were the rubrene crystals discussed earlier; and (*c*) the reaction occurs in the solid but not in solution because the $O_2$ molecules in the channel are held in an orientation favorable for reaction while in solution this specifically favorable orientation is much less probable.

In a possibly related phenomenon, the cephalosporin antibiotic cephradine (**38**) crystallizes as a monohydrate and is packaged under nitro-

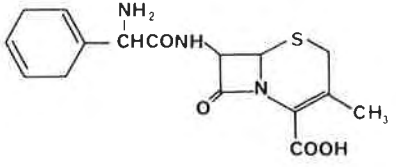


38

gen. This might imply that it undergoes a solid-state reaction; however, there is no published evidence to substantiate this idea. It is interesting to note that aromatization of the dihydrophenylalanine ring would produce another commercially available antibiotic, cephalexin.

## B. DESOLVATION AND SUBSEQUENT OXYGEN ADDITION TO PORPHYRIN MODELS

The oxygen-binding ability of solid bis(salicyaldehyde)ethylenediimine cobalt(II) (**39**) is related to its crystallization with solvents of crystalliza-

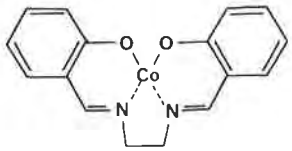

39

tion (Martell and Calvin, 1952; Vogt *et al.*, 1963). The cobalt complex (**39**) crystallizes in several forms, some of which reversibly bind oxygen and others of which are inactive. The crystal structure of one of the active forms, a chloroform solvate, has been reported (Schaefer and Marsh, 1969). This structure shows **39** as a square-planar complex with chloroform solvent tunnels running parallel to the crystallographic *a* axis. The crystal readily desolvated in marked similarity to caffeine, and it has been suggested that the desolvation was required before reversible oxygen binding could occur (Martell and Calvin, 1952; Vogt *et al.*, 1963). It is quite reasonable that, as with dihydrophenylalanine, the solvent departs, leaving the crystals easily penetrable by oxygen. This explanation is substantiated by the crystal structures of the inactive forms of **39**, which show a pentacoordinate cobalt atom without tunnels (DeIsai *et al.*, 1971; Bruckner *et al.*, 1969). In this regard it should be noted that loss of tetrahydrofuran of crystallization may play a role in the activation of iron(II) porphyrin complexes toward reversible oxygen binding (Collman *et al.*, 1974).

## C. SPECIFIC SOLID-STATE OXIDATION OF STEROIDS

Hydrocortisone 21-*tert*-butylacetate (**40**) yielded, upon standing at room temperature for 1 to 2 years, 40% of the 11-one (**41**) (Lewbart, 1969;

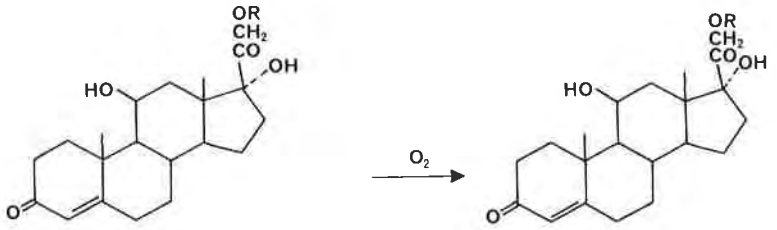

40a R = $COCH_2C(CH_3)_3$
40b R = $COC_2H_5$

41

Bremer *et al.*, 1969). In contrast, other esters including the ethyl ester (**40b**) were completely resistant to air oxidation, even after 15 years at

room temperature. The oxidation of (**40a**) is accelerated by heat and greatly accelerated by free-radical initiators and ultraviolet light.

In our laboratory, hydrocortisone 21-*tert*-butylacetate has been obtained in five crystalline forms (Lin *et al.*, 1982).

Crystal forms I, II, and III of hydrocortisone 21-*tert*-butylacetate were obtained from absolute ethanol solution either at room temperature or in the refrigerator. X-Ray powder diffraction studies indicated that they were different forms and elementaly analysis showed that they contained varying amounts of ethanol within the crystals. The table results of these studies are shown in Table II.

During recrystallization, a mixture of crystal forms I, II, and III often appeared, but a pure single form could be obtained under certain conditions. A new form designated form IV was produced when forms I, II, and

**TABLE II**
*Crystal Forms of Hydrocortisone 21-*tert*-Butylacetate*

| Crystal form | Solvent of crystallization | Ethanol content[a] | X-Ray data | mp[b] (°C) | Ultraviolet oxidation |
|---|---|---|---|---|---|
| I | Ethanol, propanol, *n*-amyl alcohol, acetonitrile | 0.9[e] | Hexagonal, $P6_1$, $a = b = 17.485$. $c = 15.376$; $\alpha = \beta = 90°$, $\gamma = 120°$ | 170–180 | Reaction |
| II | Ethanol | 1.0 | Monoclinic, 110–120[c] $P2_1$, $a = 12.440$, $b = 7.710$, $c = 14.724$; $\alpha = \gamma = 90°$, $\beta = 88.7°$ | 110–120[c] | No reaction |
| III | Ethanol, *t*-butanol | — | Triclinic, $a = 23.0$, $b = 12.5$, $c = 29.0$; $\alpha = 74°$, $\beta = 147°$, $\gamma = 74°$ | 123–126[d] | No reaction |
| IV | Heat forms I, II, or III | — | — | 234–238 | No reaction |
| V | Pyridine | — | Unstable | | Reaction |

[a] No other solvents of crystallization were observed.
[b] The exact melting temperature may vary from one crystal to another.
[c] Opaque at this temperature range, with final melting at 234°–238°C.
[d] After melting, the melt resolidified as the temperature was rising and finally remelted at 234–238°C.
[e] When crystallized from ethanol, form I contains ethanol; when crystallized from the other solvents no solvent of crystallization is present.

III were heated at 120°C. Forms I and II underwent desolvation and phase transformation to form IV, while form III changed from one phase to another. Recently, another form (form V) was isolated from pyridine. All crystal forms except forms I and V were inert to irradiation with ultraviolet light.

Form I was oxidized from hydrocortisone 21-*tert*-butylacetate to cortisone 21-*tert*-butylacetate under irradiation with ultraviolet light in air. A known weight and given size of crystals were put in vials and irradiated at 30°C. The extent of formation of ketone (**41**) was determined by integrating the C(18)methyl NMR signal, and the content of ethanol was measured by gas chromatography. The percent desolvation and oxidation of the hydrocortisone ester (**40**) are shown in Table III. Apparently the loss of ethanol was faster than the oxidation. However, this behavior is different from that of dihydrophenylalanine hydrate, in which water loss almost completely precedes the oxidation. In addition, the crystal opaqueness phenomenon of desolvation has not been found in crystal form I. The behavior of a single crystal of form I is shown in Figure 4. A significant change in appearance of form I (or other similar crystals studied) can only be observed under polarized light. After a week a circle pattern of decolorization moved from the ends toward the center, but the crystal remained clear under transmitted light even after 42 days. Crystallographic studies show that desolvated form I is still a single crystal with a resonably good diffraction pattern. This behavior is termed crystal pseudopolymorphism and indicates that the crystal packing of this form is stable and is not disrupted by solvent loss.

The crystal structure of form I has been determined. The structure of this form is consistent with structures of other hydrocortisone derivatives (see Figure 5) (Weeks and Duax, 1973, 1976). The steroid molecules in hydrocortisone *tert*-butylacetate are arranged in helices linked together by

**TABLE III**
*Percent Desolvation and Oxidation of Crystalline Hydrocortisone 21-*tert*-Butylacetate · 0.9 Ethanol upon Exposure to Ultraviolet Light*

| Days | % Cortisone (**39**) formed | % EtOH lost |
|---|---|---|
| 1 | 20.0 | 43.3 |
| 2 | 38.9 | 75.6 |
| 3 | 50.0 | 83.3 |
| 6 | 52.9 | 88.9 |
| 10 | 56.3 | 93.3 |
| 14 | 66.7 | 95.6 |
| 21 | 71.4 | 96.7 |

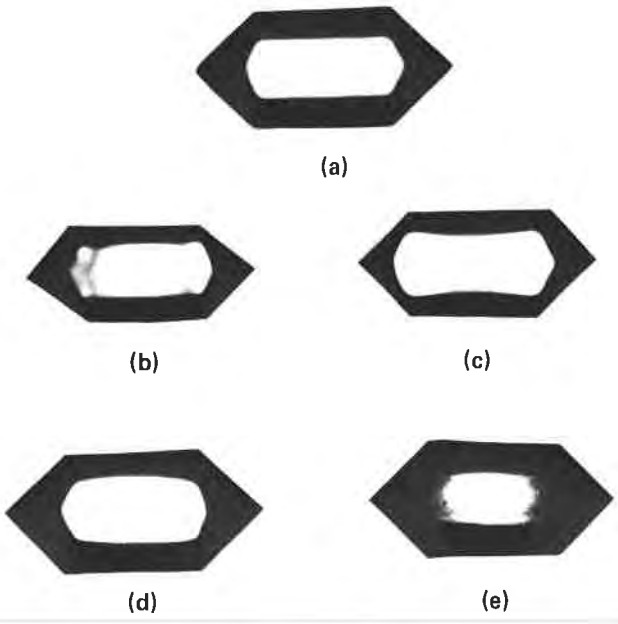


**FIGURE 4.** Behavior of a crystal of form I of hydrocortisone 21-*tert*-butylacetate upon exposure to ultraviolet light at 30°C: (*a*) at start, no polarizing filters; (*b*) after 11 days under crossed polarizing filters; (*c*) after 13 days under crossed polarizing filters; (*d*) after 22 days using crossed polarizing filters; (*e*) after 42 days using crossed polarizing filters.

$O_{29}H \cdots O_{23}{=}C$ hydrogen bonds between the carbonyl oxygen of the *tert*-butylacetoxy group and the OH attached to C(17). This hydrogen bonding, which is not possible in the unesterified hydrocortisones, may be the major reason for the helical packing arrangement observed.

It is speculated that the reactivity of form I toward oxygen is due to the crystal packing, which allows penetration of oxygen down the helix axis of the crystal. It is further speculated that ethanol of crystallization is normally along this helix axis, and that its exit further aids oxygen penetration. However, further crystallographic studies are required to confirm these speculations.

Finally, it is clear that solid-state crystal forms and polymorphs can be used for different purposes. Not only can certain crystal forms be used to cause reactions when they are desired, but also other crystalline forms can be used to prevent reactions when they are to be avoided.

Cholesterol is another steroid that oxidizes in the solid state (Beckwith,

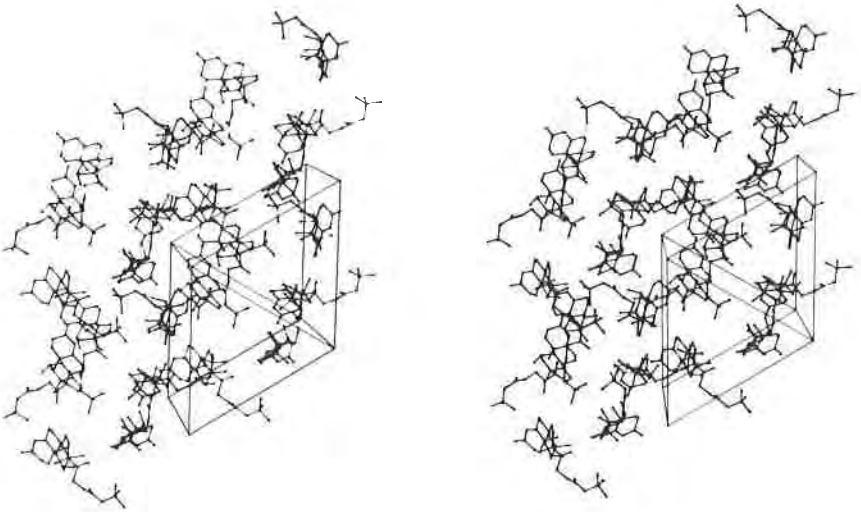

**FIGURE 5.** Stereoscopic view of the crystal packing of hydrocortisone *tert*-butylacetate.

1958). Irradiation of cholesterol for 5 days with a 150-W ultraviolet lamp gave 25-hydroxycholesterol. Beckwith postulated that cholesterol crystals have their hydrocarbon chain exposed on both major surfaces of the platelike crystals. The molecules are evidently sufficiently closely packed to prevent attack at the reactive 3-hydroxyl position and at the 5,6-double bond; the tertiary carbon, C(25), can then be attacked.

## D. OXIDATION OF PHORBOL ESTERS DURING STORAGE

When a powder of TPA (12-*O*-tetradecanoylphorbol-13-acetate, **42**) was stored at 25°C in daylight for 3 months, it was converted preferentially into its 7-peroxide (**43**) and 20-aldehyde (**44**). Different products were

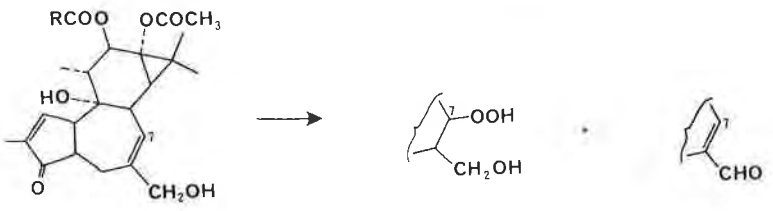


42 43 44

obtained when the reaction was run in solution or in a thin film (Schmidt and Hecker, 1975).

In addition, phorbol and some of its other esters are highly susceptible to autooxidation (Hecker and Schmidt, 1974). Phorbol crystallizes as a bromobenzene, bromothiophene, iodobenzene, a 1:1 5-bromofuronate–$CHCl_3$ solvate, and without solvent of crystallization (Petterson *et al.*, 1968; Brandl *et al.*, 1971). In a related observation, the 5-bromofuronate–$CHCl_3$ solvate decomposed rapidly when exposed to x-rays.

## XI. Solid-State Oxidation of Dialuric Acid Monohydrate: The Importance of Moisture in Accelerating Solid-State Reactions

Dialuric acid monohydrate (**45**) rapidly dehydrates at 76°C in the solid state to yield the anhydrous form. This form then slowly oxidizes over a period of 2 months to form alloxantin (**46**).

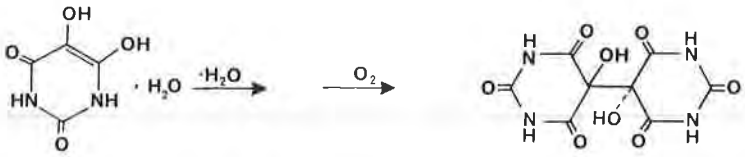


45 46

Surprisingly, in atmospheres of >93% relative humidity, solid dialuric acid oxidizes to alloxantin in less than 2 days at room temperature (Clay, 1979). Microscopic examination of reacting crystals shows no obvious signs of dissolution. However, in solution dialuric acid is oxidized to alloxantin in a few minutes.

These data indicate that a 76°C a slow solid-state oxidation reaction of dialuric acid to alloxantin occurs over a few months. The formation of alloxantin in the solid dialuric-acid matrix is feasible since the reacting carbon atoms are within 5 Å of each other. In high humidities at room temperature, dialuric acid is oxidized to alloxantin in a few days. This rapid reaction is best explained in terms of an oxidation reaction that occurs in a sorbed moisture layer on the surface of the crystal. To test this idea, the rate of reaction of anhydrous dialuric acid (formed by heating at 76°C) at various humidities was studied. The results of these studies are shown in Table IV. At humidities below 30%, rehydration to hydrated dialuric acid was not complete and no rapid oxidation occurred. At humidities between 30 and 93%, rehydration was complete but again rapid oxidation did not occur. At humidities greater than 93%, rehydration and rapid oxidation occurred, substantiating the idea of a sorbed moisture layer.

**TABLE IV**
*Structure Changes of Anhydrous Dialuric Acid at Room Temperature and Various Relative Humidities*

| Relative humidity (%) | Initial weight gain equivalent | Structure change[a] |
|---|---|---|
| 2 | None | None |
| 15 | None | None |
| 30 | 0.018 g (1 · $H_2O$) | Anhydrous to hydrate |
| 47 | Same as 30% | |
| 72 | Same as 30% | |
| 84 | Same as 30% | |
| 93 | 0.018 g | Anhydrous to hydrate → alloxantin hydrate, (>24 hr) |
| 100 | 0.018 g | Anhydrous to hydrate → alloxantin hydrate (>3 hr) |

[a] As determined by infrared and x-ray powder diffraction after 5 days exposure, except where noted.

To our knowledge, this is the first illustration of the effect that sorbed moisture can have on a solid–gas reaction.

## XII. Solid-State Reduction of the Ammonium Oxalate–Hydrogen Peroxide Adduct $(NH_4)_2C_2O_4 \cdot H_2O_2$

Although this chapter has emphasized oxidation reactions, the reported transformation of $(NH_4)_2C_2O_4 \cdot H_2O_2$ to $(NH_4)_2C_2O_4 \cdot H_2O$ is of sufficient interest to merit inclusion.

The crystal packing of $(NH_4)_2C_2O_4 \cdot H_2O_2$ shows that there are tunnels of $H_2O_2$ molecules parallel to the shortest crystal axis ($c$ = 3.81 Å) (Pederson, 1972). Upon standing, this peroxide decomposes to $(NH_4)_2C_2O_4 \cdot H_2O$, which has a similar crystal structure, and studies of this reaction using Weissenberg photography showed that the product crystal was ordered (Pederson, 1972).

We have reinvestigated this reduction (Lin and Perrier, 1979). Our studies show that this reaction is not a single-crystal-to-single-crystal reaction, but the product crystal is somewhat ordered since its diffraction pattern shows both powder lines and spots. Comparison of the reaction of

a crystal in a nitrogen stream to that of a crystal in an open container indicates that the reaction does not involve loss of $H_2O_2$ and addition of $H_2O$, since both crystals reacted to the same extent. However, further studies of this reaction using TGA are planned.

We have also investigated the reaction of the potassium and rubidium salts, $K_2C_2O_4 \cdot H_2O_2$ and $Rb_2C_2O_4 \cdot H_2O_2$. These salts react much more slowly than $(NH_4)_2C_2O_4 \cdot H_2O_2$. For example, the reaction of the ammonium salt is complete in 2 months at 25°C, while the reactions of the potassium and rubidium are complete in 10 hr at 70°C.

## XIII. Summary

In this chapter, reactions of solids with oxygen were reviewed. The important points illustrated in this chapter include:

1. Different crystal forms of a drug exhibit different oxygen reactivity.
2. The oxygen sensitivity of a drug in some cases decreases as the melting point increases.
3. Some solid-state oxidation reactions of crystal solvates require prior desolvation; stabilization of these compounds could thus be accomplished by preventing desolvation.
4. Solid-state oxidation reactions of drugs can be accelerated in high humidities. Thus stabilization of these compounds can be accomplished by storage under dry conditions.

## References

Adler, G. (1972). *Isr. J. Chem.* **10,** 563.
Akopyan, A. A., Avoyan, R. L., and Struchkov, Y. T. (1972). *J. Struct. Chem.* (*USSR, Engl. Trans.*) **3,** 576.
Baxter, J. G., and Robeson, C. D. (1942). *J. Amer. Chem. Soc.* **64,** 2407.
Beckwith, A. C. J. (1958). *Proc. Chem. Soc.*, 194.
Bhattacharayen, S. (1969). *J. Inst. Chem.* (*India*) **41,** 33.
Brandl, V. F., Rohnl, M., Zeehmeister, K., and Hoppe, W. (1971). *Acta Cryst.* **B27,** 1718.
Bremer, G., Roberts, F. E., Hoinowski, A., Budavari, J., Powell, B., Hinkley, D., and Schoenewaldt, E. (1969). *Angew. Chem. Int. Ed.* **8,** 975.
Bruckner, S., Calligaris, M., Nardin, G., and Randaccio, L. (1969). *Acta Cryst.* **B25,** 1671.
Canet, M. M., Mani, J. C., Farie, C., and Lerner, D. (1966). *C. R. Hebd. Seances Acad. Sci., Ser. C* **262,** 153.
Clay, R. J. (1979). Ph.D. Thesis, Purdue University, West Lafayette, Indiana.
Collman, J. P., Gagne, R. R., and Reed, C. A. (1974). *J. Am. Chem. Soc.* **96,** 2629.
DeIasi, R., Holt, S. L., and Post, B. (1971). *Inorg. Chem.* **10,** 1498.
Desvergne, J. P., and Thomas, J. M. (1975). *J. Chem. Soc., Perkin Trans. 2,* 584.

Desvergne, J. P., Bouas-Laurent, H., Blackburn, E. V., and Lapouyade, R. (1974). *Tetrahedron Lett.*, 947.
Dobrucki, R. (1971). *Farm. Pol.* **27,** 353.
Eble, T. E., and Garrett, E. R. (1954). *J. Am. Pharm. Assoc., Sci. Ed.* **43,** 536.
Emery, W. O., and Wright, C. D. (1954). *J. Am. Chem. Soc.* **43,** 2328.
Everhard, M. E., and Goodhart, F. W. (1963). *J. Pharm. Sci.* **52,** 281.
Funkelstein, E. I., Alekseev, E. V., and Kozlov, E. I. (1974). *Zh. Org. Khim.* **10,** 1027.
Garrett, E. R. (1954). *J. Am. Pharm. Assoc., Sci. Ed.* **43,** 539.
Garrett, E. R., and Eble, T. E. (1954). *J. Am. Pharm. Assoc., Sci. Ed.* **43,** 385.
Gilmour, H. S. A. (1963). *In* "Physics and Chemistry of the Organic Solid State" (D. Fox, M. M. Labes, and A. Weissberger, eds.), p. 329. Interscience Press, John Wiley and Sons, New York.
Guillory, J. K., and Higuchi, T. (1962). *J. Pharm. Sci.* **51,** 100.
Hakkesteegt, J. (1970). *Pharm. Weekbl.* **105,** 829.
Haleblian, J., and McCrone, W. C. (1969). *J. Pharm. Sci.* **58,** 911.
Hecker, E., and Schmidt, R. (1974). *Prog. Chem. Organic Natural Prod.* **31,** 377.
Henn, D. E., Williams, W. G., and Gibbons D. J. (1971). *J. Appl. Cryst.* **4,** 256.
Hochstrasser, R. M., and Porter, G. B. (1960). *Quart. Rev.* **14,** 146.
Hochstrasser, R. M. (1959). *Can. J. Chem.* **37,** 1123.
Hodgkin, D. C., Webster, M. S., and Dunitz, J. D. (1957). *Chem. Ind.*, 148.
Hoffmann, R., and Woodward, R. B. (1970). "The Conservation of Orbital Symmetry," pp. 52, 80, and references therein. Verlag Chemie, New York.
House, H. O. (1972). "Synthetic Reactions," 2nd ed., pp. 338–352 and references therein. W. A. Benjamin Inc., New York.
Iwamoto, K. (1935). *Bull. Chem. Soc. Jap.* **10,** 420.
Janzen, E. G., Johnston, F. J., and Ayers, C. L. (1967). *J. Am. Chem. Soc.* **89,** 1176.
Kanzawa, T., and Kotaku, S. (1953). *J. Pharm. Soc. Jap.* **73,** 1357.
Kasche, V., and Lindquist, L. (1964). *J. Phys. Chem.* **68,** 817.
Kautsky, H. (1939). *Trans. Faraday Soc.* **35,** 216.
Kekher, J., and Ark, P. A. (1949). *Antibiot. Chemother.* **9,** 327.
Keuning, K. J. (1965). *Pharm. Weekbl.* **100,** 889.
Kitaigorodskii, A. J. (1973). "Molecular Crystals and Liquid Crystals," p. 168. Academic Press, New York.
Knobler, C., Romers, C., Braun, P. B., and Hornstra, J. (1972). *Acta Cryst.* **B28,** 2097.
Kuramoto, R., Lachman, L., and Cooper, J. (1958). *J. Am. Pharm. Assoc., Sci. Ed.* **47,** 175.
Lachman, L., Swartz, C. J., Urbanyi, T., and Cooper, J. (1960). *J. Am. Pharm. Assoc., Sci. Ed.* **49,** 165.
Lerner, D., Mani, J. C., and Mousseren-Canet, M. (1970). *Bull. Soc. Chim., Fr.*, 1968.
Leszczynska, B., Halina, S., and Krowczynska, H. (1970). *Cesk. Farm.* **19,** 109.
Lewbart, M. L. (1969). *Nature (London)* **222,** 663.
Lin, C. T., and Byrn, S. R. (1976). *J. Am. Chem. Soc.* **98,** 4004.
Lin, C. T., Perrier, P., Clay, G. G., Sutton, P. A., and Byrn, S. R. (1982). *J. Org. Chem.*, **47,** 2978.
Lin, C. T., and Perrier, P. (1979). Unpublished results, Purdue University.
Martell, A. E., and Calvin, M. (1952). "Chemistry of the Metal Chelate Compounds," p. 336. Prentice-Hall, New York.
Miller, R. S., Curtin, D. Y., and Paul, I. C. (1971). *J. Am. Chem. Soc.* **93,** 2784.
Pederson, B. F. (1972). *Acta Cryst.* **B28,** 746.
Petterson, R. C., Birnbaum, G. I., Ferguson, G., Islam, K. M. S., and Sime, J. G. (1968). *J. Chem. Soc., B*, 980.

Pfoertner, K., and Weber, J. P. (1972). *Helv. Chim. Acta* **55,** 921.
Ressler, C. (1972). *J. Org. Chem.* **37,** 2933.
Rubin, S. H., DeRitter, E., and Johnson, J. B. (1976). *J. Pharm. Sci.* **65,** 963.
Schaefer, W. O., and Marsh, R. E. (1969). *Acta Cryst.* **B25,** 1675.
Scheffer, J. R., and Ouchi, M. D. (1970). *Tetrahedron Lett.,* 223.
Schmidt, R., and Hecker, E. (1975). *Cancer Res.* **35,** 1375.
Schmidt, G. N. J. (1971). *Puare Appl. Chem.* **27,** 647.
Stewart, B. A. (1978). M.S. Thesis, Purdue University.
Taylor, W. (1936). *Z. Kristallogr., Kristallgeom., Kristallphys., Kristallchem.* **93,** 151.
Tingstad, J. E., and Garrett, E. R. (1960). *J. Am. Pharm. Assoc.* **49,** 352.
Tschitschibabin, A. E. (1907). *Chem. Ber.* **40,** 3056.
United States Pharmacopeia, XX (1980), U.S. Pharmacopeial Convention, Inc., Rockville, Md. 20852
Usui, Y., Toh, K. I., and Loizuma, M. (1965). *Bull. Chem. Soc. Jap.* **38,** 1015.
Vogt, L. H., Jr., Faigebaum, H. M., and Wiberley, S. E. (1963). *Chem. Rev.* **63,** 269.
Wilk, I. J. (1975). *169th Nat. Mt. Am. Chem. Soc., Philadelphia,* April.
Weeks, C. M., and Duax, W. L. (1973). *Acta Cryst.,* **B29,** 2210.
Weeks, C. M., and Duax, W. L. (1976). *Acta Cryst.,* **B32,** 2819.
Wright, G. E., and Tang, T. Y. (1972). *J. Pharm. Sci.* **61,** 299.

# 7 Additions of Gases to Solids—Solid-State Hydrolyses

In this chapter, reactions of solids with gases are reviewed. The solid-state hydrolysis of aspirin is discussed in detail, as well as reactions of solids with ammonia, chlorine, and fluorine. These latter reactions provide models to guide future studies of solid–gas reactions.

## I. Reactions of Crystals with Ammonia Gas

Miller, Curtin, and Paul (1974) showed that crystals of many carboxylic acids react with ammonia gas to give ammonium salts ($RCOONH_4$). The acid crystals retain their original shape. These reactions are anisotropic as shown in Figure 1. In this reaction, ammonia reacts at different rates along different crystallographic directions of 4-chlorobenzoic acid. Figure 2 shows the crystal packing of 4-chlorobenzoic acid, and Figure 3 shows the crystal packing of 4-chlorobenzoic acid with respect to the Miller indices of the crystal faces. As seen in Figure 1, the ammonia gas does not react on the (100) face but instead reacts on the $(2\bar{1}0)$, $(1\bar{1}0)$, (001), and $(\bar{1}01)$ faces, and the reaction proceeds from these faces toward the center of the crystal.

This anisotropic behavior is explained in terms of the crystal packing of 4-chlorobenzoic acid. The ammonia gas reacts from the $(2\bar{1}0)$, $(1\bar{1}0)$,

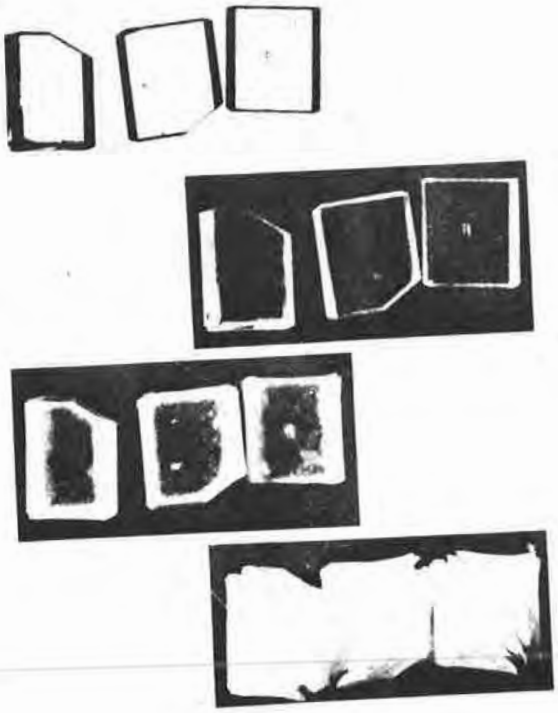

**FIGURE 1.** Reaction of a group of crystals of 4-chlorobenzoic acid with ammonia gas. The upper picture is with rear illumination before reaction. The next three are taken at 21, 100, and 1280 min of reaction with top illumination (Miller *et al.*, 1974). (Reprinted with permission from R. S. Miller, D. Y. Curtin, and I. C. Paul [1974]. Copyright 1974 American Chemical Society.)

(001), and ($\bar{1}$01) directions because penetration into the crystal from these faces allows the ammonia gas to be solvated by the carboxyl groups during penetration. On the other hand, penetration from the (100) face would require the polar gas to pass through alternate layers of nonpolar functionalities, as shown in the packing diagram (Figure 3).

Similarly, crystals of benzoic acid, 4-bromobenzoic acid, 4-nitrobenzoic acid, phthalic acid, adipic acid, 4-chlorobenzoic anhydride, and 4-bromobenzoic anhydride react with ammonia in an anisotropic manner. As with 4-chlorobenzoic acid, the behavior of these crystals can be explained in terms of crystal packing (Miller *et al.*, 1974).

In addition to these studies, some unique types of solid-state reactions involving ammonia gas have been observed. The reactions of carboxylic acids just discussed show that the ammonia gas penetrates the crystal from two directions. In principle it is possible to imagine cases where ammonia penetration would be allowed to penetrate along only one direc-

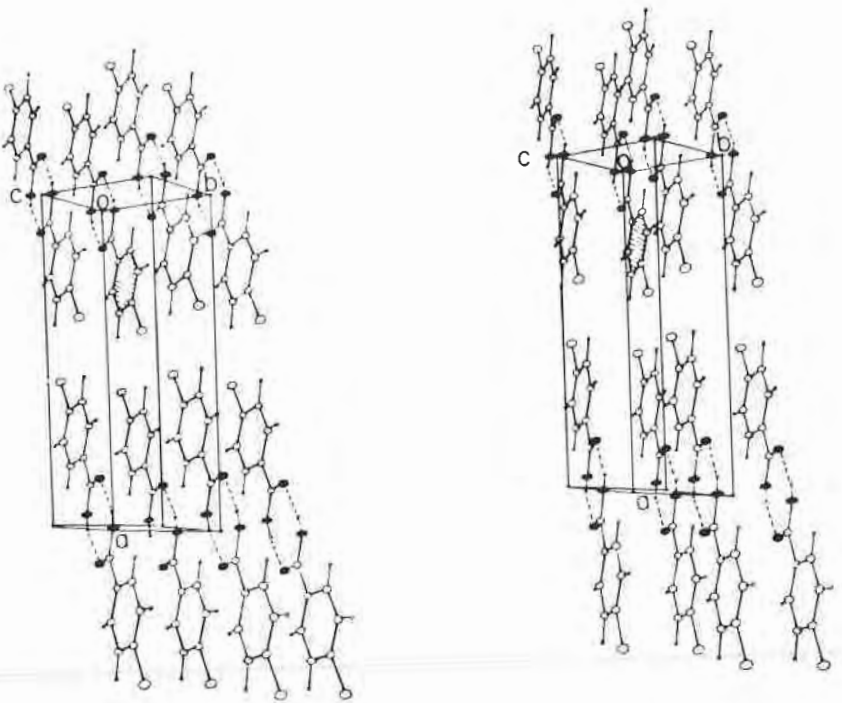


**FIGURE 2.** Stereo view of the crystal packing of 4-chlorobenzoic acid (Miller *et al.*, 1974). (Reprinted with permission from R. S. Miller, D. Y. Curtin, and I. C. Paul [1974]. Copyright 1974 American Chemical Society.)

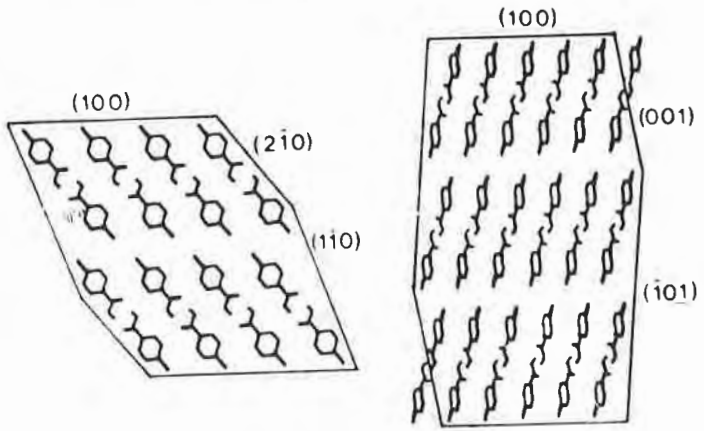


**FIGURE 3.** Drawings showing the crystal packing of 4-chlorobenzoic acid with respect to the developed crystal faces (Miller *et al.*, 1974). (Reprinted with permission from R. S. Miller, D. Y. Curtin, and I. C. Paul [1974]. Copyright 1974 American Chemical Society.)

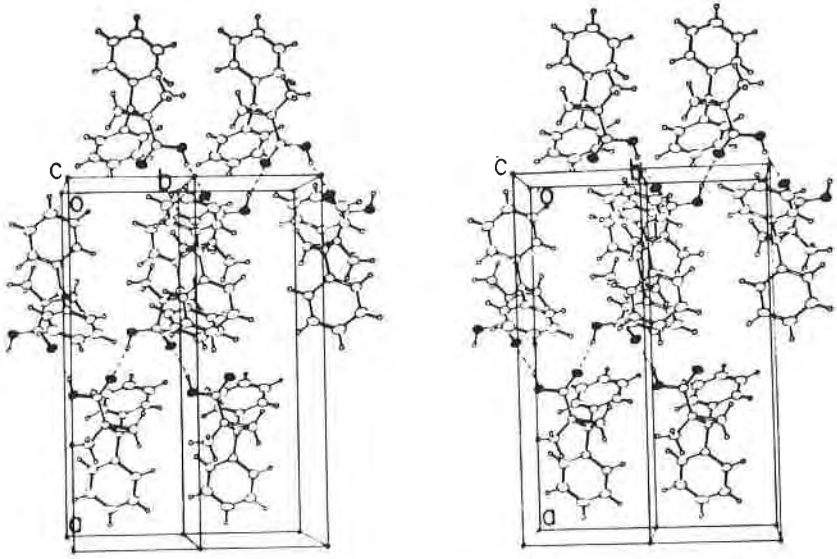


**FIGURE 4.** Stereoscopic view of the crystal packing of **1**. The (100) face is at the top, and the dark circles represent oxygen atoms (Lin *et al.*, 1974a). (Reprinted with permission from C. T. Lin, T. C. Paul, and D. Y. Curtin [1974a]. Copyright 1974 American Chemical Society.)

tion. Indeed, the carboxylic acid (**1**) has a packing arrangement (Figure 4)

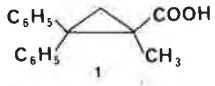


**1**

that provides tunnels of polar groups that should allow penetration along only one direction. Figure 5 shows that only reaction along this direction is observed. This reaction along the tunnel is closely related to the desolvation of organic crystalline solvates, which often desolvate anisotropically along the water tunnel direction.

In addition, reaction of solid optically active carboxylic acids with optically active amines can be used to distinguish between left-handed and right-handed crystals of an enantiomeric pair (Lin *et al.*, 1974b). Many enantiomers crystallize as mixtures of crystals that, taken individually, are either dextro- or levorotatory. This process has been termed spontaneous resolution. However, there is no way to accomplish this resolution if the dextro and levo crystals cannot be identified. While in a few cases the crystals can be separated using the Pasteur method, which involves separating the dextro and levo crystals on a microscope, many types of crystals cannot be distinguished and separated in this way. Lin, Curtin and Paul (1974b) found that they could distinguish between the (+) and (−) crystals of 2,2-diphenylcyclopropanecarboxylic acid, mandelic acid, and tartaric acid by reacting them with (+)-1-phenylethylamine. While it was

impossible to predict whether the (+) or (−) crystals would react faster with (+)-1-phenylethylamine, it is clear that this method provides a convenient procedure for separating the optical isomers of these crystals.

In a related study, the reaction of acenaphthylene-1-carboxylic acid (**2**) was investigated (Desvergne and Thomas, 1973). The reaction was aniso-

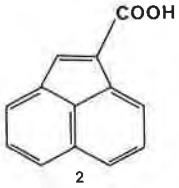


2

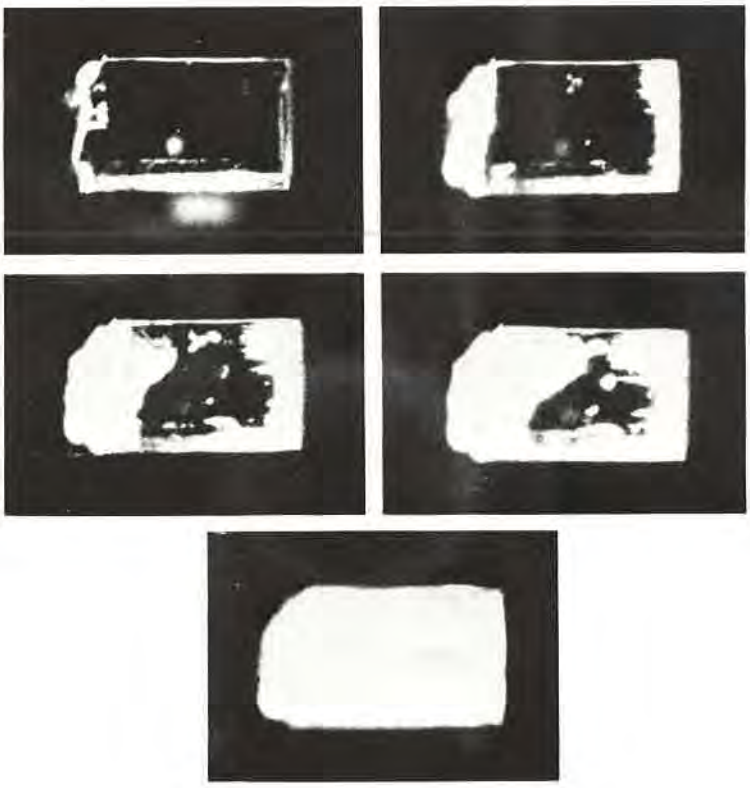

**FIGURE 5.** Reaction of a crystal of (R)-(+)-2,2-diphenyl-1-methylcyclopropane carboxylic acid with ammonia vapor. The *b* crystal axis is across, *c* vertical, and *a* into the plane of the paper (Lin *et al.*, 1974a). At the upper left, $t = 0$; upper right, $t = 1$ hr; center left, $t = 1.5$ hr; center right, $t = 2$ hr; bottom, $t = 24$ hr. The crystal was illuminated between crossed polarizing filters and was in the extinction position initially. (Reprinted with permission from C. T. Lin, I. C. Paul, and D. Y. Curtin [1974a]. Copyright 1974 American Chemical Society.)

tropic, fastest along the (010) and (100) directions and slowest along the (001) direction. Measurement of the effective area for entry of $NH_3$ along these directions gave 27.6 Å², 58 Å², and 23 Å² for the (100), (010), and (001) directions respectively. These areas are qualitatively consistent with the relative rates of reaction. In addition, it was found that the reaction could occur from the (001) direction in the presence of mechanically induced defects (Desvergne and Thomas, 1973).

In addition to the reactions of solid carboxylic acids with ammonia, ammonia gas can cause elimination of bromine from solid dibromo compounds. For example, solid 2,3-dibromo-1,2-dicyanobutane (**3**) reacts with gaseous ammonia to give dienes **4, 5,** and **6** (Friedman *et al.*, 1972, 1975).

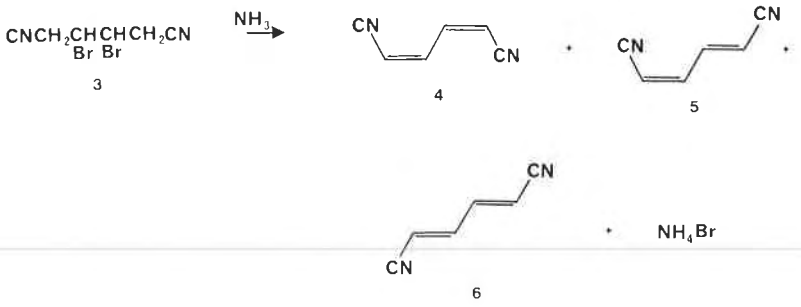


## II. Rates of Reaction of Crystalline Carboxylic Acids with Ammonia Gas

Miller, Curtin, and Paul (1974) have studied the reactions of carboxylic acid crystals with ammonia gas at constant pressure. Attempts were made to fit the rate data to three theoretical rate equations (In these equations, $w$ is weight, $M$ is the mole fraction of reactant remaining, $t$ is the time, and $k$ is the rate constant.)

1. *Three-Dimensional Diffusion.* If it is assumed that a single particle is reacting at a rate proportional to the surface area of the remaining reactant and that the reaction begins at the surface and moves inward, then:

$$-\frac{dw}{dt} = kw^{2/3}$$

and

$$M^{1/3} = 1 - k_{2/3}t \qquad (1)$$

2. *Two-Dimensional Diffusion.* If it is assumed that only the sides of the crystal are reactive and that no reaction occurs on the top or bottom faces, then:

$$-\frac{dw}{dt} = kw^{1/2}$$

and

$$M^{1/2} = 1 - k_{1/2}t \tag{2}$$

3. *First-Order Reaction.* If a mixture of particles of varying size are reacting, then the kinetic order depends on the distribution law, and certain distribution laws give the well-known first-order equation:

$$M = e^{-k_1 t} \tag{3}$$

For reference, the reader should note that these three equations correspond to Eqs. (4), (5), and (12) of Chapter 3.

Attempts to fit the data to Eqs. (1), (2), and (3) showed that plots of $M^{1/3}$ versus $t$ or $M^{1/2}$ versus $t$ gave better straight lines than plots of the first-order equation ln $M$ versus $t$. The plot of $M^{1/2}$ versus $t$ gave the best fit to the data. However, a definitive conclusion among these alternatives is not possible, particularly if data is collected for the first 50% of the reaction. This result is completely consistent with the results of studies of the rate of desolvation of crystal hydrates (Perrier, 1980). In these studies, the observed data was found to fit several rate equations and a definitive conclusion was not possible. Because of the problems of finding the proper rate equation Miller, Curtin, and Paul (1974) reported the relative rates of several crystalline acids with ammonia gas as shown in Table I.

It is clear from Table I that the rate of reaction of the acid does not correlate with its acidity, crystal density, or melting point. (Both crystal

**TABLE I**

*Relative Rates of Reaction of Crystalline Acids with Ammonia Gas*[a]

| Acid | Melting point (°C) | Density (g/cm³) | Relative rates | | Relative $K_a$ in water |
|---|---|---|---|---|---|
| | | | Single crystal | Powder | |
| 2-Naphthoic | 186 | 1.32 | 1.0 | 1.0 | 1.9 |
| 4-Nitrobenzoic | 242 | 1.60 | 1.0 | 0.6 | 10.0 |
| Phthalic | 210 | 1.58 | 2.6 | 2.0 | 35 |
| 1-Naphthol | 96 | 1.29 | | 2.0(calc.) | $10^{-5}$ |
| 4-Bromobenzoic | 255 | 1.86 | 3.5 | | 2.9 |
| α-*trans*-Cinnamic | 136 | 1.24 | 4.2 | 3.0 | 1.0 |
| Benzoic | 122 | 1.32 | 3.8 | 2.6 | 1.7 |
| 4-Chlorobenzoic | 243 | 1.54 | 9 | 25.0 | 2.8 |
| Ammonium hydrogen 4-Chlorobenzoate | | 1.49 | 17 | 18 | |

[a] From Miller *et al.* (1974). (Reprinted with permission from R. S. Miller, D. Y. Curtin, and I. C. Paul [1974]. Copyright 1974 American Chemical Society.)

density and melting point are rough measures of the crystal stability and crystal packing efficiency.) This lack of correlation is consistent with other studies where small changes in structure have produced large changes in rate. For example, the oxidation of tetramethylrubrene is much faster than rubrene (see Chapter 7), and the oxidation of one crystal form of hydrocortisone is much faster than three other crystal forms. It is interesting to note that the rates of reaction of these acids are nearly equal except for the last two entries in the table. It is also noteworthy that powders produced by grinding are of approximately the same reactivity as crystals, even though they are expected to contain many more defects.

## III. Reactions of Solids with $Cl_2$ or $Br_2$

A large number of phenols can be chlorinated in the solid state. The reaction is usually carried out by exposing the crystalline phenol to chlorine under anhydrous conditions (Lamartine and Perrin, 1974). It is proposed that the reaction proceeds via an addition elimination mechanism, where chlorine is added and then both a chloride ion and a proton are eliminated (Scheme I). Table II lists the starting materials and products of many of these reactions.

In addition to the reactants and products shown in Table II, the reaction of solid 2-methylphenol with chlorine gas was studied (Lamartine and Champtier, 1974). The products of this reaction were 2-methyl-4-chlorophenol and 2-methyl-6-chlorophenol. The ratio of the 4-chloro to 6-chloro product depended on which face of the crystal is exposed to gaseous

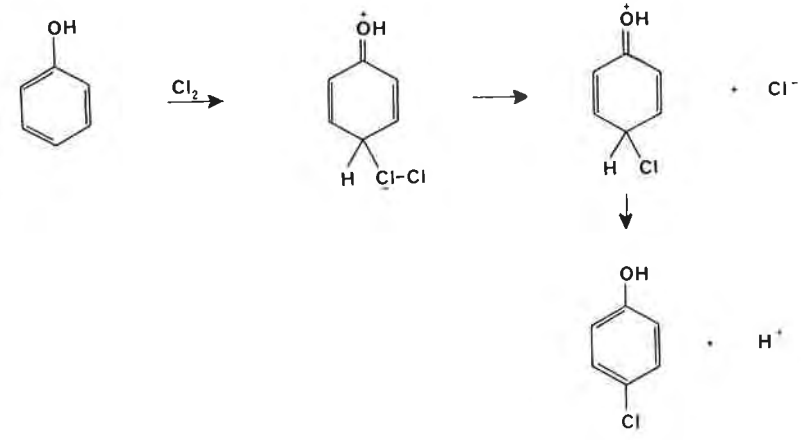


Scheme I

**TABLE II**

*Starting Materials and Products of the Chlorination of Alkylphenols in the Solid State*[a]

| Starting material | Product | Yield (%) |
|---|---|---|
| Phenol | 2,4,6-Trichlorophenol | 97 |
| | 2,4-Dichlorophenol | 3 |
| 4-Methylphenol | 2-Chloro-4-methylphenol | 20 |
| | 2,6-Dichloro-4-methylphenol | 80 |
| 4-Ethylphenol | 2-Chloro-4-ethylphenol | 30 |
| | 2,6-Dichloro-4-ethylphenol | 70 |
| 4-Isopropylphenol | 2-Chloro-4-isopropylphenol | 30 |
| | 2,6-Dichloro-4-isopropylphenol | 65 |
| | Chlorocyclohexanedione | 5 |
| 4-*tert*-Butylphenol | 1,2,4,6-Tetrachloro-4-*tert*-butyl-2,5-cyclohexanedione | 32 |
| | 2,6-Dichloro-4-*tert*-butylphenol | 68 |
| 2,6-Dimethylphenol | Chlorophenols | 55 |
| | *o*-Chlorocyclohexanediones | 25 |
| | Chlorocyclohexenones | 20 |
| 3,5-Dimethylphenol | 2,4,6-Trichloro-3,5-dimethylphenol | 20 |
| | 2,4-Dichloro-3,5-dimethylphenol | 78 |
| | 4-Chloro-3,5-dimethylphenol | 2 |
| 3-Methyl-5-ethylphenol | 2,4,6-Trichloro-3-methyl-5-ethylphenol | 98 |
| | 2,4-Dichloro-3-methyl-5-ethylphenol | 2 |
| 3,5-Diethylphenol | 2,4,6-Trichloro-3,5-diethylphenol | 80 |
| | 2,4-Dichloro-3,5-diethylphenol | 20 |
| 3-Methyl-5-isopropylphenol | 2,4,6-Trichloro-3-methyl-5-isopropylphenol | 94 |
| | 2,4,4,6-Tetrachloro-3-methyl-5-isopropyl-2,5-cyclohexanedienone | 6 |
| 3-Methyl-2-isopropylphenol | 6-Chloro-3-methyl-2-isopropylphenol | 5 |
| | 4,6-Dichloro-3-methyl-2-isopropylphenol | 95 |
| 2-Methyl-3-isopropylphenol | 6-Chloro-2-methyl-3-isopropylphenol | 8 |
| | 4,6-Dichloro-2-methyl-3-isopropylphenol | 92 |
| 3,5-Diisopropylphenol | 2,4,6-Trichloro-3,5-diisopropylphenol | 73 |
| | 2,4-Dichloro-3,5-diisopropylphenol | 4 |
| | 2,4,4,6-Tetrachloro-3,5-diisopropyl-2,5-cyclohexanedione | 23 |
| 2,6-Di-*tert*-butylphenol | 4-Chloro-2,6-di-*tert*-butylphenol | 45 |
| | 4-Chloro-2,6-di-*tert*-butyl-2,5-cyclohexanedienone | 20 |
| | 4,6-Dichloro-2,6-di-*tert*-butyl-2,4-cyclohexanedione | 35 |
| 2,5-Di-*tert*-butylphenol | Chlorophenols | 40 |
| | 4,4,6-Trichloro-2,5-di-*tert*-butyl-2,5-cyclohexanedione | — |
| | 4,4,6-Trichloro-2,5-di-*tert*-butyl-2,4-cyclohexanedione | 60 |
| | 2,4,6-Trichloro-2,5-di-*tert*-butyl-3,5-cyclohexanedienone | — |

**TABLE II** (*continued*)

| Starting material | Product | Yield (%) |
|---|---|---|
| 2,4-Di-*tert*-butylphenol | Chlorophenols | 37 |
| | 4,6-Dichloro-2,4-di-*tert*-butyl-2,5-cyclohexanedione | — |
| 3,5-Di-*tert*-butylphenol | Chlorophenols | 37 |
| | 2,4,4-Trichloro-3,5-di-*tert*-butyl-2,5-cyclohexanedione | — |
| | 2,4,4,6-Tetrachloro-3,5-di-*tert*-butyl-2,5-cyclohexanedienone | 63 |
| 2,4,6-Trimethylphenol | Chlorocyclohexenones | 30 |
| 3,4,5-Trimethylphenol | Chlorocyclohexenones | 40 |
| 4-Methyl-3,5-diisopropyl phenol | Chlorophenols | 90 |
| | Chlorocyclohexadienones | 10 |
| 4-Methyl-2,5-diisopropyl-phenol | Chlorophenols | 85 |
| | Chlorocyclohexadienones | 15 |
| 2,6-Dimethyl-4-*tert*-butyl-phenol | 2,5,6-Trichloro-2,6-dimethyl-4-*tert*-butyl-3-cyclohexenone | 95 |
| 4-Methyl-2,6-di-*tert*-butyl-phenol | 4-Chloro-4-methyl-2,6-di-*tert*-butyl-2,5-cyclohexadienone | 47 |
| 2,4,6-Triisopropylphenol | Chlorocyclohexenone | 40 |
| | Chlorocyclohexadienone | 60 |
| 2,4,6-Tri-*tert*-butylphenol | 4-Chloro-2,4,6-tri-*tert*-butyl-2,5-cyclohexadienone | 92 |

[a] Data from Lamartine and Perrin (1974).

chlorine (Lamartine and Champtier, 1974). This is an interesting result, indicating that these reactions are true solid–gas reactions. In addition, it suggests that the products of a solid–gas reaction can be controlled by controlling the face exposed to the gas. This control may result from anisotropic migration of the reactive gas into the crystal along a direction nearly perpendicular to the exposed face. The anisotropic migration is probably controlled by crystal packing.

Solid $C_6H_5ONa$, $C_6H_5OK$, $C_6H_5ORb$, $(C_6H_5O)_2Mg$, $(C_6H_5O)_3Al$, $(C_6H_5O)_3Ga$, $(C_6H_5O)_3In$, and $(C_6H_5O)_4Ti$ all react with gaseous chlorine to give quantitative yields of chlorinated products. The *ortho* to *para* ratio of the products depends upon the cation as well as the crystal structure (Vincent-Falquet-Berny and Lamartine, 1975).

Solid-state brominations are also known. For example, powdered samples of the olefins **7** and **8** reacted with bromine in light to give addition products **9** and **10**, respectively (Naae, 1977).

In addition, several asymmetric halogenations have been performed

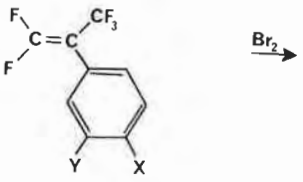

7 X=COOH Y=H
8 X=H Y=COOH

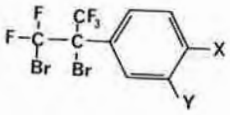

9
10

(Penzien and Schmidt, 1969). In these reactions, the chirality of the crystals provides the sole asymmetric influence. Reaction of a single crystal of 4,4′-dimethylchalcone (**11**) (which crystallizes in the acentric space group

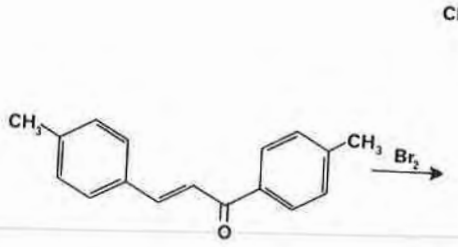

11

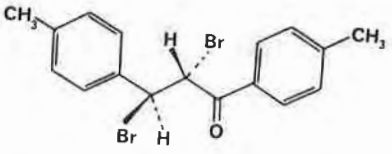

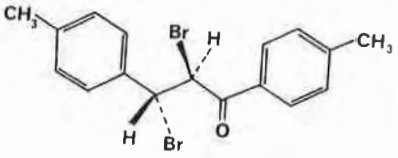

$P2_12_12_1$) with bromine vapor yields one of the enantiomeric erythro dibromides in 6% excess over the other (Penzien and Schmidt, 1969; Hadjoudis *et al.*, 1972). Since a given crystal of **11** contains either *d* or *l* isomers, some crystals give an excess of the (+) dibromide while others give the (−) dibromide. A more recent study has reported optical yields of nearly 20% for this reaction (Green and Lahav, 1975). Other halogens such as chlorine also react with **11** to give optically active products. Unfortunately, brominations of other optically active crystals did not always yield optically active products (Green and Lahav, 1975), perhaps because of a competing solution reaction in pools of condensed bromine.

## IV. Solid-State Hydrolyses

In this section the reactions of solids with water vapor are discussed. It is important to note that because of the relatively low boiling point of

water and the possibility of condensation it is impossible to prove that these reactions are true solid–gas reactions.

## A. ASPIRIN HYDROLYSIS

Reaction of solids with water vapor is an important reaction in the pharmaceutical industry. For example, the degradation of numerous tablets and powders is known to accelerate when exposed to high humidities. This acceleration may be due to a solution reaction occurring in an adsorbed moisture layer as proposed for dialuric acid.

The hydrolysis of solid aspirin (**12**) has been studied in the presence of moisture at temperatures ranging from 50° to 80°C (Leeson and Mattocks,


12 13

1958). As the humidity increases, the rate of reaction increases. The kinetics of this reaction were treated in terms of a solution reaction in which water is adsorbed onto the surface of the aspirin, with the amount of water adsorbed assumed to be proportional to the vapor pressure of the water. However, the reliability of these kinetic studies is questionable since a later study shows that sublimation of salicylic acid from a cellulose-coated aspirin tablet causes appreciable errors in measurement of percent decomposition (Gore *et al.*, 1968).

The observation of sublimed salicylic acid (**13**) on the surface of cellulose-coated aspirin tablets is also difficult to interpret in terms of a solution reaction on the surface of the solid, since it is unlikely that salicylic acid (**13**) would sublime out of a water solution. On the other hand, it is possible that salicylic acid crystallizes out of a water solution and then sublimes.

It is quite likely that if the hydrolysis has proceeded rapidly the acetic acid produced will be unable to evaporate and the reaction will proceed in an acetic acid solution. The vapor pressure of acetic acid is 100 mm at 63°C, indicating the relatively low volatility of this acid.

The eutectic point of mixtures of aspirin (mp 143°–144°C) and salicylic acid (mp 157°–159°C) has not been accurately determined, but aspirin crystals containing 60.0, 23.9, 17.7, and 1.3% salicylic acid had melting points of 115°, 115°, 114°, and 136.6°C, respectively, indicating that the eutectic point is probably much greater than 80°C and thus ruling out the possiblity of reaction in a melt of these compounds in the absence of acetic acid.

Studies of aspirin crystals heated on a hot stage would perhaps provide a definitive solution to this problem. Preliminary studies of aspirin crystals grown from benzene and heated at 95°, 87°, and 68°C on a hot stage in air showed that the edges of the crystals softened and liquid appeared after a few minutes, 24 hr and 48 hr, respectively. However, the crystals did not melt. These observations substantiate the suggestion that the hydrolysis of aspirin occurs in solution at least at high temperature. It is possible that the liquefaction results because acetic acid does not evaporate rapidly enough.

The reaction of aspirin with amines has been studied in our laboratory as a model for aspirin–water reactions. Reaction of aspirin with hexamethylenetetraamine was the best behaved. Hexamethylenetetraamine is a solid with substantial volatility. When crystals of hexamethylenetetramine and crystals of several habits of aspirin were placed in a sealed cell, the aspirin crystals reacted with the amine gas. The aspirin crystals obtained from hexane reacted fastest, as shown in Figure 6. Further work is required to adequately explain this behavior; however, the greater reactivity of crystals obtained from hexane may be related to either the greater reactivity of the large crystal face on the crystal obtained from hexane, to the greater number of defects in the hexane-grown crystals (Mitchell *et al.*, 1972; Bauer and Voege, 1972), or to a greater proportion of salicylic acid in crystals grown from hexane (Mulley *et al.*, 1971). The idea of greater reactivity is an attractive explanation for this behavior. If the crystals from hexane belonged to a crystal habit in which the large face was the face providing the most access of a gas to the carboxyl groups while the crystals from other habits had a smaller reactive face, then the crystals from hexane would be the most reactive. As mentioned, further work is required to confirm or refute this explanation.

Excipients, antacids, or granulating agents accelerated the decomposition of aspirin, apparently because of solid–solid reactions or the presence of moisture. A study was made of the effect of antacids on the decomposition of aspirin. It was found that in the presence of some solid antacids such as calcium carbonate, aspirin was 4.4% decomposed after 1 year, while in the presence of others such as sodium bicarbonate there was complete decomposition in 44 weeks (Bandelin and Malesh, 1958). Diluents also affected the stability of aspirin tablets. Cellulose and calcium sulfate conferred more stability on the tablets than did mannitol–starch or amylase. The decomposition of aspirin in the presence of these diluents could be related to the amount of moisture sorption and to the tablet hardness (Lee *et al.*, 1965).

A comparison of aspirin decomposition in suspensions and in tablets in the presence of diluents and antacids showed that the rates of decomposition were nearly the same (Maulding *et al.*, 1969). Of the compounds

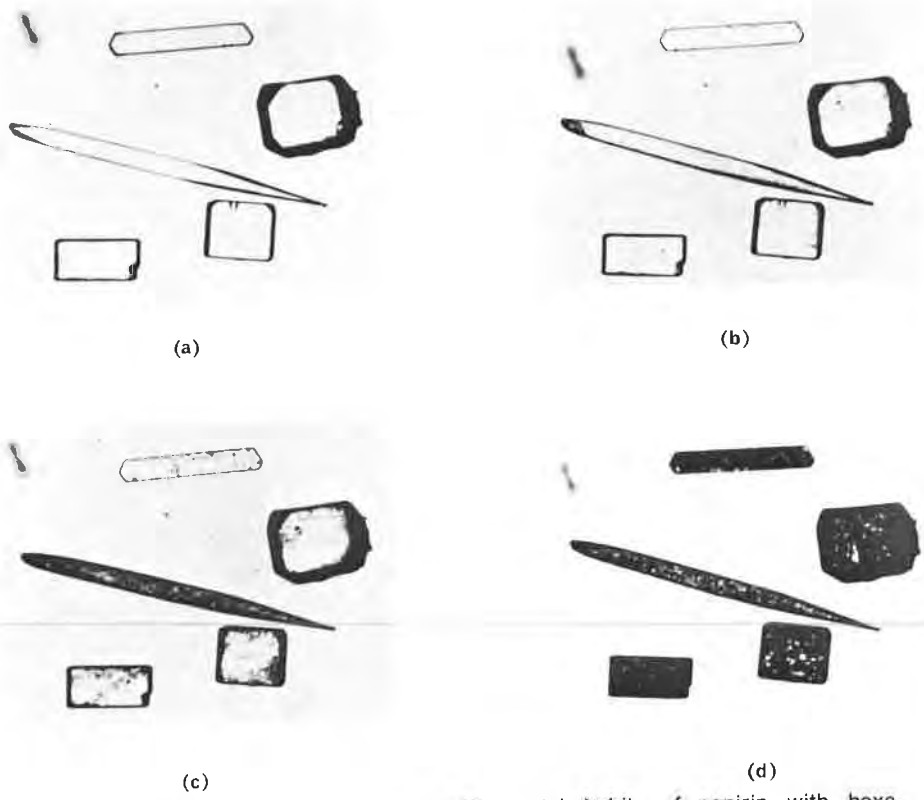


**FIGURE 6.** Reaction of five different crystal habits of aspirin with hexamethylenetetramine vapor. The times of reaction are: (*a*) 0 hr; (*b*) 3 hr; (*c*) 5 hr; (*d*) 24 hr. The crystal habit at the top was obtained from benzene. The long crystal habit in the middle on the left side was obtained from hexane. The crystal on the middle right was obtained from acetone. The crystal on the bottom left was obtained from ethanol. the crystal habit on the bottom right was obtained from chloroform.

studied, hexanoic acid conferred the most stability to aspirin and magnesium trisilicate the least.

Tablet mixtures containing aspirin and drugs with easily acylated functionalities react to give acyl compounds and salicylic acid. For example, mixtures of phenylephrine hydrochloride and aspirin contained 80% of acylated phenylephrine after 34 days at 70°C (Troup and Mitchner, 1964). A mixture of starch and magnesium stearate slowed this acylation to about 1% after 34 days, while magnesium stearate without starch caused complete decomposition after 16 days. Some diacylated product was also obtained. This reaction may proceed by direct acylation.

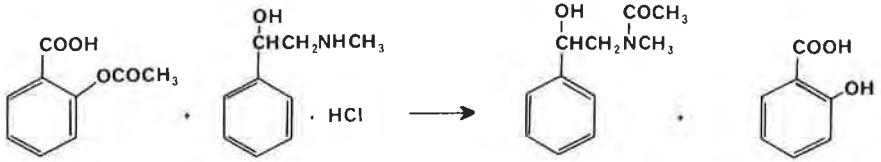


14

Similarly, tablets containing aspirin and codeine (**15**) or aspirin and acetaminophen (**17**) also yielded acylated drugs upon heating (Koshy *et al.*, 1967; Jacobs *et al.*, 1967).

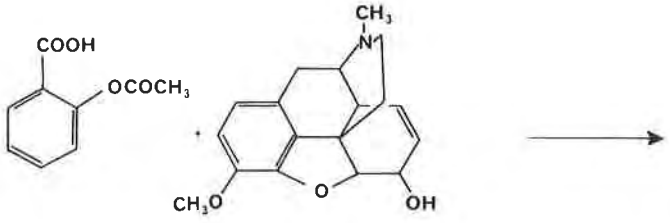


15

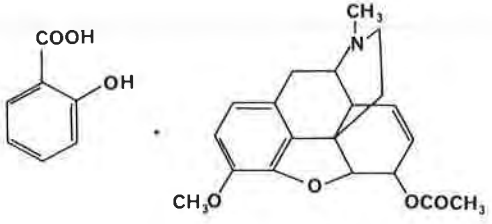


16

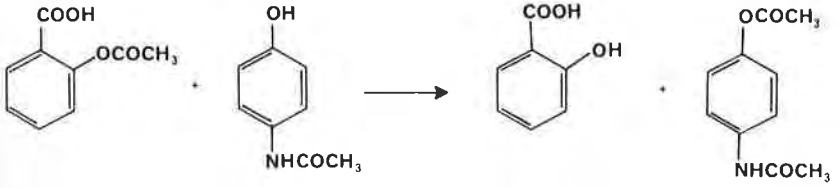


17

As a model for drug–excipient reactions and other solid–solid reactions, we have studied the reaction of *p*-aminosalicylic acid hydrochloride with sodium carbonate. The reaction proceeds anisotropically from the point when the two crystals touch. This reaction is discussed in detail in Chapter 12.

## B. NITRAZEPAM HYDROLYSIS

Nitrazepam (**18**) when mixed with microcrystalline cellulose rearranges to products **19** and **20**. Both these reactions require the presence of mois-

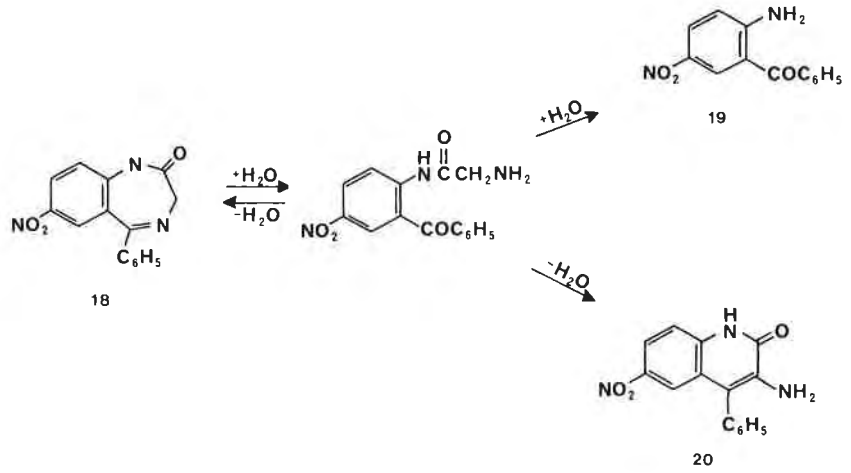


ture (Genton and Kesselring, 1977). The rate of this reaction was determined at four temperatures and six relative humidities, separating **18**, **19**, and **20** on TLC plates and scanning these plates (using diffuse reflectance spectroscopy) to quantitate the amounts of **18**, **19**, and **20**. The decomposition data was analyzed in terms of two pseudo-first-order parallel reactions where $k_1$ is the rate constant for formation of **19** and $k_2$

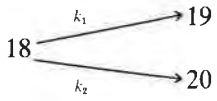


is the rate constant for the formation of 20. In addition, $K$ is defined as $k_1 + k_2$ and is the decomposition constant for **18**. Attempts were then made to mathematically relate $K$ to the temperature and the relative humidity. The term log $K$ could be fitted to a three-parameter regression equation [Eq. (1)] with terms depending on temperature and relative humidity.

$$\log K = 12.738 - 4.3804 \times 10^3\, T^{-1} + 0.03877(\%\ \text{relative humidity}) \quad (1)$$

The degradation of nitrazepam fits a kinetic equation that differs in form from that of aspirin. In fact, the decomposition of nitrazepam does not follow a sigmoid decomposition curve as aspirin does.

## C. SOLID-STATE HYDROLYSIS OF 1-METHOXY-1,2-BENZIODOXOLIN-3-ONE

The methoxyiodo compound **21** crystallizes in two polymorphs ($\alpha$ and $\beta$). The conformation of **21** in the two forms is identical, and the crystal

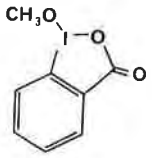


**21**

packing of these forms in shown in Figures 7 and 8 (Etter, 1976). The $\beta$ form can be converted to the $\alpha$ form in a solution-mediated phase trans-

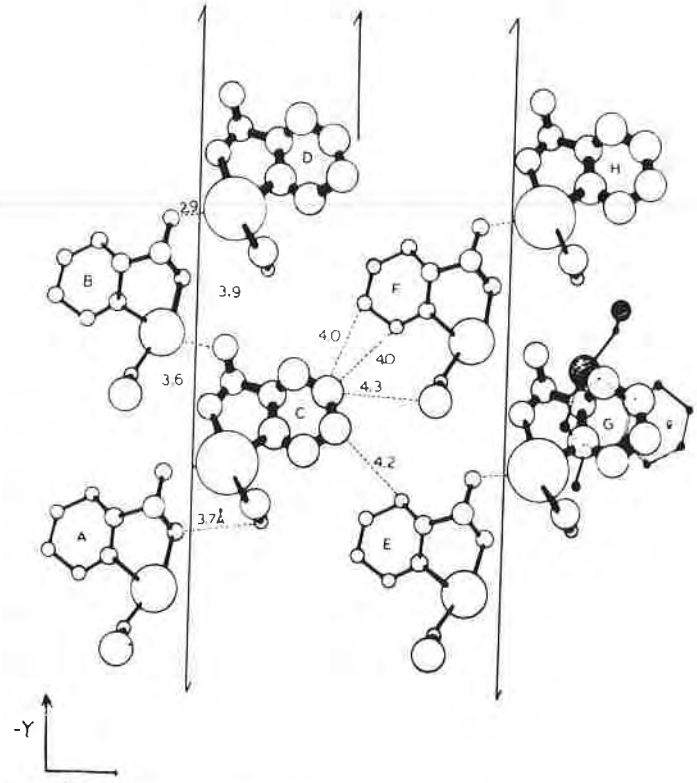


**FIGURE 7.** The crystal packing of the $\beta$ form of the methoxyiodo compound **11**, viewed along (100) (Etter, 1976). (Reprinted with permission from M. C. Etter [1976]. Copyright 1976 American Chemical Society.)

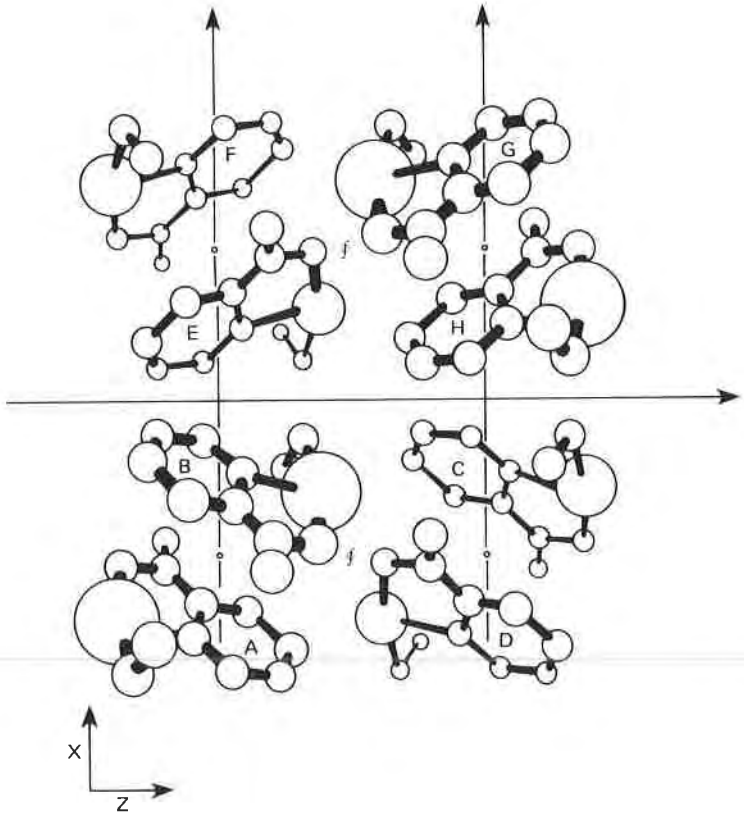


**FIGURE 8.** The crystal packing of the $\alpha$ form of the methoxyiodo compound **11**, viewed along (010) (Etter, 1976). (Reprinted with permission from M. C. Etter [1976]. Copyright 1976 American Chemical Society.)

formation, showing that the $\alpha$ form is the most stable form. Both forms are hydrolyzed by water vapor in an apparent solid–gas reaction as shown in Scheme II.

Single crystals of the $\alpha$ form decompose slowly at room temperatures and humidities, showing a loss of transparency and a generally speckled appearance after several months. In contrast, crystals of the $\beta$ form are hydrolyzed under similar conditions in a week or two. In this case, the less stable of the two polymorphs has the greater chemical reactivity. In some cases the hydrolysis reaction produced product crystals with a preferred crystallographic orientation, while in other cases amorphous crystals were produced.

The fact that different polymorphs had different rates of reaction with water vapor strongly argues that this reaction is a true solid-state reaction.

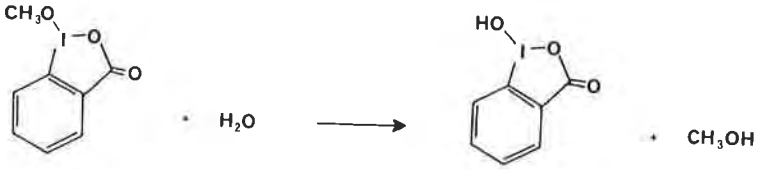

## V. Summary

This chapter has reviewed reactions of gases with solids with particular emphasis on reactions of solids with ammonia and water vapor. The following statements summarize the important conclusions and implications of this chapter.

1. Reactions of crystals with gases are sometimes (but not always) controlled by crystal packing.
2. The rates of reaction of crystals of acids with ammonia vapor could not be correlated with acid dissociation constant, crystal density, or melting point.
3. The rates of reaction of crystals with gases are dependent on a complex set of factors including temperature, gas vapor pressure, crystal-packing defects, and physical properties of the product crystal.
4. Stabilization of pharmaceuticals susceptible to hydrolysis by atmospheric moisture can probably best be accomplished by packaging under an inert gas, use of desiccants, or using an impermeable coating.

## References

Bandelin, F. J., and Malesh, W. (1958). *J. Am. Pharm. Assoc., Pract. Ed.* **19,** 152.
Bauer, K., and Voege, H. (1972). *Pharm. Ind.* **34,** 960.
Desvergne, J. P., and Thomas, J. M. (1973). *Chem. Phys. Lett.* **23,** 343.
Etter, M. C. (1976). *J. Am. Chem. Soc.* **98,** 5326.
Friedman, G., Gati, E., Lahav, M., Rabinovich, D., and Shakked, Z. (1975). *J. Chem. Soc., Chem. Commun.*, 491.
Friedman, G., Cohen, C., Wolff, D., and Schmidt, G. M. J. (1972). *Isr. J. Chem.* **10,** 559.
Genton, D., and Kesselring, U. W. (1977). *J. Pharm. Sci.* **66,** 676.
Gore, A. Y., Naik, K. B., Kildsig, D. O., Peck, G. E., Smolen, V. F., and Banker, G. S. (1968). *J. Pharm. Sci.* **57,** 1850.
Green, B. S., and Lahav, M. (1975). *J. Mol. Evol.* **6,** 99.
Hadjoudis, E., Kariv, E., and Schmidt, G. M. J. (1972). *J. Chem. Soc., Perkin Trans. 2*, 1056.

Jacobs, A. L., Dilatush, A. E., Weinstein, S., and Windheuser, J. J. (1966). *J. Pharm. Sci.* **55,** 893.
Koshy, K. T., Troup, A. E., Duvall, R. N., Conwell, R. C., and Shankle, L. L. (1967). *J. Pharm. Sci.* **56,** 1117.
Lamartine, R., and Champtier, G. (1974). *C.R. Acad. Sci., Paris, Ser. C* **279,** 429.
Lamartine, R., and Perrin, R. (1974). *J. Org. Chem.* **39,** 1744.
Leeson, L. J., and Mattocks, A. M. (1958). *J. Am. Pharm. Assoc.* **47,** 330.
Lee, S. T., Dekay, H. G., and Banker, G. S. (1965). *J. Pharm. Sci.* **54,** 1153.
Lin, C. T., Paul, I. C., and Curtin, D. Y. (1974a). *J. Am. Chem. Soc.* **96,** 3699.
Lin, C. T., Curtin, D. Y., and Paul, I. C. (1974b). *J. Am. Chem. Soc.* **96,** 6199.
Maulding, H. V., Zoglio, M. A., Pigois, F. E., and Wagner, M. (1969). *J. Pharm. Sci.* **58,** 1359.
Miller, R. S., Curtin, D. Y., and Paul, I. C. (1974). *J. Am. Chem. Soc.* **96,** 6329, 6334, 6340.
Mitchell, A. G., Milaire, B. L., Saville, D. J., and Griffiths, R. V. (1972). *J. Pharm. Pharmacol.* **23,** 534.
Mulley, B. A., Rye, R. M., and Shaw, P. (1971). *J. Pharm. Pharmacol.* **23,** 902.
Naae, D. G. *J. Org. Chem.* **42,** 1780.
Penzien, K., and Schmidt, G. M. J. (1969). *Angew. Chem., Int. Ed.* **8,** 608.
Perrier, P. (1980). Unpublished results, Purdue University; see Chapter 6.
Troup, A. E., and Mitchner, H. (1964). *J. Pharm. Sci.* **53,** 375.
Vincet-Falquet-Berny, M. F., and Lamartine, R. (1975). *Bull. Soc. Chim. Fr.*

# 8 Solid-State Decomposition Reactions of the Type A(solid) → B(solid) + C (gas)

In this chapter, decomposition reactions of solids to produce another chemically different solid and a gas are discussed. In an earlier chapter, reactions that involve loss of solvent of crystallization have been reviewed. While such desolvation reactions are also of the type A (solid) → B (solid) + C (gas), their activation energy is often much smaller than the chemical reactions discussed in this chapter.

## I. Solid-State Dehydration of Hydroxyl Compounds

There are a large number of studies of the dehydration of hydroxyl compounds in solution and in the gas phase; however, relatively little is known about solid-state dehydrations. Those that are understood are discussed in this chapter. However, it is important to know more about solid-state dehydrations.

### A. DEHYDRATION OF HYDROXYTRIARYLMETHANOLS

Lewis, Curtin, and Paul have studied the reaction of *p*-hydroxytriarylmethanols **1a**, **1b**, and **1c** (Lewis *et al.*, 1979). These

triarylmethanols dehydrate to form the fuchsones **2** upon heating or irradiation. The crystal structures of **1a, 1b,** and **1c,** which are isostructural,

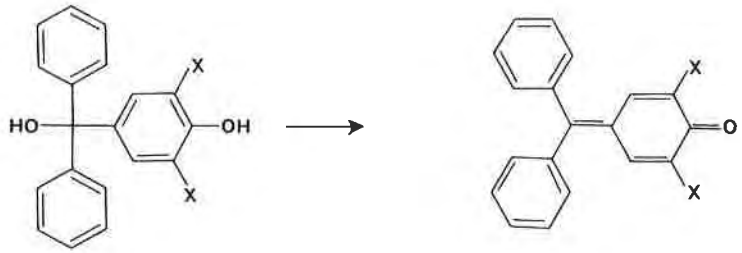


**1a** X = H
**1b** X = Br
**1c** X = $CH_3$

**2**

have been determined (Lewis *et al.,* 1979). The molecules of **1a**, **1b**, and **1c** are aligned in the solid state with the phenolic OH group hydrogen bonded to an alcoholic OH group of an adjacent molecule as shown in Figure 1. Thus these compounds constitute a series in which crystal packing aligns the molecules in a geometry favorable to reaction. Indeed, photomicrographic study of the reactions of crystals of **1c** showed a slight preference for reaction along the hydrogen-bonded chains. The reaction began by formation of a solid solution of the colored product in the parent crystal in triangular regions. Then cracks developed, and finally the product phase separated as the reaction moved through the crystal.

Comparative studies showed that crystals of **1b** reacted much faster than crystals of **1c**. The time required for 90% reaction of **1b** was 10 hr (at 110°C) versus 100 hr for **1c**. In solution, **1b** is about 10,000 times more acidic than **1c**, perhaps explaining the increased solid-state reactivity of **1b**. (However, in reactions of related crystals this argument may not apply. In addition, it should be noted that in an entirely different reaction, the reaction of solid acids with ammonia gas, the rate of reaction did not parallel the acidity of the acid.)

Crystals of **1b** or **1c** also reacted when irradiated with 254-nm light to form **2b** or **2c**. This reaction may again be due to an acidity effect, since solution photochemical studies showed that the first excited states of phenols are $10^6$ times more acidic than the ground state.

In a very interesting finding, it was shown that exposure of a part of a crystal of **1c** to ultraviolet light photonucleated the thermal dehydration process: the thermal reaction began in the exposed part and moved to the unexposed parts of the crystal.

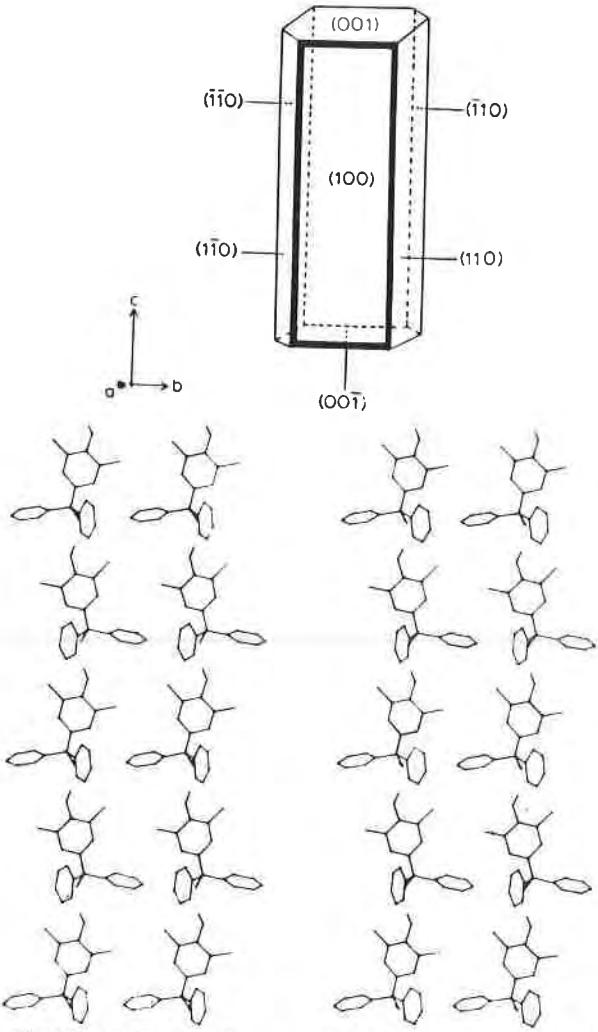


**FIGURE 1.** The upper drawing shows a crystal of the triarylmethanol **Ic** in habit I. The lower drawing shows a stereo view of the crystal packing of **Ic**, in the same orientation as the crystal above (Lewis *et al.*, 1979). (Reprinted with permission from T. W. Lewis, D. Y. Curtin, and I. C. Paul [1979]. Copyright 1979 American Chemical Society.)

## B. DEHYDRATION OF 2-HYDROXY-2-(β-BENZOYL-β-PHENYLHYDROZYL)INDANE-1,3-DIONE (3)

Crystals of the indanedione **3** dehydrate to form the indanetrione phenylhydrazone **4** upon heating (Lewis *et al.*, 1976). The crystal structure

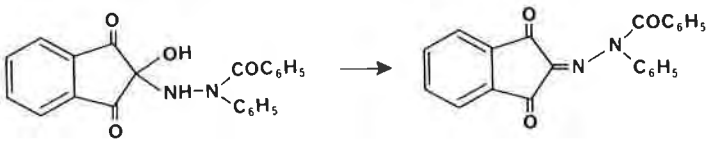

3 4

of **3** (Figure 2) showed that there was a chain of hydrogen-bonded molecules of **3** along the *b* axis. As might be expected, crystals of **3** dehydrated preferentially along this axis.

## C. DEHYDRATION OF HYDROXYARYLBENZODIHYDROFURANS

In 1906, Guyot reported that hydroxyarylbenzodihydrofurans (**5**) slowly lost water at room temperature to form **6** in solution and the solid

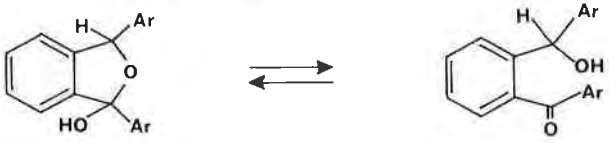

5A 5B

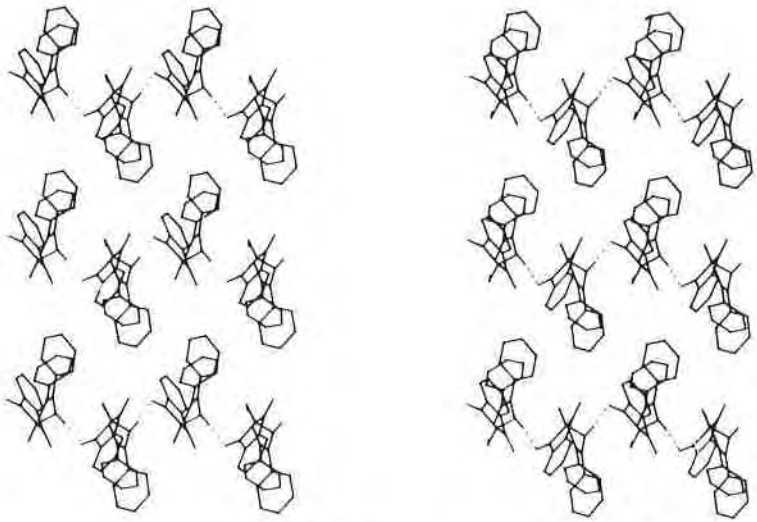

**FIGURE 2.** Stereo view of the crystal packing of the indanedione (**3**) as viewed perpendicular to the 001 layer. The preferred direction of reaction is shown (Lewis *et al.*, 1976).

state (Guyot and Vallette, 1906, 1911; Guyot and Catel, 1906). The dehydration reaction was accelerated by warming or addition of acid.

The hydroxyarylbenzodihydrofurans (**5**) can actually be viewed as ring-chain tautomers (**5A** ⇄ **5B**). While both **5A** and **5B** could conceivably

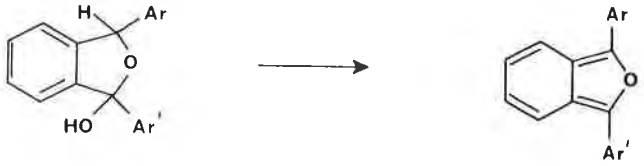


5 6

a $Ar = Ar' = C_6H_5$

b $Ar = C_6H_5$ $Ar' = p\text{-}C_6H_4CH_3$

c $Ar = p\text{-}C_6H_4CH_3$ $Ar' = p\text{-}C_6H_4NO_2$

d $Ar = Ar' = p\text{-}C_6H_4CH_3$

e $Ar = Ar' = CH_3$

f $Ar = p\text{-}C_6H_4NO_2$ $Ar' = p\text{-}C_6H_4CH_3$

dehydrate to form **6**, the dehydration of **5B** appears to be less likely since dehydration of **5B** would proceed through a high-energy carbene species. In addition, it should be noted that the formation of **6** from such a carbene would require a rearrangement of the addition product or carbene addition to oxygen. The NMR spectrum of **5** shows that the amount of **5B** in $CDCl_3$ is below detectable limits. Based on the mechanisms of the dehydration of alcohols catalyzed by either acids or bases (Konzinger, 1971), we suggest that the conversion of **5** to **6** probably proceeds via **5A** by the ionic or perhaps the concerted process.

While the stereochemistry of this elimination to form **6** has not been investigated, we suggest that the stereochemistry of the H and OH groups probably is less important in the 1,4-elimination than in 1,2-elimination reactions. The driving force for the dehydration of hydroxybenzodihydrofurans is the formation of a more conjugated system. (structure **6**).

In solution the dehydration of **5** readily takes place. However, in the solid state it is surprising that this dehydration occurs at room temperature, since in the solid the motion of atoms is restricted and the H and OH groups in a single molecule are rather far apart. Perhaps a unique type of crystal packing places these groups close together as in previous cases. Thus the solid-state reaction may not necessarily follow the same mechanism as the solution reaction but may instead be bimolecular. Further studies of this reaction are obviously needed.

## D. DEHYDRATION OF *N*-(*p*-CHLOROPHENYL)PHTHALANILIC ACID

Farmer and Lando (1974) have reported studies of the dehydration of solid *N*(*p*-chlorophenyl)phthalanilic acid (**7**) to form the phthalimide (**8**).

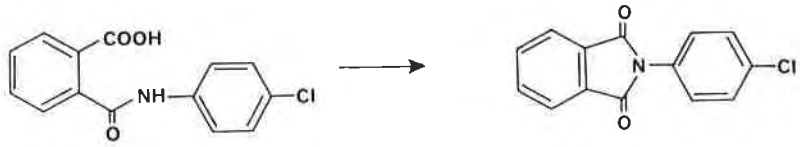


7 8

They reported that this reaction was topotactic. In addition, the reaction was suggested to proceed through the intermediate **9**.

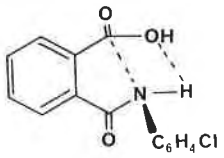


9

## E. DEHYDRATION OF TETRACYCLINES

Tetracycline antibiotics, including tetracycline (**10a**), chlortetracycline (**10b**), oxytetracycline (**10c**), and rolitetracycline (**10d**), dehydrate in both the solid state and solution.

### *1. Solid-State Dehydration*

Powders of tetracycline (**10a**), oxytetracycline (**10b**), chlortetracycline (**10c**), and rolitetracycline (**10d**) degrade when stored at 37° and 100% relative humidity (Walton *et al.*, 1970).

The most important degradation products are anhydrotetracycline (**11**) and 4-epianhydrotetracycline (**12**). These products are particularly important because they have been implicated as the causative agents in tetracycline-induced renal dysfunction (Fulop and Drapkin, 1965).

The rate and extent of the solid-state dehydration depends on the salt. For example, solid tetracycline phosphate contains 14% of **11** and 6% of **12** after 30 days at 37°C and 100% humidity, while solid tetracycline hydrochloride contains only 3.7% of **11** and 2.2% of **12** under identical conditions. Tablets of tetracycline hydrochloride are also unstable and

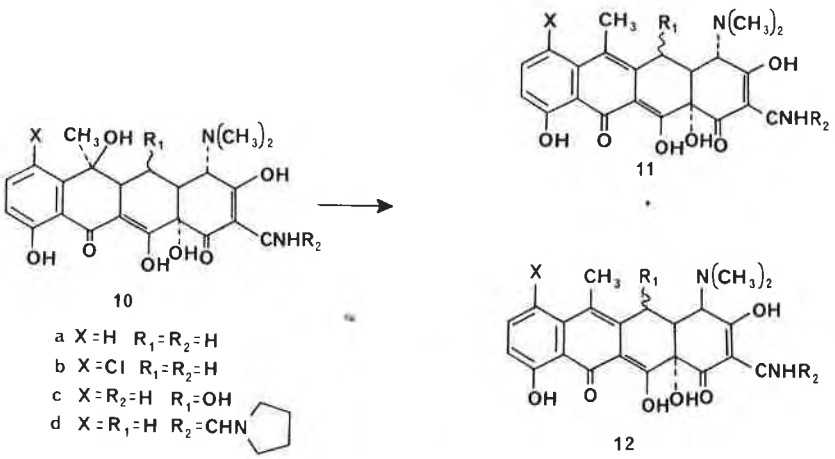


degrade to form approximately 6% **11** and 6% **12** after storage at 70°C for 6 weeks (Simmons *et al.*, 1966).

There have been extensive studies of the crystallographic properties of the tetracycline antibiotics (**10**). These studies show that, in general, these compounds crystallize in numerous crystal forms with different physical properties.

Two crystal forms of tetracycline (**10a**), chlortetracycline (**10b**), and oxytetracycline (**10c**) have been reported by Miyazaki *et al.* (1975). These forms are summarized in Table I. Each of the forms listed in Table I had significantly different dissolution rates and different bioavailabilities. The most striking differences in bioavailability were for the two forms of tetracycline. Form II of tetracycline reached a blood concentration of 3 times that of form I in rats and approximately $1\frac{1}{4}$ times that of form I in human subjects. This illustrates the dramatic effect crystal form can have on bioavailability.

The crystal structure of form I of oxytetracycline has been reported (Stenzowski, 1976). In addition, the crystal structure of tetracycline

**TABLE I**
*Crystal Forms of Tetracyclines*[a]

| | | |
|---|---|---|
| Tetracycline (**10a**) | Form I | $C_{22}H_{24}O_8N_2 \cdot 3H_2O$ |
| Tetracycline (**10a**) | Form II | $C_{22}H_{25}O_8N_2 \cdot 2H_2O$ |
| Chlortetracycline (**10b**) | Form I | $C_{22}H_{23}O_8N_2Cl \cdot \frac{5}{2}H_2O$ |
| Chlortetracycline (**10b**) | Form II | $C_{22}H_{23}O_8N_2Cl \cdot \frac{3}{2}H_2O$ |
| Oxytetracycline (**10c**) | Form I | $C_{22}H_{24}O_9N_2 \cdot 2H_2O$ |
| Oxytetracycline (**10c**) | From II | $C_{22}H_{25}O_9N_2 \cdot \frac{1}{2}H_2O$ |

[a] Data from Miyazaki *et al.* (1975).

hexahydrate and the anhydrous form of oxytetracycline have been determined (Donohue *et al.*, 1963). The crystal structure of chlortetracycline hydrochloride has also been determined. No studies of the reactivity of these forms have been reported and thus no conclusions concerning the relationship between crystal structure and the different reactivities of these forms can be made. A study of the relationship between structure and reactivity of these forms would help explain the mechanism of the solid-state reaction as well as suggest methods to improve the stability of the tetracycline antibiotics.

#### *2. Solution Degradations of Tetracyclines*

The solution reactions of tetracycline have been extensively studied and will not be completely reviewed here. However, several important aspects of these reactions will be discussed in order to relate the solution and solid-state reactions.

An early study reports that in acid solution chlortetracycline forms both the anhydro (**11**) and epianhydro (**12**) products, while in base a product termed isochlortetracycline is formed (Huang *et al.*, 1956). This study was substantiated by another early study, showing that the epimerized product is formed via a mechanism solely involving epimerization at the C(4) carbon atom (McCormick *et al.*, 1957). These reports are consistent with more recent studies (Faith *et al.*, 1972; Thorpe *et al.*, 1969).

The kinetics of dehydration of tetracycline in acidic aqueous solution have also been investigated and obey the rate law:

$$\text{Rate} = k[\text{tetracycline}][H^+]$$

A study of the rate at different temperatures gave an activation energy of 25.1 kcal/mole (Schlecht and Frank, 1975).

## II. Solid-State Decarboxylation Reactions

In this section, reactions of the type A (solid) → B (solid) + $CO_2$ are discussed.

### A. DECARBOXYLATIONS OF SALICYLIC ACIDS

In our laboratories, the decomposition of salicylic acids **13**, **14**, **15**, **16**, **17**, and **18** have been studied (Lin *et al.*, 1978). At 100°C, only *p*-aminosalicylic acid (**10**) decarboxylated. *p*-Aminosalicylic acid decarboxylated in 10 hr, while the other salicylic acids did not decarboxylate

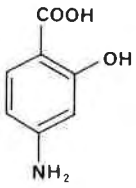


13

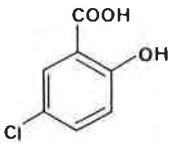


14

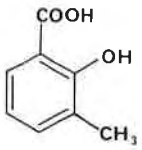


15

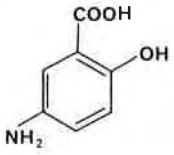


16

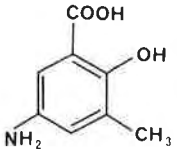


17

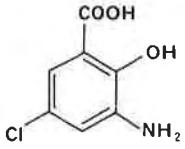


18

even when heated for 1 week. This is consistent with the predicted decomposition rates of salicylic acids based on the mechanism of the solution reaction and studies of the solid-state decomposition of benzoic acids. The rate constants for decarboxylation of $p$-$NH_2$, $p$-OH, $p$-$OCH_3$, and $p$-$CH_3$ salicylic acids obeyed a Hammett $\rho^+$ plot, with $\rho = 4.38$. Based on this data, the predicted relative rates of decarboxylation of **13**, **17**, **15**, **16**, **18**, and **14** are approximately 1, $10^{-4}$, $10^{-5}$, $10^{-5}$, $10^{-6}$, and $10^{-7}$, respec-

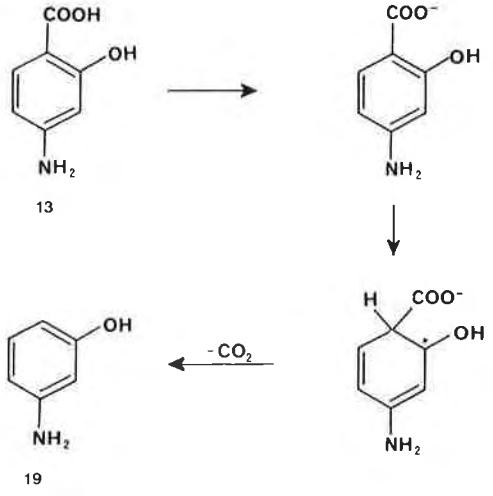


SCHEME I

tively. (The $\rho$ value for the metasubstituents was used in estimating these rates.) In addition, sodium *p*-aminosalicylate was stable at temperatures of 100°C and below, ruling out the possibility that these salicylic acids could decompose via a carbanion mechanism at temperatures of 100°C and below. A carbanion mechanism is apparently operative in the decarboxylation of trinitrobenzoic acid (Schubert and Gardner, 1953).

This evidence suggests that the solid-state reaction follows a path similar to the solution reaction (Scheme I). The proton required for the electrophilic addition may come from an adjacent ArCOOH or ArOH group. An analysis of the crystal packing shows that there are at least four carboxyl protons and two phenolic protons with 5 Å of the aromatic carbon atom. These protons (and symmetry positions) are: C(1) · · · HOOC $(x,1+y,z)$, 3.98 Å; C · · · HOOC $(2-x,1-y,-z)$, 4.99; C · · · HOOC $(2-x,-y,-z)$, 4.60; C · · · HOOC $(1-x,1-y,-z)$ 4.42; C · · · HO $(x,1+y,z)$, 4.17; and C · · · HO $(x,y-1,z)$, 4.77. Figure 3 shows these protons and the carbon atom involved in these contacts.

Morsi and Williams (1978) have used emission spectroscopy to study the decomposition of *p*-aminosalicylic acid and particularly the source of the proton for electrophilic substitution. They suggest that the fluorescence spectrum of *p*-aminosalicylic acid is consistent with the presence of **13A** in the solid state. Furthermore, they suggest that this isomer is an intermediate in the decomposition of *p*-aminosalicylic acid to *m*-aminophenol. They argue that the fact that sodium *p*-aminosalicylate decomposes at high temperatures dispenses with the requirement that the carboxylic proton be responsible for the decomposition of *p*-aminosalicylic acid. Caution should be used in making this latter argument, since sodium *p*-aminosalicylate decomposes at a temperature more than 100°C higher than *p*-aminosalicylic acid. This salt probably decom-

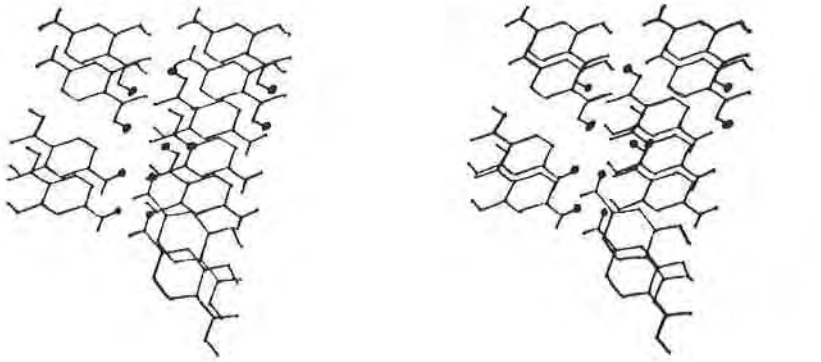

**FIGURE 3.** Stereo view of the crystal packing of *p*-aminosalicylic acid. The COOH protons and OH protons within 5 Å of the nucleophilic carbon atom are denoted with dark circles (Lin *et al.*, 1978).

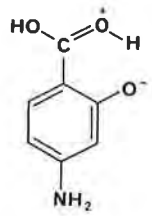

13A

poses via the carbanion mechanism in similarity to trinitrobenzoic acid. In addition, because of rapid proton transfers it is virtually impossible to distinguish between the two sources of proton (ArCOOH or ArOH) for electrophilic substitution.

Surprisingly, *p*-aminosalicylic acid hydrochloride showed a slight amount of decomposition after 10 hr at 100°C, even though its predicted relative rate in solution is $10^{-10}$. After longer times, sublimed *m*-aminophenol hydrochloride could be isolated near the top of the closed vial. The material remaining on the bottom of the vial was mostly *p*-aminosalicylic acid hydrochloride and a trace of *p*-aminosalicylic acid. In contrast, the hydrochloride salts of **16**, **17**, and **18** did not decarboxylate after 1 week at 150°C. However, analysis showed that these compounds had lost HCl.

These data are consistent with resonance considerations that suggest that p-aminosalicylic acid hydrochloride should dehydrochlorinate more readily than the hydrochlorides of **16**, **17**, and **18**.

Based on this evidence, we suggest that the decarboxylation of *p*-aminosalicylic acid hydrochloride follows the mechanism shown in Scheme II (Lin, *et al.*, 1978). No solid–solid reaction between *m*-

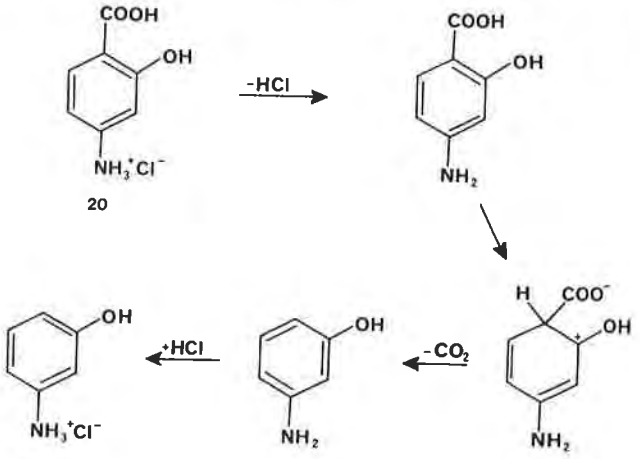

20

SCHEME II

aminophenol and *p*-aminosalicylic acid hydrochloride could be detected. Thus the alternative mechanism involving solid–solid transfer of $H^+$ (or HCl) to *m*-aminophenol and reaction of *p*-aminosalicylic acid could be ruled out.

## B. DECARBOXYLATION OF SODIUM BICARBONATE

The thermal transformation of sodium bicarbonate (**21**) to anhydrous sodium carbonate was studied at temperatures ranging from 82°–95°C using x-ray powder diffraction (Shefter *et al.*, 1974).

$$\underset{\mathbf{21}}{2NaHCO_3} \longrightarrow Na_2CO_3 + H_2O + CO_2$$

In this study, powder diffraction was used to monitor diffraction peaks of both $NaHCO_3$ and $Na_2CO_3$. These studies indicate that the only product is $Na_2CO_3$; no hydrates or other crystal forms were observed, suggesting that the loss of $H_2O$ and $CO_2$ may be simultaneous or essentially simultaneous. Unfortunately, the intermolecular hydrogen bonding and crystal packing of $NaHCO_3$ has not been analyzed in terms of this possibility.

Figure 4 shows a plot of the reaction of $NaHCO_3$ by the cube root law.

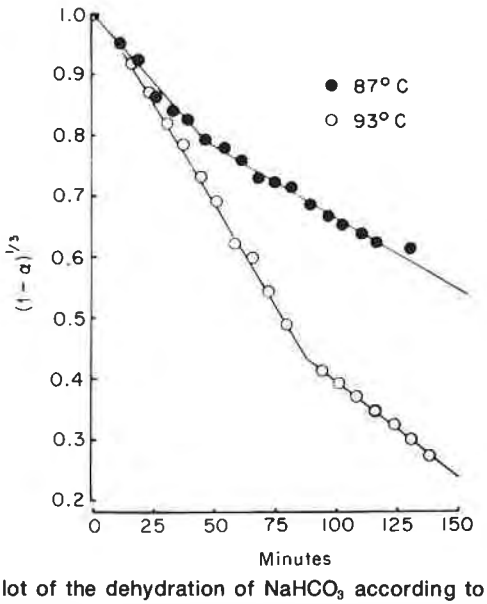


**FIGURE 4.** A plot of the dehydration of $NaHCO_3$ according to the cube root law (Shefter *et al.*, 1974). (Reprinted from E. Shefter, A. Lo, and S. Ramalingam [1974]. *Drug Dev. Commun.* **1**, 29, by courtesy of Marcel Dekker, Inc.)

This plot which is based on the Avrami–Erofeev equations (Sharp *et al.*, 1966) is biphasic, indicating that this equation does not apply. Unfortunately, the fit of the data to other equations was not examined.

Scanning electron micrographs indicate that the reaction is surface-controlled, since crystals of $Na_2CO_3$ appear on the surface of $NaHCO_3$ after heating.

## C. THE PHOTOCHEMICAL DECARBOXYLATION OF DIBENZOYLPEROXIDE

Morsi, Thomas, and Williams (1975) have reported a study of the solid-state thermal and photochemical decomposition of dibenzoylperoxide (**22**). The reaction is quantitative, and electron spin resonance

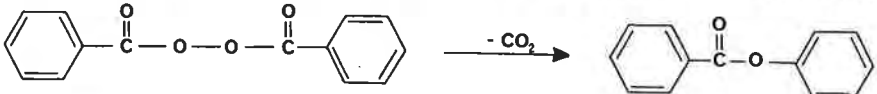


22 23

(ESR) studies show that at 4°K only phenyl radicals are formed. No benzoyl radicals could be detected. Thus the mechanism of this reaction is probably that shown in Scheme III.

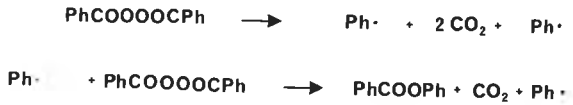


SCHEME III

The thermal reaction occurs on the 010 face and involves both randomly and [100]-aligned nuclei. Similar behavior is seen in the photolytic reaction.

TGA studies on both deliberately deformed crystals and as-grown crystals showed that plots of $[-\log(1-\alpha)]$ versus $t$ gave a straight line for $\alpha$ between 0.1 and 0.95. This indicates but does not prove that the reaction follows a phase-boundary-controlled or contracting-envelope model.

Microscopic studies show that decomposition is rapid along the [010] direction. This anisotropic behavior is consistent with preferential migration of phenyl radicals along this direction.

## D. PHOTOLYSIS OF ACETYLBENZOYLPEROXIDE

The photolysis of crystalline acetylbenzoyl peroxide (**24**) at low temperature gives methyl benzoate and toluene (Karch *et al.*, 1975). Labeling

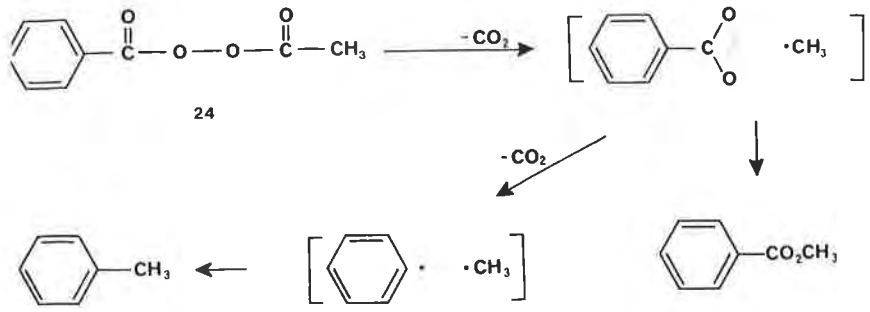

24

experiments show that these products are probably formed from reaction in a cage, and low-temperature ESR suggests that the radical pairs shown are the intermediates. In addition, labeling experiments show that there is oxygen discrimination in ester formation. This discrimination is apparently due to crystal packing and the position of the accompanying $CO_2$ molecule.

## III. Decomposition of Explosives

One of the best known examples of solid-state reactions that have gases as products is the decomposition of organic explosives. These compounds have, of course, been extensively studied and reviewed, and these reviews will not be repeated here (Morawetz, 1963). It is important to note that these reactions begin at and spread from nuclei. The rate of expansion of these nuclei is determined by the heat given off during the explosive reaction. Their nature is not known but could involve mechanical imperfections, impurity sites, or product sites.

## IV. Decompositions That Produce Nitrogen Gas

The behavior of diazonium salts **25a–25d** has been studied in the solid state (Gougoutas and Johnson, 1978; Gougoutas, 1979). The diazonium salts with X = Br and X = Cl are isostructural and decompose to form the corresponding 3-halo-2-naphthoic acids. In addition, both of these com-

25

a X = I
b X = Br
c X = Cl
d X = $HSO_4$

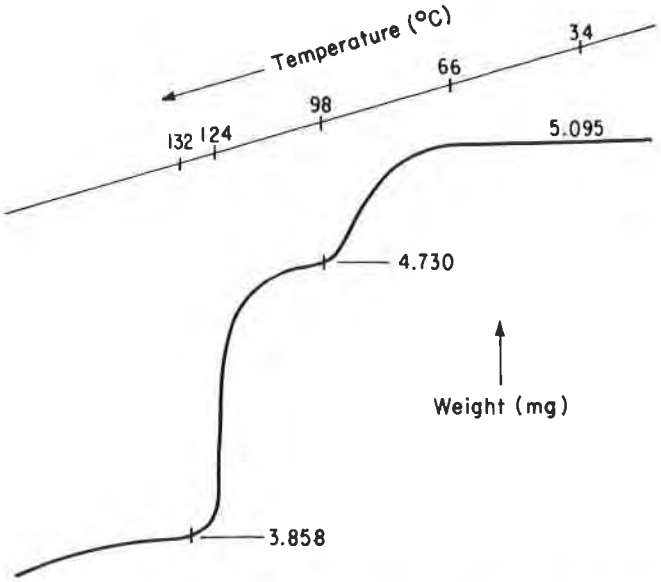


**FIGURE 5.** Thermal gravimetric analytical (TGA) studies of the diazonium salt **25b** at a heating rate of 2.5°C/min. Temperature is shown on the upper line, and weight is shown on the lower line (Gougoutas and Johnson, 1978). (Reprinted with permission from J. Z. Gougoutas and J. Johnson [1978]. Copyright 1978 American Chemical Society.)

pounds (**25b** and **25c**) crystallize with solvent of crystallization. DSC and TGA studies (Figure 5) show that water of crystallization is lost at ~65°C and $N_2$ is lost at 110°–137°C. X-Ray studies show that the loss of water is topotactic, giving a new phase with different reflections that have not been indexed. This phase is then topotactically transformed to a second phase at about 90°C.

TGA studies indicate that the iodo salt **25a** is much less stable than the chloro and bromo salts (**25b** and **25c**). These studies also show that the decomposition of **25a** involves more or less simultaneous loss of $N_2$ and $H_2O$, rather than the stepwise process found for **25b** and **25c** (Figure 6).

While the overall packing of **25a** and **25b** are different, the environment of the diazonium group in these two compounds is similar. Thus the difference in stability of these two compounds is probably not related to crystal packing but instead to the greater ease of oxidation of $I^-$ to $I_2$ versus $Br^-$ to $Br_2$ or $Cl^-$ to $Cl_2$. Thus it is suggested that these reactions proceed via an electron transfer mechanism.

The photolysis of crystalline azobisisobutyronitrile (**26**) has been studied in solution and in two crystalline modifications (Jaffe *et al.*, 1972). The reaction in the crystals gives 95% disproportionation and 5% recombina-

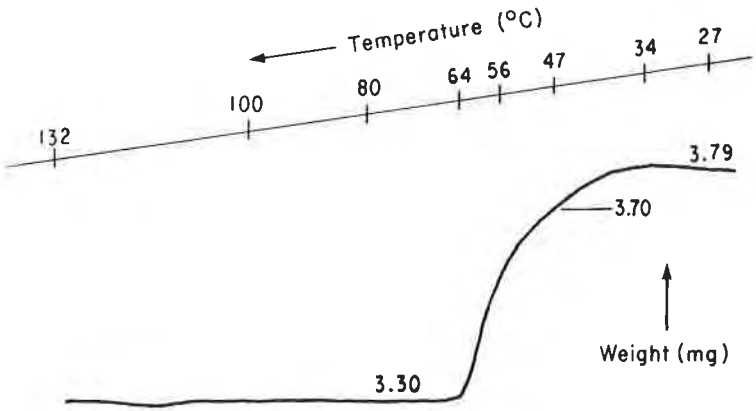


**FIGURE 6.** TGA studies of the diazonium salt **25a** at a heating rate of 2.5°C/min. The upper line is temperature and the lower line is weight (Gougoutas, 1979). (Reprinted with permission from J. Z. Gougoutas [1979]. Copyright 1979 American Chemical Society.)

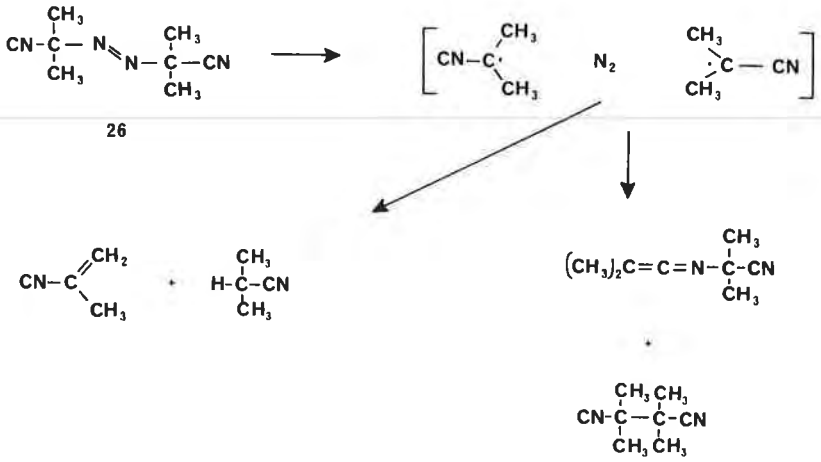

26

tion while the reaction in solution gave 5% disproportionation and 80% recombination. The difference in products is apparently due to a specific type of crystal packing which disfavors recombination.

In contrast, the products of irradiation of **27** are the same in the solid state and in solution, perhaps indicating that the crystal packing that changes the proportion of products in **26** is not present in **27**.

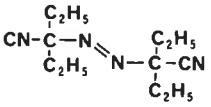

27

## V. Summary

This chapter discusses a number of solid-state reactions of the type A (solid) → B (solid) + C (gas). These reactions appear to be governed by chemical as well as crystal-packing factors. This is reasonable, since they involve the dissociation of covalent bonds.

From a pharmaceutical viewpoint these reactions can sometimes be avoided by careful handling. In particular, care should be taken to avoid exposure of the solids to high temperatures.

## References


Donohue, J., Dunitz, J. D., Trueblood, K. N., and Webster, M. S. (1963). *J. Am. Chem. Soc.* **85,** 851.

Faith, L., Georch, D., and Springer, V. (1972). *Cesk. Farm.* **21,** 353.

Farmer, B. C., and Lando, J. B. (1974). *Z. Naturforsch., Teil B* **29,** 769.

Fulop, N., and Drapkin, A. (1965). *N. Engl. J. Med.* **272,** 986.

Gougoutas, J. Z. (1979). *J. Am. Chem. Soc.* **101,** 5672.

Gougoutas, J. Z., and Johnson, J. (1978). *J. Am. Chem. Soc.* **100,** 5816.

Guyot, A., and Catel, J. (1906). *Bull. Soc. Chim. Fr.* **35,** 1124.

Guyot, A., and Vallette, F. (1911). *Ann. Chim. Paris* **23,** 363.

Huang, Y. T., Nee, D. N., Tsung, H. C., and Tai, L. H. (1956). *Acta Chim. Sinica* **22,** 85.

Jaffe, A. B., Skinner, K. J., and McBride, J. M. (1972). *J. Am. Chem. Soc.* **94,** 8510.

Karch, N. J., Koh, E. T., Whitsel, B. L., and McBride, J. M. (1975). *J. Am. Chem. Soc.* **97,** 6729.

Knozinger, H. (1971). *In* "The Chemistry of the Hydroxyl Group," Part 2 (S. Patai, ed.), p. 641. Interscience, New York.

Lewis, T. W., Puckett, S. A., Curtin, D. Y., and Paul, I. C. (1976). *Mol. Cryst. Liq. Cryst.* **32,** 111.

Lewis, T. W., Curtin, D. Y., and Paul, I. C. (1979). *J. Am. Chem. Soc.* **101,** 5717.

Lin, C. T., Siew, P. Y., and Byrn, S. R. (1978). *J. Chem. Soc., Perkin Trans. 2,* 959, 963.

McCormick, J. R. D., Fox, S. M., Smith, L. L., Bitter, B. A., Reichenthal, J., Origoni, V. E., Muller, W. H., Winterbottom, R., and Doerschik, A. P. (1957). *J. Am. Chem. Soc.* **79,** 2849.

Miyazaki, S., Nakano, M., and Arita, T. (1975). *Chem. Pharm. Bull.* **23,** 552.

Morawetz, H. (1963). *In* "Physics and Chemistry of the Organic Solid State" (D. Fox, M. M. Lakes, and A. Weissberger, eds.), p. 316. Interscience, New York.

Morsi, S. E., and Williams, J. O. (1978). *J. Chem. Soc., Perkin Trans. 2,* 1280.

Morsi, S. E., Thomas, J. M., and Williams, J. O. (1975). *J. Chem. Soc.,* 1857.

Schlecht, K. D., and Frank, C. W. (1975). *J. Pharm. Sci.* **64,** 352.

Schubert, W. M., and Gardner, J. D. (1953). *J. Am. Chem. Soc.* **75,** 1401.

Sharp, J. H., Brindley, G. W., and Narahariachar, B. N. (1966). *J. Am. Ceramic Soc.* **49,** 379.

Shefter, E., Lo, A., and Ramalingam, S. (1974). *Drug Dev. Commun.* **1,** 29.

Simmons, D. L., Woo, H. S. L., Koorengevel, C. M., and Seers, P. (1966). *J. Pharm. Sci.* **55,** 1313.
Stezowski, J. J. (1976). *J. Am. Chem. Soc.* **98,** 6012.
Thorpe, R. F., Stretton, R. J., and Watson-Walker, J. (1969). *Loughborough Univ. Technol., Dep. Chem., Summ. Final Year Stud. Proj. Theses,* **10,** 64.
Walton, V. C., Howlett, M. R., and Selzer, G. B. (1970). *J. Pharm. Sci.* **59,** 1160.

# IV

# Solid-State Photochemical Reactions

# 9 Solid-State Photochemical Reactions

In this chapter, solid-state photochemical reactions are reviewed. In particular, experimental evidence for the topochemical postulate, which explains a large number of these reactions and is one of the most important ideas in solid-state chemistry, is presented. In addition, several solid-state photochemical reactions of drugs are discussed and reviewed.

In general, solid-state photochemical reactions can involve either reaction inside the crystal as exemplified by the extensive studies of Schmidt and co-workers, or, in the presence of oxygen, photochemical oxidations can occur. Examples of photochemical oxidations are less well known but include both the oxidation of crystals of vitamin $D_2$ and the oxidation of crystals of hydrocortisone-21-*tert*-butyl acetate. Solid-state oxidation reactions were discussed in Chapter 6.

## I. Photochemistry of Solid Cinnamic Acids, Styrylthiophenes, and Dienes: The Topochemical Postulate

The topochemical postulate is based on the solid-state photochemistry of the *trans*-cinnamic acids, which can be generalized as follows (Schmidt, 1971).

*Trans*-cinnamic acids solidify in three forms—$\alpha$,$\beta$, and $\gamma$—which can be distinguished by their short crystallographic cell dimensions. The shortest cell dimensions of 38 cinnamic acid polymorphs fall into three ranges: (*a*) 3.9 ± 0.2 Å ($\alpha$ type); (*b*) 4.94 ± 0.2 Å ($\beta$ type); and (*c*) >5.1 Å ($\gamma$ type). Upon photolysis, each type yields characteristic cyclobutane products with symmetries indicated in Table I. These products have been rationalized in terms of the spatial relationship of the monomers and the separation between neighboring double bonds (Schmidt, 1964, 1971). In crystals of the $\alpha$ type, the double bonds of the monomers are parallel and are centrosymmetrically related and 3.6 to 4.1 Å apart (for example, cinnamide and the $\alpha$ form of cinnamic acid). In the $\beta$-type crystals—e.g., *p*-chlorocinnamic acid—the double bonds of the monomers are separated by about 4.0 Å, and the molecules are arranged in stacks and are related only by translational symmetry. Both *trans*-$\alpha$-bromocinnamic acid and *trans*-*m*-chlorocinnamic acid belong to the $\gamma$ type, with monomers related by translational symmetry but with their double bonds more than 4.2 Å apart. This correlation of packing geometry and the distance of the double bonds from each other with the shortest cell dimension is surprising, since the choice of unit cell is arbitrary in many of the cases studied. However, the significance of the correlation is underscored by the specificity of the solid-state photodimerizations.

Topochemical control of these solid-state photochemical reactions is illustrated by the dimerization of the two ($\alpha$ and $\beta$) polymorphic forms of *trans*-cinnamic acid shown schematically below. Upon exposure to sunlight in cellophane-covered petri dishes or Pyrex cylinders, the centrosymmetric $\alpha$ forms (**1**) gives with 74% yield the centric dimer $\alpha$-truxillic acid (**2**), while the unstable $\beta$ form (**3**) gives pure $\beta$-truxillic acid (**4**) upon irradiation, provided care is taken to insure that the photolysis is run below the $\alpha$-to-$\beta$ transition temperature. These results are consistent with the idea that the crystal packing of the reactant crystal controls the geometry of the product.

Schmidt has tentatively suggested that in the majority of cases solid-

**TABLE I**
*Cinnamic Acid Polymorphs*

| Crystal type | Shortest cell dimension (Å) | Crystallographic relationship of monomers | Double-bond separation (Å) | Symmetry of product |
|---|---|---|---|---|
| $\alpha$ | >5.1 | $\bar{1}$ (centric) | 3.6–4.1 | $\bar{1}$ (centric) |
| $\beta$ | 3.9 ± 0.2 | translation | 3.9–4.1 | *m* (mirror) |
| $\gamma$ | 4.9 ± 0.2 | translation | 4.2–5.1 | No reaction |

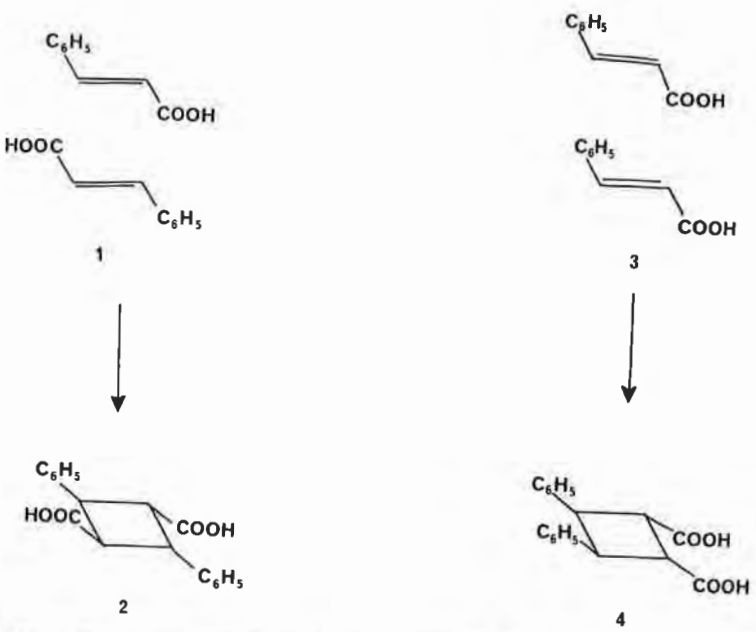


state photodimerization proceeds from the singlet state (Schmidt, 1971). This suggestion is based on experiments on solid solutions of cinnamides where the products indicate that the dimerization is faster than energy transfer, and on studies of thymine dimerization in frozen solution. However, none of these experiments clearly rules out the possibility that the photodimerization of cinnamic acids proceeds through the triplet state.

Schmidt has also made the striking observation that the reacting double bonds of cinnamic acids must be aligned and parallel or no cycloaddition reaction is observed (Schmidt, 1971). For example, *trans*-methyl *m*-bromocinnamate does not photodimerize over long periods of irradiation. This ester has its double bonds 3.93 Å from each other but nonparallel (the double bonds are related by a glide plane). This observation is consistent with studies of the polymerization of 1,1-trimethylene-bisthymine (Leonard *et al.*, 1973; Frank and Paul, 1973).

The photochemistry of solid *cis*-cinnamic acids was at first glance unexpected on the basis of the topochemical postulate (Bergman *et al.*, 1964). Many of the cis acids studied by single-crystal x-ray techniques crystallize with their double bonds within 4 Å of each other and in position to yield cis dimers; however, irradiation yielded either *trans*-cinnamic acid or photoproducts derived from the trans acid. Powder x-ray experiments indicated that the cis acids isomerized to trans acids and then dimerized to give trans-type products (Bergman *et al.*, 1964). For the trans acids that

crystallize in several polymorphic forms, dimers expected from all the polymorphs were often obtained. In contrast, coumarin (**5**)—a *cis*-cinnamic-acid derivative pinned in the cis configuration—and the coumarin–$HgCl_2$ complex crystallized with the double bonds 4 Å apart and gave upon irradiation the cis–syn dimer (**6**), as expected from the topochemical postulate.

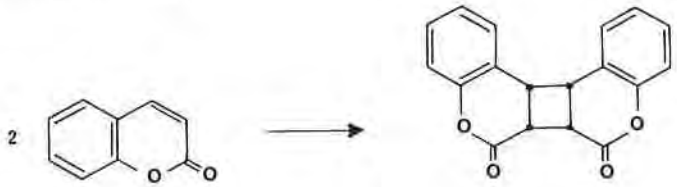

5 6

Careful study of the solid-state photochemistry of *cis-o*-methoxycinnamic acid showed that at room temperature mainly *o*-methoxy-$\alpha$-truxillic acid (a derivative of **2**) was formed upon irradiation, while at low temperatures (between $-80°$ and $-180°C$) the *trans-o*-methoxycinnamic acid accumulated but no dimer was formed (Schmidt, 1971). Control experiments showed that the dimerization of *trans*-cinnamic acids was not temperature-dependent (between 25° and $-180°C$). On this basis, Schmidt has explained the reaction of *cis*-cinnamic acids as follows. Crystals of the cis acid upon irradiation are transformed to a solid solution of trans acid (formed by cis → trans photoisomerization) in the cis host crystal. Then the trans acid crystallizes out of the solid solution, and these crystals dimerize to trans products. At low temperatures, the crystallization of trans crystals from the solid solution is slowed or stopped, allowing the noncrystalline, hence nonreactive, trans acid to accumulate.

It should be noted that solid-state photochemical reactions may offer distinct advantages over the corresponding solution reactions, since they allow control of the sterochemistry of the product (truxillic acids) and control of the course of the reaction. For example, *trans*-cinnamic acid yields 98% polymer when irradiated in solution.

The solid state behavior of styrylthiophenes **7**, **8**, and **9** is crystal-lattice-controlled in similarity to the cinnamic acids. Thiophene **7** and two crystalline modifications of **9** are light-stable while, crystals of **8** yield a mirror-symmetric dimer. In contrast, in solution, **7**, **8**, and **9** dimerize. For example, **8** yields two dimers, both of which have the cis,anti,cis stereochemistry, and **9** gives all four possible cyclobutane dimers.

The difference between the solid-state and solution photochemistry of

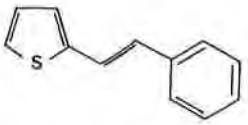


7

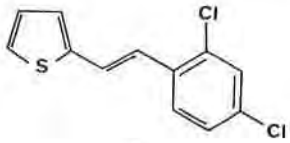


8

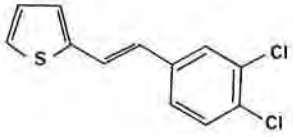


9

these styrylthiophenes illustrates the control the solid state can have on the stereochemistry of reaction products. Dienes also dimerize in the solid state. For example, the diene **10** gives photodimer **11** in good yield when

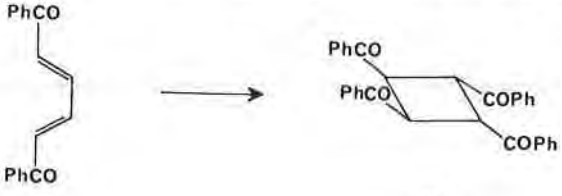


10 11

irradiated in the solid state (Perlmutter and Trattner, 1978). Topochemical control of solid-state reactions can also be used to perform asymmetric reactions (Elgavi *et al.*, 1973). Irradiation of chiral mixed crystals of the dienes **12** and **13** lead to the formation of chiral heterophotodimers. The dienes **12** and **13** form mixed chiral crystals (space group $P2_12_12_1$) upon crystallization from ethanol. Irradiation of one of these crystals showed that one of the two possible chiral dimers predominates, giving an optical rotation of about $\pm 1°$.

Quina and Whitten reported an interesting study of the behavior of the styrylpyridine **14** in monolayer assemblies, crystals, and micelles (Quina and Whitten, 1977). In crystals and monolayers, dimer formation and red-shifted fluorescence is observed. The red-shifted fluorescence probably arises from an excimer, although other explanations are possible. In addition, the excimer may be on the path to formation of the dimer.

In contrast, in micelles, only cis–trans photoisomerization, which also occurrs in solution, is observed.

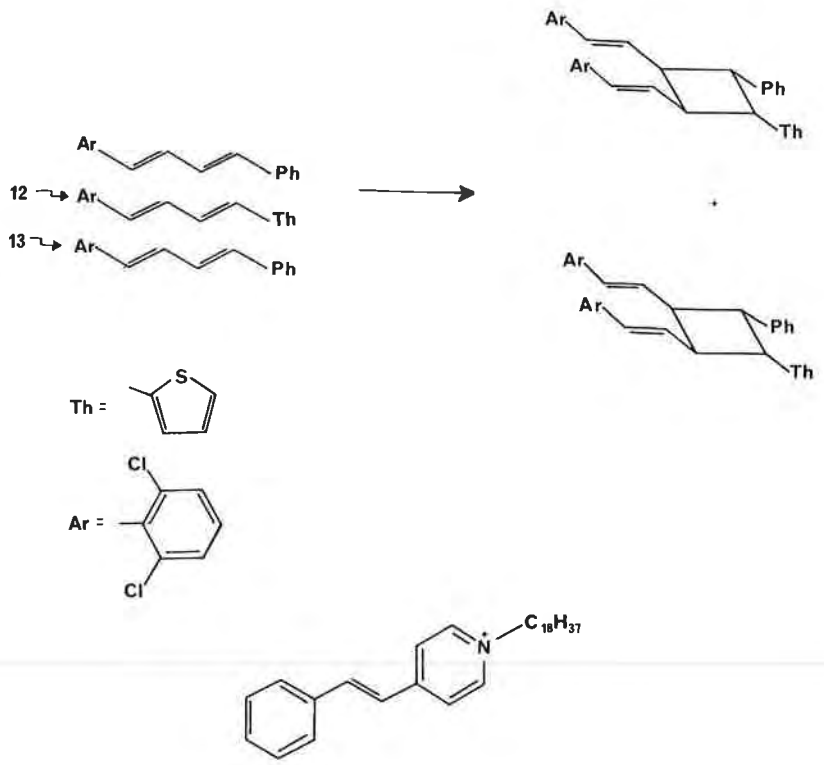


14

This study again illustrates the importance of crystal packing effects in controlling the reaction products in both crystals and condensed monolayers.

In addition, in some cases the activated complex and the products fit so well in the reaction cavity that products occur as a solid solution in the starting crystal. Thus, a topochemically controlled reaction is expected to give the product that best fits the reaction cavity. This is best demonstrated by lattice-controlled polymerizations where the products are formed as a solid solution in the starting crystal. For example, the divinyl compound **15** polymerizes with lattice control, and the product **16** is formed as a solid solution in the monomer crystal (Hasegawa *et al.*, 1970).

## II. Solid-State Photochemistry of Anthracenes: Exceptions to the Topochemical Postulate

Substituted anthracenes can in principle give either head-to-head or head-to-tail dimers. For 9-substituted anthracenes, only the head-to-tail

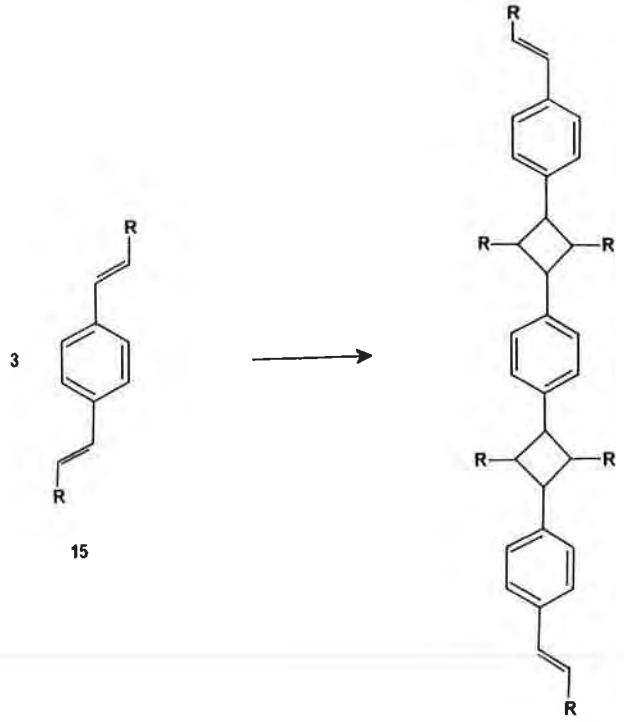


15 16

(centrosymmetric) dimer is formed upon irradiation in solution. In the solid state, crystals that have head-to-tail (centrosymmetric) packing yield head-to-tail dimers upon irradiation, while crystals with head-to-head crystal packing are either light-stable or give the head-to-tail dimer, which is inconsistent with the topochemical postulate. For example, crystals of 9-cyanoanthracene (**17**) yield the unexpected head to tail dimer (**18**) upon irradiation (Cohen *et al.*, 1971; Houk and Northington, 1972).

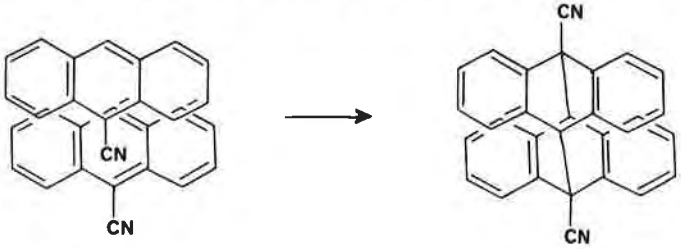


17 18

Two explanations are possible for this behavior. The first is that in crystals with head-to-head geometry that form head-to-tail dimers, the

energy is absorbed and rapidly transferred to defect sites, where the reaction occurs between molecules in the head-to-tail orientation. A second explanation is that the production of head-to-tail dimers in crystals containing head-to-head-oriented monomers is due to the mutual rotation of two molecules in an excimer. While this may be energetically unlikely in the bulk crystal, it could occur at defects (Kawada and Labes, 1972; Baum, 1970).

In contrast, 1,4,5,8-tetrasubstituted anthracenes (**19**) obey the topochemical postulate. Irradiation of crystals that have the head-to-head orientation of monomers gives predominantly head-to-head dimer (**20** in

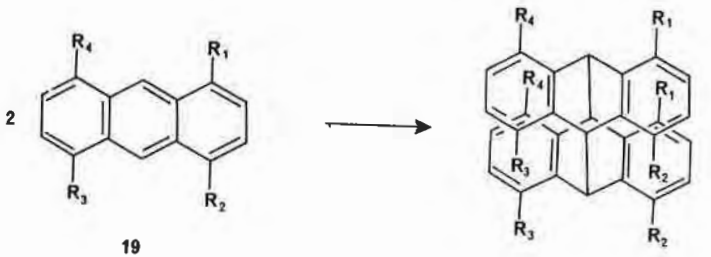


**19** **20**

>80% yield). In solution, mostly head-to-tail dimer is obtained. This reaction is viewed by Desvergne as occurring at defects; however, the alternate view that it occurs from excimers cannot be completely ruled out (Desvergne *et al.*, 1978).

An analysis of crystal packing indicates that photodimerizable anthracenes containing a bulky chiral group may crystallize only in the nonreactive $\gamma$-packing type. On the other hand, racemic crystals of these compounds can crystallize in either the reactive $\alpha$ crystals or the unreactive $\gamma$ crystals. Thus, attachment of a bulky chiral handle to an enantiomerically enriched sample and subsequent irradiation should lead to an enrichment, since the racemic crystals will react while the chiral crystals will remain unreactive. Such a resolution was accomplished by condensing three 1-aryl ethanols with 9-anthroic acid (for example, **21**) and irradia-

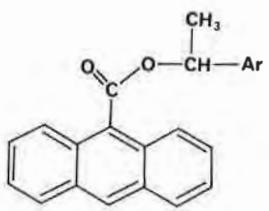


**21**

tion and extraction. Significant improvements in optical purities were obtained, and the enantiomeric purities of unreacted monomers were often >80% (Lahav *et al.*, 1976).

## III. Solid-State Photochemistry of Quinones

The solid-state photochemistry of *p*-quinones has been carefully investigated (Rabinovich and Schmidt, 1967). Both 2,5- and 2,6-dimethyl-*p*-benzoquinone give dimers with the geometry expected from the monomer crystal packing, which has parallel double bonds with center-to-center distances of less than 4.3 Å. However, the third dimethylbenzoquinone isomer, 2,3-dimethylbenzoquinone, does not give the products expected from crystal packing. In addition, *p*-benzoquinone and duroquinone polymerize upon irradiation in the solid state, perhaps due to the fact that the nearest neighbor C=C groups are not parallel and thus react to form a diradical that initiates polymerization.

The photochemistry of the tetrahydronaphthoquinone **22** and eight of its substituted derivatives has been investigated in the solid state and in

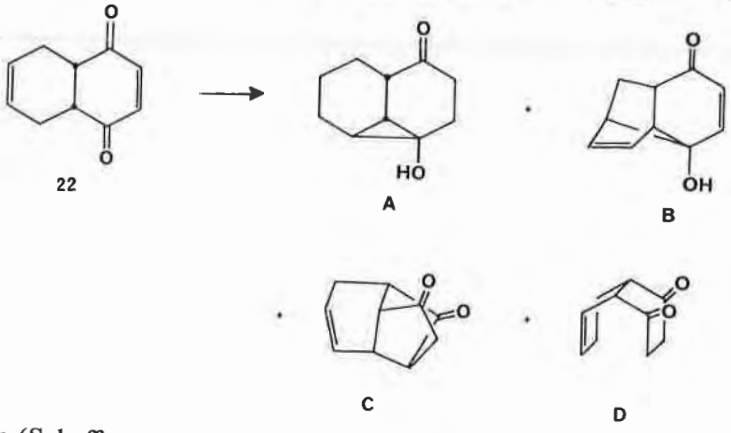


solution (Scheffer and Dzakpasu, 1978). In solution, photoproducts with general structures A, B, C, and D have been isolated. In the solid state, the products depend on crystal packing, conformation, and relative rates of reaction of different excited states. The five tetrahydronaphthoquinones **23–27** give products with the B structure upon irradiation in the solid state. All of these (**23–27**) have similar conformations in the solid state, and the products are apparently formed because this conformation favors formation of B-type products (presumably according to the mechanism shown in Scheme I).

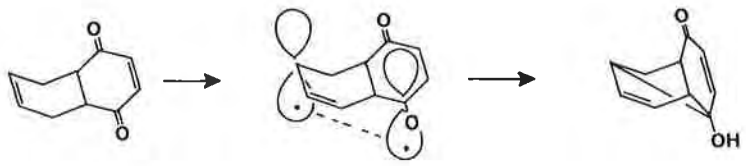

SCHEME I

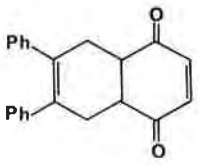

23

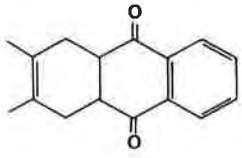

24

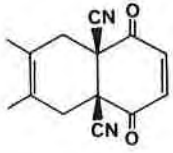

25

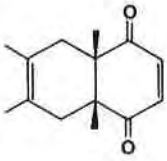

26

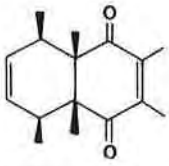

27

The tetrahydronaphthoquinones **26** and **27** also give products with the C-type structure upon irradiation in the solid. This may be due to the fact that the reaction leading to B-type products proceeds through an excited state different from that leading to C-type products so that the reactions of compounds **23, 24,** and **25** differ from those of **26** and **27.**

The tetrahydronaphthoquinones **28**, **29**, and **30** give 2 + 2 dimers upon irradiation in the solid state. This is entirely new chemistry for these

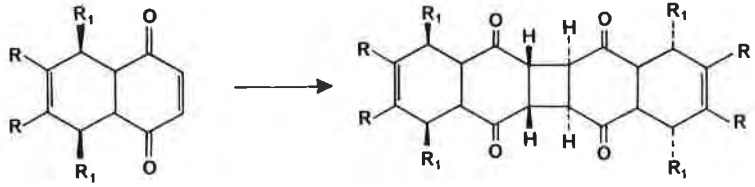

**28** R=H $R_1$=$CH_3$

**29** R=$R_1$=H

**30** R=$CH_3$ $R_1$=H

compounds, and no dimers are observed in solution. This is apparently due to the fact that the crystal packing places the double bonds parallel

and within 4.1 Å, thus favoring dimerization, even though the molecular conformation would appear to allow the formation of B- or C-type products.

Finally, compound **31** gives only the oxetane product **32** upon irradiation in the solid state. This reaction is apparently due to the fact that

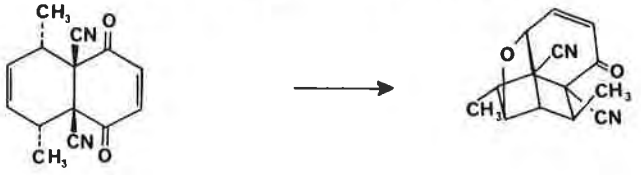

**31** **32**

crystal packing does not favor 2 + 2 dimerization and that the rate of formation of the B- and C-type products is very slow, thus allowing another product to be formed.

In a related study, the photochemical reactions of the tetrahydro-1,4-naphthoquinols **33** and **34** in the solid state and solution have been investi-

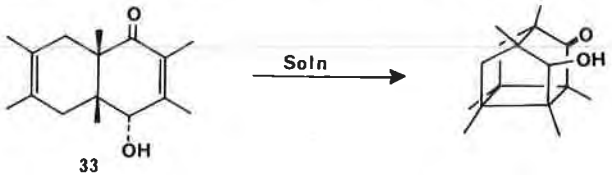


**33**

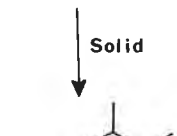


**34**

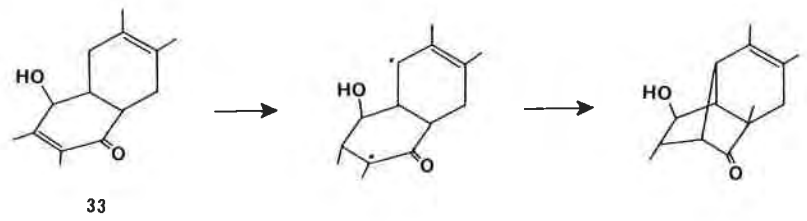


33

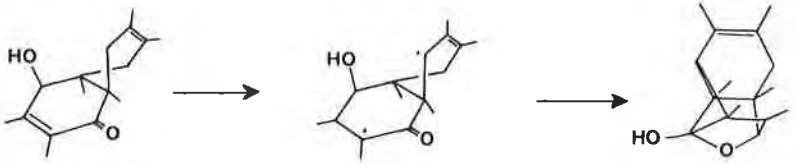


34

SCHEME II

gated (Appel *et al.*, 1980). The different products of the solid-state reaction were shown to be due to the presence of different conformers in the solid state. The naphthoquinol **33** was shown to be in the conformation shown in Scheme II in the solid, and diradical formation would lead to the product observed. The isomer **34** is in a different conformation in the solid state (Scheme II) and thus leads to a different product.

These reactions appear to be controlled by a reaction cavity that allows only a minimum of motion. That is, the crystal forms an environment in which motion is restricted, and products that can be formed with a minimum of molecular motion and that have a shape similar to the starting material are favored. In solution, numerous conformers are present and motion is not restricted, so that different products are obtained.

The reaction of the tetrahydronaphthoquinone **35** also appears to be controlled by the reaction cavity. Different products are obtained in the solid state and in solution (Appel *et al.*, 1979). Examination of the conformation of **35** in the solid state (Figure 1) shows that it is in a conformation that favors the formation of the cyclobutanone **36**.

The solid-state products formed appear to depend on the solid-state conformation, which is controlled by the crystal packing or, put another way, the shape of the reaction cavity. In solution, different conformers react and there is no rigid reaction cavity—thus, different products are formed.

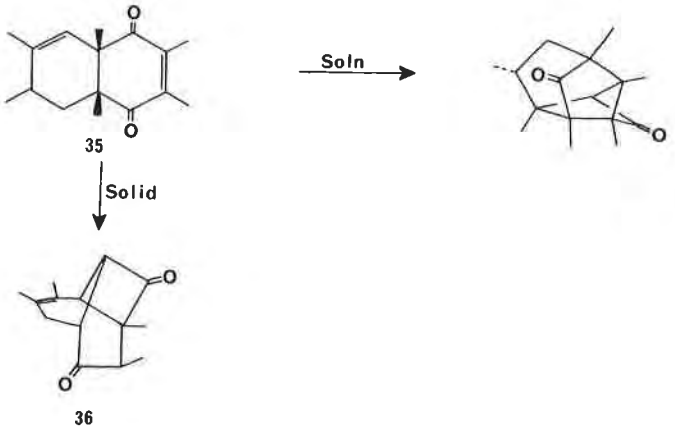


## IV. Solid-State Photosynthesis of Indigo: The Role of Molecular Conformation in Solid-State Reactions

In the solid-state photosynthesis of indigo (Engler and Dorant, 1895), the molecular conformation of the reactant (i.e., the nitrochalcone **37**) imposed by the lattice plays an important role in the reaction. The first step in this reaction involves the attack of the nitro group on the benzylidine carbon atom. The most favorable geometry for this reaction is the

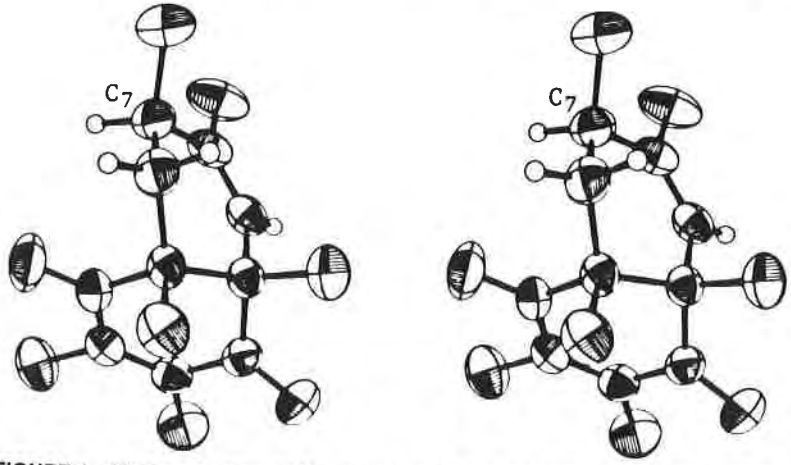


**FIGURE 1.** Stereo pair view of the structure of the quinone **35** in the solid state. It is clear that a minimum of motion is required to form **36** (Appel *et al.*, 1979). (Reprinted with permission from W. K. Appel, T. J. Greenhough, J. R. Scheffer, and J. Trotter [1979]. Copyright 1979 American Chemical Society.)

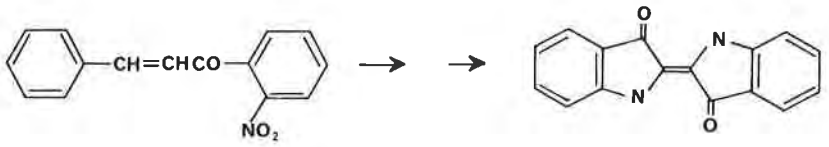


37 38

*S*-trans geometry of the ethylene linkage with respect to the carbonyl group. Indeed, the crystal structure of **37** shows that the molecules are in the *S*-trans geometry in the solid state (Rabinovich and Schmidt, 1970).

However, this conformation while necessary is apparently not sufficient to ensure reaction, since *S-trans*-4-bromo-2′-nitrochalcone does not give the corresponding indigo (Jungk and Schmidt, 1970). In addition, 4-bromo-2′-nitrochalcone, also crystallizes in the *S*-cis conformation, but then does not give the corresponding indigo upon irradiation (Jungk *et al.*, 1977).

## V. Solid-State Polymerizations

This is an extensive area which will not be completely reviewed here. It is important to note, as mentioned in Section II, that dienes such as **15** polymerize under lattice control to yield a product that is formed as a solid solution in the monomer crystal (Hasegawa *et al.*, 1970).

In a series of related studies, Wegner and co-workers showed that 1,3-diacetylenes (**39**) polymerize in the solid state to form the polymer

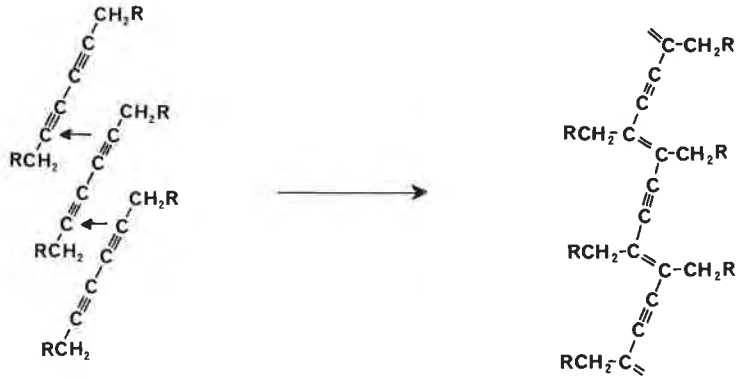


39

product as a solid solution in the monomer crystal (Kaiser *et al.*, 1972). In fact, a complete conversion to product can be obtained without a phase change, since the polymer is isomorphous with the starting material.

## VI. Dimerizations of Pyrones in the Solid State

Irradiation of pyrone **40** in the solid state gave the dimer **41**, while irradiation in benzene gave dimers **42** and **43** (Rieke and Copenhafer,

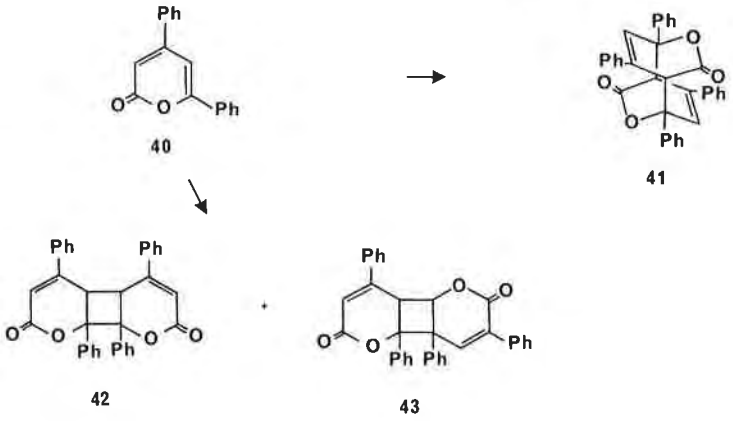


1971). This research provides another example of the role that crystal packing plays in solid-state reactions.

## VII. Solid-State Photochemistry of Nucleic Acids

The reversible dimerization of 2,5-diketopyrimidines is concentration-dependent, and in crystals of these compounds the equilibrium is shifted to the dimer side, perhaps due to the close proximity of the reactants in the solid state. In addition, the photodimers of solid thymine, 1-methylthymine, and 1,3-dimethylthymine are consistent with the ones predicted from the crystal packing of the monomers (Lisewski and Wierzchowski, 1970). The quantum yields of the solid-state reactions of these compounds decrease as the distances between the reacting double bonds increase. This observation is consistent with the topochemical postulate (Lisewski and Wierzchowski, 1970).

Photochemical reactions of nucleic acids in frozen solution are also well known (Fahr, 1969). For example, irradiation of 6-methyluracil (**44**) in frozen solution leads to the formation of the cis–syn dimer **45** (Konnert *et al.*, 1970). Similarly, irradiation of 1,3-dimethylthymine (**46**) in frozen aqueous solution yields the cis–syn dimer **47** (Camerman and Camerman, 1970).

The importance of a knowledge of the phase behavior of frozen aqueous solutions was discussed by Pincock more than 10 years ago (Pincock,

44 45

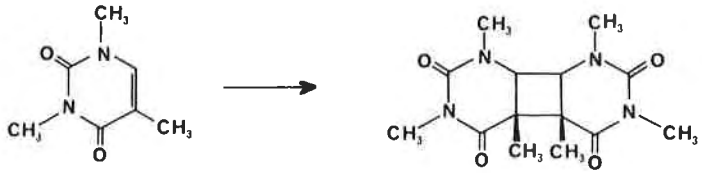

46 47

1969). He pointed out that in a two-component system, the following phase diagram can be drawn (Scheme III). He also pointed out that frozen-state reactions often appear faster than solution reactions due to a concentration effect where the solid contains ice while the liquid contains a concentrated solution of reactants. This effect is particularly important for reactions with kinetic orders $> 1$. Thus the reaction is accelerated. It has been shown that the dimerization of thymine in frozen solutions, however, was a true solid-state reaction since it occurred below the eutectic point (Fuchtbauer and Mazur, 1966; Wang, 1966).

Some nucleic acid derivatives have been observed to polymerize in the solid state (Leonard *et al.*, 1973; Frank and Paul, 1973). For example, 1,1′-trimethylenebisthymine (**48**) polymerizes to yield a polymer made up of *trans–syn*-thymine cyclobutane dimer units joined by a trimethylene chain. The crystal structure of **48** is consistent with the fact that crystals do not yield intramolecular dimers and is consistent with Schmidt's observation that the reacting orbitals must be aligned for reaction. This observation leads to the suggestion that the orientation of the participating orbitals may be as important as the distance between the reacting carbon

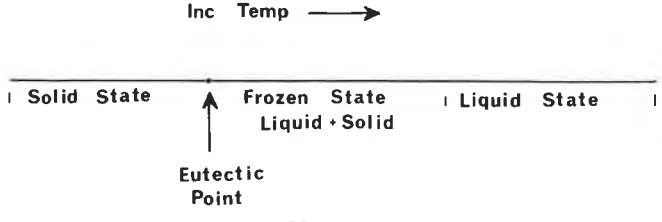


SCHEME III

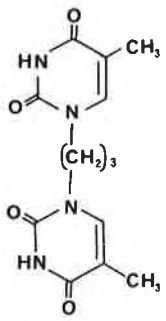

48

atoms in controlling solid-state photochemical reactions (Frank and Paul, 1973).

## VIII. Effect of Ionizing Radiation on Crystals of Biologically Important Compounds

### A. EFFECT OF γ-IRRADIATION ON CRYSTALS OF NUCLEIC ACIDS

Irradiation of crystals of nucleic acids leads to the formation of radical pairs that can be identified by ESR spectroscopy.

For example, γ-irradiation of 1-methyluracil (**49**) leads to radical pairs formed by abstraction of one of the $CH_3$ hydrogen atoms (Dulcic and Herak, 1973).

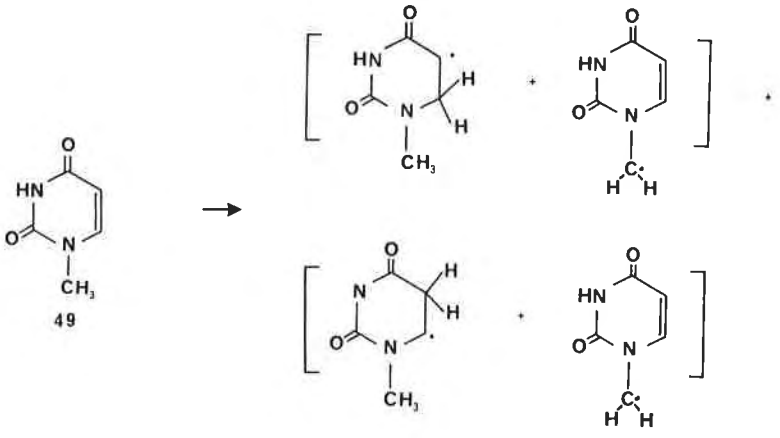

49

Similarly, irradiation of 1-methylcytosine (**50**) gives radical products (Elliott, 1971; Rustgi and Box, 1974).

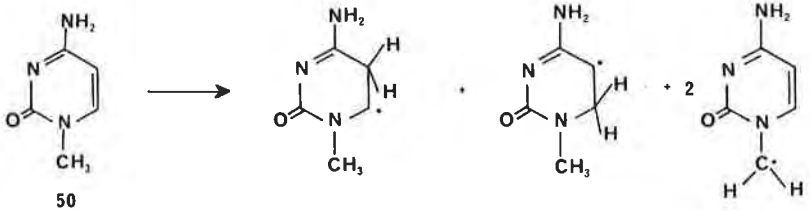

**50**

## B. IRRADIATION OF CRYSTALS OF AMINO ACIDS

Irradiation of single crystals of amino acids at room temperatures shows two predominate processes. In cases such as alanine (Miyagawa and Gordy, 1960), or D,L-aspartic acid (Jasya and Anderson, 1962), a radical is formed by rupture of a C–N bond. In crystals of L-leucine (Patten and Gordy, 1961) and D,L-valine (Shields *et al.*, 1967), the C–N bond remains intact, and in D,L-threonine (**51**) crystals a radical resulting from hydrogen abstraction is formed (Close and Anderson, 1974).

**51**

These studies may provide knowledge that can be used to understand radiation damage in biological systems.

## C. IRRADIATION OF CHOLINE CHLORIDE CRYSTALS

The effect of ionizing radiation on crystals of choline chloride (**52**) is a particularly interesting example of the effect of polymorphism on solid

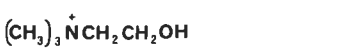

**52**

state reactivity. Choline chloride crystallizes in a stable $\alpha$ form and an unstable $\beta$ form that is present at temperatures greater than 78°C (Tomkiewicz *et al.*, 1973; Nath *et al.*, 1971, 1974; Hjortas and Sorum, 1971). The $\alpha$ form is the most sensitive to ionizing radiation of all compounds known (Nath *et al.*, 1971). That is, it has the highest G factor (molecules

destroyed/100 ev) of any compound known. The G factor for radical formation is about 2, while the G factor for radiolysis is as high as 55,000. In contrast, the high-temperature $\beta$ form is not abnormally radiation-sensitive. The difference in radiation sensitivity of these polymorphs may be related to the crystal packing of the two forms. The choline molecules in the crystals of the $\alpha$ form are apparently in a geometry favoring the propagation step in the radiolysis reaction scheme shown below. This step involves the attack of an excited H atom on a ground state choline cation. Examination of the packing in the $\alpha$ polymorph (Figure 2) indicates that the abnormal radiation sensitivity of $\alpha$-choline chloride may be due to the fact that the propagation step (step 3) proceeds rapidly through the stacks of choline molecules, much like a topochemically controlled polymerization. A knowledge of the structure of the $\beta$ polymorph of choline chloride would be of great interest, and a comparison of the packing in the two polymorphs would provide more insight into this reaction:

$$(CH_3)_3N^+CH_2CH_2OH \rightarrow [(CH_3)_3N^+CH_2CH_2OH]^* \rightarrow (CH_3)_3N \cdot \cdot CH_2CH_2OH \quad (1)$$

$$\cdot CH_2CH_2OH + e^- \rightarrow [:CH_2CH_2OH^*]^- \quad (2)$$

$$[:CH_2CH_2OH^*]^- + (CH_3)_3N^+CH_2CH_2OH \rightarrow CH_3CHO + (CH_3)_3N^+H + [:CH_2CH_2OH^*]^- \quad (3)$$

$$(CH_3)_3N \cdot^+ + [:CH_2CH_2OH^*]^- \rightarrow (CH_3)_3N^+CH_2CH_2OH + e^- \quad (4a)$$

$$(CH_3)_3N \cdot^+ + [:CH_2CH_2OH^*]^- \rightarrow (CH_3)_3N^+H + CH_3CHO + e^- \quad (4b)$$

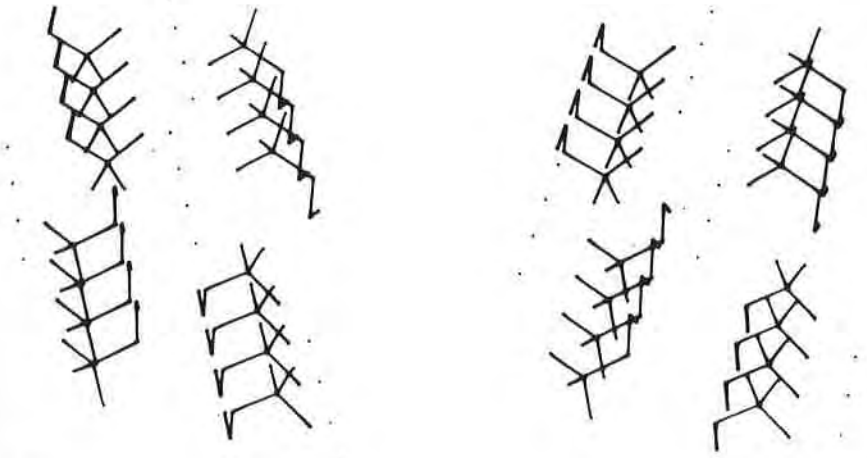

**FIGURE 2.** Stereo pair view of the crystal packing of the $\alpha$ form of choline chloride. The Cl atoms are represented as dots, and the H atoms are not drawn (Byrn, 1976). (Reproduced with permission of the copyright owner.)

The overall reaction is

$$(CH_3)_3N^+CH_2CH_2OH \rightarrow (CH_3)_3N^+H + CH_3CHO$$

### D. IRRADIATION OF HIRSUTIC ACID

The *p*-bromophenacyl ester of hirsutic acid (**53**) undergoes a rearrangement to **54** when exposed to x-rays (Comer *et al.*, 1967). Crystal

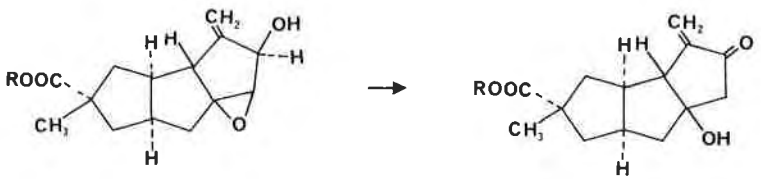


53 54

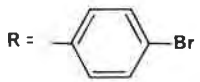


exposure to 53 to 60 hr of Mo radiation gave a 60% yield of **54**. The product, **54**, exists as a solid solution in **53**. Irradiation of the parent compound (**53**, R = H) and other related compounds gave no reaction, indicating that crystal packing plays an important role in these reactions.

## IX. Solid-State Photochemistry of Drugs and Natural Products

Few extensive studies have been reported in this area. Thus, this section by necessity reviews a number of studies where the products have not been identified. However, this clearly indicates that solid-state photochemical reactions of drugs do occur. One reason this area has not been extensively studied is that such reactions can often be prevented by storing the drug in an amber or opaque container.

### A. NOVOBIOCIN

The sodium salt of novobiocin (**55**) is light-sensitive. The degradation products are not known but could either involve oxidation or photoreaction of the coumarin functionality (Mullins and Macek, 1960).

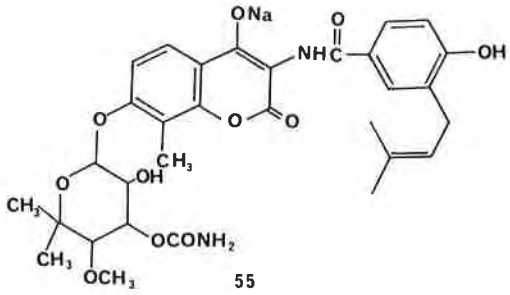


55

## B. FUMAGILLIN

Fumagillin (**56**), which contains a polyene functionality, oxidizes in the solid state when exposed to light in air. However, the structure of the

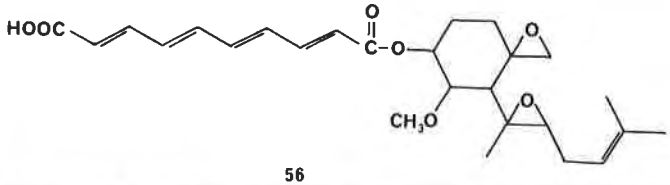


56

oxidation products are unknown (Garrett and Eble, 1954; Garrett, 1954; Eble and Garrett, 1954). Thermal degradation of fumagillin has also been observed (Garrett and Eble, 1954).

## C. RESERPINE

Reserpine (**57**) crystals discolor when exposed to light; however, the loss of potency is usually small. In solution, reserpine is quite sensitive to

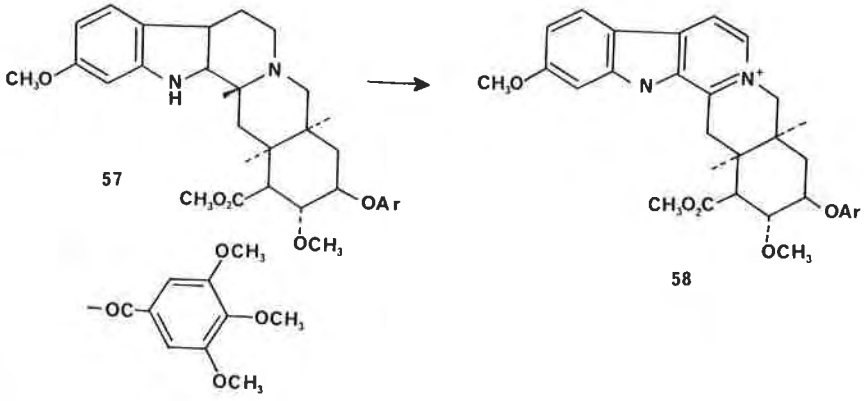


57 58

light and degrades via light-induced oxidation. This reaction in solution or the solid state is apparently due to the formation of 3-isoreserpine (**58**) (Wright and Tang, 1972; Hakkesteegt, 1970). The extent of solid-state degradation was approximately 35% in 4.5 years.

## D. STEROIDS

A recent study of the effect of FD&C colorants on the stability of norethindione (**59**) and ethinyl estradiol (**60**) gave interesting results. Table

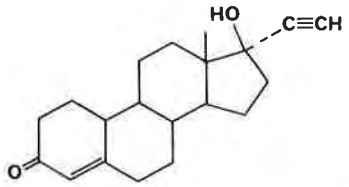


**59**

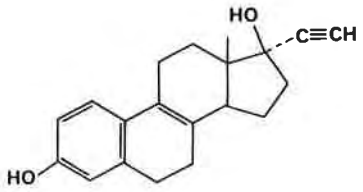


**60**

II summarizes these, which were obtained from studies in a light cabinet containing both incandescent and fluorescent lights (approximate intensity 1000 foot-candles) (Kaminski *et al.*, 1979).

All preparations were stable except **60**—pink. The dye used for the pink preparation was erythrosine, which is a sensitizer for singlet oxygen. The dye used for the orange preparation is not known to be a singlet-oxygen sensitizer. The degradation of 60—pink is thus explainable in terms of a singlet-oxygen-induced degradation of **60**. However, it is not clear why **59**—pink does not degrade, unless the crystal structure of **59** prevents oxygen penetration. A related study of the oxidation of hydrocortisone 21-*t*-butylacetate is discussed with the solid–gas reactions in Chapter 6.

**TABLE II**
*Degradation of the Steroids Norethindione* (**59**) *and Ethinyl Estradiol* (**60**) *in a Light Cabinet*[a]

| | % After | | | |
|---|---|---|---|---|
| Steroid preparation | 5 days | 10 days | 21 days | 30 days |
| **59**—White | 100.4 | 97.4 | 96.8 | 94.0 |
| **59**—Pink | 100.6 | 98.8 | 97.8 | 96.8 |
| **59**—Orange | 102.0 | 98.0 | 99.2 | 99.2 |
| **60**—White | 101.1 | 98.0 | 95.8 | 96.1 |
| **60**—Pink | 86.9 | 86.9 | 78.9 | 78.9 |
| **60**—Orange | 99.7 | 98.6 | 98.6 | 99.4 |

[a] Data from Kaminski *et al.* (1979).

## E. GIBBERELLINS

A few examples of solid-state photoreactions of natural products are known. For example, Adam's group has found that 3-keto-gibberellin $A_3$ (**61**) dimerizes upon irradiation in the solid, while intramolecular reaction or solvent addition occurs in solution (Adam and Voigt, 1971).

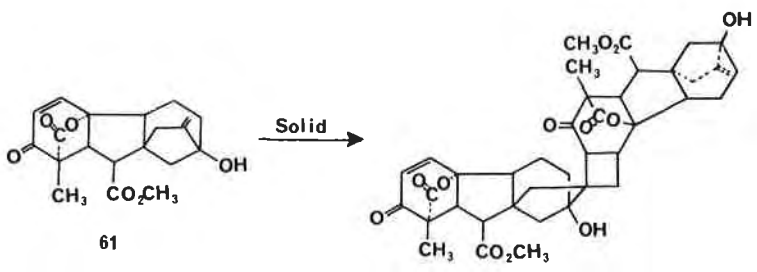


The natural pyrone **62** was also found to dimerize upon irradiation of the solid with visible light (Gottlieb *et al.*, 1975).

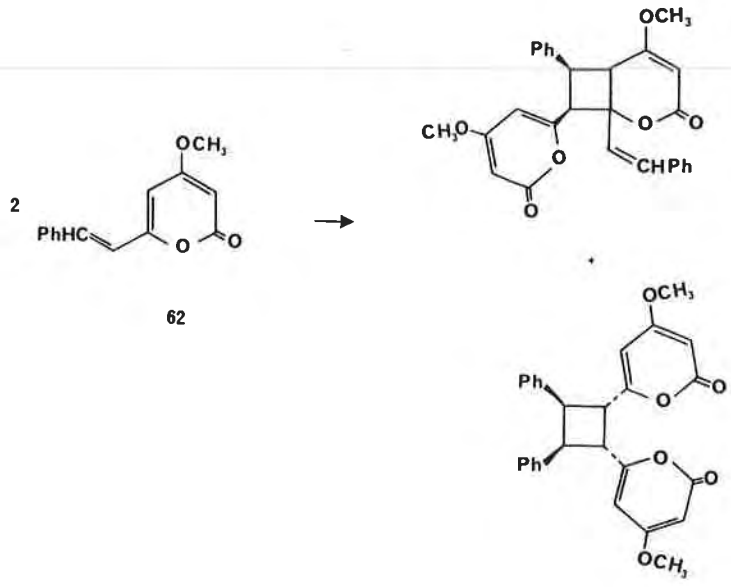


## F. PHORBOLS

Tumor-promoting phorbal esters oxidize upon storage in light. For example, TPA (**63**) decomposes to peroxide (**64**) and aldehyde (**65**).

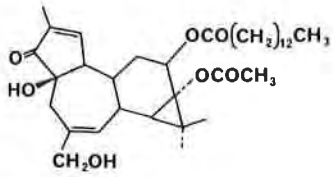


63

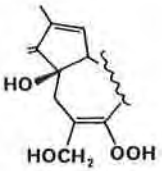


64

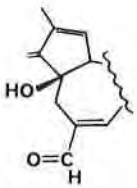


65

## G. INSECTICIDES

The insecticide dieldrin (**66**) reacts when irradiated in thin films to form **67** (Benson, 1971). This reaction may be important for understanding the environmental fate of this insecticide.

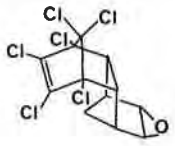


66

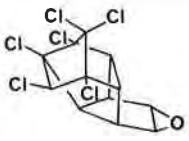


67

## X. Summary

Solid-state photochemical reactions of unsaturated compounds are well known and provide several examples of the control the solid can exert on the products of a reaction. These reactions generally obey the topochemical postulate, which states that the products formed will result from the reaction of double bonds that are parallel and less than 4.1 Å apart. The topochemical postulate appears to be a specific example of the general concept that solid-state reactions are controlled by the reaction cavity, which favors products that have a shape similar to the starting material and that can be formed with a minimum of molecular motion.

## References


Adam, G., and Voigt, B. (1971). *Tetrahedron Lett.*, 4601.

Appel, W. K., Greenhough, T. J., Scheffer, J. R., and Trotter, J. (1979). *J. Am. Chem. Soc.* **101,** 213.

Appel, W. K., Greenhough, T. J., Scheffer, J. R., Trotter, J., and Walsh, L. (1980). *J. Am. Chem. Soc.* **102,** 1158, 1160.

Baum, E. J. (1970). *In* "Excited State Chemistry" (J. N. Pitts, ed.), p. 121. Gordon and Breach, New York.

Benson, W. R. (1971). *J. Agr. Food Chem.* **49,** 66.

Bergman, J., Osaki, K., Schmidt, G. M. J., and Sonntag, F. I. (1964). *J. Chem. Soc.*, 2021.

Byrn, S. R. (1976). *J. Pharm. Sci.* **65,** 1.

Camerman, N., and Camerman, A. (1970). *J. Am. Chem. Soc.* **92,** 2523.

Close, D. M., and Anderson, R. S. (1974). *J. Chem. Phys.* **60,** 2820.

Cohen, M. D., Ludmer, Z., Thomas, J. M., and Williams, J. O. (1971). *Proc. R. Soc. London, Ser. A* **324,** 459.

Comer, F. W., McCapra, F., Qureshi, I. H., and Scott, A. I. (1967). *Tetrahedron* **23,** 4761.

Desvergne, J. P., Chekpo, F., and Bouas-Laurent, H. (1978). *J. Chem. Soc., Perkin Trans. 2,* 84.

Dulcic, A., and Herak, J. N. (1973). *Mol. Phys.* **26,** 605.

Eble, T. E., and Garrett, E. R. (1954). *J. Am. Pharm. Assoc., Sci. Ed.* **43,** 536.

Elgavi, A., Green, B. S., and Schmidt, G. M. J. (1973). *J. Am. Chem. Soc.* **95,** 2058.

Elliott, J. P. (1971). *First Eur. Biophys. Congr.* **2,** 17.

Engler, C., and Dorant, K. (1895). *Chem. Ber.* **28,** 2497.

Fahr, E. (1969). *Angew. Chem., Int. Ed. Engl.* **8,** 578.

Frank, J. K., and Paul, I. C. (1973). *J. Am. Chem. Soc.* **95,** 2324.

Fuchtbauer, W., and Mazur, P. (1966). *Photochem. Photobiol.* **5,** 323.

Garrett, E. R. (1954). *J. Am. Pharm. Assoc., Sci. Ed.* **43,** 539.

Garrett, E. R., and Eble, T. E. (1954). *J. Am. Pharm. Assoc., Sci. Ed.* **43,** 385.

Gottlieb, O. R., Veloso, D. P., and Pereira, M. O. (1975). *Rev. Latinoam. Quim.* **6,** 188.

Hakkesteegt, T. J. (1970). *Pharm. Weekblad.* **105,** 829.

Hasegawa, M., Sozuki, Y., and Tamaki, T. (1970). *Bull. Chem. Soc. Jap.* **43,** 3020.

Hjortas, J., and Sorum, H. (1971). *Acta Cryst.* **B27,** 1320.

Houk, K. N., and Northington, D. T. (1972). *Tetrahedron Lett.* 303.

Jasya, T. S., and Anderson, R. S. (1962). *J. Chem. Phys.* **36,** 2727.

Jungk, A. E., and Schmidt, G. M. J. (1970). *J. Chem. Soc., B,* 1427.

Jungk, A. E., Luwisch, M., Pinchas, S., and Schmidt, G. M. J. (1977). *Isr. J. Chem.* **16,** 308.

Kaiser, J., Wegner, G., and Fisher, E. W. (1972). *Isr. J. Chem.* **10,** 157.

Kaminski, E. E., Cohn, R. M., McGuire, J. L., and Carstensen, J. T. (1979). *J. Pharm. Sci.* **68,** 368.

Kawada, A., and Labes, M. M. (1970). *Mol. Cryst. Liq. Cryst.* **11,** 133.

Konnert, J., Gibson, J. W., Karle, I. L. Khattak, M. N., and Wang, S. Y. (1970). *Nature (London)* **227,** 953.

Lahav, M., Laub, F., Gati, E., Leiserowitz, L., and Ludmer, Z. (1976). *J. Am. Chem. Soc.* **98,** 1620.

Leonard, N. J., McCredie, R. S., Logue, M. W., and Crindall, R. L. (1973). *J. Am. Chem. Soc.* **95,** 2320.

Lisewski, R., and Wierzchowski, K. L. (1970). *Photochem. Photobiol.* **11,** 327.

Miyagawa, I., and Gordy, W. (1960). *J. Chem. Phys.*, **32,** 255.

Mullins, J. D., and Macek, T. J. (1960). *J. Am. Pharm. Assoc.* **49,** 245.
Nath, A., Agarwal, R., and Lemmon, R. M. (1974). *J. Chem. Phys.* **61,** 1542.
Nath, A., Agarwal, R., Marton, L., Subramanyan, V., and Lemmon, R. M. (1971). *J. Am. Chem. Soc.* **93,** 2103.
Patten, F., and Gordy, W. (1961). *Radiat. Res.* **14,** 573.
Perlmutter, H. D., and Trattner, R. B. (1978). *J. Org. Chem.* **43,** 2056.
Pincock, R. E. (1969). *Acc. Chem. Res.* **2,** 97.
Quina, F. H., and Whitten, D. G. (1977). *J. Am. Chem. Soc.* **99,** 877.
Rabinovich, D., and Schmidt, G. M. J. (1967). *J. Chem. Soc., B,* 144.
Rabinovich, D., and Schmidt, G. M. J. (1970). *J. Chem. Soc., B,* 6.
Rieke, R. D., and Copenhafer, R. H. (1971). *Tetrahedron Lett.,* 829.
Rustgi, S. N., and Box, H. C. (1974). *J. Chem. Phys.* **60,** 3343.
Scheffer, J. R., and Dzakpasu, A. A. (1978). *J. Am. Chem. Soc.* **100,** 2163.
Schmidt, G. M. J. (1964). *J. Chem. Soc.,* 2014.
Schmidt, G. M. J. (1971). *Pure Appl. Chem.* **27,** 647.
Shields, H., Hammrick, P., and DeLaigle, D. (1967). *J. Chem. Phys.* **46,** 3649.
Tomkiewicz, Y., Agarwal, R., and Lemmon, R. M. (1973). *J. Am. Chem. Soc.* **95,** 3144.
Wang, S. Y. (1966). *Photochem. Photobiol.* **5,** 323.
Wright, G. E., and Tang, T. Y. (1972). *J. Pharm. Sci.* **61,** 299.

# V | Solid-State Thermal Reactions

# 10 Solid-State Thermal Reactions

In this chapter, solid-state thermal reactions are discussed. For purposes of classification, heat-induced reactions that do not involve gases as reactants or products are considered in this chapter. Other solid-state reactions induced by heat are considered in the chapters on polymorphs and desolvations. Unlike the reactions discussed in this chapter, polymorphic transformations and desolvations do not involve the formation or breaking of any covalent bonds.

## I. Solid-State Rearrangement Reactions

### A. REARRANGEMENT OF TEREPHTHALATE ESTERS

Byrn, Curtin, and Paul (1972) reported the reaction of the yellow dimethyl 3,6-dichloro-2,5-dihydroxyterephthalate (**1Y**). This ester transforms to the white isomer (**1W**) upon heating. Photomicrographic analysis of this reaction shows that the transformation of the yellow crystal to the white usually begins on an edge and proceeds through the crystal in a front. Chemically, this reaction involves only a change in hydrogen bond-

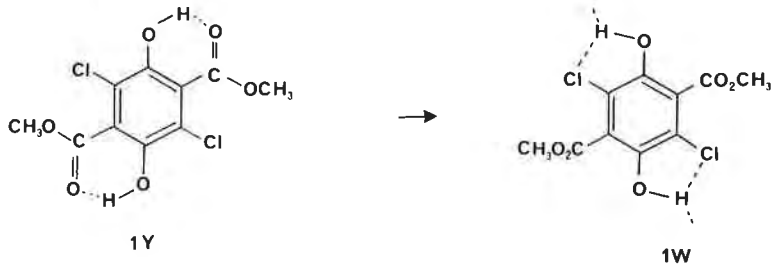


1Y 1W

ing and a conformational change. As shown in Figure 1, upon conversion of **1Y** to **1W** the carboxyl groups rotate out of the plane of the aromatic ring and form hydrogen bonds to the hydroxyl groups of adjacent mole-

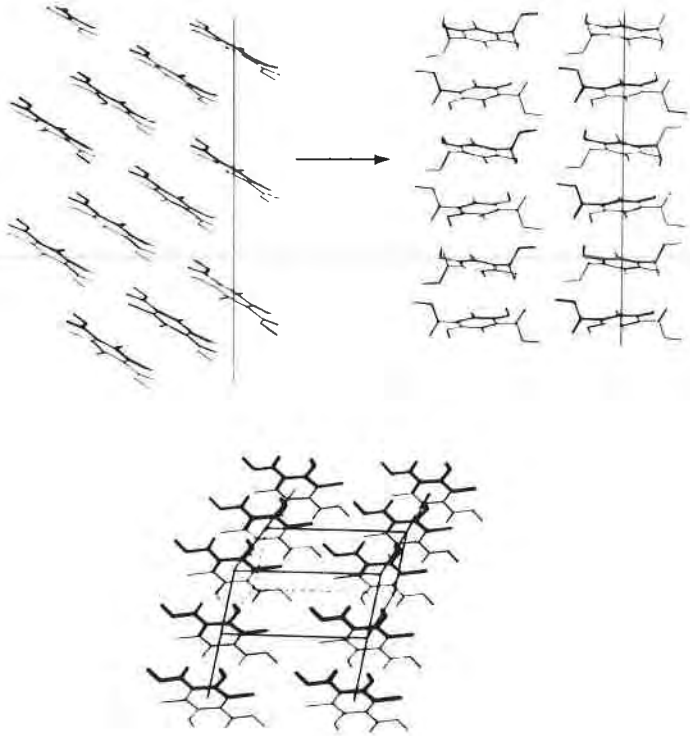

**FIGURE 1.** The top photograph shows the change in molecular structure that occurs when **1Y** (left structure) is converted to **1W** (right structure). The view is perpendicular to the direction of front advancement. The bottom photograph shows a different view of the molecular structure. In this view the direction of front advancement is across the page (from left to right). This view indicates that it is reasonable to postulate that disorientation of one of the vertical stacks is not readily transmitted to the next (Paul and Curtin, 1973). Reprinted with permission from I. C. Paul and D. Y. Curtin [1973]. Copyright 1973 American Chemical Society.

cules in the stack. In addition, the conversion of **1Y** to **1W** requires that every other molecule in a stack rotate 180° about the Cl–Cl axis or some other equivalent motion. It is possible to explain the behavior of crystals of **1Y** shown schematically in Figure 1 in terms of rapid reaction in a given stack and transmission to adjacent stacks in one direction but not to stacks in the other direction. Anisotropic behavior such as that observed for **1Y** is also characteristic of some solid-state reactions such as desolvation. Thus anisotropic behavior might be considered another criterion for a solid-state reaction.

In addition, the conversion of **1Y** to **1W** was almost instantaneous in solution, indicating that $k_{liq}/k_{solid}$ was very large for this reaction.

## B. BECKMAN–CHAPMAN REARRANGEMENT OF PICRYL ETHERS

McCullough, Curtin, and Paul (1972) have studied the Beckman–Chapman rearrangement of the benzophenone *o*-picryl ethers (**2**) to give the *N*-picrylbenzanilide (**4**). The same product, **4**, was formed whether the

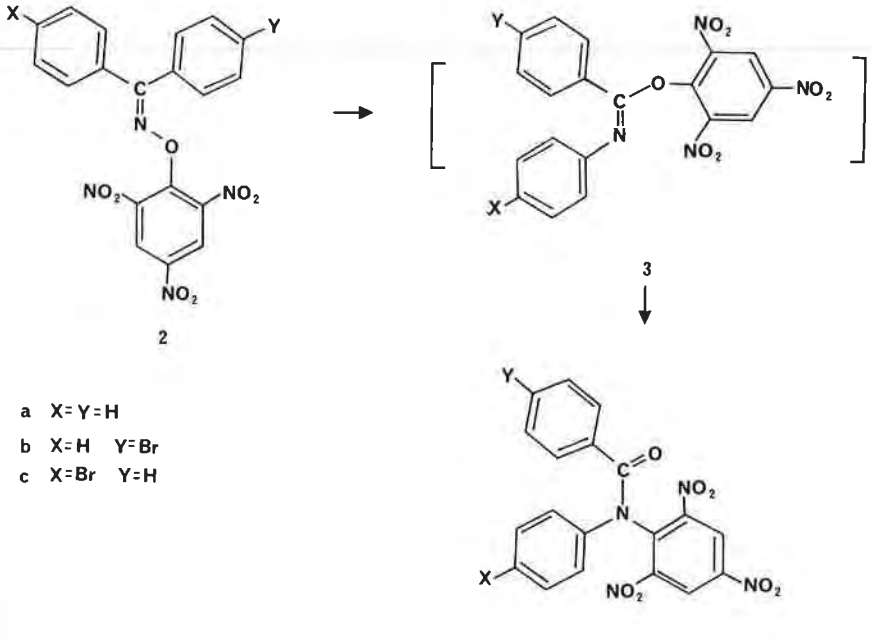


reaction was run in the solid or solution. This reaction, which proceeds via intermediate **3**, involves migration of two groups to form **3** and then migra-

tion of the trinitrobenzyl group to form **4**. In the solid state, great variation in the behavior of individual crystals was observed. Large crystals cracked and broke during reaction. This may indicate that the reaction initially forms a solid solution of **4** in crystals of **2** and then crystals of the product **4** separate causing the cracking and breaking.

Thus this reaction illustrates the solid-solution step and the separation of product step in Paul and Curtin's four-step sequence of solid-state reactions. In addition, the molecular change in this reaction is apparently the same in both the solid and solution reactions.

Comparison of the rates of the solid-state and solution reactions showed that the solution reaction was only 6–14 times faster than the solid-state reaction. These rates are in the middle of the expected $k_{liq}/k_{solid}$ ratios and indicate that the reaction cannot be occurring via a gas-phase rearrangement of a small amount of vapor in equilibrium with the crystalline solid. Such a process would have a much larger ratio, since the rate of reaction in the vapor should be comparable to that found in nonpolar solvents and only a small amount of reactant could be present as a vapor at any one time.

These kinetic studies thus appear to indicate that the molecular mechanism of the solid-state reaction is quite similar to that of the solution reaction. This reaction was also studied by differential thermal analysis (DTA) in hopes of further defining the mechanism: it showed that the $\Delta H$ of the reaction of **2c** (solid) → **4c** (solid) is about −80 kcal/mole. This $\Delta H$ is consistent with values predicted from bond-dissociation energies.

## C. BENZOYL-TRANSFER REARRANGEMENTS IN AZOTRIBENZOYLMETHANES

The rearrangement of phenylazotribenzoylmethane (**5**) to $\alpha$-phenylazo-$\beta$-benzoyloxybenzalacetophenone (**6**) and the hydrazone (**7**) occurs in

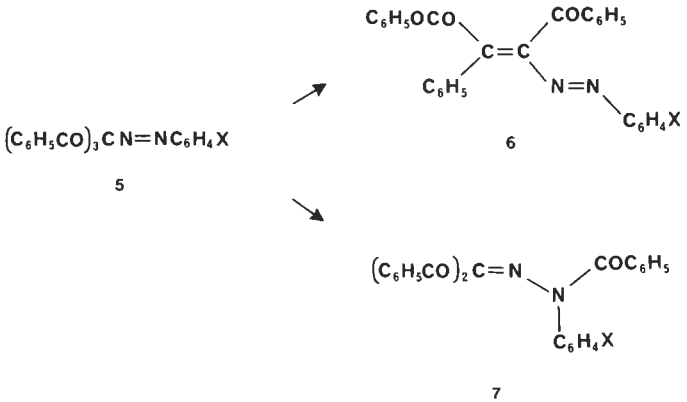


5 6 7

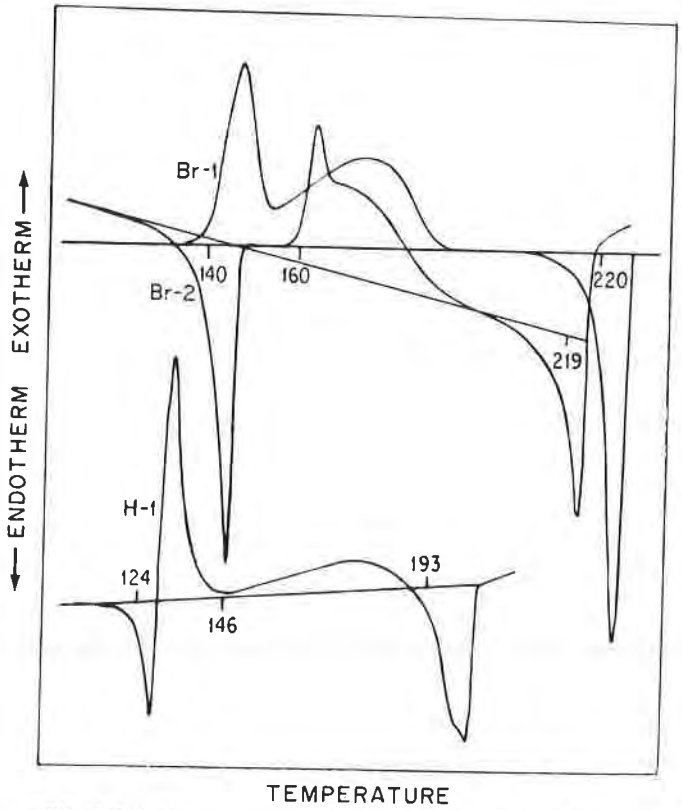


**FIGURE 2.** The differential thermal analysis (DTA) thermograms of **5**, X = H (labeled H-1); **5**, X = Br (labeled Br-1); and **6**, X = Br (labeled Br-2). For **5**, X = H, the heating rate was 5°C/min; for **6**, X = Br, the heating rate was 10°C/min. The baseline is indicated for each thermogram, as well as the temperature of onset of each thermal change (Curtin *et al.*, 1969). (Reprinted with permission from D. Y. Curtin, S. R. Byrn, and D. B. Pendergrass, Jr. [1969]. Copyright 1969 American Chemical Society.)

the solid state (Puckett *et al.*, 1966; McCullough *et al.*, 1970; Pendergrass *et al.*, 1972). The rearrangement of the starting material **5** to the red product **6** involves a 1,3-C to O acyl migration, while the formation of white **7** from **5** involves a 1,3-C to N acyl migration. Figure 2 shows the DTA thermograms of **5**, X = H (labeled H-1); **5**, X = Br (labeled Br-1), and **6**, X = Br (labeled Br-2). To identify the chemical changes associated with the various thermal changes, the heating was interrupted at various times by rapid cooling of the sample with dry ice. The reaction mixture was then analyzed by UV–visible spectroscopy. This analysis showed that the endotherm at 124°C in the thermogram of **5**, X = H, was associated with partial melting and that the subsequent exotherm corresponded to the rearrangement to approximately equimolar mixtures of **6**

and **7**. The exotherm beginning at 145°C was associated with a slower rearrangement of the remaining **6** to **7**. The endotherm at 200°C was due to melting of **7** (reported mp 199–200°C). The thermogram Br-1 of **5**, X = Br, was similar to that of **5**, X = H, except the initial endotherm was absent. Chemical analysis showed that the interpretation of this thermogram was identical to that of **5**, X = H. The thermogram of **6**, X = Br, shows an endotherm at approximately 140°C that corresponds to melting, an exotherm at 140°C that corresponds to rearrangement to **7**, and subsequent melting of **7**.

Estimates of the $\Delta H$ of the melting endotherms of the product **7** in these reactions indicate that the product is formed in a highly ordered state, since the $\Delta H$ of melting of crystalline **7** is approximately the same as that of the product formed.

Kinetic studies of this reaction in the solid state indicate that it is first-order after an induction period. Since **5** can be obtained in a number of crystalline forms, an analysis of the rate constant in terms of the crystalline form can be made (Table I). These rates show the wide variation that can occur under different conditions. Nevertheless, the solid-state reaction was at least 100 times slower than the liquid reaction. The ratio of **6**:**7** formed from **5** ranges from 0.5 at 65°C to 1.21 at 102–8°C in the solid versus 0.97 at 58.8°C and 0.92 at 77.1°C in dioxane solution. These different product ratios show the influence that the solid state can exert on product ratios. Both the differences in ratios of solid versus liquid product and in rates argue that this reaction is a true solid-state reaction at least in part, even though melting was observed in the DTA reaction. Note that these kinetic studies were done at 90°C, more than 30°C below the temperature at which melting was observed.

## D. REARRANGEMENT OF THE YELLOW FORM OF 2-(4′-METHOXYPHENYL)-1,4-BENZOQUINONE

Desiraju, Paul, and Curtin (1977) reported an interesting study of the solid-state rearrangement of the yellow form of 2-(4′-methoxyphenyl)-

**TABLE I**
*Rates of Reaction (First-Order) of Crystals of* ***5*** *at 90°C*

| Crystal | $k \times 10^6$ ($sec^{-1}$) |
|---|---|
| Crystals from xylene–hexane | 25.0 ± 2.0 |
| Crushed crystals from xylene–hexane | 14.6 ± 0.8 |
| Desolved crystals of an ether solvate | |
| Pointed form | 324 |
| Blunt form | 50 |
| Crushed | 12.8 ± 0.5 |

1,4-benzoquinone (**8**) to the red form. The crystals of the yellow form rearrange to the red form upon heating. Individual crystals of the yellow

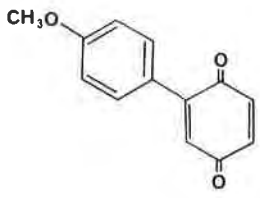


**8**

form show an enormous variation in the rate of reaction. Some reacted in a few hours at room temperature, while others rearranged only when heated above 100°C.

Reaction of a yellow crystal begins at a nucleation site inside the crystal and spreads through the crystal in well-defined fronts. This behavior is reminiscent of the behavior of **1Y.** The crystal structures of the two forms of **8** are shown in Figure 3.

In the yellow form there are stacks of quinone and anisyl groups coming out of the plane of the paper. In the red form, the stacks contain quinone, anisyl, quinone, etc. Thus the conversion of yellow **8** to red **8** requires either slippage along *c* or rotation of half the molecules 180° about a direction perpendicular to the *c* axis. Experimentally it is impossible to distinguish between these explanations.

## E. THERMAL REARRANGEMENTS OF IODOBENZOYL PEROXIDES

Gougoutas, Etter, Clardy, Lessinger, and Naae, at both Harvard University and the University of Minnesota at Minneapolis, have conducted extensive studies of the thermal solid-state rearrangement of the iodobenzoyl peroxide (**9**) to the iodoso compounds **10** and **12** and the benzoic acid **11** (Gougoutas and Clardy, 1972; Gougoutas and Lessinger, 1973; Gougoutas and Naae, 1976; Gougoutas, 1977; Etter, 1976). These reactions are generally considered thermal reactions; however, at least one of these also occurs photolytically. The conversion of **9** and **10** to **11** requires the presence of atmospheric moisture and is thus a solid-state hydrolysis reaction related to other reactions such as the hydrolysis of solid acetylsalicylic acid discussed earlier. The conversion of **9** to **10** is most likely a free-radical reaction. All of these reactions have also been observed in solution.

Studies of a series of crystalline benzoyl peroxides (**9**) shows that these crystals belong to two general groups based on their reactivity. Crystals of group A react to form the benzoxiodo isomers **10**. Crystals of group B

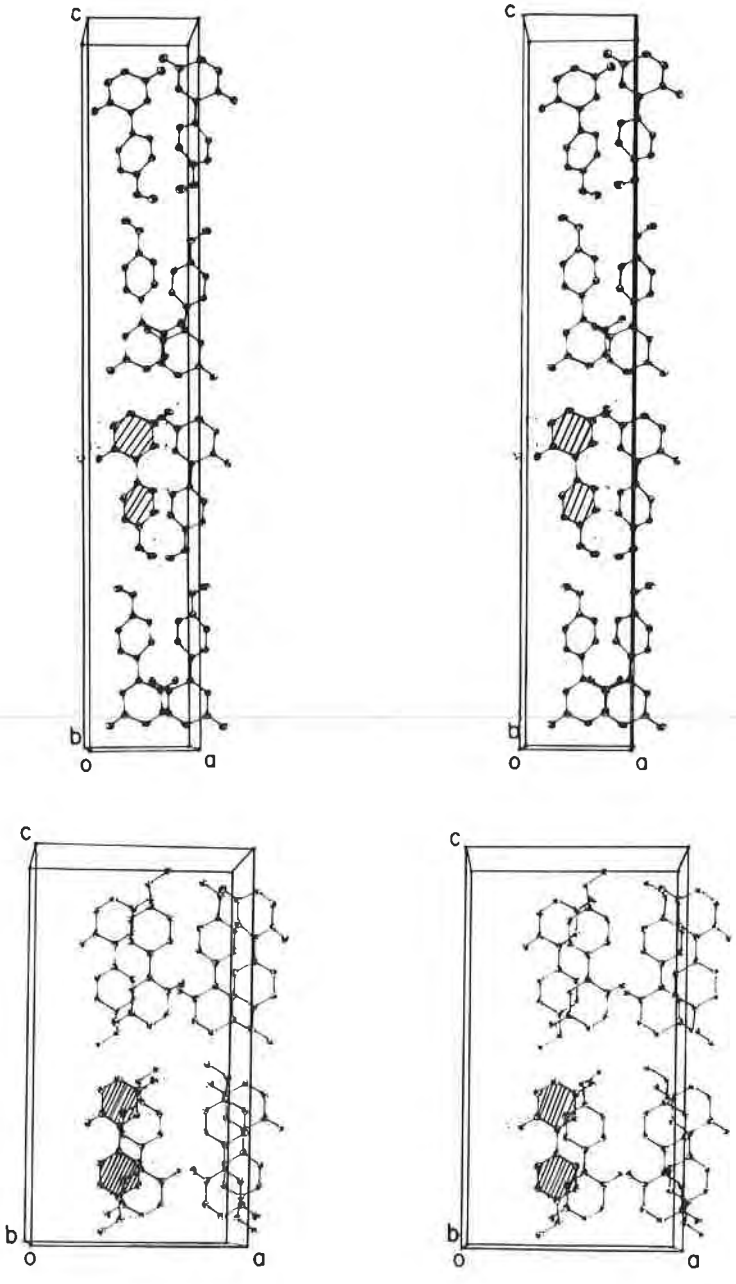


**FIGURE 3.** Stereo views of the crystal packing of the yellow form of **8** (upper panels) and red form of **8** (lower panels) (Desiraju *et al.*, 1977). (Reprinted with permission from G. R. Desiraju, I. C. Paul, and D. Y. Curtin [1977]. Copyright 1977 American Chemical Society.)

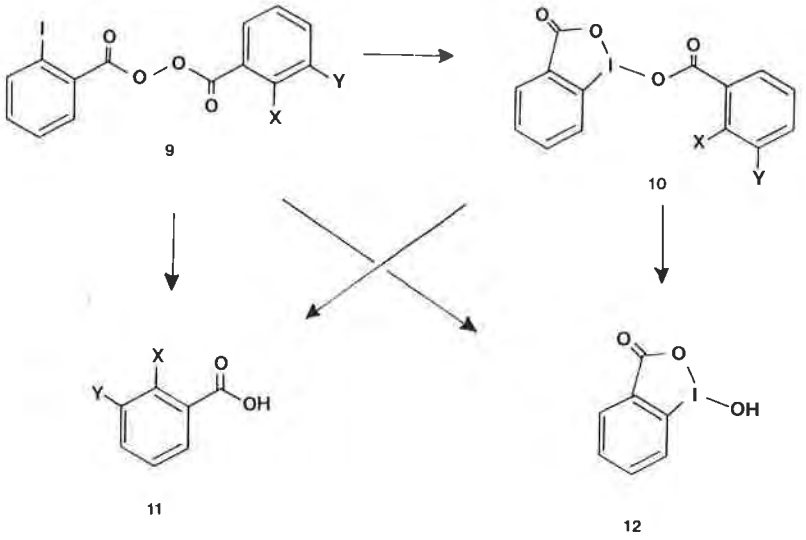

9 10 11 12

| GROUP A | | GROUP B | |
|---|---|---|---|
| X | Y | X | Y |
| I | H | F | H |
| Br | H | H | H |
| Cl | H | H | Cl |

appear to be more susceptible to hydrolysis by atmospheric moisture and thus give the hydrolysis product **11** and the product **12**, the hydrolysis product of 10. In addition, these crystals exist in several polymorphs.

The differences in reactivity are in general consistent with the structures of the crystals of groups A and B. Crystals of group A have a crystal structure that would allow the intermolecular reaction shown in Scheme I. Thus the reaction of **9** to form **10** is favored by the crystal structure of the group A crystals. In the group B crystals, there are no short I · · · X contacts: thus rearrangement to form **10** is not favored and other reactions occur. This reasoning predicts that after electronic effects, if any, have been subtracted, crystals of group A should react faster than those of group B. Unfortunately, the relative rates of reaction of these crystals have not been reported. Nevertheless, the fact that chemically similar compounds give entirely different products upon reaction in the solid state meets one of Morawetz's criteria for solid-state reaction.

In addition, single crystals of the type I polymorphs of group A are transformed topotactically into single crystals of products (Gougoutas and Clardy, 1972; Gougoutas and Lessinger, 1973; Gougoutas and Naae,

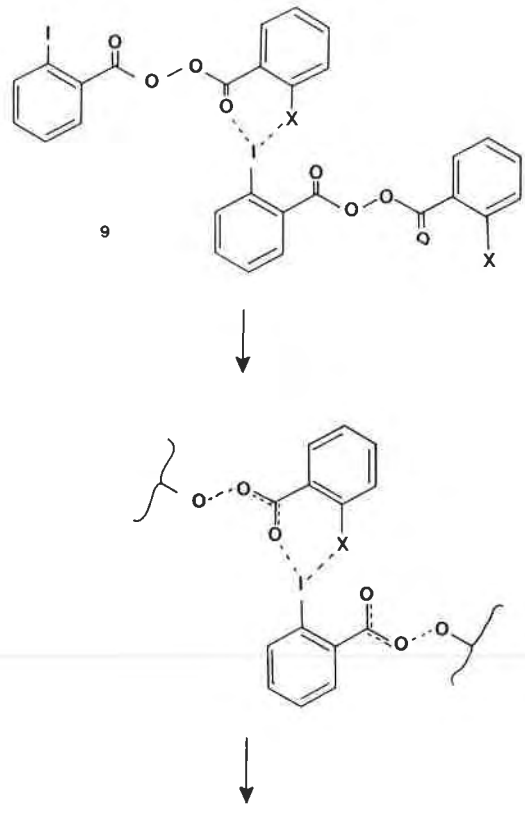

9

10

SCHEME I

1976). Thus these reactions meet a second criterion for solid-state reactions.

In the case of **9**, X = Br, Y = H, the product is dimorphic and in humid conditions the other two products **11** and **12** are formed. All of these phases are single crystals: thus five different single crystalline phases coexist. Studies on the reaction of **10** show that different orientations of single-crystalline **11** and **12** are formed in this reaction. This indicates that the orientation of **11** and **12** from the peroxide **9** is governed by the crystal structure of **9** and not the structure of the first product **10**. Thus crystalline **9** appears to control the orientation of the two phases of **10** as well as that of **11** and **12** (Gougoutas, 1977).

In another study, Gougoutas and Naae (1976) have compared the photochemical and thermal behavior of **9**, X = Cl, Y = H. Scheme II

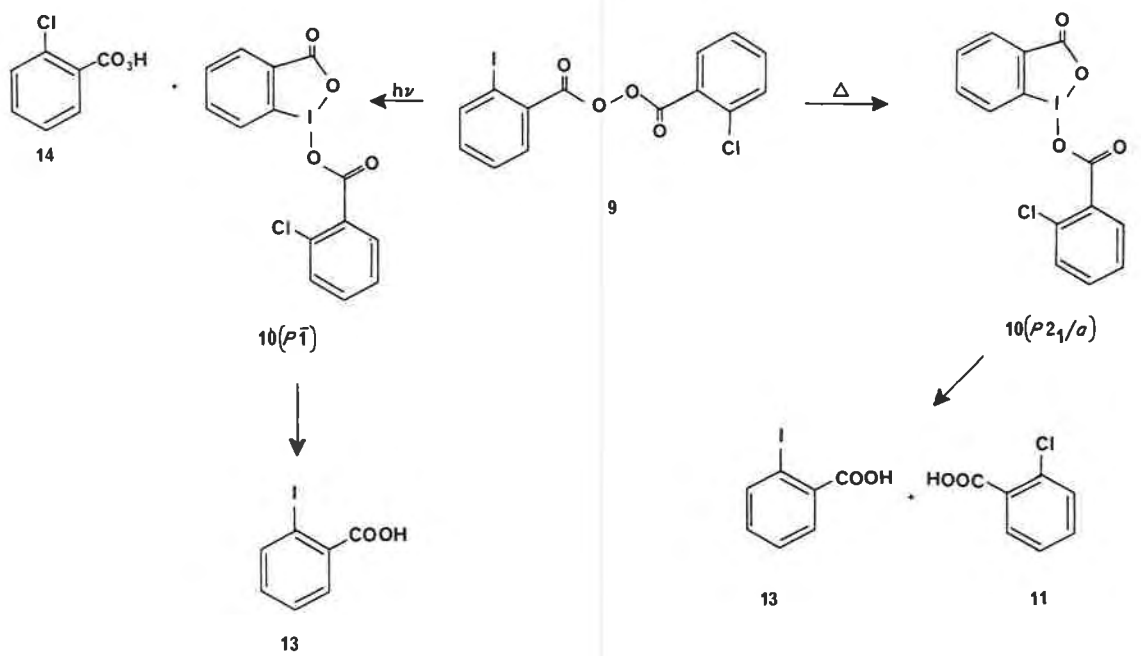


SCHEME II

summarizes the results of their studies. The peroxide **9** rearranges to the iodoso compound **10,** which is in space group $P2_1/a$. This product then decomposes to a solid solution of **11** in **13.** These two components appear to be mutually soluble over almost all concentration ratios. The rearrangement of **9** to **10** and then decomposition to **13** and **11** is the reaction that has just been discussed.

In contrast, irradiation of **9** produced **10** in space group $P\bar{1}$ and chloroperbenzoic acid (**14**) as whiskers on the starting crystal. The iodoso compound **10** then further decomposed to **13.**

The fact that a different polymorph of **10** is formed in the photochemical reaction may indicate a difference in mechanism. This is consistent with the vastly different rates and the formation of a different product, **14**, in the photochemical reaction. However, since both the thermal and photochemical reactions are free-radical reactions the reason for a difference in mechanism is not obvious.

These studies illustrate the wide range and consequences of topotactic reactions that occur in the iodobenzoyl peroxides.

## II. Thermal Retro Cycloaddition Reactions

While a number of solid-state cycloaddition reactions have been reported, especially by the researchers at the Weizmann Institute (see Chapter 9), relatively few studies of the reverse reaction have been reported. In this section, three thermally induced solid-state retro Diels–Alder reactions are discussed.

### A. THERMAL MONOMERIZATION OF 9-CYANOANTHRACENE DIMERS

The *syn*-9-cyanoanthracene dimer (**15**, R = H) and the *syn*-9-cyano-10-acetoxyanthracene dimer (**15**, R = $OCOCH_3$) are thermally converted to the monomer (Donati *et al.*, 1972). These reactions have been studied by differential scanning calorimetry (DSC). The DSC studies show that the

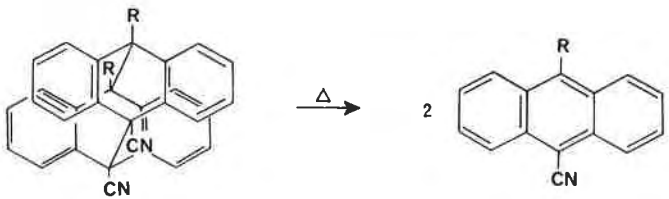


15

monomerization occurs at 30°–130°C below the melting point of the monomer. While the eutectic melting point of the monomer–dimer mixture was not determined, it is reasonable to consider this a solid-state reaction.

In addition, it is quite reasonable to expect that the dimer crystals could accommodate a significant amount of monomer as a solid solution. Thus this monomerization could occur in a reaction cavity of the type visualized by Cohen and could even be a topotactic reaction. However, crystallographic studies of this reaction are needed to test these suggestions.

## B. THERMAL REACTION OF BI[ANTHRACENE-9,10-DIMETHYLENE] (16)

The thermal reaction of **16** to yield **17** has been investigated in the solid state and in solution (Mau, 1978). Differential thermal analysis was used to

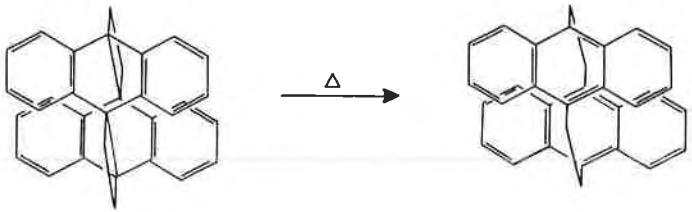


**16** **17**

get the rate constants of the solid-state reaction, and conventional methods were used to get the rates of the solution reaction.

For the solid-state reactions, first-order kinetics were assumed. However, plots of $\ln k$ versus $1/t$ were not linear, and the researchers proposed an autocatalytic mechanism to explain the kinetics. Plots of $\ln [k/(1 - \alpha)]$ versus $1/t$ were linear and yielded reasonable rate constants. To the extent that these assumptions are invalid, the absolute value of the rate constants are incorrect. However, the relative value of the rate constants is a reasonable measure of the relative reactivity in the solid state. Table II compares rate constants in different media.

These data show that the solid-state reaction has a rate with the same order of magnitude as in the solution reaction. This rules out a mechanism involving monomerization of a small amount of **16** in the vapor state and crystallization of the product. Such a mechanism would have a $k_{liq}/k_{solid}$ ratio much larger than unity, since the vapor-phase rate would be approximately the same as the rate in nonpolar solvents and the concentration of reactant in the vapor would be small.

The rate of reaction of **16** homogenously dispersed in product crystals

**TABLE II**
*Rate Constants for the Conversion of* **16** *to* **17**

| Reaction medium | Rate constant at 298 K, $k_{298}$, ($sec^{-1}$) |
|---|---|
| Toluene solution | $4.1 \times 10^{-6}$ |
| Product host crystal (isothermal data, 100°C) | $1.0 \times 10^{-5}$ |
| Initial stage of reaction, normal crystal | $1.4 \times 10^{-7}$ |
| **16** Homogenously dispersed in crystals of **17** | $3.5 \times 10^{-6}$ |

was measured by photolyzing crystals of **17** until they contained about 15% of **16** and then measuring the rate of reversion of **16** to **17**. The fact that this rate is slower than the rate of conversion of **16** to **17** when pure crystals of **16** are reacted seems to substantiate the idea that during reaction of pure crystals of **16**, some sort of autocatalytic mechanism is in operation.

Further crystallographic studies of this reaction aimed at determining whether it is topotactic are in order.

## C. RING-OPENING OF TRICYCLO[4,2,0.$0^{2,5}$]OCTANES

The tricyclo[4,2,0.$0^{2,5}$]octane (**18**) is stereospecifically converted to the (*Z*,*E*)cycloocta-1,5-diene (**19**) in 96% yield via a solid-state reaction (Bel-

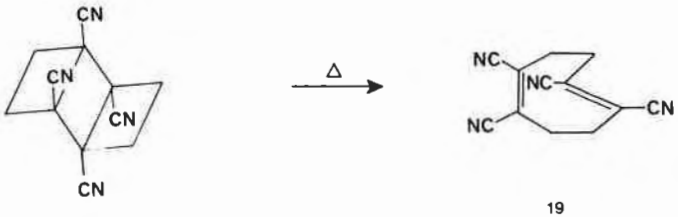


18 19

lus *et al.*, 1974). This is the first known example of this reaction, which is an allowed process according to orbital symmetry rules. Heating **18** in solution did not form **19** but instead yielded **20**, which is not predicted on the basis of orbital symmetry.

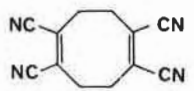


20

The conversion of **18** to **19** occurs at temperatures 60°–90°C below the melting point of **18**, and the rate data fit first-order kinetics after an initial induction period. The rate constant for the solid-state reaction is $10^3$ times less than the rate constant for the solution reaction of a structurally related model compound.

These three facts (different products are formed from the solution reaction, the low temperature of the reaction, and the slow rate of the solid state reaction) all argue that this reaction is a true solid-state process. Further studies of the crystallography of this reaction would provide even more insight into this reaction.

## III. Solid-State Thermal Reactions of Drugs and Biologically Important Compounds

The reactions discussed thus far in this chapter have not involved biologically important compounds; however, the study of these organic solid-state reactions lays the groundwork for understanding solid-state thermal reactions of drugs.

In this section, three solid-state thermal reactions of biologically important compounds are considered, relying on the previous discussion to put the reaction in perspective and to suggest further experiments.

### A. METHYL-TRANSFER REACTIONS

The methyl ester of tetraglycine (**21**) rearranges to the corresponding methylammonium salt (**22**) when heated at 100° in the solid state (Sluyter-

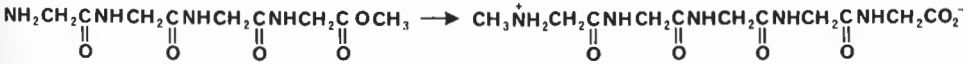

**21** **22**

man and Veenendaal, 1952; Sluyterman and Kooistra, 1952). It is unlikely that this methyl-transfer rearrangement is unimolecular, and it may be facilitated by crystal packing that places the $CH_3$ group near the $NH_2$ group.

The solid-state reaction is quite different from the solution reaction, in which tetraglycine methyl ester polymerizes upon heating. This means that one of the criteria for solid-state reactions is met: a solid-state reaction gives different products from the corresponding solution reaction.

Further studies of the kinetics of this reaction and the crystal structure of tetraglycine methyl ester would certainly shed light on this reaction. In

the absence of these studies, it is instructive to consider the solid-state methyl-transfer reaction of methyl *p*-dimethylaminobenzenesulfonate (**23**) to form *p*-trimethylammonium benzenesulfonate (**24**) (Sukenik *et al.*,

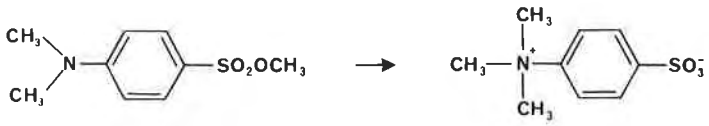

23 24

1977). The intermolecularity of this reaction was studied via a labeling experiment performed by reacting a 50 : 50 mixture of **23** and $d_6$-**23**. The distribution of deuterium atoms in the product indicated that the reaction is $\geq$76% intermolecular.

Studies of the kinetics of the solid-state reaction revealed that it was 25 to 40 times faster than the reaction in the melt. This evidence strongly indicates that the reaction is a true solid-state reaction, even though studies of the reaction were done at only 15°C below the melting point. In addition, a determination of the crystal structure of the reactant **23** provided a ready explanation for the accelerated solid-state reaction. Figure 4 shows a view of the stacking of the molecules in crystals of methyl *p*-dimethylbenzenesulfonate (**23**).

It is obvious from Figure 4 that very little molecular movement is required for the reaction to occur, and in fact the molecules are in an almost perfect orientation for reaction. This explains why the solid-state reaction is faster than the liquid reaction. It is perhaps surprising that the favorable orientation present in the solid state results in only a 25- to 50-fold increase in rate.

The data on the benzenesulfonate (**23**) makes it tempting to speculate that a similar type of crystal packing favors the methyl transfer in the tetraglycine methyl ester. Such packing would also explain why tetraglycine methyl ester polymerizes when heated in solution. Further studies aimed at explaining the reaction of tetraglycine methyl ester are definitely in order.

## B. REACTIONS OF BENZENEARSENOUS ACIDS

In the late 1940s, Banks, Controulis, Walker, and Sultzaberger (1947) reported an interesting study of the important antisyphilitic drug, 3-amino-4- hydroxybenzenearsenous acid (oxyphenarisine) (**25**) (Banks *et al.*, 1948; Banks, 1949). Crystalline 3-amino-4-hydroxybenzenearsenous acid (**25B**) can be prepared by published procedures and yields (upon

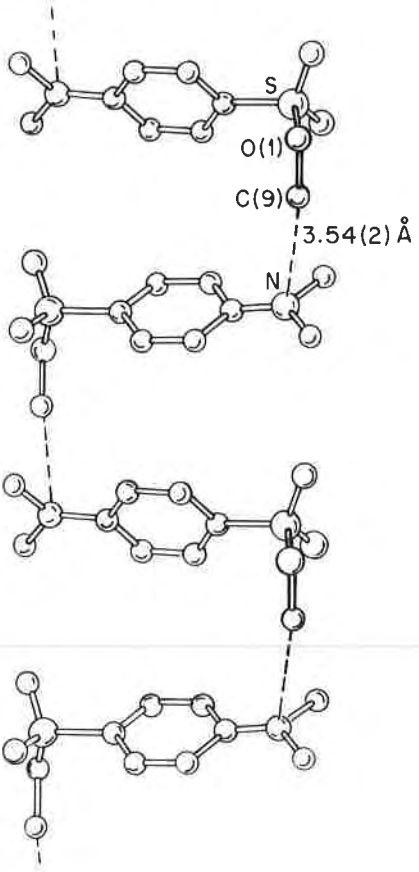


**FIGURE 4.** The stacking of one chain of methyl *p*-dimethylaminobenzenesulfonate molecules, viewed perpendicular to the (101) plane. The C(9) atom is of the methyl group that is transferred to the connected nitrogen atom during the reaction (Sukenik *et al.*, 1977). (Reprinted with permission from C. N. Sukenik, J. A. P. Bonapace, N. S. Mandel, P. Y. Lau, G. Wood, and R. G. Bergman [1977]. Copyright 1977 American Chemical Society.)

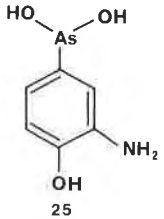


25

crystallization from oxygen-free water at pH 6.5) large colorless crystals of analytically pure 3-amino-4-hydroxybenzenearsenous acid (**25C**). Al-

though no crystallographic studies such as powder diffraction analysis have been performed, it has been suggested that **25B** and **25C** are different crystalline forms (Banks *et al.*, 1948). These were quite different from the amorphous form **25A**, particularly in their solid-state reactivity.

The amorphous form, **25A**, is much more reactive than the crystalline forms **25B** and **25C**. Form **25A** decomposes in a few days in the absence of air, while **25B** and **25C** are stable for 3 and 6 months, respectively, under similar conditions. These data are consistent with the reaction of all three forms being true solid-state reactions. The reactivity of the amorphous form is consistent with other studies in which it is found that amorphous forms are more reactive than their crystalline counterparts. The reasons for the greater reactivity of the amorphous forms may be related to the nature of these forms. Usually a solid is termed amorphous if it gives no x-ray diffraction pattern. The reason for a failure of a solid to give a diffraction pattern could be that (*a*) the solid has no crystalline structure or (*b*) the solid has a crystalline structure but the size of the crystallites are so small no diffraction is observed. If case (*a*) applies, it is easy to explain the enhanced reactivity of an amorphous form since the reaction would not be subjected to the usual restraints of a rigid, close packed crystal. However, if case (*b*) applies it is difficult to explain differences in reactivity between crystalline and amorphous solids.

In addition to the acid **25**, the anhydrous compound **26** can be prepared by azotropically removing water and alcohol from a benzene solution of

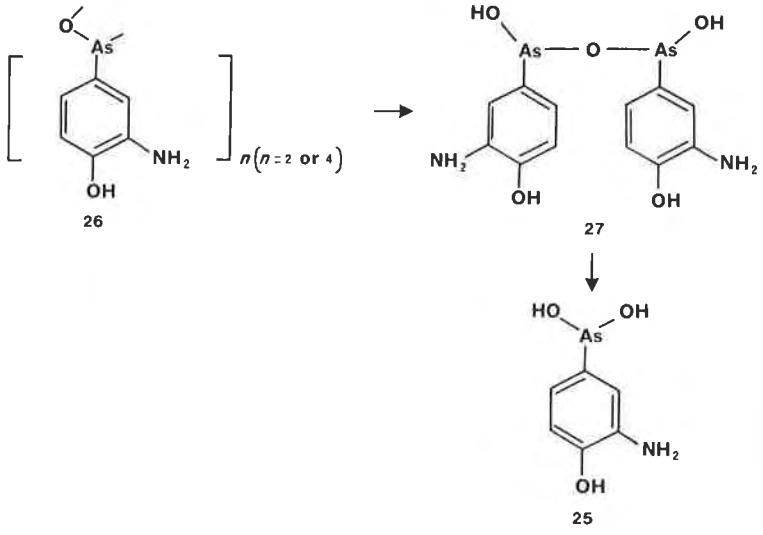

**25**. Evaporation of the benzene then yields **26**, which is reported to be a mixture of dimers and tetramers. Exposure of **26** to moist air yields the hemihydrate **27** and eventually **25**.

The hydrochloride salts of the acid **25** can also be prepared. Preparation of a concentrated solution of **25B** or **25C** in water in the presence of exactly 1 equivalent of HCl gave upon freeze drying a powder analyzed as $C_6H_6AsNO_2 \cdot HCl \cdot H_2O$, suggested to have the structure **28**. Careful dehydration of this hydrate gave $[C_6H_6AsNO_2 \cdot HCl]_2 \cdot H_2O$ (**29**), which is apparently the compound listed in "The Merck Index." Further dehydration yielded $C_6H_6AsNO_2 \cdot HCl$, which may have the dimer structure **30**.

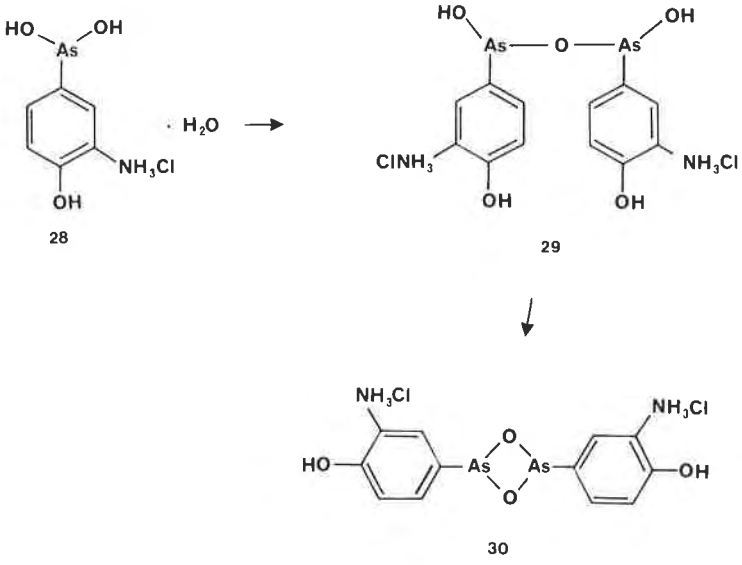


As mentioned previously, it should be noted that none of these structures have been rigorously established by crystallographic analysis and, for example, "The Merck Index" lists **29** as structure **31**. Obviously,

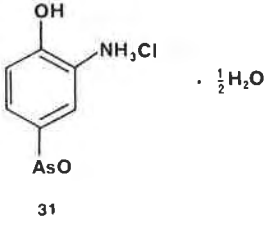

further crystallographic research is required to rigorously establish the structure of these compounds.

The solid-state decomposition of the anhydrous hydrochloride salt (**30**), the hydrated hydrochloride salt (**28**), and the free base (**25**) have been carefully studied by Banks (1949). The anhydrous salt (**30**) was very stable in the solid state; however, the hydrate (**28**) and the free base (**25**) decom-

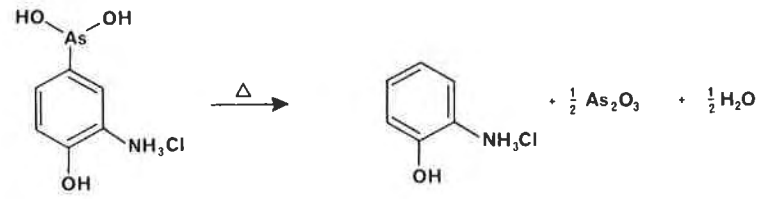


28 32 · HCl

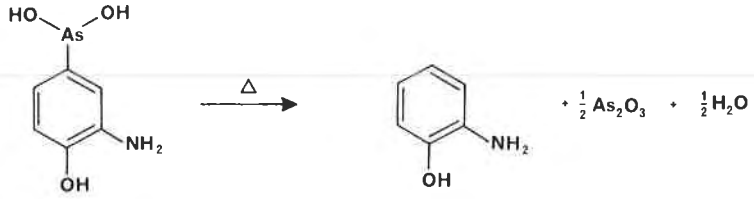


25 32

posed to give *m*-aminophenol hydrochloride (or *m*-aminophenol) and inorganic arsenic. In the presence of oxygen, the *m*-aminophenol formed is oxidized to **33** and **34**.

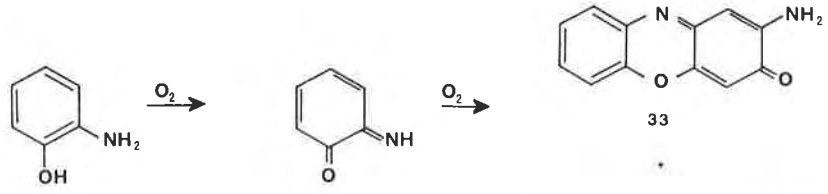


32 33

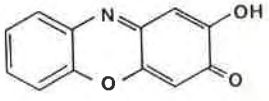


34

Further studies of the structures of these compounds and their solid-state reactivities would yield much useful information.

## C. REACTIONS OF ASPIRIN ANHYDRIDE

Aspirin anhydride (**35**), which at one time was thought to be a superior form of aspirin, has a rich and varied solid-state chemistry, and its stabil-

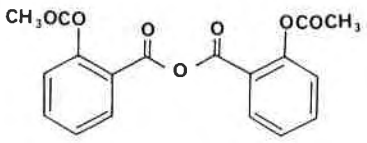


35

ity has been extensively investigated (Garrett *et al.*, 1959). The stability of three lots of crystals was investigated at 40°–70°C. Lot 1 was the least stable and liquified before the other lots. Analysis showed that this lot contained 1.2% water, much less than that for the monohydrate; however, this 1.2% represents a significant amount of residual water. The other lots contained significantly less water, so the instability and early liquefication of lot 1 was probably related to the high percentage of residual water.

In addition, the degradation of a particular lot was much faster in "soft" glass than in "hard" glass. This may be related to differences in water content in glasses, with soft glass containing more water.

These experiments show that aspirin anhydride can best be stabilized by careful drying and storage in "hard" glass containers.

Other experiments showed that contact of aspirin anhydride with salicylic acid accelerated the decomposition of aspirin anhydride. This acceleration was perhaps due to depression of the melting point, since salicylic acid is not an initial product of the decomposition reaction. However, the acceleration could also be due to moisture in the salicylic acid. Also, removal of the liquid and gaseous products of the decomposition of aspirin anhydride (mainly acetic anhydride and acetic acid) by a stream of warm air stabilized the remaining aspirin anhydride. Probably the removal of these products prevented liquefication.

The decomposition products of aspirin anhydride under both dry and moist conditions has been investigated. Under moist conditions, aspirin anhydride is reported to yield acetylsalicoylsalicylic acid (**36**) and acetic acid (**37**) as the final products. The acetylsalicoylsalicylic acid may arise from hydrolysis of the main product of the reaction in dry air.

Under dry conditions, aspirin anhydride yields mainly 2,2′-bis(2-acetoxybenzoyloxy)-benzoic anhydride (**38**) and acetic anhydride (**39**). The products of the reaction in moist air may arise from hydrolysis of **38** and **39**. In addition, smaller amounts of other transacylated products are probably also present.

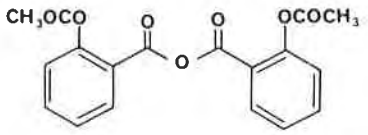


35

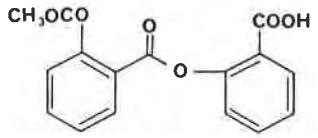


36

+

$CH_3COOH$

37

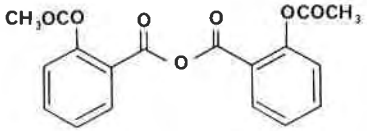


35

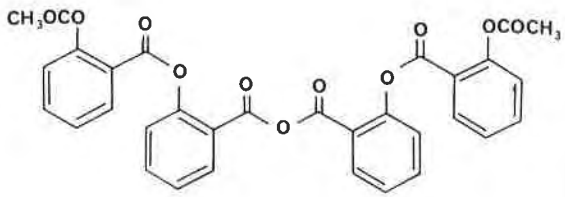


38

+

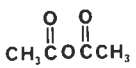


39

The crystal structure and behavior of single crystals of aspirin anhydride have been determined in our laboratory (Byrn and Siew, 1981).

Aspirin anhydride belongs to the tetragonal crystal system, space group $P4_12_12_1$ with $a = 8.457$ (1), $c = 23.166$ (6), and $Z = 4$. With $Z = 4$, each aspirin anhydride molecule is situated on a twofold rotation axis. The structure was solved by direct methods and refined to a final $R$ of 0.067. The bond lengths and bond angles were reasonable based on related molecules, and a stereo drawing of the molecule is shown in Figure 5.

The molecule geometry would allow facile transfer of a


group from O(3) to O(2) as shown in Scheme III. However, the products of this reaction are not obvious intermediates in the formation of **38**. Thus it is unlikely that such an intermolecular rearrangement is involved in the its formation.

Study of the intramolecular contacts show no close contacts ($\leq$4.0 Å)

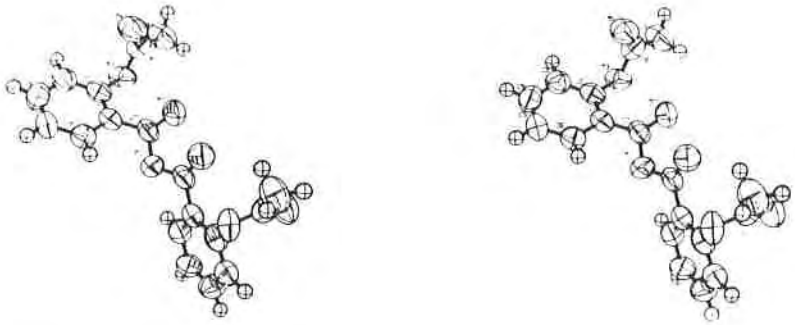

**FIGURE 5.** Stereo view of the conformation of aspirin anhydride in the crystal, along the (018) axis.

between C(7) and O(3), which are the two atoms that need to bond to form **38** from aspirin anhydride.

The crystallographic results do not indicate that the decomposition of aspirin anhydride takes place in a reaction cavity rigidly defined by the crystal structure and controlling the products formed. This is consistent with photographs of a crystal of aspirin anhydride during reaction. These do not indicate any anisotropic or crystallographically controlled reaction, and in fact show the presence of a pocket of liquid at one point.

## D. REACTIONS OF A TRIAZENOIMIDAZOLE

In the late 1960s, the synthesis of a potentially useful antileukemic agent was reported (James *et al.*, 1969; Shealy *et al.*, 1968; Shealy and Krauth, 1966). This compound, 5-[3,3-bis(2-chloroethyl)-1-triazeno]imidazole-4-carboxamide (**40**), however, rapidly isomerized in the solid state to form an ionic chloride. Subsequent single-crystal x-ray studies showed that the ionic chloride had structure **41**. This solid-state reaction was complete in 126 days at room temperature. The crystal structure of **40** has not been determined, but it is considered likely that the solid-state conformation of **40** allows facile cyclization to **41**.

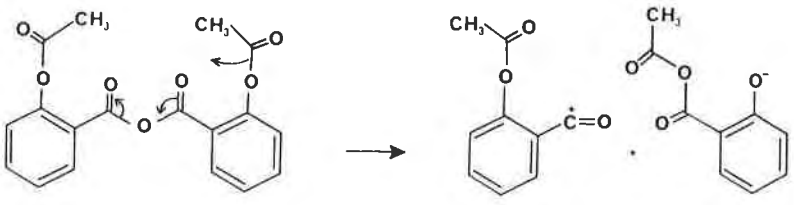

SCHEME III

40 41

This may thus be an example of a solid-state reaction facilitated by the orientation of the reactant in the crystal. This possibility makes the reaction very attractive for future studies.

## IV. Summary

The chapter indicates that drugs can show a wide range of behavior in the solid state, including reactions that give different products depending on crystalline form and on whether the reaction is run in the solid state or solution. Furthermore, at least one study shows that amorphous solids are much less stable than crystalline forms, and further studies are needed to determine the reasons for this behavior.

This chapter shows that x-ray crystallographic studies of the solid-state structure and behavior of the benzenearsenous acids and the tetraglycine methyl ester are urgently needed to explain the solid-state chemistry of these compounds.

## References

Banks, D. K. (1949). *J. Am. Pharm. Assoc., Sci. Ed.* **38,** 503, 509.
Banks, C. K., Controulis, J., Walker, D. F., and Sultzaberger, J. A. (1947). *J. Am. Chem. Soc.* **69,** 6.
Banks, C. K., Controulis, J., Walker, D. F., Tillitson, E. W., Sweet, L. A., and Gruhzit, O. M. (1948). J. Am. Chem. Soc. **70,** 1762.
Bellus, D., Mez, H. C., Rihs, G., and Suater, H. (1974). *J. Am. Chem. Soc.* **96,** 5007.
Byrn, S. R., and Siew, P. Y. (1981). *J. Pharm. Sci.*, **70,** 280–283.
Byrn, S. R., Curtin, D. Y., and Paul, I. C. (1972). *J. Am. Chem. Soc.* **94,** 890.
Curtin, D. Y., Byrn, S. R., and Pendergrass, D. B. Jr. (1969). *J. Org. Chem.* **34,** 3345.
Desiraju, G. R., Paul, I. C., and Curtin, D. Y. (1977). *J. Am. Chem. Soc.* **99,** 1594.
Donati, D., Guarini, G., and Sarti-Fantoni, P. (1972). *Mol. Cryst. Liq. Cryst.* **17,** 187.
Etter, M. C. (1976). *J. Am. Chem. Soc.* **98,** 5326.
Garrett, E. R., Schumann, E. L., and Grostic, M. F. (1959). *J. Am. Pharm. Assoc. Sci. Ed.* **48,** 684.
Gougoutas, J. Z. (1977). *J. Am. Chem. Soc.* **99,** 127.
Gougoutas, J. Z., and Clardy, J. C. (1972). *J. Solid State Chem.* **4,** 230.
Gougoutas, J. Z., and Lessinger, L. (1973). *J. Solid State Chem.* **7,** 175.
Gougoutas, J. Z., and Naae, D. G. (1976). *J. Solid State Chem.* **16,** 271.

James, R. H., Sternglanz, P. D., and Shealy, Y. F. (1969). *J. Pharm. Sci.* **58,** 1193.
Mau, A. W. H. (1978). *J. Chem. Soc., Faraday Trans. 1* **74,** 603.
McCullough, J. D. Jr., Curtin, D. Y., Miller, L. L., Paul, I. C., and Pendergrass, D. B. Jr. (1970). *Mol. Cryst. Liq. Cryst.* **11,** 407.
McCullough, J. D. Jr., Curtin, D. Y., and Paul, I. C. (1972). *J. Am. Chem. Soc.* **94,** 874, 883.
Paul, I. C., and Curtin, D. Y. (1973). *Acc. Chem. Res.* **6,** 217.
Pendergrass, D. B., Jr., Curtin, D. Y., and Paul, I. C. (1972). *J. Am. Chem. Soc.* **94,** 8722, 8730.
Puckett, R. T., Pfluger, C. E., and Curtin, D. Y. (1966). *J. Am. Chem. Soc.* **88,** 4637.
Shealy, Y. F., and Krauth, C. A. (1966). *Nature (London)* **210,** 208.
Shealy, Y. F., Krauth, C. A., Holum, L. B., and Fitzgibbon, W. E. (1968). *J. Pharm. Sci.* **57,** 83.
Sluyterman, L. A. A., and Kooistra, M. (1952). *Recl. Trav. Chim. Pays-Bas* **71,** 277.
Sluyterman, L. A. A., and Veenendaal, H. G. (1952). *Recl. Trav. Chim. Pays-Bas* **71,** 137.
Sukenik, C. N., Bonapace, J. A. P., Mandel, N. S., Lau, P. Y., Wood, G., and Bergman, R. G. (1977). *J. Am. Chem. Soc.* **99,** 851.

# VI Miscellaneous Topics

# 11

# Miscellaneous Topics in the Solid-State Chemistry of Drugs

In this chapter we review three important topics—defects in solid-state reactions, solid–solid reactions, and solid-state NMR Spectroscopy. In the future, we expect that these areas, particularly solid state NMR, will expand greatly.

## I. Role of Defects in Solid-State Reactions

Thomas and his group have carried out extensive studies of the influence of defects on solid-state reactions of inorganic compounds. They have also studied the influence of defects on the solid-state photochemical reactions of organic compounds. The objective of their study of solid-state photochemical reactions of organic compounds was to explain the breakdown of the topochemical postulate in certain solid-state photochemical dimerizations. For example, they hoped to show that the dimerization of 9-cyanoanthracene, which leads to the centrosymmetric photodimer (rather than the minor symmetric photodimer predicted on the basis of the topochemical postulate), occurs at defects that bring the monomer into a centrosymmetric relationship with another monomer.

Thomas and co-workers used both transmission electron microscopy

and optical microscopy to study these reactions. In the electron microscopic procedure, single crystals are cleaved and one of the matched faces is irradiated while the other is wet-etched. The faces are then compared. In general, these studies show that photochemical reactions begin at defects (Thomas and Williams, 1969; Thomas, 1970; Thomas *et al.*, 1972; Desvergne, 1973; Sloan *et al.*, 1975; Jones and Williams, 1975).

The studies by Thomas and co-workers have mainly involved the identification of three types of defects: (*a*) the screw dislocation, (*b*) the slip dislocation, and (*c*) the orientation defect. Screw and slip dislocations can bring molecules into different spatial orientations and create different molecular cavities from the bulk crystal. The topochemical postulate and the principle of least motion will still apply, but the products will be determined by the geometry at the screw or slip dislocation and not by the geometry in the bulk crystal (Thomas, 1972).

For example, reaction at screw or slip dislocations could explain why 9-cyanoanthracene forms centrosymmetric photodimers rather than the minor symmetric dimers predicted from the bulk crystal structure. Unfortunately, it is difficult to prepare stable thin samples of this solid, so this explanation cannot be considered confirmed. In addition, it is important to realize that reaction at defects cannot occur unless photochemical energy is transferred to the defect site. If energy transfer is slow relative to the rate of reaction, then reaction will occur in the bulk crystal. If energy transfer is fast relative to the rate of reaction then the reaction will occur at defects, because defects often trap the energy. For example, the 9-cyanonanthracene dimerization is apparently a defect-sensitive reaction, since the quantum yield of this reaction increases as the reaction proceeds. This idea is further confirmed by the fact that a small concentration of fluorescent dopants decreases the yield of dimers (Cohen *et al.*, 1971).

At orientational defects, the tenant molecule takes up an abnormal orientation. This defect is believed to occur in 1,5-dichloroanthracene, which when irradiated produced 20% of the head-to-tail dimer and 80% of the head-to-head dimer (Thomas, 1979).

In our laboratory, we have observed the effect of defects on dehydration reactions of crystal solvates. Three observations on different crystal hydrates illustrate the effect of defects on these solid → solid + gas reactions. First, the temperature (and/or time) at which a desolvation occurs is dependent upon defects. For example, individual crystals of cycloserine began to desolvate at very different times when heated at 50°C. Apparently, the faster reacting crystals had defects that initiated the reaction. Second, mechanical defects produced by cutting the ends off the crystal greatly accelerate the reaction. For example, crystals of dihydrophenylalanine · 0.75 $H_2O$ lost $H_2O$ much more rapidly when the ends of

the crystal were removed with a razor blade. Similar observations were made for *p*-dichlorobenzene where mechanical defects initiated the phase transformation. Third, Perrier, at Purdue (1980), recently found that seeding unreacted crystals with desolvated powder in some cases accelerated the desolvation. However, in other cases this treatment had no effect. For example, brushing the desolvated powder of cytosine hydrate onto the ends of single crystal of cytosine hydrate induced the reaction to begin on the ends of the crystal and move to the center.

In conclusion, it should be noted that defects can have important influences on the solid-state reactions of drugs. In particular, defects can determine when the reaction begins and in special cases possibly even the products of solid-state reactions.

## II. Solid–Solid Reactions

Solid–solid reactions have not been extensively studied, even though they are sometimes used industrially because no solvent disposal or recovery is required. In addition, drugs in dosage forms sometimes degrade via solid–solid reactions. However, only a few studies of solid–solid reactions of drugs have been reported.

A solid–solid reaction can be thought of as occurring in three steps: (*a*) surface migration of one or both reactants, (*b*) diffusion of one reactant into the grains and channels of the other reactant, and (*c*) penetration of one reactant into the crystal lattice of the other reactant (Rastogi *et al.*, 1977a,b). This three-step mechanism has been shown to explain the solid–solid reactions of powders of 8-hydroxyquinoline (**1**) with phthalic anhydride (**2**), maleic anhydride (**3**), succinic anhydride (**4**), catechol (**5**), and resorcinol (**6**). In these reactions a yellow molecular complex is

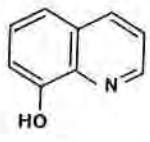


1

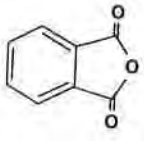


2


3

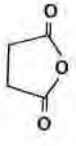


4

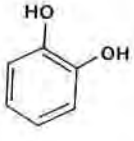


5

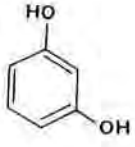


6

formed that dissociates upon dissolution. The kinetics of diffusion of 8-hydroxyquinoline into the solid anhydrides **2**, **3**, and **4** and the phenols **5** and **6** were measured using a capillary technique. The powders of 8-hydroxyquinoline and the reactant were placed in capillary tubes, in contact or with an air gap separating them. The reaction was monitored by measuring the increase in thickness of the yellow product layer. When the powders were in contact, the data fit Eq. (1), where $k$ is the rate constant, $t$ is the time, and $n$ is an integer.

$$\text{Thickness of product layer} = kt^n \tag{1}$$

The activation energy for this reaction was determined by measuring the rate at various temperatures and was 3–5 kcal/mole. This low activation energy was interpreted in terms of a surface migration of 8-hydroxyquinoline into the anhydrides or phenols (Rastogi *et al.*, 1977a,b). No migration of the phenols or anhydrides into the 8-hydroxyquinoline layer was observed.

When there was an air gap separating 8-hydroxyquinoline from the reactants, the reaction was much slower and followed a different kinetic equation, Eq. (2). As the lengths of the air gap increased, the rate of reaction decreased.

$$\text{Thickness of the product layer} = kt \tag{2}$$

These results indicate that when the powders are in contact the reaction proceeds by a mechanism other than vapor diffusion.

The diffusion of 8-hydroxyquinoline inside the grains of the reactant anhydrides and phenols was also studied. This was sutidied by reacting 8-hydroxyquinoline vapor with solid anhydride or phenol. This has an activation energy of 23.0 kcal/mole and may occur by vapor-phase diffusion.

This study points out several important aspects about solid–solid reactions. Of particular interest to pharmacal scientists is the observation that intimate contact of the reactant powders allows surface migration of the reactant. This study indicates that surface migration has a very low activation energy relative to vapor-phase diffusion.

Lin, Siew, and Byrn (1978) have studied the reaction of single crystals of *p*-aminosalicylic acid (**7**) hydrochloride with powdered sodium carbonate. This reaction was carried out by placing $Na_2CO_3$ in contact with single crystals of *p*-aminosalicylic acid hydrochloride crystals, and thus can be viewed as a study of the details of the penetration of reactants. The *p*-aminosalicylic acid exists in three crystal habits, and all three undergo solid–solid reaction with sodium carbonate (see Figure 1 for photographs of a typical reaction). These reactions always began at the point where the

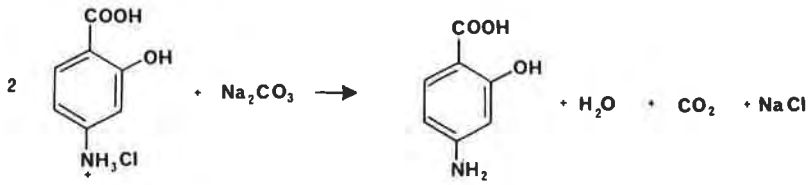


7

acid crystal and base touched. They were quite slow and took more than 40 days to reach completion at 60°C.

When the reaction was carried out at room temperature, droplets of water could be observed after a few days; however, at 60°C no water droplets were observed. The water droplets probably resulted from the breakdown of carbonic acid. Apparently at elevated temperatures the vapor pressure of water was sufficiently large to prevent condensation.

Analysis of the end-products of the reaction indicated that both

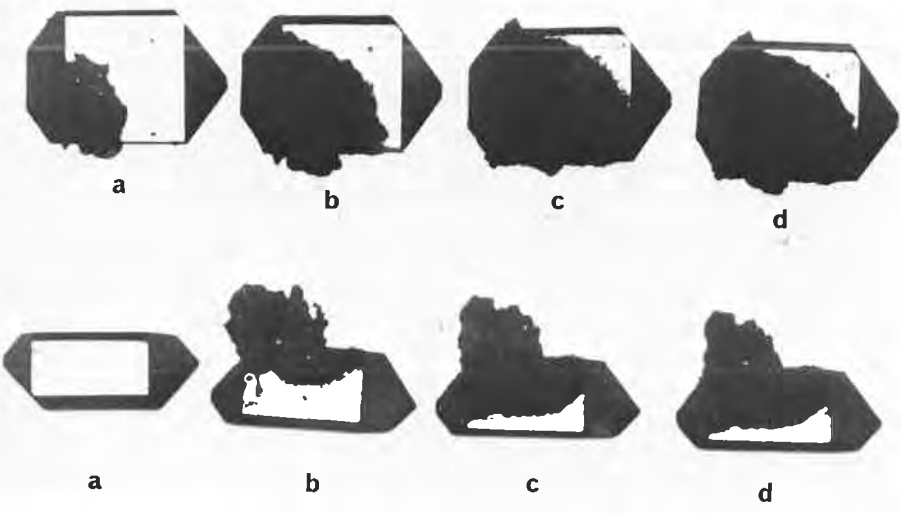


**FIGURE 1.** Upper sequence: reaction of a crystal of habit II of *p*-aminosalicylic acid with $Na_2CO_3$ (dark mass) viewed from the *c* crystallographic direction. (a) Start, (b) after 13 days, (c) after 21 days, and (d) after 30 days. Direction of the crystal axes *a* up, *b* across, and *c* into page. Lower sequence: reaction of the same crystal viewed from the *a* crystallographic direction. This sequence was obtained by turning the crystal in the upper sequence on its side. (a) Start, (b) after 13 days, (c) after 21 days, and (d) after 30 days. Direction of crystal axes *b* across, *c* down, and *a* into page (Lin *et al.*, 1978).

*p*-aminosalicylic acid and *p*-aminosalicylate ion were present. Thus solid–solid acid–base reactions do occur and are slow in comparison to their solution counterparts. The slow rate is probably due to slow diffusion (Jost, 1964; Schmalzried, 1968, 1974; Hauffe, 1955) of ions in the *p*-aminosalicylic acid hydrochloride crystal lattice. In addition, the fact that these reactions always began at the point of contact of the acid crystals and base and spread through the crystal from that point indicates that these reactions can be artificially nucleated and that the reaction proceeds from the nucleation site (which may involve a defect) throughout the crystal. This behavior is similar to that of single crystals of *p*-aminosalicylic acid hydrochloride at 95°C, since once these crystals begin to react the reaction spreads from that nucleation site throughout the crystal. It should be noted that while the thermal reaction of *p*-aminosalicylic acid hydrochloride probably involves loss of HCl by diffusion, these solid–solid acid–base reactions could involve either diffusion of HCl to the sodium carbonate or counterdiffusion of the $H^+$ and $Na^+$ ions to form $H_2CO_3$ in the base and NaCl in the acid lattice.

Although organic solid–solid reactions are relatively rare, solid–solid reactions that form spinels from metal oxides (e.g., $Al_2O_3$ and MgO) at high temperatures have been carefully studied (Jost, 1964; Schmalzried, 1968, 1974; Huaffe, 1955); the most probable mechanism of these reactions involves counterdiffusion of cations.

The behavior of a crystal of habit I of *p*-aminosalicylic acid hydrochloride in contact with sodium carbonate on the (011) and (011) crystal faces is quite similar to that of crystals of habit I upon heating, except that in the former case the reaction begins on the end where the $Na_2CO_3$ is touching and moves to the other end. As in the thermal reaction of crystals of habit I, the photographs give the impression that the reaction is proceeding in layers and that it is slower in the *c* than in the *b* crystallographic direction.

When a crystal of habit I of *p*-aminosalicylic acid hydrochloride is placed in contact with sodium carbonate on the (102) face, the reaction begins at the point of contact; after 5 days the distance of the reaction front from the point of contact indicates the reaction is equally fast in the *a* and *b* crystallographic directions. After 40 days the reaction stopped before it reached completion. The reaction rates in the *a* and *b* directions are consistent with the crystal packing, which indicated that ion migration along either the *a* or *b* direction would be favorable.

Figure 1 shows the behavior of a crystal of habit II of p-aminosalicylic acid hydrochloride when $Na_2CO_3$ was placed on the *c* face. Measurement showed that the ratio of distances which the front had to move to reach completion in the *a* : *b* : *c* direction was 3.5 : 5 : 5. After 13 days the reac-

tion had proceeded equally far in the *a* and *b* crystal directions, and after 21 days the reaction had reached completion in the *a* and *b* direction but was not completed in the *c* direction. This data qualitatively shows that the reaction of habit II is faster in the *a* and *b* directions than in the *c* direction. These relative rates are consistent with the crystal packing, which showed that migrating ions encounter more hydrocarbon functionalities when migrating in the *c* than in the *a* and *b* directions (Lin *et al.*, 1978).

This reaction is a model to explain drug physical incompatibilities that have been known for many years and indicates that, as with other solid-state reactions, solid–solid acid–base reactions are slower than their solution counterparts.

Tablets containing aspirin and easily acylated drugs degrade to give acylated drugs and salicylic acid. These reactions have been reviewed in Chapter 7 while discussing solid–gas reactions, since the first step of these reactions may involve hydrolysis of aspirin to form acetic acid. For example, mixtures of phenylephrine hydrochloride and aspirin contained 80% of acylated phenylephrine after 34 days at 70°C. A mixture of starch and magnesium stearte slowed this acylation to only about 1% after 34 days, while magnesium stearate without starch caused complete decomposition after 16 days. Some diacylated product was also obtained. This reaction may proceed by direct acylation.

The solid state acetylation of codeine phosphate by aspirin has been studied in a recent paper by Galante *et al.* (1979). The kinetics of this reaction were complex and a single equation could not be obtained. The kinetics of codeine phosphate disappearance were pseudo-first-order after an initial lag time; however, the kinetics of acetylcodeine formation were a complex order and were not related to codeine disappearance. This result suggests that there is an intermediate in this reaction. The kinetics of aspirin disappearance also did not follow any specific order.

One complicating factor in this reaction is the source of water for the hydrolysis of the aspirin. For the hydrolysis of the initial few molecules, residual water in the mixture is available. After this, each molecule of acetylcodeine formed releases one molecule of water for further hydrolysis of aspirin. Based on this argument it is surprising to note that the reaction does not go to completion but instead uses up all of the residual water and continues to the extent of about 7% and then stops. This may be due to the fact that a coating of product is formed on the reactant at this point, preventing any further reaction.

It is clear from these few studies that further investigations are required to establish the factors controlling solid–solid reactions and the course of these reactions.

## III. Solid-State Carbon NMR Spectroscopy—A New Method for the Study of Solid Drugs

Drugs that crystallize in different forms show a wide range of physical and chemical properties, including different melting points and spectral properties (Halleblian and McCrone, 1969; Byrn, 1976). The crystal form is particularly important since it can alter the dissolution rate, bioavailability, chemical stability, and physical stability (Haleblian and McCrone, 1969; Byrn, 1976).

The existence of crystalline forms is best established by crystallographic examination; however, other methods can be used including optical microscopy, infrared spectroscopy, and thermal methods of analysis (see Chapters 2 and 4).

In addition, drugs often precipitate as amorphous solids. These solids give no x-ray diffraction pattern and are in general difficult to characterize. However in some cases—that is, nabilone (Thakkar *et al.*, 1977) and novobiocin (Mullins and Macek, 1960)—the amorphous form is the pharmaceutically desirable form, since the crystalline forms are insoluble.

There are numerous activities in the pharmaceutical industry that require consideration of the polymorph present, as reviewed by Haleblian and McCrone (1969). Tableting behavior depends on the crystal form present. Some forms tablet properly while others cause powder bridging and capping problems. Phase transformations of suspensions can lead to caking and problems in syringeability. Phase transformation to a more stable form can also lead to gritty and otherwise unacceptable creams. In addition, the form present can affect chemical stability. For example, overdrying of cephalosporin antibiotics can lead to a product that is probably amorphous and is extremely unstable. Similar observations have been made for steroids. Finally, the form present can affect bioavailability. For example, two of the crystalline forms of nabilone are completely unavailable when given perorally to dogs and thus have no biological effect (Thakkar *et al.*, 1977).

Unfortunately, the mechanism of the solid-state degradation of drugs and the structure and nature of amorphous forms are not adequately understood. Thus new methods for the study of solid drugs could eventually lead to improved effectiveness and quality of pharmaceuticals by improving our understanding of these processes.

### A. ADVANTAGES IN CHARACTERIZING SOLID DRUGS

While infrared spectroscopy and thermal analysis (particularly differential scanning calorimetry, DSC) have been used to characterize crystalline

forms, some forms known to be different show identical infrared spectra and DSC properties. In addition, DSC measures the bulk properties of the solid and is difficult to interpret when mixtures of crystal forms are present. Infrared spectroscopy, of course, measures the vibrational energies of the bonds and, except for hydrogen bonding, crystal packing forces are sometimes not strong enough to cause changes in bond vibrations. Thus infrared spectroscopy is not always extremely sensitive to changes in crystal packing. X-Ray diffraction is sensitive to differences in crystal packing but is an averaging technique, not extremely useful for solid solutions or at all for amorphous forms. In addition, these techniques do not allow examination of the change in conformational or motional properties of functional groups of a solid during drying or a phase transformation.

Solid-state carbon-13 NMR spectroscopy appears to offer significant advantages over these techniques for the study of solid drugs. Figure 2 shows the solid-state carbon-13 NMR spectra of three crystal forms of nabilone. These spectra clearly show that different crystal forms have different spectra. Apparently the crystal packing differences in these forms are great enough to expose the different carbon nuclei to different environments with respect to the NMR experiment. This shows that the NMR method is in principle able to detect small differences in the environment of functional groups in solids. This result is consistent with reports in the literature which show that different polymorphs of cellulose show different C-13 NMR spectra (Atalla *et al.*, 1980) and that (+) crystals of tartaric acid show different spectra from (±) crystals (Hill *et al.*, 1979).

Because solid-state carbon-13 NMR spectroscopy is not an averaging technique, it offers the potential for the analysis of mixtures of crystalline forms as well as the analysis of a particular form in the presence of excpients, provided a unique resonance can be found. Both of these potential applications could lead to its widespread use in the pharmaceutical industry.

Moreover, solid-state carbon-13 NMR spectroscopy also offers the possibility of the analysis and characterization of amorphous forms. A particularly important question in this area is whether amorphous forms are liquid-like or solid-like.

Finally, the technique can be used to examine conformational and dynamic changes that occur in solid drugs during solid-state transformations and reactions.

## B. THEORY OF SOLID-STATE CARBON-13 NMR SPECTROSCOPY

In this section, the theory leading to the development of solid-state carbon-13 nmr spectroscopy is briefly reviewed, along with several impor-

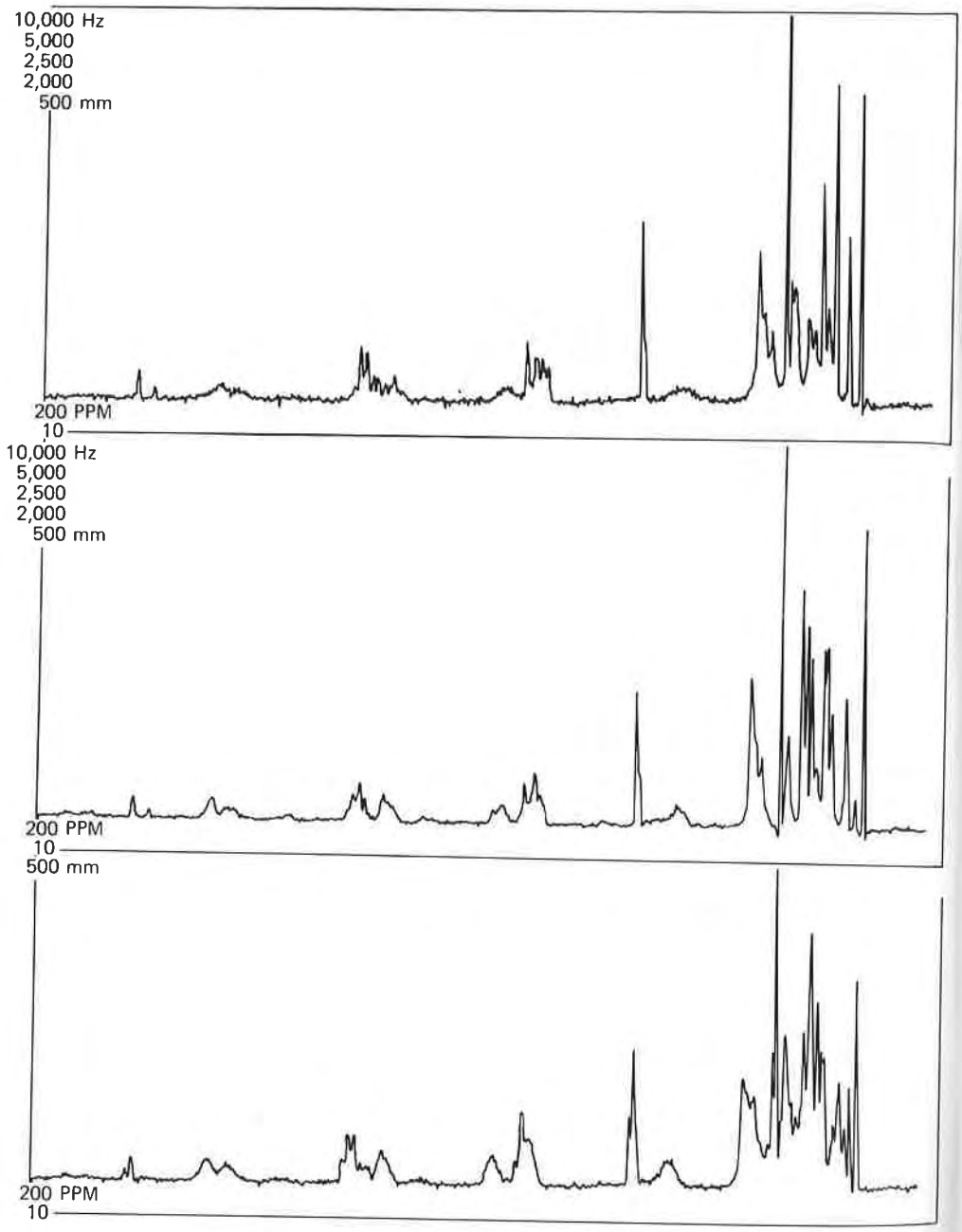


**FIGURE 2.** Solid state nmr spectra of three polymorphs of nabilone.

tant papers in the literature. This is intended to provide the reader with state-of-the-art knowledge.

Classical carbon-13 NMR spectra of solids obtained in Fourier transform (FT) experiments are characterized by broad featureless line shapes that obscure any chemical-shift information. The large linewidths are due to both the strong interaction of the observed nucleus with neighboring nuclei and the wide variety of orienations that it experiences with respect to the applied field in a randomly oriented powder.

Strong proton decoupling can be used to remove the interaction of the observed nucleus with neighboring nuclei, and the effect of random-oriented powders can be removed by very rapid spinning at the "magic angle" (54°44′).

A third problem involves the long spin–lattice relaxation in ($T_1$) of the C-13 nuclei in solids. This long time permits only a slow pulse repetition and thus limits the amount of data that can be accumulated per unit time. However, cross-polarization techniques can be used to allow a much faster acquisition of data. This sequence involves four steps:

1. The proton nuclear spin magnetization is allowed to build up along **Bo**.
2. The proton spin set is prepared in a state of low spin temperature (excess of ground-state spins).
3. The low-spin-temperature protons are put in contact with the high-spin-temperature carbon nuclei. This results in a relaxation of the carbon nuclei to the lower spin state (low spin temperature).
4. The FID decay of the carbon nuclei is measured. The actual pulse sequence required to accomplish this is described in the various instrument operation manuals.

A combination of strong proton decoupling, magic-angle spinning, and cross polarization allows the observation of carbon-13 solid-state NMR spectra with linewidths of a few hertz. The spectra shown in Figure 2 were obtained using these techniques.

As already mentioned, solid-state carbon-13 NMR spectra of two polymorphs of cellulose (Atalla *et al.*, 1979) and the (+), (±), and meso crystals of tartaric acid have been measured (Hill *et al.*, 1979). In these cases, the different polymorphs (or crystalline forms) gave different solid-state NMR spectra.

In addition, Shiau *et al.* (1980) at the University of Illinois at Urbana have used solid state carbon-13 NMR to show that solid naphthazarin B exists in the phenolquinone tautomer in the solid state at both 25° and −160°C.

Recently, a pulse sequence involving interrupted decoupling has been

introduced as an aid to assigning the peaks in the solid-state carbon-13 NMR spectrum. (Opella and Frey, 1979). This technique causes the intensities of all signals from CH or $CH_2$ carbons to decrease, leaving only the signals from quaternary or $CH_3$ carbons. Gray used this technique to assign some of the peaks in the solid-state spectrum of nabilone. In many cases, the peaks can also be assigned using the solution spectra.

Solid-state carbon-13 NMR spectroscopy has improved and developed to the point at which it has great potential for the study of solid drugs.

## IV. Conclusion

There is no data, except for the spectra presented herein, concerning the applicability of solid-state carbon-13 NMR spectroscopy to the investigation of solid drugs. Because solid-state carbon-13 NMR spectroscopy has advanced to the point where spectra such as those of hydrocortisone-*tert*-butylacetate and nabilone can be obtained, this method can be extended to other pharmaceutically important solids. In addition, the effect of the following factors on solid-state carbon-13 NMR spectra are of interest: (*a*) the presence or absence of water of hydration; (*b*) two crystallographically unique molecules per asymmetric unit; (*c* different tautomers in different crystalline forms; (*d*) different conformers in different crystalline forms; and (*e*) different ionization states in different crystalline forms.

Other potential applications include using solid-state carbon-13 NMR spectroscopy for the study of amorphous forms, solid-state reactions, and drug–polymer interactions.

## References

Atalla, R. H., Gast, J. C., Sindorf, D. W., Bartuska, V. J., and Maciel, G. E. (1980). *J. Am. Chem. Soc.* **102,** 3249.

Byrn, S. (1976). *J. Pharm. Sci.* **65,** 1.

Cohen, M. D., Ludmer, Z., Thomas, J. M., and Williams, J. O. (1971). *Proc. R. Soc. London, Ser. A* **324,** 459.

Desvergne, J. P. (1973). Ph.D. Thesis, University of Bordeaux.

Galante, R. N., Visalli, A. J., and Patel, D. M. (1979). *J. Pharm. Sci.* **68,** 1494.

Haleblian, J., and McCrone, W. C. (1969). *J. Pharm. Sci.* **58,** 911.

Hauffe, K. (1955). "Reactionen in und an Festen Stoffen." Springer-Verlag, Berlin.

Hill, H. D. W., Zens, A. P., and Jacobus, J. (1979). *J. Am. Chem. Soc.* **101,** 7090.

Jones, W., and Williams, J. O. (1975). *J. Mater. Sci.* **10,** 379.

Jost, W. (1964). "Diffusion." Academic Press, New York.

Birifalco, L. A. (1964). "Atomic Migration in Crystals." Blaisdell, New York.

Lin, C. T., Siew, P. Y., and Byrn, S. R. (1978). *J. Chem. Soc., Perkin Trans. 2,* 963.

Mullins, J. D., and Macek, T. J. (1960). *J. Pharm. Sci.* **49,** 245.
Opella, S. J., and Frey, M. H. (1979). *J. Am. Chem. Soc.* **101,** 5854.
Perrier, P. (1980). Unpublished results. Purdue University.
Rastogi, R. P., Singh, N. B., and Sungh, R. P. (1977a). *Ind. J. Chem.* **15A,** 941.
Rastogi, R. P., Singh, N. B., and Sungh, R. P. (1977b). *J. Solid State Chem.* **20,** 191.
Schmalzried, H. (1968). *In* "Reactivity of Solids," *Proc. 6th Int. Symp., Schenectady, New York,* August.
Schmalzried, H. (1974). "Solid-State Reactions" (English translation). Verlag-Chemie and Academic Press, New York.
Shiau, W., Duesler, E. N., Paul, I. C., Curtin, D. Y., Blann, W. G., and Fife, C. A. (1980). *J. Am. Chem. Soc.* **102,** 4546.
Sloan, G. J., Thomas, J. M., and Williams, J. O. (1975). *Mol. Cyrst. Liq. Cyrst.* **30,** 167.
Thakkar, A. L., Hirsch, C. A., and Page, J. G. (1977). *J. Pharm. Pharmacol.* **29,** 783.
Thomas, J. M. (1970). *Carbon* **8,** 413.
Thomas, J. M. (1972). *Isr. J. Chem.* **10,** 573.
Thomas, J. M. (1979). *Pure Appl. Chem.* **51,** 1065.
Thomas, J. M., and Williams, J. O. (1969). *J. Chem. Soc., B,* 2749.
Thomas, J. M., Williams, J. O., and Jones, W. (1972). *In* "Reactivity of Solids" (J. S. Anderson, M. W. Roberts, and F. S. Stone, eds.), p. 515. Chapman and Hall, London.

# 12 Conclusion

The purpose of this chapter is to demonstrate that the molecular approach to studying the solid state chemistry of drugs leads to the development of new knowledge. This new knowledge in turn leads eventually to the development of new methods for the stabilization of drugs.

Crystals are one of the important media in which solid-state reactions occur. The arrangement of molecules in crystals is defined using single-crystal x-ray techniques, so that the reaction environment and geometry of the reactant is completely defined. Synthetic chemists use this defined geometry to enable the preparation of polymers and other molecules of defined stereochemistry.

Crystal habits are known. The crystal habit affects the pharmaceutical properties of the crystal. For example, different crystal habits in suspension have different syringeability. Different crystal habits also have different tableting behavior. These differences are primarily due to differences in shape of the different crystal habits.

Crystal polymorphs are common for drugs. The polymorph present can alter both the chemical reactivity and the pharmaceutical properties including bioavailability of the compound. For example, one of the polymorphs of hydrocortisone-*tert*-butyl acetate is oxidized in light and air. Three other polymorphs of hydrocortisone-*tert*-butyl acetate are sta-

ble under identical conditions. In another example, two polymorphs of nabilone show pharmaceutically acceptable dissolution rates while two others do not dissolve.

A special type of polymorphism involves crystal solvates. Crystal solvates incorporate solvent of crystallization in stoichiometric or nonstoichiometric amounts. As with polymorphs, solvates show different chemical and pharmaceutical properties.

Solids also exist as amorphous forms. Amorphous solids do not contain molecules in a regular arrangement. They are difficult to define. In addition, these forms are sometimes hygroscopic and are often more reactive than crystalline forms.

Not all reactions involving crystalline or amorphous forms occur in the solid state. Observation of reacting crystals under a microscope can often reveal whether the reaction is occurring in the solid state or whether liquid is present. In addition, a solid-state reaction should meet at least one of the following criteria:

1. A reaction occurs in the solid when the liquid reaction does not occur or is much slower.
2. A reaction occurs in the solid when pronounced differences are found in the reactivity of closely related compounds.
3. A reaction occurs in the solid when different reaction products are formed in the liquid state.
4. A reaction occurs in the solid if the same reagent in different crystalline modifications has different reactivity or leads to different reaction products.
5. A reaction occurs in the solid if it occurs at a temperature below the eutectic of a mixture of the reactants.

Solid-state reactions of drugs are viewed in terms of a four-step process:

1. *Molecular Loosening*. The reactant molecules gain enough molecular motion to react. For solid–gas reactions this step also involves diffusion of the gas to the reaction site.
2. *Molecular Change*. The chemical reaction occurs and new chemical bonds are formed and old bonds are broken.
3. *Solid Solution Formation*. A solid solution of the product in the starting crystal is formed.
4. *Separation of the Product Phase*. The product phase crystallizes out of the solid solution.

The first two steps of this process (molecular loosening and molecular change) are most important, since they are the rate-determining steps for

most solid-state reactions. These two steps are profoundly affected by crystal packing. Crystal packing controls the molecular looseness of the molecules and the size and shape of the reaction cavity. Crystal packing also controls the relationship between molecules in the solid. Its influence on solid-state photochemistry has led to the topochemical postulate, which states that reactions within crystals will proceed with a minimum of atomic and molecular motion.

With these generalizations and principles in mind, we review the various solid-state reactions in terms of these principles.

Polymorphic transformations convert one crystal form of a drug or organic compound to another. These reactions often proceed through the crystal in a front. Polymorphic transformations can be understood on a molecular level in terms of Kitaigorodskii's closest packing theory. They almost always produce the most closely packed, densest crystal. However, in some cases, particularly favorable crystal packing such as hydrogen bonding can result in one of the less dense forms being most stable.

An interpretation of the stability of polymorphs in terms of the molecular packing in each polymorph provides insight into the factors that are responsible for the stability of crystals. These factors are the density of the crystal, and hydrogen bonding, which adds additional stabilization to the crystal.

Polymorphs are interconvertible via dissolution–recrystallization processes as well as solid-state reactions. These interconversions produce the most stable crystal form as the product. In these interconversions, which are called solution-mediated phase transformations, crystals of the most stable form grow while crystals of the less stable forms dissolve.

Desolvation reactions are a particular type of polymorphic transformation that involves the loss of solvent of crystallization. Crystallographic study shows that a desolvation reaction can form one of three types of crystals: (*a*) a desolvated crystal with the same crystal structure as the solvate; (*b*) an anhydrous form with a crystal structure different from the solvate; or (*c*) an amorphous form. The crystal formed plays an important role in the reactivity of desolvated crystals. For example, if an amorphous form is produced, then the desolvated crystal will be more reactive than the solvate.

Study of the factors influencing the facility of desolvation indicates that these reactions are influenced by molecular loosening and the strength of the hydrogen bonds of the solvent to the host crystal. Molecular loosening really means the looseness with which the solvent is held in the crystal. It can be correlated with the cross-sectional area of the solvent tunnels. The larger the cross-sectional area, the greater the molecular looseness and the more facile the desolvation. The strength of hydrogen bonding between

the solvent and the host crystal of course affects the facility of removal of the solvent. The weaker the hydrogen bonding, the easier it is to remove the solvent. The influence of molecular looseness and hydrogen bonding on desolvation reactions are excellent examples of the influence of the molecular-loosening and molecular-change steps on solid-state reactions.

Solid-state oxidation reactions can be understood in terms of the molecular looseness of the crystal. In several instances the oxidation of one crystal form of a substance occurs while other crystal forms of the substance are stable. For example, tetramethylrubrene is oxygen-sensitive while the nonmethylated derivative, rubrene, is stable. The best explanation of this behavior is that oxygen can penetrate into the loosely packed tetramethylrubrene crystal but not the more closely packed rubrene crystal.

Crystals undergoing solid–gas reactions show anisotropic behavior. Addition of ammonia gas to crystals of carboxylic acids proceeds in a front that moves through the crystal. Similarly, desolvation reactions that involve loss of solvent of crystallization proceed in a front which moves through the crystal. The direction in which the front migrates through the crystal can be explained in terms of the crystal packing, which is a particular aspect of the molecular looseness of the crystal. In both the ammonia addition to carboxylic acid crystals and desolvation reactions, the gas migrates in the direction in which it encounters the least number of nonpolar hydrocarbon functionalities.

Another factor that influences solid–gas reactions is relative humidity. For example, the oxidation of dialuric acid in high relative humidities can be interpreted in terms of the formation of a water layer a few molecules thick. The extremely fast solution oxidation of dialuric acid apparently occurs in this water layer. Of course, solid-state hydrolysis reactions are also accelerated in high humidities.

Solid-state decarboxylation reactions, which are a special type of solid gas reactions, are influenced by the molecular-change step. In contrast to other solid–gas reactions where molecular looseness plays a role, the decarboxylation of salicyclic acids in the solid state parallels the rate of reaction in solution. This observation is best explained in terms of the hypothesis that decarboxylation reactions are controlled mainly by the molecular change occurring, rather than by the molecular looseness of the crystal.

The major factor controlling the structure of the products of solid-state photochemical reactions is the geometry in which the reactants are held in the crystal. This control by crystal packing is an example of the profound effect that the lack of molecular looseness can have on the products of such reactions. For these, the fact that the molecules are held in a fixed

geometry in the crystal results in complete control of the stereochemistry of the products.

The control of the stereochemistry of the products of a solid-state photochemical reaction by the crystal packing is the experimental basis for the topochemical postulate, which states that the products of a solid-state photochemical reaction will be those formed by the least molecular motion of the reactants. Numerous solid-state photochemical reactions obey the topochemical postulate. These include the dimerization of cinnamic acids and derivatives, the reactions of naphthoquinones, and many solid-state polymerizations.

Solid-state photochemical reactions also provide insight into steps 3 and 4 (solid-solution formation and separation of the product phase) of the hypothetical solid-state reaction. Because of the nature of these reactions, the product is formed in the crystal lattice of the reactant. In some cases, a large percentage of product is formed before it separates into its own phase. In fact, the separation of the product into its own phase is not a desirable process because of the possibility that this separation will disrupt the crystal packing of the reactant. For solid-state photochemical reactions, a large extent of solid-solution formation is almost required in order to maintain the reactants in the required geometry.

Solid-state thermal reactions can be understood by realizing that these reactions are controlled by both the molecular looseness of the crystal and the molecular change occurring in the reaction. Some thermal reactions are accompanied by front advancement, in a direction that can be understood by considering both the molecular looseness and the crystal packing. The products and relative rates of these reactions can best be understood by considering the molecular change involved in the reaction. The influence of the molecular-change step on these reactions is expected, since they often have relatively high activation energies.

In conclusion, this book demonstrates an understanding of solid-state reactions in terms of a four-step process: molecular loosening, molecular change, solid-solution formation, and separation of the product phase.

## Glossary

Accelerated stability tests—Tests for the stability of drugs, using high temperatures and/or humidities to accelerate the degradation. This accelerated degradation data is then used to predict the expiration date.

Activation energy (Arrhenius activation energy)—A physicochemical quantity that represents the barrier for a chemical reaction.

Amorphous form—A solid that does not give a distinctive powder x-ray